2009

The effects of biomass pretreatments on the products of fast pyrolysis

Randall Dennis Kasparbauer
Iowa State University

The effects of biomass pretreatments on the products of fast pyrolysis

by

Randall Dennis Kasparbauer

A thesis submitted to the graduate faculty
in partial fulfillment of the requirements for the degree of
MASTER OF SCIENCE

Major: Mechanical Engineering

Program of Study Committee:
Robert C. Brown, Major Professor
James Bernard
Raj Raman

Iowa State University
Ames, Iowa
2009

TABLE OF CONTENTS

LIST OF FIGURES

LIST OF TABLES

ABSTRACT

Fast pyrolysis thermochemically degrades lignocellulosic material into solid char, organic liquids, and gaseous products. Using fast pyrolysis to produce renewable liquid bio-oil to replace crude oil is gaining commercial interest. The production of pyrolysis bio-oil needs to be improved through standardization. Only with standard operational methods can pyrolysis bio-oil be commercially refined into chemicals or transportation fuels. Pretreatments such as washing or torrefaction of biomass prior to pyrolysis are not required to produce high liquid yields, but may improve the end products' yield or quality. Improved quality will offset future processing costs that would otherwise be required. Solid biochar and non-condensable gas products are also formed during fast pyrolysis. Water wash, torrefaction, grinding, and drying pretreatments of biomass were studied to determine how each affects the products of fast pyrolysis.

Three modified central composite experimental designs were developed to study a control and two major biomass pretreatments: washing, and torrefaction for effects of grinding, moisture content or torrefaction, and pyrolysis temperature. A fluidized bed fast pyrolyzer was operated at 0.1 kg/hr to complete the three separate experimental design studies, in a total of sixty tests.

The experimental study was used to develop model equations that express how feedstock pretreatments (grinding and moisture content or torrefaction) and pyrolysis temperature affected the products of fast pyrolysis. In each case, a model equation was derived for the three major studies. Model equations were developed for: biochar yield and composition; bio-oil yield, moisture content, and water insoluble content; and non-condensable gas yield and composition. The results showed pyrolysis temperature was the most significant variable in product modeling. The grind size impacted the extent of decomposition during pyrolysis and the biomass moisture content affected mass balances of low moisture biochar and high moisture bio-oil products.

Results showed that water washing reduced the inorganic mineral content of the biomass but did not eliminate it. A 75% ash reduction in the feedstock was

realized from the water wash. Pyrolysis product yields were not significantly affected by the pretreatment. Torrefaction caused non-moisture volatile mass loss in the biomass of 3.8% at 180°C to 15.4% at 250°C during the pretreatment step. The mass loss included the moisture (12 wt. % on a dry basis) as well as other volatile compounds contained in the biomass. The mass reduction caused reduced bio-oil yields of 5% during fast pyrolysis. The bio-oil yield reduction during pyrolysis was realized as an increase in biochar yield. Torrefaction reduced the production of water and light compounds collected in the bio-oil during fast pyrolysis because the compounds were removed during the pretreatment.

The average biochar yield from the tests was 17.6 ± 1.5% on a wet basis of the biomass fed. The biochar yield decreased with temperature for all biomass types from 30% to 10% for pyrolysis temperatures from 426°C to 544°C. The biochar elemental analysis showed hydrogen and carbon content varied with pyrolysis temperature. Hydrogen content decreased from 5.5% to 3.5% and carbon increased from 60% to 70% when increasing pyrolysis temperature from 426°C to 544°C.

A fractionated bio-oil collection method was used that collected four separate fractions of bio-oil. The first three fractions had higher heating values (HHV) above 20 MJ/kg and water content below 5 wt. %. The fourth fraction had an average HHV of 6 MJ/kg and an average water content of 58 wt. %. The first three fractions were also more viscous, contained higher amounts of water insolubles, and contained more elemental carbon and less oxygen compared to bio-oil collected in the fourth fraction (elemental carbon contents of 61.4%, 53.6%, 60.1%, and 37.9% and oxygen contents of 31.4%, 39.1%, 33.1%, and 56.0% respectively for bio-oil fraction 1, 2, 3, and 4). Hydrogen, nitrogen, and sulfur content were constant between all four fractions with hydrogen content at 6%, nitrogen content below 1%, and sulfur content below 0.1%.

The total bio-oil mass yield from the tests was 58.7 ± 1.3% on a wet basis of biomass fed. The first fraction accounted for 18% of the total bio-oil. It collected compounds that condensed at higher temperatures from 400°C to 100°C. The fraction was close to 50 wt. % insoluble in water, had higher energy density, and had the highest viscosity compared to the other fractions. The fraction exhibited solid properties at room temperature. The second fraction collected compounds that condensed at lower temperatures: 100°C to 80°C. The second fraction accounted for

13% of the total collected bio-oil. The second fraction was an energy dense liquid that contained close to 25 wt. % water insolubles and remained a liquid at room temperature. The third fraction collected the majority of aerosol liquids collected by an electrostatic precipitator. The fraction accounted for 53% of the total bio-oil. The third fraction was composed of close to 45 wt. % water insolubles and had a high viscosity. The fourth fraction collected all remaining compounds that condensed above 10°C. The fourth fraction accounted for 16% of the bio-oil collected in each test. The fraction had a low viscosity, less than 1 wt. % water insolubles, and low energy content due to the increased water content.

The non condensable gasses that were formed during fast pyrolysis were measured with a micro gas chromatograph. The non-condensable gas yield averaged 11.9 ± 0.7%. It was determined the total non-condensable gas yield increased with pyrolysis temperature from 10% to 16%. The non-condensable gas carbon monoxide concentration increased and carbon dioxide concentration decreased with increasing pyrolysis temperature. No significant differences in non-condensable gas yield or composition were found between the three biomass pretreatment types studied.

CHAPTER 1: OVERVIEW

The world requires energy to function. Crude oil energy is arguably the most important commodity in the world market. The free-flowing liquid with high energy density and relatively stable properties is the base ingredient for fuels, chemicals, pharmaceuticals, plastics, lubricants, and much more. Crude oil of the 20th and early 21st century, known as a "fossil fuel," is pumped from underground. It was created over millions of years under proper conditions from buried organic matter (Encarta Encyclopedia, 2008). Fast pyrolysis creates a dark liquid, derived from biomass, which has the potential to replace the limited global crude oil supply. Fast pyrolysis of biomass uses an extremely fast heating rate in an oxygen-free reactor to decompose biomass into solid, liquid, and gas products.

1.1 Biomass

Biomass is defined as any carbonaceous material of recent origin (Brown, 2003). This not only includes all raw herbaceous material, but also refuse-derived material that originated as herbaceous material. The latter includes cardboard, wood demolition waste, paper, and plant-derived clothing. Biomass is primarily made of carbon, hydrogen, and oxygen, but is very complex in specific structure. Other minerals are also present in any raw, untreated biomass, but normally in very low concentrations. These minerals can be any available element or compound that comes into contact with the biomass. Some minerals are vital to the growth and health of the plant when it is alive and remain in the plant after harvest. These minerals may include but are not limited to: aluminum (Al), calcium (Ca), iron (Fe), magnesium (Mg), sodium (Na), potassium (K), phosphorus (P), silicon (Si), and sulfur (S) (Raveendran, et al., 1995).

Prior to the advent of coal and oil, biomass was the only fuel available for heat. After initial discovery, other fossil fuel sources became much more popular due to the higher energy density and lower cost of extraction. Previously, wood or grass had been used for combustion to create heat in a furnace or simple campfire.

Biomass is commonly categorized by its three major components: cellulose, hemicellulose, and lignin. These three compounds make up the majority of raw biomass (Mohan, et al., 2006). The remaining material in the biomass can be categorized as extractives and ash. The extractives include small fractions of biomass that are particular to the original plant type. They can include oils, gums, waxes, pectin, and proteins (NREL, 2008). The ash is the mineral matter and all other non-combustible components of raw biomass.

The main components, cellulose, hemicellulose, and lignin, create a very strong natural physical matrix in the biomass. Each component is made of large polymers of primarily carbon, hydrogen and oxygen elements. Tiny crystalline fibrils of cellulose are tied together with the hemicellulose structure. Lignin is the glue that then fills in all the gaps and holds everything together. Each component can be broken apart using a wide array of different processing methods with an end result shown in Figure 1 (Mosier, et al., 2005). The processing can be either biochemical or thermochemical. When broken apart, the resulting compounds can then be restructured or processed into more usable products. The amount of each

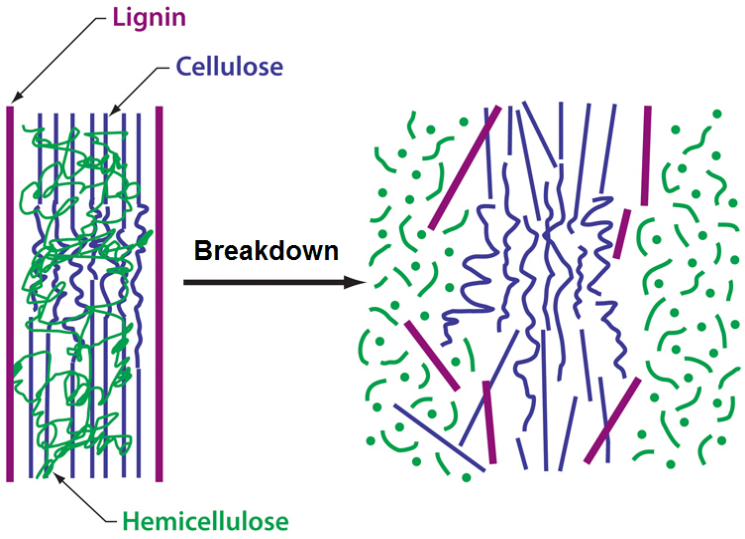

Figure 1: Graphic of three biomass components before and after breakdown (adapted from Mosier, et al., 2005).

component, as well as other constituents, can vary widely between different types of biomass and even between biomass from different regions and growing seasons. The values of these compositions in some commonly used biomass types are shown in Table 1 (U.S. DOE, 2006).

Table 1: Cellulose, hemicellulose, and lignin content in various sources of biomass (U.S. DOE, 2006).

Feedstock	Cellulose	Hemicellulose	Lignin	Other[1]
Corn stover	36.4	22.6	16.6	24.4
Wheat straw	38.2	24.7	23.4	13.7
Rice straw	34.2	24.5	23.4	17.9
Switchgrass	31	24.4	17.6	27
Poplar	49.9	20.4	18.1	11.6

1: Other components include undefiened extractives

1.1.2 Biomass pretreatments

When biomass is used as an energy source it will usually require pretreatment. If the biomass is to be processed thermochemically, grinding and drying are almost always necessary. Using an acid or alkaline soak to break down lignocellulose is common in biochemical biomass-to-energy conversion methods (U.S. DOE, 2006). Water alone can be used to simply clean biomass prior to treatment. All pretreatments create additional costs but are beneficial in the end due to higher end product yields.

1.1.2.1 Washing

When biomass is to be processed into pure chemical compounds, mineral contaminations become a problem. A simple rinsing of the biomass with water will remove large amounts of minerals from the surface (Davidsson, et al., 2002).

Surface minerals can come from previous contact with soil during harvest or transportation.

1.1.2.2 Grinding

Grinding is done mechanically by cutting or breaking biomass apart into smaller dimensions. This is required for efficient conversion by increasing the surface area-to-volume ratio for a feedstock. As the material is ground smaller, the ratio becomes greater. Since heat energy enters the biomass through the surface, the higher this ratio becomes, the faster the particles can heat up in order to react (Wei, et al., 2006).

Grinding is commonly used to reduce the size of biomass at harvest or immediately thereafter. Biomass grinding decreases the bulk density that makes the biomass easier to transport long distances.

For experimental research, the particle size of biomass needs to be reduced to accommodate smaller reactor sizes in experimental equipment. As process equipment is scaled up in size, beyond lab scale, the larger equipment should be capable of processing larger particle size feedstock.

1.1.2.3 Drying

A common problem when using biomass for fuel is the water content in the biomass. Freshly cut biomass can have a moisture content of 60-85 wt% (Brown, 2003). Air drying can reduce the moisture content to around 20 wt. %. Mechanical pressing can reduce moisture content in biomass to 15 wt. %. Heated drying can be used to remove all moisture from biomass. A moisture content of 5-10 wt% is required for prolonged preservation without fermentation effects (Brown, 2003).

1.2 Thermochemical processing

The thermochemical energy platform includes several technologies for converting biomass into fuel. Research has been done on the various methods to increase yields and product quality. Each method has positives and negatives

concerning the implementation and economics on an industrial scale. Thermochemical processing methods include combustion, gasification, fast pyrolysis, and torrefaction. Each operates at specific conditions and can be optimized to produce particular products (Goyal, et al., 2006).

1.2.1 Combustion

Combustion is the traditional method of burning biomass to create heat or light. This is the oldest method for using stored energy to fuel human needs. Due to the relative age of combustion technology, the methods are defined and mature. The basic principles of combustion are utilized in all other thermochemical processes. Complete combustion is the chemical reaction of biomass being oxidized at high temperatures into carbon dioxide and water; releasing all of its stored energy as heat and light.

1.2.2 Gasification

Gasification is a well-known technology that is a precursor to fast pyrolysis. Gasification converts solid biomass into a gaseous product of hydrogen and carbon monoxide. Gasification is considered “fuel agnostic” due to the ability to process any feedstock that is deconstructible with heat. Gasification uses temperatures higher than pyrolysis and below complete combustion to chemically react all of the compounds from the feed into gaseous products.

Oxygen is fed into the gasifier allowing partial combustion to occur. Combustion is used to increase the reactor temperature to above 800ºC. At this temperature a chemical equilibrium is achieved turning solid biomass into a primarily gaseous product. The purity of the gas outlet requires only partial combustion of biomass. Oxygen is added at a specific equivalence ratio either as pure oxygen mixed with steam or as oxygen in air.

The reactor temperature is dependent on the equivalence ratio and freeboard height of the gasifier (Ergudenler, et al., 1997). When conditions are right, the gas outlet is rich in hydrogen, carbon monoxide, and carbon dioxide. The gas is useful

for heat generation, power generation, or chemical upgrading such as via Fisher-Tropsch synthesis (Zwart, et al., 2006).

The exit gas is known as “syngas” if in a purified form, with high carbon monoxide and hydrogen concentrations; when diluted with an inert gas such as nitrogen it is known as “producer gas”. The exiting gas also contains small concentrations of higher molecular weight hydrocarbon compounds (tar), sulfur oxides (SOx), and nitrous oxides (NOx) from incomplete conversion and impurities in the feedstock. The carbon dioxide in the gas is from the partial combustion that occurred during gasification.

Gasification reactors become more thermally efficient as they increase in size. Another method to increase the efficiency of a gasifier is to increase the operating pressure and temperature, promoting increased chemical conversion. Char and tar are also formed during gasification, but at a much smaller mass percentage compared to the gas production. Energy remaining as char or tar reduces the energy conversion efficiency of a gasification unit. Two major problems with operating a large scale gasification plant are the large amount of biomass required and the issues with feeding biomass into the reactor.

The limit for a large gasifier is the ability to feed large quantities of biomass in a reliable and economical manner. Gasification reactors can easily process liquid feeds. When coal is gasified it is mixed with water to form a slurry that is easily fed at high temperatures and pressures (The American Coal Foundation, 2007). Biomass has hydrophilic qualities that diminish slurry formation. An important option to solve these issues is to gasify biomass-derived fast pyrolysis bio-oil.

1.2.3 Fast pyrolysis

Fast pyrolysis is defined as the thermal decomposition of organic material in the absence of oxygen (Bridgwater, et al., 2001). Most commonly, fast pyrolysis is operated at 500°C and at atmospheric pressure (Goyal, et al., 2006). Fast pyrolysis is an attractive choice for increasing the energy density of biomass for economical transportation or creating high value chemicals.

During the process, heat is supplied to the reaction chamber. Extremely fast biomass heating rates are a requirement for fast pyrolysis. Reactions with slow heating rates are referred to as slow pyrolysis. Very short residence times are also critical for fast pyrolysis operation. This is often accomplished by using an inert sweep gas.

The fast pyrolysis process requires moderately high heat to fully convert biomass to liquid at the most efficient rate. The heat inputs hamper the attractiveness of producing bio-oil. Current concern for the environment, the desire for clean energy, and prospected increases in crude oil cost help to make bio-oil an attractive energy source.

The industry standard way to collect bio-oil is to quench the pyrolysis vapors as quickly as possible. Commonly, the produced vapors are quenched within seconds after production. An alternative method uses staged cooling to collect separate bio-oil liquids (Boateng, et al., 2007).

Fast pyrolysis also creates char and gas during operation. The byproducts of bio-oil production can be used to fuel the heat required for the reactor, or they can be sold to other industries. The yields of bio-oil, biochar, and gas are highly dependent on reaction temperature, residence time, and biomass type (Bridgwater, et al., 2001).

1.2.3.1 Bio-oil

The condensed compounds from fast pyrolysis form a crude oil-type liquid known as pyrolysis–oil or bio-oil (Brown, et al., 2006). Bio-oil consists of thousands of different organic compounds that can be combined into similar groups (Bridgwater, 1999). These major groups include: acids, alcohols, aldehydes, alkenes, esters, furans, ketones, phenols, and sugars (Mahfud, 2007). Fast pyrolysis bio-oil can be burned as a low-grade heating fuel. It is also possible to upgrade the bio-oil into more desirable chemicals. Industrially produced bio-oil is currently inferior in quality and stability to fossil fuel crude oil. The most important criteria for fuel-oil quality are low solids content, good homogeneity and stability, and reasonably high flash point (Oasmaa, et al., 2005 b).

Processing methods for producing high quality bio-oil from fast pyrolysis are needed to standardize the industry before production can be increased to meet current energy needs. Biomass that is used for fast pyrolysis can come from anywhere and can contain a very wide range of compounds, elements, or contaminants. The wide range of contaminants can cause poor bio-oil stability and quality.

1.2.3.2 Biochar

After biomass has been completely devolatilized, the remaining solid particulate is called biochar. This solid matter has a low density and can easily entrain into a gas stream. Common industrial cyclone filters work well to remove biochar from a gaseous flow stream. Biochar is very similar in composition and appearance to common commercial charcoal made by slow pyrolysis. The mass yield of biochar produced is inversely proportional to the temperature of the fast pyrolysis reactor until complete devolatilization occurs (McHenry, 2009).

Biochar can be burned after being formed to provide heat to the reactor or to generate steam power for electricity or district heating. The fixed carbon is oxidized into CO_2 similar to coal combustion. Biochar could be co-fired with common commercial charcoal for heat generation.

An alternative end use for biochar is as soil amendment. Biochar has been credited with improving soil quality in ancient Amazonian civilizations (Morris, 2006). The same result is possible today by returning biochar back to soils that contain low levels of carbon caused by centuries of agricultural production (Hottle, 2008).

1.2.3.3 Non-condensable gas

The gas that is not condensed during oil-collection is referred to as non-condensable gas. Similar to gasification, the gas can be referred to as syngas if it is pure, or a producer gas if diluted with inert gas. The non-condensable gas is composed of carbon dioxide, carbon monoxide, hydrogen, and other light gaseous

hydrocarbon compounds. This gas can be used for heat production to fuel a fast pyrolysis reactor or to produce other products.

1.2.3.4 Distributed pyrolysis

Gasification of fast pyrolysis bio-oil can benefit from large economies of scale without incurring high transportation costs. A bio-oil gasifier can complete the conversion of biomass into syngas if the syngas is the most desirable product. Biomass requires more resources and energy to pressurize prior to gasification. Several small fast pyrolysis reactors very close to biomass sources could efficiently supply a central gasification unit with cost-effective liquid energy (Wright, et al., 2008); (Zwart, et al., 2006). The bio-oil has a higher bulk density allowing for more energy to be transported per transport vehicle. This situation would require fast pyrolysis units to supply bio-oil that can remain stable from the time it is produced until it is gasified. Reducing the water content in bio-oil can further increase the energy transport efficiency of the model.

1.2.4 Torrefaction

Torrefaction heats biomass in an inert atmosphere to mild temperatures for a prolonged period of time to improve the energy density and grindability of biomass (Prins, et al., 2006), (Zanzi, et al., 2008). The process temperatures can range from 120-300ºC and process residence times from fifteen minutes to several hours. Torrefaction is also referred to as mild pyrolysis due to its similarity to pyrolysis (Arias, et al., 2008). The difference being that torrefaction is performed at lower temperatures to maximize solid product yields.

Torrefaction of biomass can be performed at a wide range of temperatures and residence times. The temperature at which biomass is torrefied defines the extent to which the biomass is depolymerized (Prins, et al., 2006 b). Lower temperatures merely remove the water and a few lightweight compounds. These compounds include: carbon monoxide, carbon dioxide, methanol, and formic,

lactic, and acetic acid. Higher temperatures remove a majority of the hemicellulose, as well as begin to break the cellulose chains (Prins, et al., 2006 b).

The removal of lightweight compounds and water from the biomass prior to fast pyrolysis may give the resulting bio-oil better stability. Torrefaction causes depolymerization of cellulose into shorter fiber lengths making the biomass more brittle (Bergman, et al., 2005 b). This could improve pyrolysis due to the increased number of chain end locations for chemical reactions to begin. It may also cause fast pyrolysis to break down the material too fast at standard conditions, greatly reducing the amount of high quality products produced. Torrefaction is being explored by companies such as the Netherlands' entity ECN. Torrefaction is used to improve the biomass grindability for pelletizing and to preserve the biomass by preventing biological degradation that is a common problem with biomass storage (Bergman, et al., 2005 b).

1.3 Carbon sequestration

When the carbon in crude oil and coal is burned it produces carbon dioxide (CO_2) as an exhaust. The fossil-fuel carbon is centuries old. The use of fossil fuels causes widespread exhaust of carbon into the atmosphere. Combusting fuel from biomass, rather than fossil fuels, exhausts carbon compounds that were only recently removed from the atmosphere. Biomass energy is carbon-neutral because the carbon was not stored millions of years ago.

The biochar products of fast pyrolysis present the opportunity to produce carbon-negative energy. The carbon rich biochar is formed from to carbon in the biomass not oxidizing with oxygen to form CO or CO_2. Biochar can be burned for heat to create a carbon-neutral process or it can be returned to the earth to create a carbon-negative process (Hottle, 2008). The process is carbon-negative because only the carbon in the bio-oil and producer gas are used as energy fuel. The rest of the carbon from the biomass is returned to the ground as biochar. The total amount of carbon released back into the atmosphere is less than what was removed while the biomass was living. Carbon-negative practices are the only way to reverse fossil fuels' negative effects on Earth's ecosystems.

Fast pyrolysis is an efficient method to produce liquid, gas, and solid fuel from biomass. Returning the biochar to the soil renders the process carbon-negative. The process also yields a renewable liquid and gas product that can be transformed into heat or power. Adding the biochar to soil not only can decrease atmospheric CO_2, but it can also increase biomass production. Based on the observations of ancient Amazonians, black earth known as “terra preta” is a very productive agriculture soil that is composed of poor soil mixed with charcoal. This is a tremendous win-win scenario for returning biochar to the soil for future fast pyrolysis facilities (Morris, 2006).

CHAPTER 2: REVIEW OF TECHNOLOGY

The thermochemical biofuel industry is still in the early stages of commercialization. Combustion and gasification are mature technologies with many currently operating facilities. Torrefaction is a relatively new development. It is being commercialized in the biomass industry for the economic pelletizing of biomass. Pelletizing is critical for transporting biomass long distances for combustion or gasification. Fast pyrolysis is an undeveloped technology for biofuel production but is promising for future applications.

The bio-oil that is collected during fast pyrolysis has the potential to be a high-value commodity to be used for sustainable fuels or chemicals. The biochar also has potential to be a high-value product. Standards for producing each are vague, and the quality of each is questionable. The operating conditions of a fast pyrolysis reactor greatly affect the yields and qualities of each product. This research explores how biomass treatments can affect the production of bio-oil, biochar, and non-condensable gas during fast pyrolysis.

2.1 Biomass

The biomass for this study was loblolly pine slash. It is a lignocellulosic softwood forest product that is left over after traditional logging practices have removed all high value lumber. Slash is a mixture of branches, twigs, needles, and foreign plant matter that was picked up during collection.

Loblolly pine, pinus taeda, extends through fourteen southern states in the United States. It is the most commercially important forest species in the southern United States, dominant on 11.7 million hectares (Baker, et al., 1990). With a fifty year base age, it can grow 18 to 30 m tall depending on soil type and environment (Baker, et al., 1990).

Dependent on the end use, biomass can be collected in several different ways. Biomass types used specifically for biofuels are very early in commercialization and do not yet have a base of proper harvesting equipment. Biomass used for biofuels should be as clean as possible. Inorganic material

creates inefficiencies in transportation and conversion. For thermochemical conversion, the moisture content should be low. If the biomass is to be hydrolyzed, moisture content is not an important factor. Another factor important to harvesting economics is the overall size and density of the biomass.

The use of pine slash for a fuel source requires efficient harvesting methods. The slash and brush is normally burned or left to rot on the forest floor during a tree harvest due to the complexity of collection. This can be both an environmental hazard and a fire hazard. Traditional brush removal methods utilize controlled burning or chemical herbicides. Several commercially available machines can be used to harvest loose biomass slash from the forest. The machines can also be used for brush removal anywhere biomass is available as a fuel source. An average harvest is projected to yield twenty tons of slash per acre of felled forest land (Kock, et al., 1976).

A traditional method for harvesting the biomass is a harvesting machine that mechanically chops the biomass into a cart that is pulled behind the harvester. This is best used when the biomass will be moved off-site. A machine can otherwise windrow the biomass to the side for use in mulching beds or bailing. Tight cylindrical bales are sometimes used if the biomass is to be transported off-site (Kock, et al., 1976).

The pine slash feedstock is only one of many possible sources of lignocellulosic energy. The feedstock studied in this research is practical and could be used in a large future processing facility. Any impurities in the biomass used in this study will simulate a genuine feedstock. Several treatments can be done to improve the biomass quality. Washing, torrefying, grinding, and drying were each studied in this project.

2.2 Fast pyrolysis

There is a substantial and growing knowledge of fast pyrolysis methods and reactor designs. Despite that, exact sizing parameters and operating conditions are still in research stages. Overall, the ultimate goal of fast pyrolysis is to produce a bio-oil at a high yield that can be sold for a profit. The low value of bio-oil is

attributed to its high water content, high acidity, poor homogeneity, and poor stability (Oasmaa, et al., 2005 b). An improved method for producing bio-oil can make the fast pyrolysis of biomass a viable option to generate affordable renewable energy.

2.2.1 Current state of art

Fast pyrolysis can be performed by several reactor types and under a wide range of operating conditions. Using a fluidized bed reactor for fast pyrolysis is common because of the high heat transfer and turbulent mixing characteristics of a fluidized sand-bed.

Other common reactor styles for fast pyrolysis include the following: auger (with and without additional heat carrier such as sand or steel pellets), circulating fluidized bed, ablative, vacuum, rotating cone, and drop tube. Each reactor has known advantages and disadvantages in operation and scaling (Brown, et al., 2006). The fluidized bed reactor was chosen due to its relative ease of scalability and simple operation when compared to other fast pyrolysis reactor types.

Fast pyrolysis reactors have been researched for many years, but a market need for production has not yet been realized. This is evident in production quantities of pyrolysis oil being far less than other low-value renewable fuel liquids produced in the United States shown in Table 2 (Holmgren, et al., 2008). Renewable liquid fuel available in the United States from oil, grease, and animal fats accounted for almost 100,000 barrels while pyrolysis oil accounted for only 750 barrels in 2005. The volumes available for fuel are also far less than the total produced in the United States. The primary reason that bio-oil is not mass produced is the relatively poor fuel quality it exhibits compared to its fossil fuel and other biofuel competition.

Table 2: Availability of biorenewable liquids in the United States (Holmgren, et al., 2008).

Biorenewable Feedstock	Definition	Amount produced in the U. S. (bpd)	Amount available for fuel production in U.S. (bpd)
Vegetable Oils	soy, cottonseed, canola, peanut	194,000	33,500
Recycled	yellow grease, brown (trap) grease	51,700	33,800
Animal Fats	tallow, lard, fish oil	71,000	32,500
Pyrolysis Oil	made from pyrolysis of waste biomass (cellulosic)	1,500	750

2.2.2 Bio-oil properties

The quality problems with bio-oil involve its energy density, homogeneity, particle contamination, and phase stability over time. These problems must be solved before bio-oil can be mass-produced. Poor bio-oil quality can result from its high water content as well as the low molecular weight and highly acidic compounds that are in solution with the bio-oil (Oasmaa, et al., 2001). Some of these compounds can be traced back to particular components of the biomass used. Particularly, the hemicellulose and lignin components of the biomass contain some of the undesirable compounds. The inorganic minerals present in the biomass may be another source of undesired compounds. The minerals promote reactions from desired bio-oil compounds such as levoglucosan into unwanted compounds such as acetic acid (Di Blasi, 2008). Using a feedstock that is free of these contaminants could greatly increase the quality and stability of bio-oil. High quality and stable bio-oil could compete with the industry-standard fossil crude oil. Common properties of published bio-oil liquids that can be used as a baseline are shown in Table 3 (Oasmaa, et al., 2001).

Table 3: Properties of pyrolysis liquids from different souces and feedstocks (Oasmaa, et al., 2001).

Source	VTT[1]	VTT[1]	Ensyn	NREL
Feedstock	Pine	Forest residue[2]	Mixed hardwood	Poplar[3]
Physical Property				
Water, wt.%	16.6	24.1	22	18.9
pH	2.6	2.9	2.5	2.8
Density (at 15°C), kg/dm^3	1.24	1.22	1.18	1.2
Elementals (dry), wt.%:				
C	55.8	56.36	56.4	57.3
H	5.8	6.2	6.2	6.3
O (by diff.)	38.2	36.9	37.1	36.2
N	0.1	0.1	0.2	0.18
S	0.02	0.03	<0.01	0.02
Ash	0.03	0.08	0.01	<.01
K+Na, ppm	20	60	460	10
Cl, ppm	30	<100	3	8
HHV, MJ/kg	19.1	17.4	17	18.7
HHV (dry), MJ/kg	22.9	23	23.1	22.3
Viscosity, cSt:				
20°C	n.d.	152	n.d.	128
50°C	31	29 (40°C)	50	13.5
Flash point, °C	n.d.	42	55	64
Pour point, °C	-19	-12	-25	-36
Solubility, wt.% insolubles in:				
ethanol	0.3	0.1	0.045	0.045
methanol-dichloro-methane	n.d.	0.02	n.d.	n.d.

1: VTT Technical Research Centre of Finland
2: Bottom phase (90% of total liquid)
3: Hot gas filtered

Bio-oil may be upgraded into additional useful compounds (Bridgwater, 1996). Iowa State University has also explored the use of bio-oil as an asphalt binder in the road paving industry (Williams, et al., 2008). Both of these end uses of bio-oil have not been commercialized but are promising technologies to increase the overall value of bio-oil.

Bio-oil can be gasified (Wright, et al., 2008). It allows for gasification to easily operate at higher pressures due to the simplicity of pressurizing a liquid feed rather than the solid biomass (Venderbosch, et al., 2008). Bio-oil is denser than

raw biomass. It also has a higher energy density. This increases the efficiency of transporting energy to a centralized processing facility. Currently, pyrolysis bio-oil is not an ideal fuel source for direct combustion or upgrading. The foreign minerals, water, and oxygen in the bio-oil do not allow for robust use in standard combustion chambers or oil refineries (Czernik, et al., 2004).

On an energy basis, bio-oil contains as much as 66% of the original biomass energy in a dense liquid state (Uslu, et al., 2008). Fast pyrolysis is relatively efficient at a small scale. Potentially, this allows for the distribution of a large number of fast pyrolysis reactors to be placed where biomass is available. The bio-oil can then be transported to a large processing facility where it can be either upgraded or gasified at a more economic scale.

The instability of bio-oil is an issue when producing bio-oil at a commercial level. Bio-oil can polymerize over time, changing from a liquid to a solid state. Often, bio-oil collected into one fraction separates into two distinct fractions (Asadullah, et al., 2007). The bio-oil stability issues can be minimized by keeping the bio-oil at low temperatures. A possible catalyst for the polymerization of the bio-oil is predicted to come from inorganic minerals or the presence of water and acidic compounds in the bio-oil (Oasmaa, et al., 2005 b).

2.2.3 Pyrolysis kinetics

Kinetic studies of fast pyrolysis are used to understand the basic methods of how biomass degrades into the various compounds found in biochar, bio-oil, and producer gas. The kinetic studies of biomass conversion in fast pyrolysis use a variety of methods.

Thermogravimetric analysis (TGA) is a method used to identify how biomass begins to volatilize in relation to temperature. The data gives insight into what happens overall during fast pyrolysis, but discrepancies between theoretical data and experimental data leave much to be determined (Antal, et al., 1998).

The TGA uses slow heating rates compared to what is used in fast pyrolysis. At high heating rates, the instrument experiences large temperature lag and thus forms large errors in the data (Antal, et al., 1998). Another issue is that sweep gas

velocity and residence time play key roles in the initial, secondary, and tertiary reactions that occur during fast pyrolysis. Overall, the TGA kinetic information cannot be extrapolated to meet the conditions found in fast pyrolysis (Kersten, et al., 2005), (de Jonga, et al., 2003).

A TGA can identify the degree of mass loss that occurs during the heating of biomass. Lignin was found to volatilize slowly and continuously over large temperature ranges. The lignin does not fully volatilize and leaves large mass fractions behind as biochar. Hemicellulose volatilized quickly at 275°C; it showed a more substantial mass loss, but also left biochar residue. Cellulose volatilized in a very fast and complete manner at 355°C. TGA also allows researchers to monitor how gas compounds that are volatilized at specific temperatures (Yang, et al., 2007).

Biochar becomes more porous with increased temperature (Bonelli, et al., 2001), (Della Rocca, et al., 1999). Other kinetic models for fast pyrolysis describe the interactions of reacting compounds both inside and outside the biomass particle (Di Blasi, 2002). The possibility of compounds such as water having a catalytic effect on the formation of pyrolysis vapors has been proposed (Ball, et al., 1999).

The model presented by Ball, et al. (1999) describing cellulose degradation is shown in Figure 2. This illustrates how water vapor can affect the production of products during fast pyrolysis. Water vapor is produced during the decomposition of cellulose but is also available from the original moisture content of the feedstock. In this model, volatiles are the vapor compounds of what is to become liquid bio-oil. The model showed that with sufficient water, reactions take a lower energy route and produce more biochar and gas than volatiles. The high energy reactions creating volatiles occur when enough heat energy is available. The balance between the two pathways becomes even more complicated when dealing with whole biomass.

This model and others like it focus only on the decomposition of cellulose in pyrolysis conditions. Whole biomass, containing far more than cellulose, will degrade with alternate reactions. The reactions become extremely complex and are not currently fully understood. The water vapor in biomass was shown to influence

catalytic effects on the extra-particle processes of volatile decomposition: higher moisture content biomass produced additional biochar and gases (Di Blasi, 2002).

The formation of biochar can be described in several ways. Pure cellulose would theoretically produce no biochar in the absence of water vapor. The other constituents of biomass including hemicellulose, lignin, extractives, and ash further contribute to the biochar production. Cellulose also degrades to produce char when water is available in the reactor (Figure 2). The vapor-solid reactions have been identified as a major factor in biochar formation from both cellulose and whole biomass (Di Blasi, 2008).

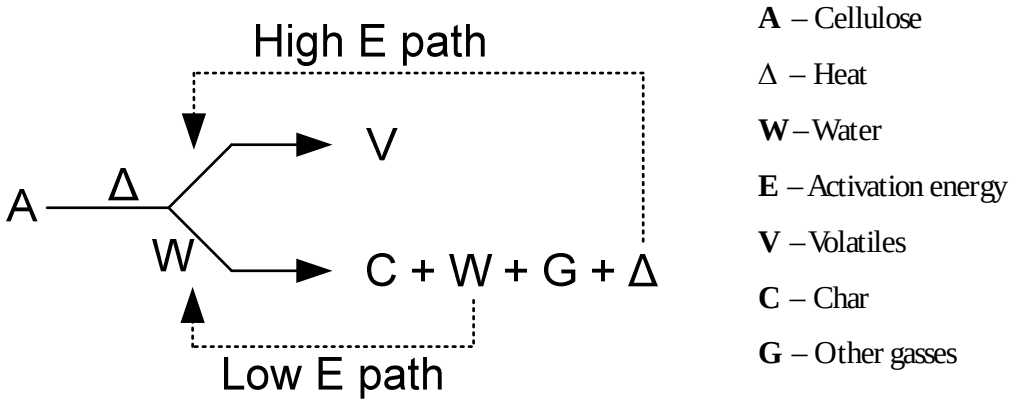

Figure 2: Basic model showing how chemical and thermal feedback effect cellulose decomposition (Ball, et al., 1999).

As heat energy is available in the reactor, volatile matter also reacts to form char and gas. These are referred to as secondary reactions. It is unclear as to whether water vapor or ashes catalyze these reactions, but ash content does play a role in reducing the amount of bio-oil directly from secondary reactions (Agblevor, et al., 1994).

Cellulose decomposition reactions may result in either levoglucosan-rich or hydroxyacetaldehyde-rich volatile products, depending on the ash concentration of the biomass (Scott, et al., 2001). The formation of levoglucosan is more desired to hydroxyacetaldehyde and formation of the latter is catalyzed by cations available in natural occurring inorganic minerals in biomass (Scott, et al., 2001). Removing the minerals from the biomass will cause a decrease in hydroxyacetaldehyde yield and increase levoglucosan yield (Scott, et al., 2001).

2.2.4 Reactor configuration

Many pyrolysis reactors built at different locations of different sizes and with different operating parameters have been used to explore converting biomass into a more useful form. A reactor developed by the University of Waterloo, Ontario, Canada was used for several fast pyrolysis research projects at Aston University, Birmingham, United Kingdom (Figure 3) (Bridgwater, et al., 2001), (Coulson, et al., 2003). It utilized pneumatic biomass feeding at a rate of 100 g/hr. It had a headed cyclone and used heat exchangers and an electrostatic precipitator to collect the bio-oil liquid.

Feeding systems on large pyrolysis reactors are commonly auger-feed systems. Auger feed systems are not used for very small reactors. Small laboratory reactors utilize pneumatic feeding to transport biomass into the heated reactor. The reactor used for this project utilizes a pneumatic feed system. Rather than feeding through the top, as in Aston University's, the reactor for this project feeds into the side of the fluidized bed reactor.

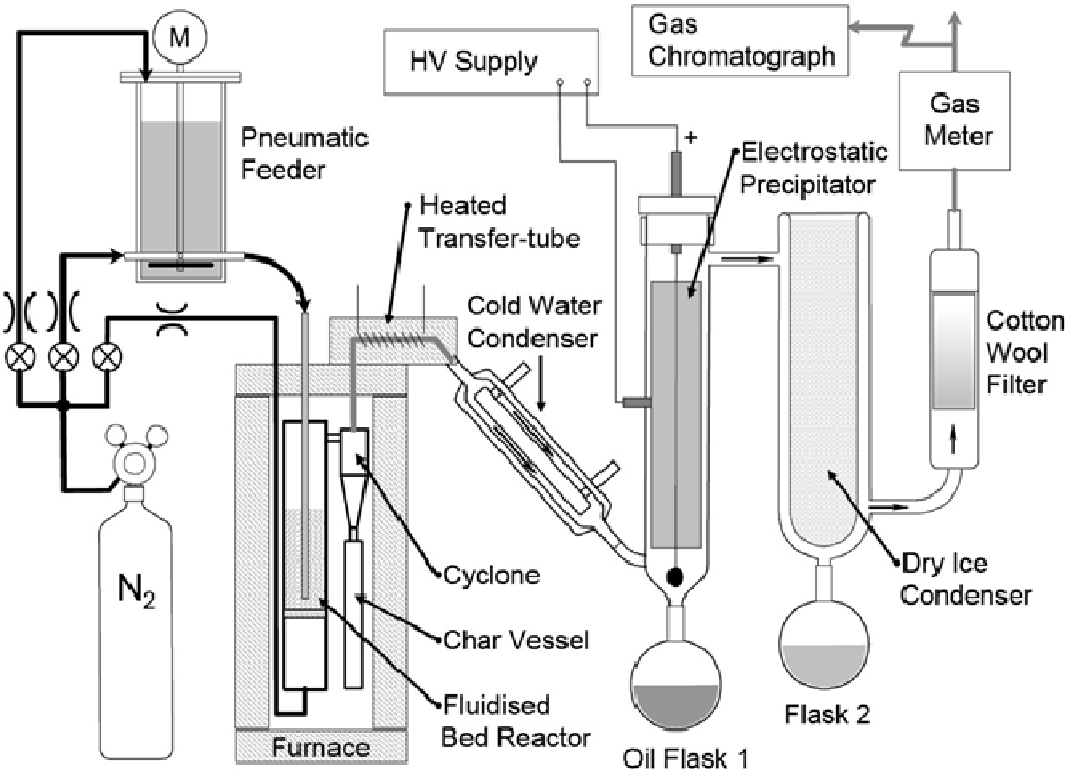

Figure 3 : Fluidized bed fast pyrolyzer with 100 g/hr pneumatic feeding and oil collection used by Aston University (Coulson, et al., 2003).

Fast pyrolysis consists of simultaneously occurring exothermic and endothermic reactions. The energy required to sustain pyrolysis is much less than what is needed to initially preheat the reactor and offset heat losses. Overall, endothermic reactions are more dominant requiring heat energy to achieve a steady state. The enthalpy of pyrolysis on a dry basis for pine is 1.64 MJ/kg (Daugaard, et al., 2003). Due to the high level of control, electric heat is commonly used for lab-scale reactors. Other methods include using combustion heat jackets or a heat carrier.

The moderately high temperatures and corrosive requirements of pyrolysis operation require the reactors to be constructed from stainless steel. The bio-oil product of fast pyrolysis is very acidic and requires 316-stainless steel to prevent any corrosion problems. Some commercial reactors use other steel types depending on the particular operating conditions (Fransham, 2001).

Any inert gas can be used as the fluidizing gas in pyrolysis reactors. Nitrogen was used in this research due to its availability. This is a commonly recognized gas that is used in a majority of pyrolysis experiments.

Fast pyrolysis operating temperatures have been reported in a range of 250°C to 900°C (Wang, et al., 2005), (Suarez, et al., 2006). Ideal operation for maximum measured bio-oil yield is reported to be near 500°C (Gerdes, et al., 2002). The fast pyrolysis operating conditions can determine the overall quality of the pyrolysis bio-oil (Fagbemi, et al., 2001). Heating rates, residence time, pyrolysis temperature, particle geometry, and biomass composition are given as major parameters for proper pyrolysis operation (Fagbemi, et al., 2001).

Several other reactors that perform in a similar manner, but use alternative designs are found in literature. These include a fixed bed reactor (Onay, et al., 2004), an auger reactor (Leonard Ingram, 2008), and a free-fall reactor (Wei, et al., 2006). Each alternative setup greatly reduced inert sweep gas flow in contrast to what a fluidized bed requires.

Dimensions of the feedstock particles are important to the rate that they completely volatilize (Babu, et al., 2004). Particles larger than 10 mm in diameter are considered to be thermally thick. Particles of this size may exhibit alternative pyrolysis reactions pathways (Luo, et al., 2004). Smaller particles are expected to also exhibit the alternate pathways, but are less evident.

Gas cyclones are used to remove particulate matter elutriated from fluidized bed fast pyrolysis reactors. When used with pyrolysis vapors, a solid filter at high temperatures does not operate properly, due to the difficulty of removing the char cake (Scahill, et al., 1997). Cyclones are popular with a fluidized bed reactor because of the high gas flow rates at the exit. Cyclones can be designed to remove a specific diameter particle and limit the pressure drop according to the amount of gas passing through it. This is an effective and efficient way to remove solid particulate from the pyrolysis gas stream, but inefficiencies allow for incomplete collection of all particulate.

Bio-oil collection can be achieved using several different methods. Maintaining a short residence time is critical to stopping the occurrence of secondary and tertiary reactions degrading liquid products into char and gas. This

is why a simple quenching method is common for many pyrolysis systems (Qiang, et al., 2009). A major issue with quenching is that the bio-oil product separates into separate phases (Scholze, et al., 2001). The bio-oil also has moderately high moisture content and contains organic acids that, over time, lead to undesirable degradation (Oasmaa, et al., 2001). An alternative technology uses staged cooling to reduce the gas temperature over a series of condensers. This method is able to separate different compounds (Boateng, et al., 2007).

Electrostatic precipitation (ESP) is the use of a high voltage differential to remove aerosols and particulates from a gas stream. This technology was originally used in coal combustion gas cleanup to remove ash and solids from the exhaust fumes. Fast pyrolysis bio-oil collectors often use an ESP to remove the aerosols from the pyrolysis gas stream (Coulson, et al., 2003).

The staged condensation method was used for this study. Theoretically, bio-oil should not begin to condense until its temperature is less than 400°C (Agblevor, et al., 1995). Effective removal of vapors requires cooling the gas to below a dew point and condensing the liquid out of the gas stream (Bridgwater, et al., 1999 b).

Carbon monoxide and carbon dioxide are the major non-condensable gas compounds exiting the reactor. A small amount of gaseous hydrocarbons, as well as pure hydrogen gas are also produced. When using an inert fluidizing gas, the concentration of the non-condensable gases becomes diluted.

2.3 Pretreatments

Commercialization and optimization of thermochemical energy production is relatively new technology and has not matured in industry. Little research has been done on how the effects of grinding and drying impact pyrolysis products. The obvious results are the size constraints with transporting and heating non-ground biomass and the increased water vapor in non-dried biomass feedstock. Altering the size of the particle being pyrolyzed has various results in the literature (Li, et al., 2004). Pretreatments such as water wash and torrefaction are studied because of the compositional impacts that are achieved through use.

2.3.1 Torrefaction

Torrefaction was originally studied as a way to increase the transport economics of using biomass as a fuel. Compared to untreated biomass, torrefied biomass exhibits a higher energy density and has improved grindability (Bergman, et al., 2005 b). Torrefied biomass also exhibits hydrophobic properties while being stored in open air (Zanzi, et al., 2008).

The operation temperature and residence times are the major control parameters for torrefaction. Temperatures are normally above 200ºC and held long enough for the biomass to fully reach this temperature. Torrefaction removes all the water from biomass. This improves the heating value, thereby increasing the energy density of the biomass. Chemical reactions also begin to occur during torrefaction. Hemicellulose begins to react first and quickly at temperatures above 225ºC (Prins, et al., 2006). At longer residence times, lignin reacts as well. This is undesirable because lignin makes up of a major energy portion of biomass.

The chemicals that are formed during torrefaction are lightweight acidic compounds often found in bio-oil and non-condensable gas from fast pyrolysis. Higher temperatures cause increased mass loss in the biomass, yielding more gaseous product (Prins, et al., 2006 b). Above 300ºC, tar cracking begins to occur, causing substantial secondary char to form on the biomass. At higher temperatures, the carbon dioxide to carbon monoxide molar ratio of the produced gas decreases. This leads to the theory that carbon monoxide is a major product of secondary reactions (Prins, et al., 2006 b).

The xylan content of the biomass can indicate the extent of hemicellulose decomposition during torrefaction. Xylan is the most reactive component of hemicellulose. Xylan is more concentrated in deciduous wood than in coniferous wood. This theory was confirmed with results that torrefied coniferous wood exhibited less mass loss when compared to deciduous wood (Prins, et al., 2006 b).

Torrefaction requires a notable amount of energy to first heat the biomass during the process and then cool the biomass afterward to prevent combustion. Torrefaction requires heating biomass without oxygen to 230 – 300°C for 10 – 180 minutes (Zanzi, et al., 2008). Due to the energy and control requirements, few commercial applications exist. Some torrefaction applications in Europe and the

United States are being explored to simplify the process of pelletizing biomass. Pelletized biomass is used for co-firing biomass with coal in power plant facilities (Bergman, et al., 2005).

The gases produced during torrefaction can be used as supplemental fuel to produce the heat required. The gas contains a high percentage of water vapor as well as only low-quality chemicals (Bergman, et al., 2005 b). Since the mass removed during torrefaction is low-quality, the remaining solid is a higher quality fuel for combustion.

One pretreatment option not studied in literature is using torrefied wood as a feedstock for fast pyrolysis. Lightweight compounds, acids, and water are undesired chemicals in bio-oil. Removing the compounds during torrefaction prior to fast pyrolysis should produce a higher quality, more stable bio-oil.

2.3.2 Water wash

Water wash is used as a biomass pretreatment to remove dirt and other minerals from biomass. The minerals on the biomass show up as ash in the biomass during proximate analysis (Raveendran, et al., 1995). The ash content in raw biomass is derived from non-combustible components. The minerals can be present due to the biomass touching soil during harvesting, transport, or storage. Some minerals are critical to the growth of biomass and are contained within the material. The minerals within the biomass are not removed with a water wash (Yang, et al., 2006). Ash reduction can coincide with an increase of bio-oil yield (Luo, et al., 2004), (Coulson, et al., 2003). At a minimum, the water wash is expected to reduce the ash content in the biomass. At best, the overall inorganic mineral content of the biomass should be significantly reduced.

High ash content in biomass is known to affect the biochar and bio-oil formation during fast pyrolysis. The catalytic effects of the ash are maximized when the ash content is above a 1.5% (Agblevor, et al., 1994). The minerals can form extremely small biochar particulates that are difficult to separate with a cyclone. The minerals are suspended in the bio-oil liquid rather than being collected with biochar. Biochar contains up to 90% of the original biomass mineral content

(Raveendran, et al., 1995). Any solids present in bio-oil greatly decrease its capability for use as turbine combustion fuel (Oasmaa, et al., 2005).

2.3.3 Drying

The drying of biomass prior to thermochemical processing is an energy conservation method. Water requires a substantial amount of heat energy to vaporize during thermochemical processing. Reducing the amount of water in the biomass feedstock will, in turn, reduce the amount of energy required to heat the feedstock to the process temperatures required. This becomes essential in fast pyrolysis because the residence time is critical. The moisture content of the biomass affects the overall heating rate and the speed for a particle to devolatilize. This was due to the high specific heat of the water (Minkova, et al., 2001). Water content of biomass is expected to be important due the significant effects water has on pure cellulose in char-forming processes (Ball, et al., 1999).

An additional energy input will be required to dry the biomass if the biomass is not dried within the reactor. A large amount of heat energy for drying is required to reduce the water content and is often very inefficient.

CHAPTER 3: METHODS AND PROCEDURES

The goal of this project was to produce statistical models that use specific parameters to predict the yields and composition of fast pyrolysis products. Full central composite investigations were used for three biomass types. One group underwent a water wash, the other group was torrefied at different temperatures, and the third group was untreated. Torrefaction temperature, moisture content, grind size, and pyrolysis temperature were each studied as well. The methods used to produce and evaluate both biomass and products are explained in this chapter. The results are presented in Chapter 4.

3.1 Design of experiments

Two biomass treatments were studied to determine how they affect the products of fast pyrolysis. Pre-washing biomass was investigated to remove inorganic elements that may impact the quality of the bio-oil and affect the reaction paths during pyrolysis. Torrefaction was explored as a biomass pretreatment to remove the biomass' water and lightweight compounds. Torrefaction started the depolymerization of biomass prior to fast pyrolysis. Each of these pretreatments was investigated beside a control group that had no major pretreatment.

The experimental design consisted of three separate central composite experimental designs of twenty experiments each. The three major groups were the untreated control group, the water washed group, and the torrefied group. The control and water wash group each consisted of three target levels of moisture content, three grind sizes, and five pyrolysis temperatures. The torrefied group differed in that it used three torrefaction temperatures in place of the various moisture contents.

A variable distribution is shown in Table 4 and the experimental design for washed and unwashed biomass is shown in Table 5. The torrefied central composite is similar in style only with torrefaction temperature replacing the moisture content variable. The grind size for the tests increased from 0.25 to 0.75 mm. The moisture content is shown to shift from 5% to 15%. For torrefied biomass,

the moisture content was changed to reflect the varied torrefaction temperature from 180°C to 250°C. A full copy of the design and analysis of experiments and the central composite experimental designs can be found in **Appendix A**. The goal of torrefaction was to reduce the water and hemicellulose in biomass, and the goal of the water wash was used to reduce the mineral contaminants in the biomass. Each experimental design was studied separately to determine how each impacted the derived model equation compared to the control group.

Table 4: Design of experiments variable grid.

	Variable location				
	-1.68	-1	0	1	1.68
Pyrolysis temperature, °C	426	450	485	520	544
Grind size, mm		0.25	0.5	0.75	
Moisture content, % db		5%	10%	15%	
Torrefaction temperature, °C		180	215	250	

Table 5: Central composite design for washed and unwashed loblolly pine slash.

Run	Moisture content	Grind size	Pyrolysis temperature
1	-1	-1	-1
2	-1	-1	1
3	-1	0	0
4	-1	1	-1
5	-1	1	1
6	0	-1	0
7	0	0	-1.68
8	0	0	0
9	0	0	0
10	0	0	0
11	0	0	0
12	0	0	0
13	0	0	0
14	0	0	1.68
15	0	1	0
16	1	-1	-1
17	1	-1	1
18	1	0	0
19	1	1	-1
20	1	1	1

3.1.1 Control

Loblolly pine slash biomass was chipped and sealed in 55-gallon steel drums. The biomass was delivered from a forest site where loblolly pine was harvested. The biomass samples were collected and shipped by B & W Logging from Brookeland, Texas.

The shipment of biomass was delivered to Iowa State at the Biomass Conversion (BECON) research facility located in Nevada, Iowa. The shipment included two-thirds of the total biomass used. The other third was delivered to ConocoPhillips Company in Ponca City, Oklahoma, to be torrefied.

The delivered biomass was immediately separated into two groups: the control group and the water wash group. The control group was bagged directly after delivery into mesh harvest bags.

The control biomass was split into three groups and dried to the respective stages at the Iowa State University Agronomy Farm, which is detailed later in this chapter. After the biomass was dried, it was ground to a uniform size. The biomass was then analyzed using the standard methods for all biomass. The control group was representative of the as received quality of biomass, without any form of pretreatment.

3.1.2 Washing procedure

Washing of the loblolly pine slash was performed to remove the mineral and inorganic material from biomass by turbulent mixing. Water was used at room temperature in an attempt to minimize any changes in biomass composition that could occur because of temperature.

The resources used for washing biomass required a large capacity of compressed air, deionized water, and fresh water. The equipment used for the test is as follows:

2 - Pneumatic stainless steel 55-gallon drum paint mixers

1 - Pneumatic diaphragm pump

3 - Clean 55-gallon steel drums

Several quick-connect air hoses and water hoses

During this test, the biomass was washed two separate times for forty-five minutes each. The water and biomass from before and after each test was sampled for analysis. Tap water was used for the first wash and deionized (DI) water was used for the second wash in order to conserve DI water and remove the salts in the tap water.

Approximately 20 kg of biomass was loosely filled into an empty 55-gallon drum. The level of the biomass just crested the bottom ring of the drums that were used (Figure 4). The drum was then filled with tap water for the first wash. A

sample of the water was collected while filling up the barrel. The sample number, its wash number, and liquid type were recorded on the sample bottle. The volume of water used was approximately 150 L for each test. The final water level was just above the top ring on the barrel (Figure 5). This level was found to be optimal for keeping the mixing fully turbulent as well as for minimizing the amount of water that ran over the sides and onto the floor.

Figure 4: 20 kg of biomass in a 55-gallon drum.

Figure 5: Drum filled with water.

After the drum was filled with water, a pneumatic mixer (Figure 6) was inserted into the drum (Figure 7). The mixer was turned on and the mixing action was monitored through a viewing hole in the mixer lid.

The mixers were originally manufactured for stirring paint. The blades on the shaft pushed the material upward in the barrel. Since the biomass floated on water, the stirring action needed to push the material down in the barrel. The stirring blades were modified before the wash to achieve the altered flow direction. The tube that was inserted into the mixer lid stopped the fluid from vortexing within the drum. It disrupted the circular flow, causing the fluid to mix violently.

After 45 minutes of washing, the mixer was stopped, and a sample of the post-wash water was then taken for analysis. A water hose was used to siphon the water from the drum. While the water drained, the biomass separated within the drum. One fraction floated and the other sank. The floating biomass was clean, large chips of wood. The bottom portion was comprised of pine needles, saturated bark, and silt (Figure 8).

Figure 6: Modified pneumatic mixers used for water washing.

Figure 7: Drums used for washing. The drum on the left has the mixer inserted.

The floating biomass was removed and transferred into a separate barrel for the second wash. The remaining water was drained out using a perforated plastic sheet. The sheet was pressed into the bottom of the drum and it was tipped on its side to allow the water to drain. The perforations were 6.35 mm holes that only allowed minimal amount of small particulate to be lost. This bottom biomass portion was hand-washed in a 5-gallon bucket of deionized water to remove the silt that had settled with it. If a large amount of sand and dirt was visible in the hand-washed biomass, it was considered too dirty and was discarded.

Figure 8: Sand (left) and saturated biomass (right) collected at the bottom of a drum.

The second wash barrel was filled with deionized water to the same level as the first wash, just above the top ring (Figure 5). A sample of the deionized water was taken and labeled for analysis. After the drum was filled, the mixer was again inserted into it and operated in the same fashion. The second wash, like the first, lasted 45 minutes. After the second wash was complete, another water sample was taken from the dirty water.

The biomass was removed from the barrel by the same method as the first wash, except that the biomass was placed into mesh harvest bags. The biomass from one barrel filled roughly three bags at 7-8 kilograms each. 17-18 kg of the final mass came from the floating top biomass and the bottom biomass contributed 4-5 kg. Each bag of biomass was allowed to drip dry after being tagged and weighed. The biomass drip-dried on wooden pallets (Figure 9). The tag noted the sample number and the respected bag's initial weight in kilograms. Random samples of washed and unwashed biomass were taken and sent to Minnesota Valley Testing Laboratories, Inc. for analysis. At the private laboratory the ultimate, proximate, and mineral analysis of each sample was completed.

Figure 9: Bagged, tagged, and weighed samples post-wash drip drying at wash site.

The minerals removed from the biomass were either dissolved into the washing liquid or entrained in the liquid and removed with phase separation. Each mineral concentration was measured in parts-per-million (ppm) for both the solid and liquid samples. As shown in Equation 1, the original biomass mineral content (B_{m1}) and water mineral content (W_{m1}) will change to a final concentration. The difference between the initial and final mineral concentration equals the minerals removed by the liquid (M_2).

Equation 1: Mineral balance

$$B_{m1} + W_{m1} = B_{m2} + W_{m2} + M_2$$

3.1.3 Drying

The biomass required drying to meet specifications for the experimental design. It was dried in a bulk fashion at the Iowa State University Agronomy Farm on the west side of Ames, Iowa. The facility featured large carts that held nine bags of biomass. The carts had large blower fans that blew warm air through the biomass (Figure 10). The carts were placed in heated rooms that were kept at 110ºC. The rooms were heated by steam heat and continually exhausted humid air.

The washed biomass required the most drying because the washing sequence increased in moisture content in the biomass. Three sets of nine bags of the washed biomass were placed into the drying rooms for certain periods of time: forty-eight, twenty-four, and six hours, respectively, for each desired moisture level of washed biomass. The unwashed biomass needed little drying. The highest moisture content was in the range of 10% water on a dry basis. This made it impossible to test at the desired range of 15% moisture. The tests were changed so that 10% was the high moisture level. The third level required no drying. Two sets of nine bags were dried for twenty-four and six hours. The driest fraction of the group was dried to 5% moisture to represent the lowest level of moisture. The mid-range of biomass that was dried only six hours was very similar to the driest biomass at around 7% moisture.

After the drying was completed, the biomass was taken back to the BECON research facility for grinding. The bags from one cart were ground and mixed together and stored in a sealed container to achieve a common moisture level. Samples that were used for the pyrolysis experiments were randomly sampled out of these sealed containers. Moisture content of the biomass was measured just before it was used for a specific test.

Figure 10: Dryer cart in drying room at Iowa State University Agronomy Farm.

3.1.4 Torrefaction procedure

The torrefaction pretreatment of loblolly pine slash was carried out in Ponca City, Oklahoma by employees of ConocoPhillips Company using a sealed oven. The oven held metal trays that were filled with biomass. The mass of biomass in each tray was measured before and after the process.

The oven was filled with the biomass sample trays, purged with nitrogen, and heated to the proper temperature. A constant purge of nitrogen was used to remove the produced vapors and to prevent any introduction of oxygen into the oven. The biomass was kept at the target temperature for forty-five minutes before being cooled down and removed from the oven. The biomass was torrefied in the same fashion for each temperature level.

Originally, the high level of torrefaction was to be 280ºC. When this was done an average weight loss of the biomass was over 35%. This was deemed unacceptable and was removed as a maximum torrefaction temperature. The high level was reduced to 250ºC, which produces a more acceptable weight loss. The center level was set at 215ºC and the low level at 180ºC.

The mass loss for each sample was recorded to monitor the overall mass loss of the biomass. The original moisture content of the biomass was measured before the analysis and it was determined to be 12% moisture on a dry basis. The total mass loss was calculated by measuring the sample mass before and after each torrefaction trial. The mass lost included the water as well as some organics driven off by the elevated temperatures. A notable color change was seen in the biomass after being torrefied (Figure 11).

The biomass was analyzed for mineral content by ConocoPhillips Company using inductively coupled plasma mass spectrometry. It was sent to Iowa State University in Ames, Iowa to be pyrolyzed. After the biomass was delivered, it was analyzed at Iowa State for inorganic elements. At Iowa State it was ground to a uniform size of 5 mm before being ground again to the specific levels for pyrolysis.

Figure 11: Loblolly pine slash biomass torrefied at 180ºC, 215ºC, and 250ºC (left to right).

3.1.5 Grinding

The biomass arrived at Iowa State in a chipped form directly from the harvest site. The biomass samples were ground to pass an initial screen size of 3.175 mm. The initial grinding was done with a 44.7 kW Arts Way twenty-six inch hammermill grinder (Figure 12). As it was ground, the ground biomass was fed directly into 5-gallon buckets. A special spout was fabricated to the grinder to efficiently feed into the buckets. The biomass was then transferred into sealed plastic 150 L tubs for storage. Biomass of similar moisture content and pretreatment was stored in the same tub in order to reach equilibrium and minimize any difference in moisture content. The containers were sealed until further grinding was needed prior to pyrolysis tests.

For the pyrolysis tests, the biomass was ground to a diameter less than 0.75 mm. From initial shake-down trials with the reactor, 0.25, 0.5, and 0.75 mm were determined to be the best sizes for proper operation. The biomass was ground to these levels using a Retsch SM2000 cutting mill grinder (Figure 13).

Biomass with higher moisture content did not readily grind to the very small diameters required for the experiments. To ease the process, biomass was ground in stages. For example, first a sample was ground to 1.0 mm, then to 0.5 mm before then being ground to 0.25 mm for a test.

Figure 12: Art's Way 26" hammer mill.

Figure 13: Retsch SM2000 cutting mill.

3.2 Fast pyrolysis

A fluidized bed reactor was designed and built to study tar and biochar formation during both fast pyrolysis and gasification run modes. This reactor was designed to operate at 500°C, atmospheric pressure, and with a 100 g/hr biomass feed rate. Due to the reactor's small size, it could quickly process a large number of tests. Up to three tests could be completed in one day. A simple process-flow diagram is shown in Figure 14. A multiple-picture collage is shown in Figure 15 with labels for each major piece of equipment. The design calculations are included in **Appendix B**, and the standard operating procedure is included in **Appendix C**.

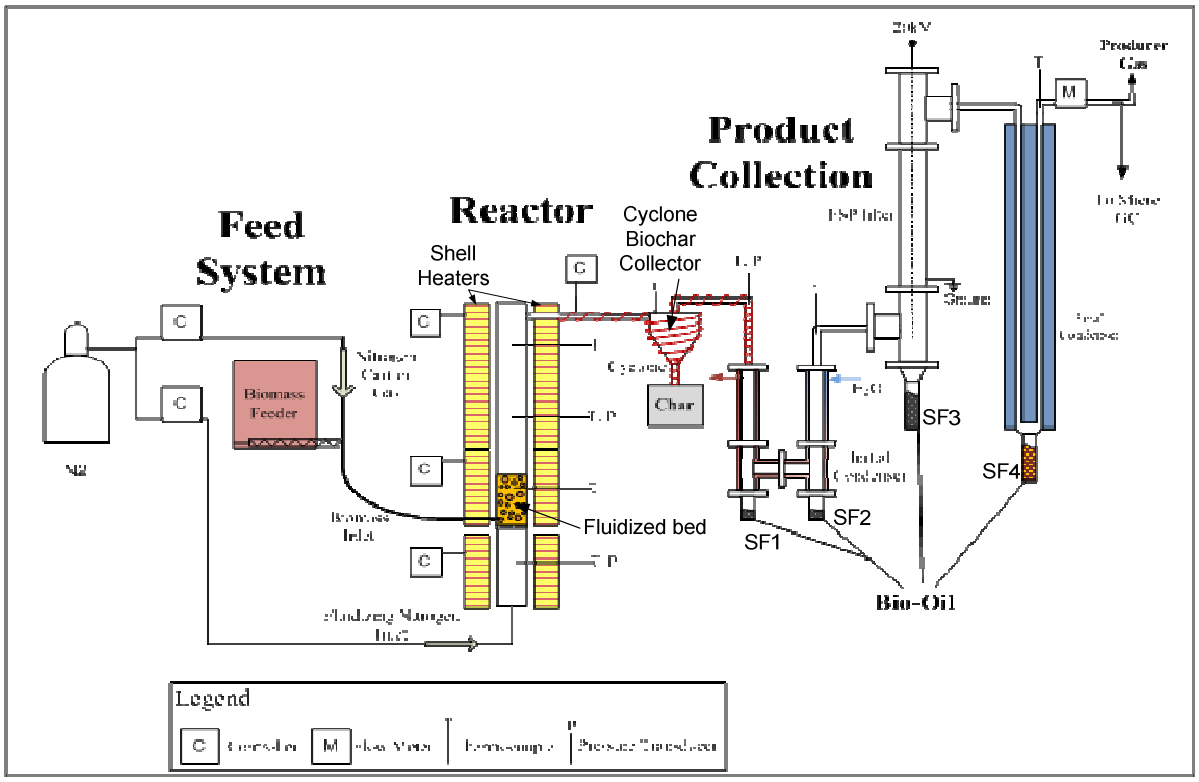

Figure 14: Basic process-flow diagram of fluidized bed pyrolysis reactor and product collection.

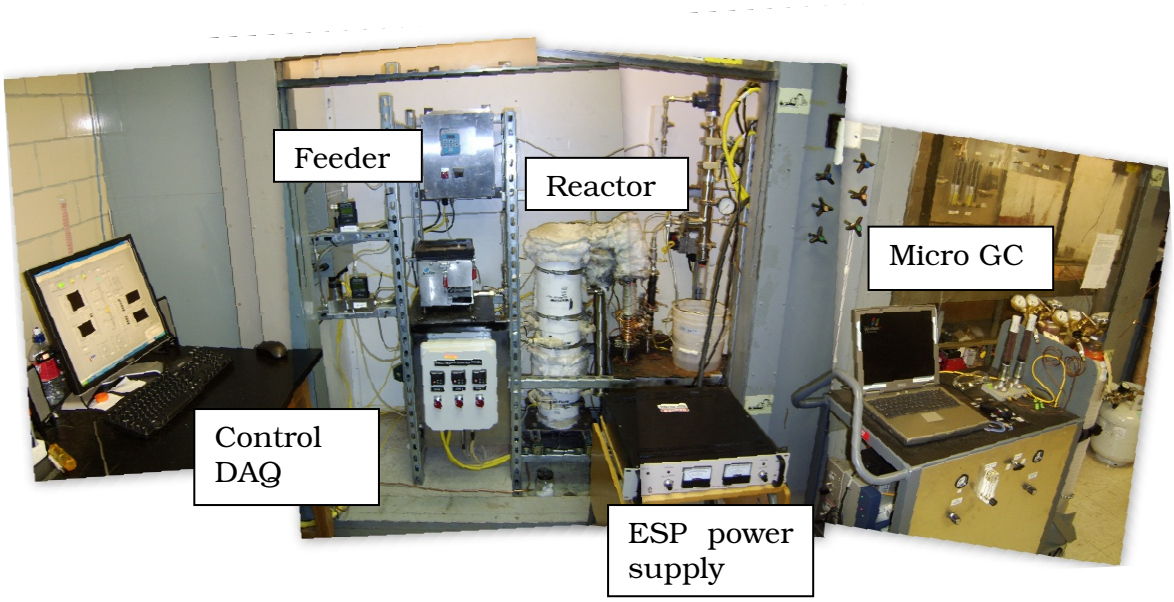

Figure 15: Collage of workspace used for experiments.

3.2.1 Feed system

The feed system used pneumatic feeding to transport biomass into the reactor. This required that the biomass was ground small enough to flow though the 6.35 mm diameter tubing. A nitrogen gas flow of 4 slpm was used to transport the biomass effectively. The biomass feed tube entered the reactor at the bottom of the sand bed. Nitrogen was also used as the inert gas to fluidize the bed. Standard industrial grade nitrogen was used and contaminants were required to be less than 0.05%.

The feeder was required to be under a slight pressure, equal to the pressure at the bottom of the sand bed. To keep the feeder under pressure, a custom lid was made from acrylic and steel. The lid was clamped down over a rubber gasket with four latches that were fastened to the feeder. The custom lid is shown attached to the feeder in Figure 16. The pressure in the feeder was less than 20 kPa.

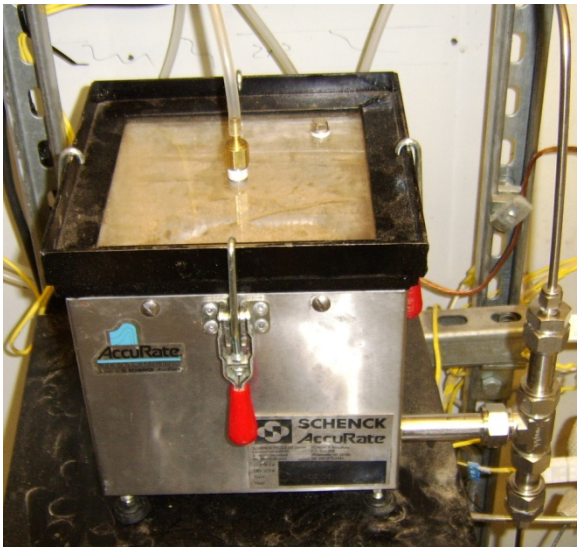

Figure 16: Feeder with sealed lid.

The feeder had a shafted auger that was 19.05 mm in diameter and fed directly into a reduction chamber. In order to achieve the gas velocity needed for biomass transport, the reduction chamber reduced the 19.05 mm diameter to 6.35 mm diameter.

The feeder featured a flexible rubber hopper equipped with a paddle. The paddle flexed the hopper to keep the biomass from bridging over the auger. The paddle tapped the bulk hopper at a rate proportional to the auger speed.

The DC voltage to the feeder motor feeder was controlled by the operator. The controller was set either manually or digitally within the control program. During a test, the feeder speed was controlled by the reactor system control program. When the auger was operating during a test, the voltage being supplied to the feeder was recorded to the data file for reference.

3.2.2 Reactor

The main reactor consisted of several custom parts. The main tube was a standard 316-stainless steel tube, 0.46 m long, and 38.1 mm in diameter. Standard bolt-flange connections were welded on each end. Three thermocouple ports were welded evenly up one side of the main reactor tube. A 6.35 mm female half-coupling was welded to the bottom of the reactor to allow for the feed tube. A

12.7 mm half-coupling was welded to the top of the reactor to allow the exit of pyrolysis vapors. The sand bed was in the bottom of the main tube. It consisted of 200 g of standard-fill sand. The sand was sieved to a range of 0.6 – 1.8 mm before use. The stagnant height of the sand bed was approximately 63 mm. The remaining height above the sand bed was the freeboard of the reactor. The freeboard was sized to allow for approximately 0.5 seconds of residence time between the top of the bed to the cyclone entrance. The top of the reactor was capped with a standard bolt-flange cap. Design calculations and drawings for the system are described in **Appendix B**.

A plenum was fixed underneath the main tube. It was made of standard 316-stainless steel tube, 152.4 mm long, and 38.1 mm in diameter. One thermocouple port was welded into the center of the plenum. The plenum was half-filled with steel beads, 6.35 mm in diameter, to disperse the entering nitrogen gas and act as a heat sink from the reactor wall to preheat the nitrogen to 500ºC. The average nitrogen flow into the plenum was 15 slpm.

A distributor plate was fixed between the plenum and the main tube. The distributor plate was a flat disk with several holes drilled evenly across it. It forced the nitrogen to enter the bed from the plenum with a uniform velocity profile. This aided in properly fluidizing the bed. It also suspended the sand bed in the reactor. A metal screen was added just above the distributor plate to keep sand from seeping through the holes when the reactor was not in operation.

3.2.3 Product collection

The biomass fed into the fluidized bed decomposed into biochar, liquid aerosols, and gas. These components exited out of the top of the reactor directly into a cyclone. A cyclone filtered out the biochar that was elutriated from the bed. The cyclone was designed according to the expected gas flow rate and biochar loading during a test. The cyclone was designed to filter 99% of particulate above 5 μm in diameter for a flow rate of 50 liters per minute of nitrogen gas at 500°C. The vapors exiting the cyclone entered the bio-oil collection system. The process piping

from the reactor to the bio-oil collection inlet was kept above 400°C to avoid any premature condensation of bio-oil.

The bio-oil collection system was composed of two condensers, followed by an ESP and a final, third condenser. Each bio-oil sample was stored separately and labeled standard fraction one through standard fraction four.

The first two condensers were designed to remove heat while the gas flow remained laminar. Bio-oil condensed and collected along the walls and ran to the bottom of each heat exchanger. A series of standard stainless steel sanitary tubing, 25.4 mm in diameter, were set up in an "H" shape (Figure 17). To remove heat, the steel condensers were wrapped with copper tubing. Water was passed through the tubing to remove heat. The first heat exchanger used water at 45°C. The water came from the laboratory hot tap water supply. The condenser wall temperature was kept relatively high to allow for condensed compounds to remain in the liquid phase as they flowed down the condenser wall. The wall temperature of the first condenser was measured at 80°C.

Figure 17: Stainless steel condenser in "H" shape.

The second heat exchanger used the laboratory cold tap water supply at 20°C. The wall temperature of the condenser was 40°C. The vapors were cooled to an exit temperature of 70-80°C, depending on the gas temperature at the condenser inlet. This removed and collected condensable compounds, including some water, which condensed at the low wall temperatures.

The process stream then flowed into an electrostatic precipitator that removed and collected aerosol compounds from the gas stream by electrostatic force. The ESP was not actively heated or cooled, but remained at room temperature. Due to this, some product condensed in the ESP and was collected with the aerosols. The gas exited the ESP at 50°C.

The ESP was a stainless steel tube, 50.8 mm in diameter and 400 mm in length. It required a 400 mm long and 2 mm in diameter electrode to be hung into the center of the ESP tube that was charged to -20 kV. It utilized electrostatic force to collect the aerosols. As the droplets entered the tube they became statically charged from the corona generated from the charged center rod. The charged droplets were attracted to the grounded tube wall surface where they collected and flowed down into a collection port at the bottom of the tube. The aerosols were visible in the gas stream as white-smoke colored gas (Figure 18).

Figure 18: ESP operation. Left: OFF aerosol bio-oil escaping. Right: ON, complete aerosol removal.

The gases are kept in a very laminar flow regime while in the tube. The electrostatic field was energized to create an electrical corona that filled the complete tube volume. The tube length was designed to collect 99.99% of the theoretical aerosol droplets from the gas stream.

After the ESP, a final condenser was used to collect the lightweight compounds still in vapor form. The temperature was reduced as much as possible by passing the gas through a turbulent heat exchanger submerged in an ice-salt bath. The gas temperature was reduced as much as possible without causing freezing. The condensed liquid was collected from a port at the bottom of the heat exchanger. The heat exchanger was a 9.5 mm diameter tube 2.5 m long. The tube

was coiled into the bath to allow liquids to flow to the bottom. This condenser collected any remaining condensable liquids. The gas exited the final condenser at 5-7°C.

The remaining gas was then vented to the exhaust. The exhausted vapors were sampled and analyzed for elemental composition during each test. A vacuum pump pulled a sample of the non-condensable gases and delivered it to the gas analysis equipment. The vapors passed through a precautionary glass wool and Drierite® filter to remove any remaining concentrations of water vapor or aerosols before being analyzed. The gas was pumped to the micro gas chromatograph to maintain a pressure head of 14 kPa to the instrument.

3.2.4 Data collection and control methods

It was important to accurately collect information to obtain mass balances through the system. The pyrolysis system was monitored and controlled using National Instruments' CompaqDAQ™ along with LabView™ software. The program could run continuously and only recorded data to an Excel file when selected to do so.

Operational parameters and recorded data were saved from each run in an overall run data file. The recorded information and control points are shown in Table 6. All manual control points were noted. The heater controllers for the ceramic heaters were controlled separately from the computer program, but the temperatures of each were recorded during the tests. When a test was recording, a data sample was taken every thousandth of a second. One thousand samples were then averaged into one data point that was recorded for each second.

After each test, the products were collected and weighed to determine the quantity that was produced. Additionally, the amount of unfed biomass was measured to determine the exact amount of biomass fed in a test. This was needed to perform a mass balance.

The micro gas chromatograph was operated as a stand-alone apparatus. It was operated when necessary. A properly calibrated sequence was used to measure the concentrations of the non-condensable gas.

Table 6: Data acquisition and control locations.

Temperature	**Pressure**
Plenum gas	Across bed top/bottom
Sand bed	Across cyclone inlet/outlet
Freeboard 1	At exhaust vent (manual)
Freeboard 2	**Control**
Cyclone wall	Nitrogen flow to fluidized bed
Gas inlet to condenser 1	Nitrogen flow to feed
Water supply to condenser 1	Feeder on/off
Water exit from condenser 1	Feeder speed
Gas exit from condenser 2/inlet to ESP	Cyclone heat tape
Water supply to condenser 2	Water flow to condensers (manual)
Water exit from condenser 2	ESP voltage (manual)
Gas exit from condenser 3/at exhaust	ceramic heaters (manual)

3.2.4.1 Controls and measurements

The data control interface was used to control the nitrogen flow rates into the system. The heat tape that kept the cyclone at elevated temperatures was controlled in the program. The program used a user-specified temperature to maintain the cyclone wall temperature. The feeder speed was controlled in the program as well.

Several parameters were set manually. This included the set operation temperatures of the ceramic heaters surrounding the reactor plenum, bed, and freeboard sections. The water flow rates to each of the heat exchangers were manually controlled with rotameters. The water used for each came from the laboratory's water supply. The ESP power and voltage level was controlled manually as well.

During a specific test, as described in Table 6, temperature was recorded in twelve separate locations. Pressure was recorded in two locations as a pressure differential. A pressure gauge was used at the vapor exit to manually monitor the reactor pressure. This allowed the operator to quickly diagnose unwanted plugging.

3.2.4.2 Biomass and products

Biomass was stored in either sealed plastic buckets or sealable plastic bags. Biochar was kept in pint-size sealable plastic bags. The mass measurements for the biomass and products were done on a digital scale located in the laboratory. The scale measured accurately to 0.01 g. Bio-oil was kept in 50 ml centrifuge tubes. The bio-oil liquid samples were stored in a cold refrigerator (7ºC) to prevent any aging of the liquids. Each bio-oil sample was kept separate for bio-oil analysis. The bio-oil was stored in a refrigerator from the time it was collected until it was analyzed.

3.2.5 Mass balance

A mass balance was done for every pyrolysis experiment. Each test was treated as a semi-batch system (Figure 19). The test used as much nitrogen as was required to keep the bed fluidized and properly feed the biomass during a test. The two inputs to the system were solid biomass and nitrogen gas. Three major outputs exited the system: solid biochar, liquid oil, and non-condensable producer gas.

The solid biochar was separated with a cyclone. The bio-oil was seperated continuously over four collectors. After each test the bio-oil collectors were manually scraped clean to collect all of the produced bio-oil. The bio-oil left after scraping was determined to be between 0.1% and 1% of the total bio-oil produced in each fraction. The bio-oil collectors were cleaned between tests with alkaline soap and water. The producer gas contained the uncondensed pyrolysis vapors and the nitrogen used for fluidization and feed operation. The exiting gas was sampled every three minutes with a micro gas chromatograph (Micro GC).

For the experiments in this study, the producer gas yield was calculated from an overall average of the micro gas chromatograph information. The concentration of each non-condensable gas produced as well as the nitrogen component was measured by the micro GC. The amount of nitrogen used during a test was known from the mass flow controllers at the inlet. With the nitrogen

supply known, the mass of produced non-condensable gases was back-calculated to give closure to the mass balance.

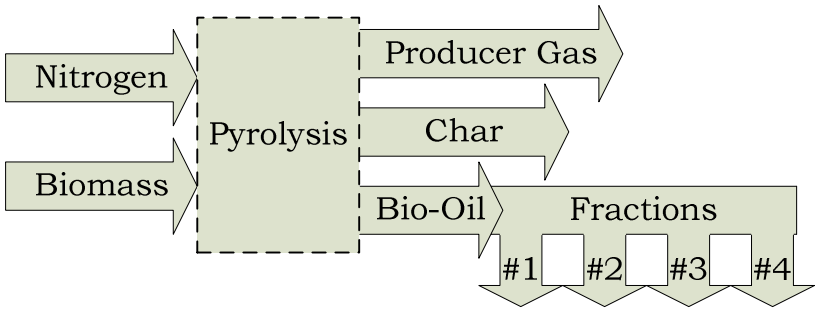

Figure 19: Mass balance inputs and outputs.

3.3 Analysis

3.3.1 Water analysis

Water used to wash the biomass during pretreatments was sampled before and after each wash. The samples were kept sealed in 50 ml centrifuge tubes until they were analyzed. When the samples were taken, some debris was suspended in the water. The suspended solids were allowed to settle to the bottom and were not used in the water analysis. The analysis only tested for dissolved minerals.

The water samples were analyzed at Iowa State University's Environmental Engineering Research Lab. Tests were done for the water soluble fractions as total Kjeldahl nitrogen, total phosphorus, sodium, potassium, magnesium, and iron.

3.3.2 Biomass analysis

Biomass samples were tested several ways. The control and washed biomass were first sent to an independent lab, Minnesota Valley Testing Laboratories (MVTL), for initial analysis. At Iowa State, biomass mineral content was measured using X-Ray fluorescence (XRF). At the Center for Sustainable Environmental Technologies' (CSET) lab at Iowa State, the ultimate analysis of the biomass was

determined. A particle size distribution of the ground biomass was done using standard sieve screens to determine the grinding affects on the final particle size.

3.3.2.1 Ultimate and proximate analysis

Initially, the ultimate and proximate analysis of the original biomass was done at an independent lab to confirm the results of the newly installed CSET equipment. This was done at Minnesota Valley Testing Laboratory.

The ultimate analysis was repeated by CSET technicians at Iowa State. A LECO TrueSpec® CHN was used to determine carbon, hydrogen, and nitrogen concentrations. LECO TrueSpec® S was used to determine the sulfur concentration and ash content. Accuracy of measurements was sufficient for carbon, hydrogen, and nitrogen. Sulfur concentrations were extremely low, below 0.05%, and were not precisely determined with the equipment. The oxygen content was measured by difference after the ash content and other elemental contents are known. The methods described in the operational manuals were used to perform each measurement.

The CHN analysis for the solid biochar followed the ASTM D5373 standard test method for instrumental determination of carbon, hydrogen and nitrogen. It required 0.1 g of sample to be wrapped into a tin-foil cup prior to analysis. The automatic sampler dropped the foil-wrapped sample into a furnace where all components were volatilized and analyzed by the instrument. Carbon and hydrogen were measured by non-dispersive infrared absorption and nitrogen was analyzed by a thermal conductivity sensor.

The sulfur analysis followed the ASTM D4239 standard test method for sulfur in the analysis sample. The sample required a 0.1 g sample placed into a ceramic boat that was manually placed into an oven. The sample was vaporized and the products were analyzed for sulfur content by infrared absorption.

3.3.2.2 Mineral analysis

The untreated biomass, washed biomass, and torrefied biomass were all analyzed using X-Ray fluorescence. The testing was done by the Civil Engineering department at Iowa State University. This test quantified the concentrations of minerals present in the biomass.

The independent lab, MVTL, also conducted a mineral analysis, using a 3050B digestion to determine potassium, phosphorus, and sodium concentrations in the washed and unwashed biomass types. ConocoPhillips performed a mineral analysis of the torrefied biomass using inductively coupled plasma (ICP) spectrometry.

3.3.2.3 Particle size analysis

A particle size distribution analysis was done on each biomass type. Standard U.S.A. testing sieves were used to perform the particle size distribution. Table 7 shows the screens that were used for the particle size distribution of the biomass. A model-B Ro-Tap testing sieve shaker was used to mechanically shake and tap the sieves during a test. Advantech Manufacturing's sieving procedures were used to conduct the analysis (Advantech Manufacturing, 2001).

At the start, all sieves to be used were cleaned and weighed. Depending on the size of screens being used, a pre-weighed sample was added to the top tray of the batch. In the procedures manual a maximum allowable volume is specified for each particular sieve tray. The Ro-Tap was then turned on to shake the trays. Every five minutes the machine was stopped and the top tray was weighed. When the percent mass change in five minutes was below one percent, the trays were all weighed, run for five more minutes, and weighed again. If all trays exhibited less than a five percent change in mass, the test was complete. If a tray was outside the range, sieving was continued until all trays passed the requirement.

Sieve sizes were used in groups of seven. The largest screen for a group was the biomass sample's particular grind size. The smallest screen was either the 38 µm screen for the 0.25 mm grind size or the 63 µm screen for the 0.75 mm grind size.

Table 7: USA Standard Testing Sieves ASTM Specification E 11-04 used for particle size distribution.

Sieve Designation		Nominal Sieve Opening
Standard	Alternative	
µm		in
850	20	0.0331
710	25	0.0278
600	30	0.0234
500	35	0.0197
425	40	0.0165
355	45	0.0139
300	50	0.0117
250	60	0.0098
212	70	0.0083
180	80	0.0070
150	100	0.0059
125	120	0.0049
106	140	0.0041
63	230	0.0025
45	325	0.0017
38	400	0.0015

3.3.3 Biochar analysis

After each test, the biochar was weighed and sealed in a plastic bag before being analyzed at Iowa State. CSET technicians analyzed each sample either three or four times to ensure the precision of the data.

3.3.3.1 Ultimate analysis

The ultimate analysis of the biochar was done in the same manner as the analysis of biomass. Due to very low concentrations of sulfur, only few samples were analyzed to show sulfur concentration was below the equipment precision. The ultimate analysis was performed to provide elemental information on the biochar as well as to determine if water washing or torrefaction had any effect on the biochar composition.

3.3.4 Bio-oil analysis

The bio-oil produced from each experiment was analyzed for moisture content and ultimate composition. Moisture analysis provided the moisture weight percent of the bio-oil. The ultimate analysis gave the proper amounts of carbon, hydrogen, nitrogen, and oxygen present in each sample. A majority of the samples were also analyzed for major compounds using gas-chromatograph mass spectrometry (GC-MS) and for water insoluble content.

Due to the relative similarity of the feedstock many of the bio-oil samples were not significantly different. Therefore, each individual bio-oil sample was not characterized. The biomass feedstock variations studied would not significantly change the properties of the bio-oil. The bio-oil samples were analyzed to find the basic characteristics of the bio-oil. Characterization tests were useful in determining possible end uses of each bio-oil fraction. These tests determined solids content, ash content, higher heating value (HHV), viscosity, and pH. Each sample analysis was done at Iowa State University by CSET lab technicians.

3.3.4.1 Moisture

The moisture analysis was done with a mechanical Karl Fisher moisture titrator. The test method followed the ASTM E203 standard test method for water using Karl Fisher reagent. The instrument used Hydranal Composite 5K as the reagent, and Hydranal Working Medium K as the solvent. Bio-oil samples of 20 – 40 mg in size were tested in triplicate on the instrument and the results were

averaged. This follows ASTM Test Method E 203-96: Standard Test Method to Water Using Volumetric KF Titration (Oasmaa, et al., 2001).

3.3.4.2 Ultimate analysis

The ultimate analysis of each bio-oil sample was done using the same equipment as the biochar and biomass analysis. The preparation procedure for liquid samples changed slightly to accommodate for the liquid properties of the bio-oil. The CHN analysis method used the ASTM D5291 standard test method for instrument determination of carbon, hydrogen, and nitrogen in petroleum products. When bio-oil had a high water content, it was mixed with 0.05 g of COM-AID powder in order to solidify the liquid sample for the test. Selected samples were tested for sulfur to confirm the low levels. The moisture content in bio-oil was needed to account for that elemental make up of the bio-oil on a dry basis. The sulfur analysis was also altered for the liquid analysis to follow the ASTM D1552 standard test method for sulfur in petroleum products.

3.3.4.3 Gas chromatograph – mass spectrometer

A Varian Saturn 2200 gas chromatograph/mass spectrometer was used to measure the concentrations of specific volatile compounds in bio-oil samples. The instrument measured the methanol soluble compounds that fully vaporized at the method temperature. Tests were done on each bio-oil sample separately to attempt to determine the basic composition of each bio-oil fraction. The bio-oil sample was diluted with methanol in a bio-oil to methanol ratio of 1:20. The solution was then filtered before being ran on the GC-MS.

Each compound measurement that was identified by the GC-MS was calibrated by using ideal compounds to determine the proper yield weight percent that was measured for each peak height shown by the instrument.

3.3.4.4 Solids content

Several solvents can dissolve compounds out of bio-oil. Methanol, the most effective solvent for bio-oil from pine wood, was used to dissolve the compounds present in the bio-oil (Oasmaa, et al., 2001). Methanol was added to the liquid sample until all non-solid components were solubalized. The bio-oil-methanol solution was then filtered in a 2.5 μm filter. The filter was dried to determine the solids content. Solids in the bio-oil can be collected due to biochar elutriating past the cyclone filter or secondary char formed from volatiles.

3.3.4.5 Ash content

To determine the ash content in the bio-oil, all volatile and combustible material are removed from the sample through controlled combustion. The ash content is recorded as the remaining mass as a weight percent of the original bio-oil. The standard method used a ceramic cup over a Bunsen burner to burn off all volatile compounds from the bio-oil. The sample was then transferred to a muffle furnace for four hours at 800ºC to completely oxidize any remaining compounds. The remaining residue was the ash content from the bio-oil sample. The largest source of error during ash analysis was from heating the sample too quickly and elutriating ash from the sample with the combustion gases. This was minimized with a larger sample cup and a ceramic cover over the sample

3.3.4.6 Water insolubles

Pyrolytic-lignin is estimated by measuring the amount of bio-oil that is insoluble in water (Scholze, et al., 2001). The measurement procedures for this analysis were developed at Iowa State from historical literature. The analysis is used to determine the heavy fraction of bio-oil that can greatly influence the downstream bio-oil upgrading process and the future bio-oil handling economics.

The extraction was performed using warm water (80°C) to remove all water soluble components from each bio-oil fraction. A two gram bio-oil sample was mixed with 80°C DI water at a 20:1 water to bio-oil ratio into a plastic centrifuge

tube. The centrifuge tube was mixed initially with a vortexer. The sample was then placed in a water bath sonicator for thirty minutes before being mixed on a shaker table for an additional one hour.

After mixing, the centrifuge tube was centrifuged for twenty minutes at 2500 rpm. The liquid in the centrifuge tube was filtered with a 2.5 µm ashless filter paper and a vacuum filtration apparatus. The filter and centrifuge tube were then dried at 50ºC for a minimum of twenty hours. The mass increase of both the filter paper and the centrifuge tube was recorded as the insoluble mass. This mass and the original bio-oil sample mass are used to calculate the percent of water insolubles in the bio-oil sample.

A complete study of the insoluble content in the bio-oil was attempted to correlate the water insoluble content with the fast pyrolysis experimental variables.

3.3.4.7 Higher heating value (HHV)

The higher heating value was determined using a Parr 1341 Oxygen Bomb Calorimeter. The sample was ignited by a metal filament and cotton string. If incomplete burning occurred, a measured amount of mineral spirits was added to the sample to promote complete combustion. Methods for measurement and calculation were used from the instrument's operational manual provided by the manufacturer that followed the ASTM D240 test method for heat of combustion of liquid hydrocarbon fuels. Separate tests were done on several bio-oil samples only to characterize the loblolly pine slash bio-oil relative to other bio-oil characteristics from literature.

3.3.4.8 Viscosity

The viscosity was measured as dynamic viscosity in a Brookfield DV-II+ Pro rotational viscometer. A correlation between kinematic and dynamic viscosity at a specific temperature can be determined by using Equation 2. The methods defined in the operational manual were used for the analysis.

Equation 2: Viscosity correlation. Nomenclature: η = viscosity, ρ= density

$$\eta[cSt] = \frac{\eta[m \cdot Pa \cdot s]}{\rho[kg / dm^3]}$$

Tests were done on bio-oil samples only to characterize the loblolly pine slash bio-oil relative to other bio-oil characteristics from literature. Viscosity of the bio-oil was measured at two separate temperatures, 20°C and 50°C. High viscous bio-oil samples followed the ASTM D5018 standard test method for coal-tar and petroleum pitch, and low viscosity bio-oil analysis followed the ASTM D803 standard test method for testing tall oil.

3.3.4.9 pH

The pH is the measure of free hydrogen ions (H+) in a fluid. The pH of the bio-oil was measured using an electronic pH meter. The pH of bio-oil was expected to be acidic. Therefore, the pH meter was calibrated for low pH values. The pH analysis was done on only samples that could be properly measured with the instrument. The pH was only done on bio-oil samples in order to characterize the bio-oil relative to other bio-oil characteristics from literature.

3.3.5 Non-condensable gas analysis

The non-condensable gas stream exiting the fast pyrolysis reactor was exhausted into the laboratory's exhaust vent. A fraction of the gas was sampled with a vacuum pump and sent to a Varian micro gas chromatograph. The gas sample stream passed through a precautionary filter before sampling. The sample line was kept at a pressure of 15-30 kPa during a test. The vacuum pump was able to supply the pressure required for this. The exhaust from the micro-GC went to the hood vent exhaust. The gas composition was analyzed for each particular test. A sample was taken every three minutes and analyzed in three separate columns.

Sample results were recorded and generated using Varian's installed Galaxy software. The fast pyrolysis reactor used for this study exhibited very low concentrations of non-condensable gas in the nitrogen-rich exit stream. Specific calibration gases were used to calibrate the instrument for the very low concentrations. Resolution accuracy for the gas concentration measurements was compromised due to the slow sampling rates, but values were correct for each sample verified by calibration gases.

The gas analysis was done with a top-down approach by analyzing the overall average of gas concentrations recorded during a test. Concentrations were recorded for nitrogen, hydrogen, methane, propane, carbon monoxide, and carbon dioxide.

The gas concentration information for nitrogen was related back to the recorded mass flow rate into the reactor. The overall mass produced as non-condensable gas was then calculated based on the nitrogen flow rates. This allowed for the mass balance to be calculated.

3.4 Modeling

The goal of the central composite study was to generate models to predict how pyrolysis products were produced according to set parameters. Three separate central composite experimental designs were the focus of this project: control, water wash, and torrefaction. Each of the models contained varied parameters that were studied for correlation: pyrolysis temperature, grind size, moisture content, and torrefaction temperature. The torrefaction model used the torrefaction temperature in place of moisture content. The control is often referenced in this study as unwashed biomass.

The statistical analysis software package JMP® was used to process the data from the experiments in order to derive the model equations. A response surface model equation was used to correlate how each variable affected a particular pyrolysis product (Equation 3). Symbols were used in the equations to denote each pretreatment parameter (Table 8).

A model equation was constructed by first using all possible factors from the central composite design in order to create a baseline response surface equation (Equation 3). In the case when two parameters are multiplied together they were first zeroed to limit the significance of the actual parameter value. The number was zeroed by subtracting the average value from the particular series of tests. This was required in response surface methodology.

Equation 3: Response surface model with all possible parameters for washed or unwashed biomass types.

$$Y(P,G,M) = a_0 + a_1(P) + a_2(G) + a_3(M) + a_4\left(P - P_{\bar{X}}\right)^2 + a_5\left(P - P_{\bar{X}}\right)\left(G - G_{\bar{X}}\right) + a_6\left(G - G_{\bar{X}}\right)^2 + a_7\left(P - P_{\bar{X}}\right)\left(M - M_{\bar{X}}\right) + a_8\left(G - G_{\bar{X}}\right)\left(M - M_{\bar{X}}\right) + a_9\left(M - M_{\bar{X}}\right)^2$$

Key:

P = Pyrolysis temperature, °C

G = Grind size, mm

M = Moisture content, wt. % db

$X_{\bar{X}}$ = Average value from data set

The response surface model equation predicted the experimental results by solving for each coefficient. A t-value and probability were calculated for each coefficient to quantify the significance the value had to the model. Large t-values showed large significance of the parameter on the model accuracy. When a t-value was less than two it was eliminated due to its insignificance to the equation accuracy. When the minimum number of parameters was determined, the equation was used as the reported model. If no parameters showed a t-value of two or higher, the model was deemed “undefined.” An undefined model may have varied between tests, but the variance was not correlated to any of the controlled variables.

The equation was tested to determine overall relevance by using an actual-by-predicted plot. An r-squared value was used to correlate how well the actual data was predicted by the new model. As the r-squared value approached the number one, the model showed better accuracy. R-squared values correlated how

well the data fit a straight line profile. As a general rule, when this correlation is above 0.80, the data is important (Brue, 2006). The model equation, r-squared value, and the t-values of each parameter are presented for each defined model. This analysis and modeling procedure was completed for each of the experimental designs. Statistical information and contour plots of each model equation were used in the analysis.

Table 8: Parameter list for response surface model development.

Model effect parameters	
Unwashed and Washed models	
M	G*G
P	P*M
G	G*M
P*P	M*M
P*G	
Torrefaction Model	
T	P*G
P	G*G
G	T*G
P*P	T*P
T*T	

Key:

T: Torrefied temperature, °C
M: Moisture content, wt. % db
P: Pyrolysis temperature, °C
G: Grind size, mm

To assist in reporting the data from the experiments, the measured values were averaged together and plotted against temperature on bar charts. The averaged data could only study one parameter at a time in relation to the product being studied. Temperature was used due to its known significant impact of fast pyrolysis products, and the fact that was not a pretreatment.

A total of ten tests were averaged together at the center temperature, 485°C. The six replicated tests from the center conditions from the design of experiments

were averaged together with four other points. The four points were at each of the two other variables' high and low points while keeping other variables at the center.

The averaged data points at the temperatures 450°C and 520°C consisted of four tests each. The tests were the combination of the high and low value of the other two parameters studied: grind size and moisture content for washed and unwashed biomass; and grind size and torrefaction temperature for torrefied biomass.

Only one test was done at the high and low temperatures, 544°C and 426°C respectively. These tests used the same center parameters used for the six center replications, with pyrolysis temperature changed. Since only one test was done, no error bars could be calculated. The differences between these two temperature extremes and the center point show how temperature affected the studied product.

These bar charts included in the results gave the data a visual interpretation, but do not show data from identical pretreatments. The statistical models mathematically developed the information and determined which varied parameters were significant in each product model.

CHAPTER 4: RESULTS AND DISCUSSION

The data from this study was presented from both the pretreating and the experimental trials. The analysis of the original biomass and treated biomass were done to determine the effectiveness of each of the treatments. The experimental results include both yield data from each fast pyrolysis test and data generated from the analysis of each product.

4.1 Pretreating

4.1.1 Water wash mineral analysis

The water from before and after each wash sequence was analyzed for dissolved mineral content. The water used for the first test was tap water. The water used for the second test was deionized water.

The water wash successfully dissolved minerals from the biomass during the wash (Figure 20). After each sequence the mineral content in the dirty water coming out was higher than the clean water going in. As expected, the DI water was more pure than tap water. This allowed for the tap water to remove a majority of the minerals during the first wash and the DI water to remove additional minerals during the second wash. The DI water also removed any salts deposited onto the biomass from the tap water. The minerals removed from the biomass were likely from the surface of the biomass. The removed minerals made up the ash content during a biomass analysis.

After the initial testing was completed, calcium analysis became available and two additional single tests were completed to measure calcium content. Two tests were done, one test used a double wash of deionized water, and one used tap water then deionized water (Figure 21).

The data showed that the tap water wash deposited calcium onto the biomass rather than dissolve it away. This was due to the large calcium content in the tap water relative to the biomass. Because the deionized water was free of calcium, the DI water wash removed the calcium from the biomass. The other test showed that after a single wash with deionized water, the calcium removal was the

same as the final wash procedure (using tap then DI water). The second deionized water wash then removed an even larger amount of calcium. Mass transfer limited the mineral removal when tap water was used. Calcium was the only mineral measured to have a larger concentration in the tap water before a wash compared to the water coming out.

The water wash showed promise in removing minerals from biomass. Complete inorganic mineral removal was not achieved found by minerals remaining in the biomass, covered in section **4.2 Biomass analysis**.

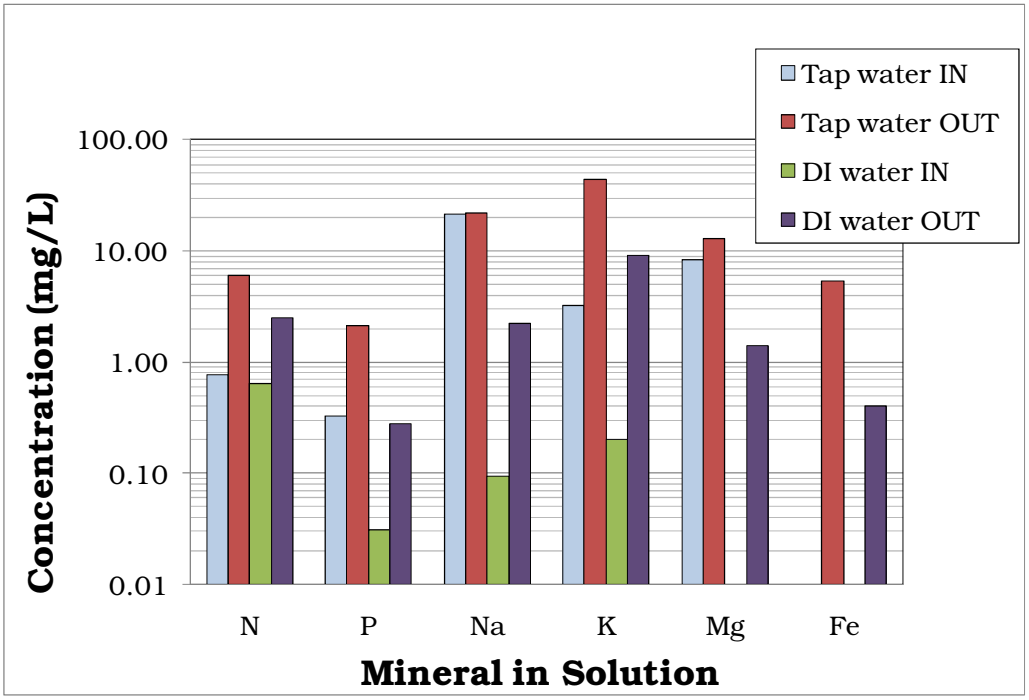

Figure 20: Total disolved minerals in water samples from biomass water washing.

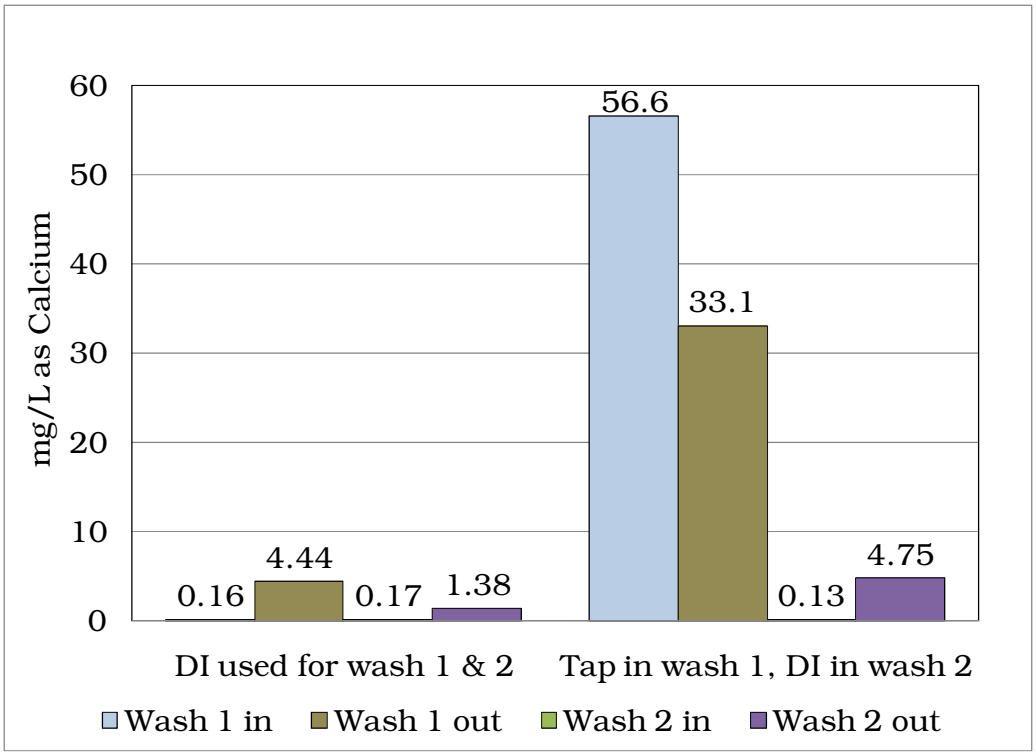

Figure 21: Total dissolved calcium analysis of water from biomass washing.

4.1.2 Torrefaction

Each torrefaction sample had a specific mass loss associated with it. The mass loss percentage determined from each test is plotted against process temperature (Figure 22). The moisture content removed from the original biomass was shown as a fraction of the mass loss. The original moisture content of the biomass was uniform 12% moisture on a dry basis. Since each biomass type had the same original moisture content, this was a baseline for determining the mass loss due to produced volatiles. The amount of volatiles produced from each sample increased with temperature. This may affect the torrefied biomass' pyrolysis product yields since the sample has already lost a substantial amount of mass.

The torrefied biomass exhibited a visual change in comparison with the untreated biomass (Figure 11; section 3.1.4 Torrefaction procedure). For higher torrefaction temperature the biomass was a darker color. This was an expected change from the torrefaction (Bergman, et al., 2005 b). Another expected change

was the ease of grinding the torrefied biomass. The biomass torrefied at 180ºC was similar to untreated biomass in color and in time required to grind. Each higher torrefaction temperature had a noticeably darker color and was progressively faster to grind.

The biomass was properly ground to the levels required by the design of experiments. Some moisture uptake was found in the torrefied biomass. The amount was very small, less than 3%, and was expected from literature examples (Bergman, et al., 2005 b). It was assumed that the mineral content of the biomass had no effect on how the biomass began to volatilize during torrefaction.

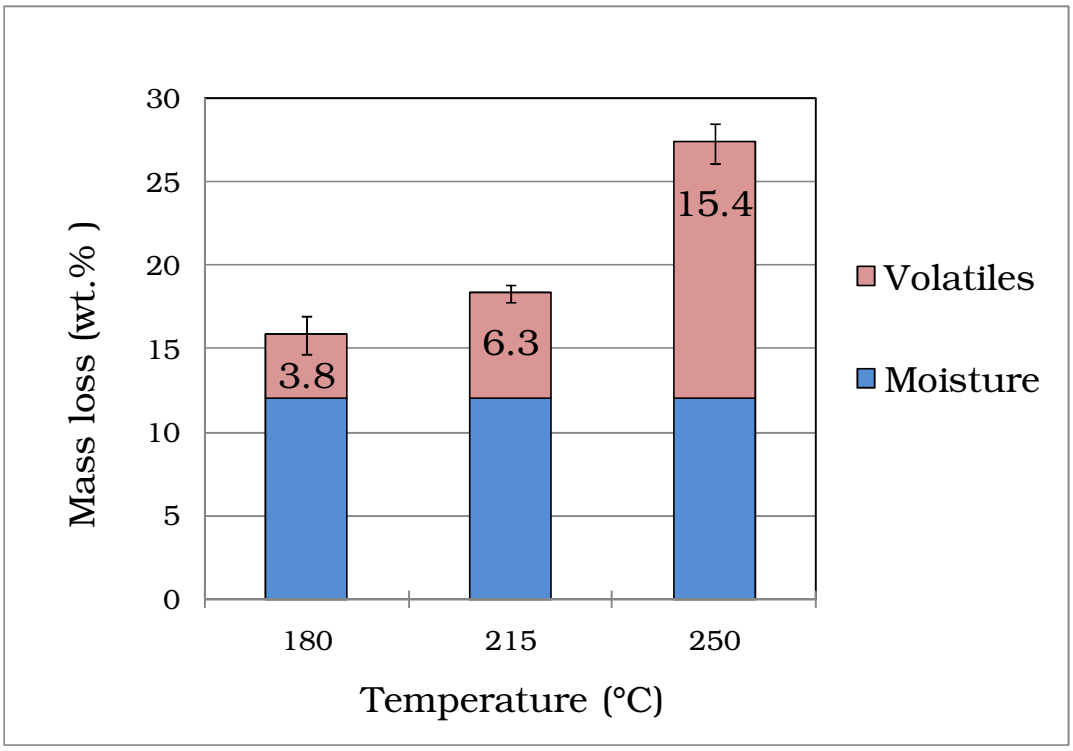

Figure 22: Total mass loss of water and volatiles from the torrefied biomass samples at particular torrefaction temperatures.

The hemicellulose begins to volatilize quickly at 275°C when using thermogravimetric analysis (Yang, et al., 2007). The hemicellulose in biomass begins to significantly break down at temperatures of 225°C (Prins, et al., 2006). The data of torrefaction weight loss showed that the weight loss increased 2.5 wt.% in the 35°C temperature change from 180°C to 215°C: equal to a 0.07 wt.% loss per degree temperature increase. The weight loss increased 9.1 wt. % in the 35°C

temperature change from 215°C to 250°C: equal to a 0.26 wt. % loss per degree temperature increase. At higher temperatures, more reactions occurred causing more mass loss. The mass loss at 250°C may be due to the higher levels of hemicellulose degradation.

4.1.3 Particle size distribution

The ground biomass had a wide particle size distribution. A particle distribution analysis was done to determine how the grinding affected the biomass particle sizes overall. The type and number of sieve trays used for each test were dependent on the particular grind size of the biomass. The mass that remained on each tray after a sieve sequence was recorded and plotted according to the original grind size of the biomass.

The geometry of the biomass was cylindrical in shape due to the inherent fibrous properties of lignocellulose. Only 0.25 mm (Figure 23) and 0.75 mm (Figure 24) grind sizes were tested, and only the differences between un-torrefied and torrefied biomass were investigated.

A significant amount of the biomass was ground smaller than the nominal grind size. The nominal grind size diameter of the biomass was used as the representative particle size in the study. The relative amount of biomass composition in each particle size tray was unknown. Each constituent of pine slash, such as bark, needles, or wood chips, may have ground differently.

Each grind size, regardless of original pretreatment, experienced similar size distribution profiles. The smallest grind size, 0.25 mm, exhibited an almost constant distribution of all particle sizes (Figure 23). The torrefied biomass exhibited easier grinding properties. When compared to other biomass, the torrefied biomass had less mass of large particles and more of small particles measured of the 45-105 μm trays. The relative profiles of the different biomasses were otherwise similar. As the grind size increased, the particle size profile shifted to the right (Figure 24). This was due to the shortened time the biomass was in the grinder before it passed out of the discharge screen. The larger screens allowed for more biomass to exit without being over-ground.

The particle size distribution of biomass ground to 0.75 mm was very similar in all treatment types (Figure 24). The plot shows a large portion of the biomass distributed around the 500 µm tray size with another peak at the lower sizes below 106 µm. The peak at the low sizes is consistent with the smaller grind sizes. Torrefied biomass, like the smaller grind sizes, showed higher quantities at small particle sizes.

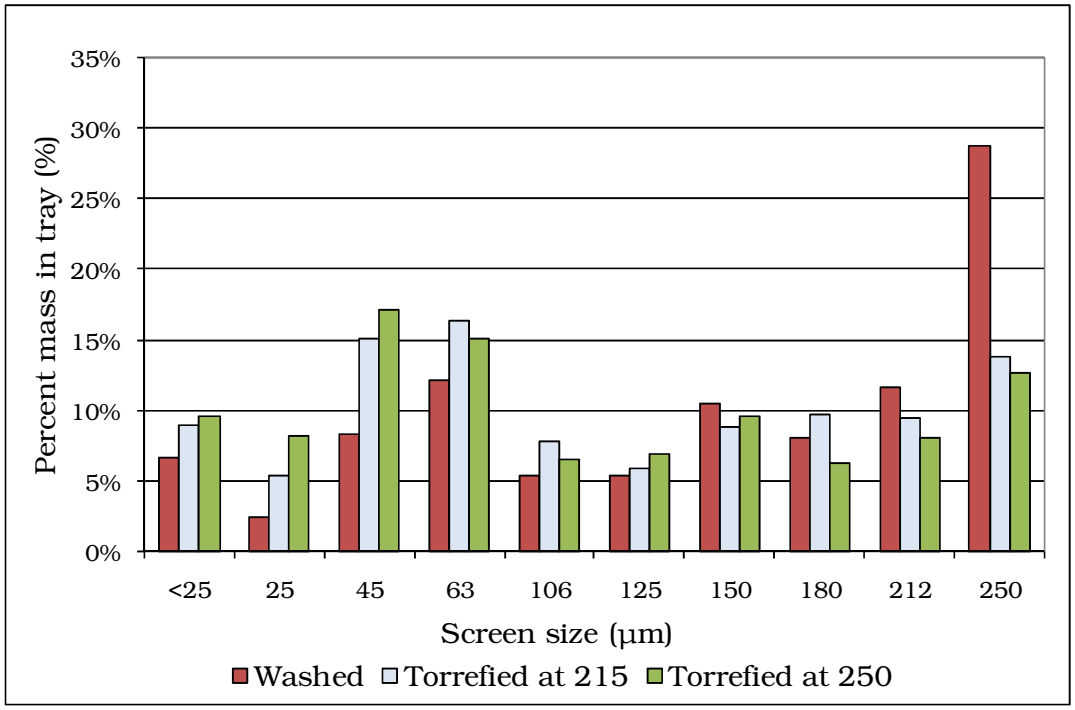

Figure 23: Particle size distribution for different biomass ground to 0.25 mm.

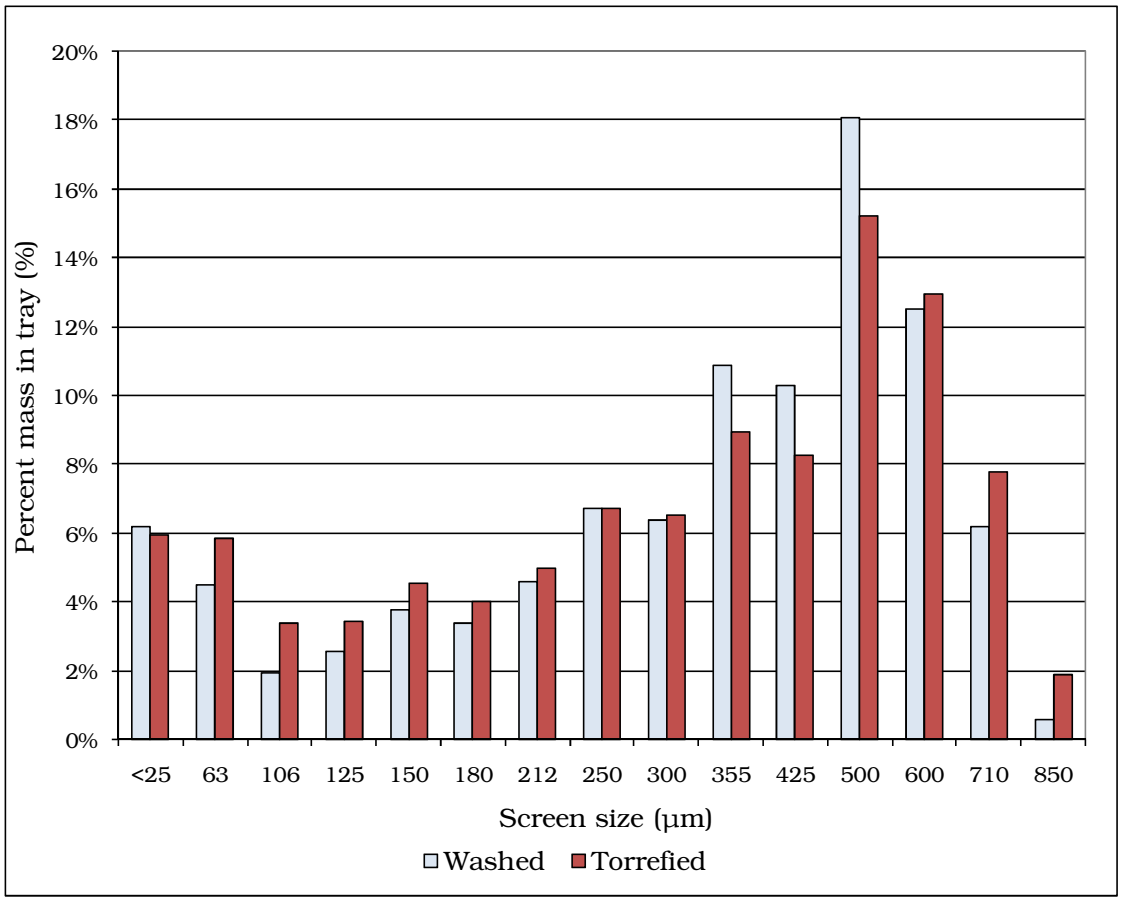

Figure 24: Particle size distribution for biomass ground to 0.75 mm.

4.2 Biomass analysis

Prior to being used for experiments, the untreated and pretreated biomass samples were analyzed for basic composition. The tests included mineral content, proximate analysis, and ultimate analysis.

4.2.1 Mineral analysis

The mineral concentration analysis in the biomass was initially completed by Minnesota Valley Testing Laboratories (MVTL). The measured mineral concentrations of the biomass from before and after a wash sequence are listed in Table 9. The mineral concentration for all but one of the minerals decreased from

the water wash. The observation of increasing sodium concentration in the washed biomass directly contradicts the water analysis results and the X-ray fluorescence analysis discussed below and shown in Table 9. It was concluded the mineral analysis done by MVTL may have not have analyzed a representative sample, and was biased by the complex nature of the slash biomass.

Several other mineral analysis tests were done on the biomass samples and included in Table 9. The wide variance of the information showed that the mineral concentration in biomass was varied and dependant on the specific measurement method.

The reduction in mineral concentration measured in the washed biomass using X-ray fluorescence (XRF) was measured with accurate repeated measurements. The smallest concentration reductions were measured for sulfur and calcium with reductions of 22% and 23% respectively. The largest concentration reductions were for silicon, aluminum, and iron with reductions of 68%, 63%, and 63% respectively. The total amount of minerals removed from the biomass was substantially higher than what was found as dissolved mineral content in the water. This suggests that a majority of the minerals were washed off as suspended solids in the water and not dissolved from the biomass. The solid minerals either settled to the bottom during a wash or were removed with the water after the completion of a wash sequence. The XRF analysis confirmed the wash sequence to be successful at removing minerals form biomass.

ConocoPhillips Company performed a separate mineral content analysis of the torrefied biomass with inductively coupled plasma (ICP) analysis (Table 9). The biomass was also analyzed at Iowa State University using XRF (Table 9). The biomass had a wide array of mineral content in comparison to the biomass delivered to Iowa State used for the wash and control groups. A reason for this could be that the minerals simply fell off after torrefaction during transport or the biomass was of slightly different slash material.

In general, each value from the mineral analysis followed similar trends. The washed biomass had a lower mineral content than untreated types. It was difficult to distinguish the change between individual elements due to the wide variation in the data.

Table 9: Complete mineral anlaysis of each biomass by different methods.

	Torrefied						Unwashed Biomass		Washed	
	Torrefied at 180°C		Torrefied at 215°C		Torrefied at 250°C					
	XRF[1]	ICP[2]	XRF[1]	ICP[2]	XRF[1]	ICP[2]	XRF[1]	305 D[3]	XRF[1]	305 D[3]
Element	ppm	ppm	ppm	ppm	ppm	ppm	ppm	ppm	ppm	ppm
Na	BQL	14.7	BQL	12.2	BQL	30	76	32.8	46	46.7
Mg	450	330	390	262	498	262	460	-	340	-
Al	1610	182	645	145	1195	408	930	-	340	-
Si	12400	-	4000	-	9600	-	6000	-	1950	-
P	345	178	280	97.5	275	57.7	390	58.5	200	20.9
S	275	-	200	-	185	-	270	-	210	-
Cl	160	-	138	-	110	-	220	142	120	54.2
K	1875	869	1610	729	2055	637	1810	1010	790	453
Ca	2745	1340	2545	949	3050	1170	3070	-	2360	-
Fe	1195	840	545	150	1130	422	810	-	300	-

1: X-Ray fluorescene scpectrometry done at Iowa State Univeristy
2: Inductively coupled plasma done at ConocoPhillips
3: 305 Digestion done by Minnesota Valley Testing Laboratories
BQL: Readings are below quantitative limit
Blank spaces are untested

4.2.2 Proximate analysis

The proximate analysis of the washed and unwashed biomass is shown on a dry basis in Figure 25. The proximate analysis shows that much of the ash content of the original unwashed biomass, reported at 2.72%, was removed during the wash, to 0.74%. The weight percent of volatiles slightly increased and the weight percent fixed carbon slightly decreased with the washed biomass in comparison to the unwashed sample. This was due to the reduction of the ash content in the biomass. This observation gave promising expectations for increased bio-oil yield during the fast pyrolysis testing. As the ash content is reduced below one percent, the effect on secondary charring should be reduced (Agblevor, et al., 1994).

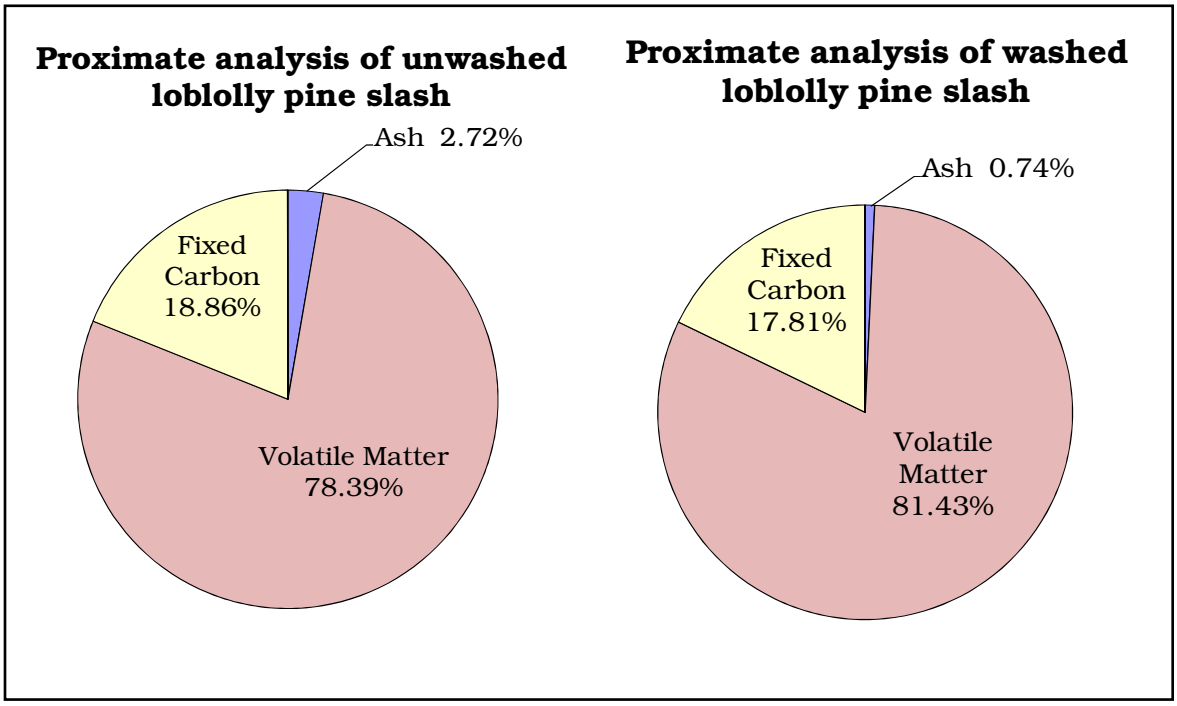

Figure 25: Proximate analysis of dry unwashed and washed loblolly pine.

4.2.3 Ultimate analysis

The ultimate analysis of the unwashed and washed biomass is shown on a dry ash free basis in Figure 26. The ultimate analysis showed little change in values between the unwashed and washed pine samples. The changes are minimal when compared to the ultimate analysis of other biomass types (Table 10). The differences are likely more dependent on the physical composition of the biomass.

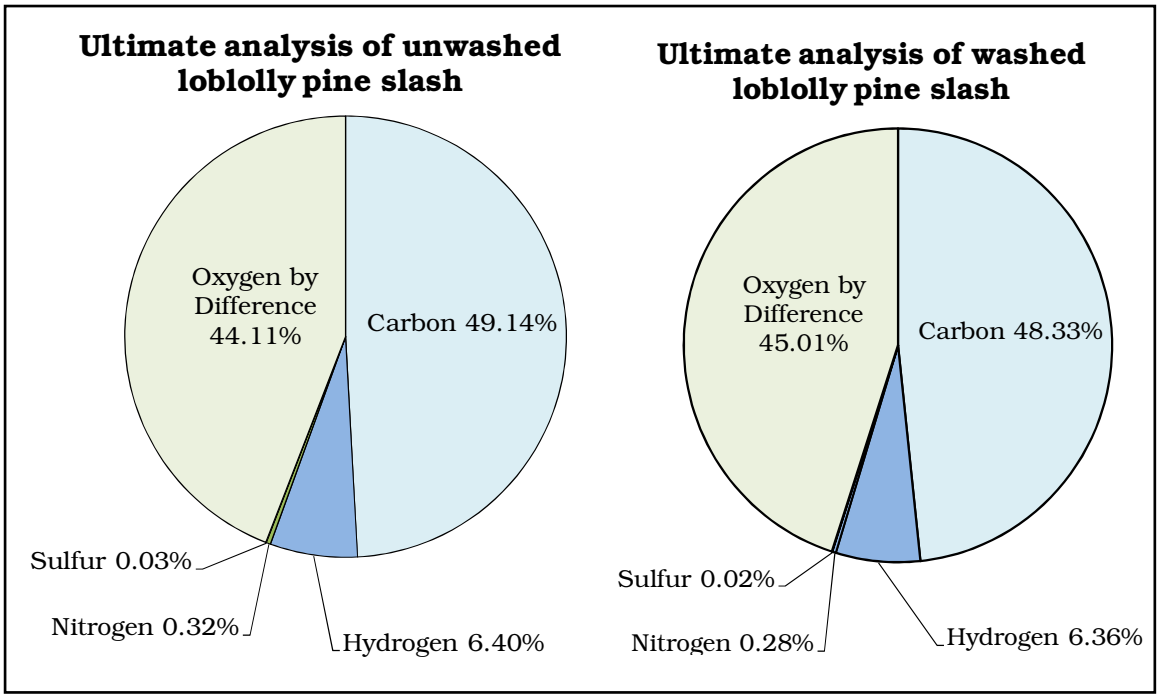

Figure 26: Ultimate analysis of washed and unwashed loblolly pine slash, wt. % dry ash free.

Table 10: Ultimate analysis of several biomass types.

Biomass Type	Carbon (wt. %) Dry Basis	Hydrogen (wt.%) Dry Basis	Nitrogen (wt. %) Dry Basis	Sulfur (wt. %) Dry Basis	Oxygen by difference (wt. %) Dry Basis
Loblolly pine slash/no wash	47.8	6.23	0.31	0.03	42.91
Loblolly pine slash/washed	47.97	6.31	0.28	0.02	44.68
Oat hulls	45.42	6.45	1.35	0.16	45.31
Oak flour	46.27	6.26	0.38	0.01	46.74
Corn stover	36.89	5.27	0.73	0.02	33.4
Wheat straw	43.3	6.05	1.14	0.1	43.87

4.3 Pyrolysis results

Experiments were carried out as specified in the design of experiments using the 100 g/hr fluidized bed fast pyrolysis reactor. Each experiment was carried out for one to two hours in length, processing 100 to 200 grams of biomass. Overall mass balances were recorded for each experiment. Data from each test included the data acquisition records and the micro-GC data.

Each test was conducted separately. The biomass was weighed before and after to determine the exact amount fed during a test. The product collection containers were weighed before and after being filled with bio-oil or biochar. All bio-oil remaining on the walls of the heat exchangers and piping were scraped clean to be precise in the collection of bio-oil. The biochar and bio-oil collected during each successful test were stored in sealed containers and later analyzed. Non-condensable gas concentration data was measured during each test using a micro GC, and the data was backed up and exported in Excel format.

The biomass sample torrefied at 250°C and ground to 0.25 mm pyrolyzed abnormally at low temperatures during four separate tests. The biomass seemed to not pyrolyze because no collectable vapors were produced from it. The reactor did not appear to function properly during any of these tests. Large amounts of biochar passed the cyclone and filled the oil collection system before any bio-oil could be collected. Due to the multiple failures, the point was deemed unmeasureable. The pretreated biomass had already reacted too completely to be pyrolyzed effectively in

the fluidized bed reactor. The small amount of volatiles produced in relation to the biochar produced was too low for the reactor to operate correctly.

4.3.1 Mass balance

The mass balance data was recorded for each test as each test was completed. The data was sorted by the three particular pretreatments being studied: unwashed, washed, and torrefied. The data was also analyzed against each of the variables for the study: pyrolysis temperature, grind size, and moisture content. The data was analyzed using statistical software to relate the data to the central composite study design.

Three products were recorded for each test: biochar, bio-oil, and non-condensable gas. The bio-oil was additionally recorded as fractions: fraction one (SF1), fraction two (SF2), fractions three (SF3), and fraction four (SF4). The overall average yield of each product is shown in Figure 27. All yield data was averaged together and shown as a weight percent of the biomass fed on a wet basis. Biochar yield averaged 17.6 ± 1.5%. The total bio-oil yield for all fractions added together averaged 58.7 ± 1.3%. The gas yield produced during the tests averaged 11.9 ± 0.7%. Overall the mass balance for the experiments averaged 87% with a 4% standard deviation. The maximum closure achieved was 96% and the minimum was 73%. The complete mass and yield records for the products from each test are shown in **Appendix D** under **D.1 Test mass balance data**. Each respective product is described in more depth in the following sections.

The incomplete mass balance closure was attributed to the method used to calculate the mass of non-condensable gas. The gas analysis on the micro GC was done every three minutes. This resolution did not offer the ability to calculate mass produced at a frequency to match the feed dynamics of the biomass feeder.

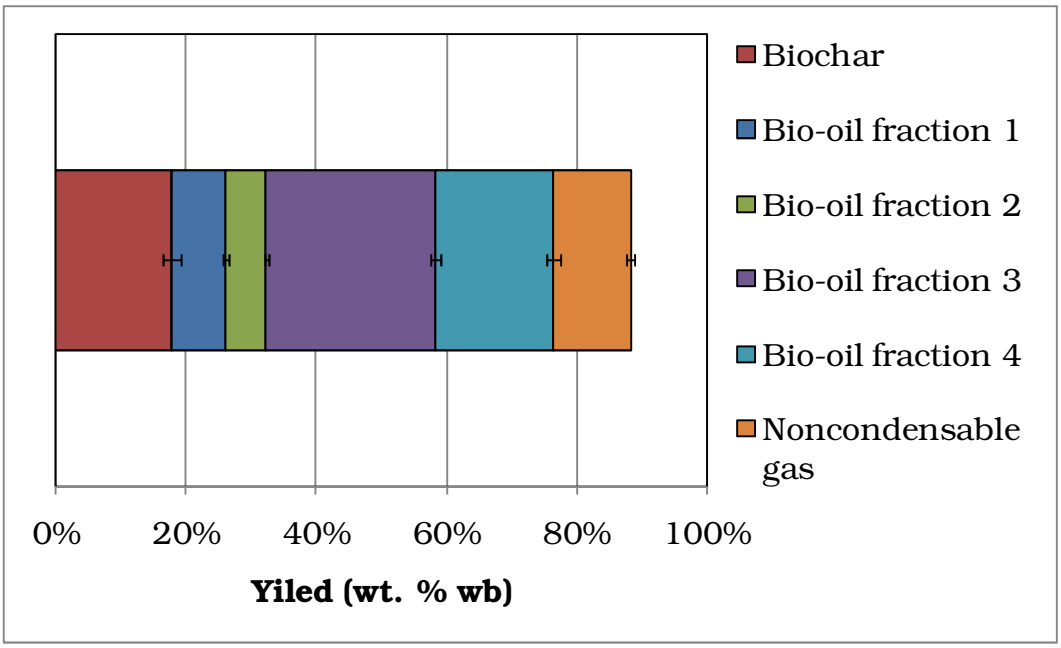

Figure 27: Averaged total yield of each pyrolysis product from all tests as a percent mass of fed biomass on a wet basis.

4.3.2 Biochar

4.3.2.1 Biochar yield

The biochar produced during fast pyrolysis was measured as a mass difference of the biochar collector from before to after a test. One biochar yield sample was collected from each test. It was all the solid material that was separated by the cyclonic filter.

The biochar was elutriated from the fluidized bed after it had completely devolatilized and decreased in density enough to be carried by the gas exiting the reactor. For each biomass type, the biochar yield decreased with increased pyrolysis temperature (Figure 28). This trend was expected from literature (Bridgwater, et al., 2001). Figure 28 shows the average biochar yield as a function of pyrolysis temperature and does not account for other varied parameters. The

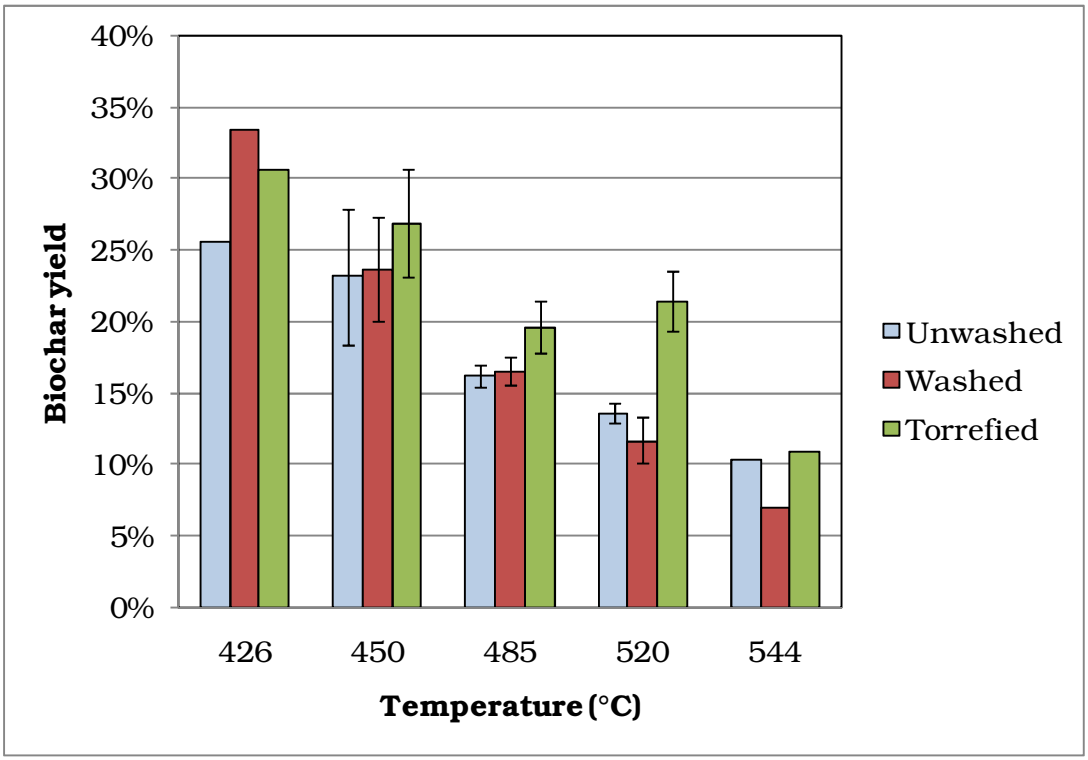

Figure 28: Average biochar yield at each pyrolysis temperature for each major pretreatment type as a percent of biomass fed on a wet basis. Samples at 426°C and 544°C are only performed once with the specified middle grind size and moisture content or torrefaction temperature from the design of experiments. Samples at 450°C and 520°C are averaged from four runs of each high and low value of grind size and moisture content or torrefaction temperature. Samples at 485°C are averaged from the six replicated center conditions and one run at each high and low variable with all other variables at the center.

data points at 485°C are averaged from the six replications of the center value for each studied parameter. The average also includes four other runs by changing one variable and holding all others at the center value. The data points at 450°C and 520°C varied particle sizes, moisture contents, and torrefaction temperatures based on the design of experiments. The variance in these measurements showed

how the other parameters other than temperature were significant in the biochar yield. The data points at 426°C and 544°C were done at the middle parameter for grind size and moisture content or torrefaction temperature. These points show the significant affect that temperature has on the biochar yield in relation to the center point.

The decreasing biochar yield with increasing temperature trend was less evident in torrefied biomass. The substantial physical changes that torrefied biomass underwent during pretreatment may be reason why the biochar yield varied for increasing pyrolysis temperature.

The indistinguishable difference between washed and unwashed biomass showed that the wash pretreatment did not greatly impact the biochar yield. The significance of other parameters seemed to be more significant at lower temperatures shown by the larger error bars at 450˚C compared to the error bars at 520˚C.

The biochar yield was modeled well for two of the three major groups (Figure 29). Torrefied biomass seemed to show a wide variance in biochar collection and could not be modeled as well shown by the lower r-squared value. Increasing pyrolysis temperature, grind size, and moisture content all reduced the biochar yield in unwashed biomass. Temperature is the most significant parameter, shown by high t-values, and controls to what degree compounds are volatilized from the biomass. The larger biomass particles were not elutriated from the bed as quickly due to the particles increased weight. The longer residence time allowed the particles to volatilize more completely which resulted in a reduced biochar yield. Moisture content in the original biomass was not collected in the biochar and therefore caused biochar yield to decrease when moisture content in the biomass was high. The statistical data for the three model equations is available in **Appendix E**.

In the washed and unwashed model equations, pyrolysis temperature and grind size were important parameters. The moisture content of the biomass was significant in only the unwashed biomass model. The t-value of the moisture content was low which showed it was the least important parameter in the model.

The biochar yield from torrefied biomass was a function of the pyrolysis temperature and torrefaction temperature only. The small particle sizes from increased grindability may have caused the biochar yield to be distorted. Since the grind size was not a significant parameter in the torrefied biomass model, the r-squared value was reduced. The torrefaction temperature was a factor because it accounted for the mass loss the torrefied biomass had already experienced. This parameter minimized biochar yield at the center torrefaction temperature. Due to the mass loss from torrefaction it was expected that biochar yield would continually increase for higher torrefaction temperature. The model showed that less biochar was produced as torrefaction temperature increased to 215°C due to the reduction of moisture and light non-biochar forming compounds similar to moisture effects in the other biomass models. As torrefaction temperatures increased above 215°C, biochar was formed in the biomass. This was evident in the significant color changes the biomass exhibited. The fast pyrolysis biochar yield increased from the biochar production during the higher temperature torrefaction pretreatment.

The biochar yields were not significantly different for washed and unwashed biomass which showed that the water wash did not impact the biochar yield. Torrefaction had a biochar yield higher than the other two biomass types; this showed the pretreatment affected the biochar yield. This was because the torrefaction pretreatment removed non-biochar components from the biomass which increased the resulting biochar yield.

Unwashed biomass biochar yield model:

$$Biochar\ yield\ (wt.\%) = 0.877 - 0.0013P - 0.0797G - 0.35M + 0.00197(P - 485)(G - 0.5)$$

R-squared = 0.925

t-value (P) = 11.7

t-value (G) = 4.4

t-value (M) = 2.7

t-value (P*G) = 3.4

Washed biomass biochar yield model:

$$Biochar\ yield\ (wt.\%) = 1.174 - 0.002P - 0.0666G + 1.1 \times 10^{-5}(P - 485)^2 + 0.0022(P - 485)(G - 0.5)$$

R-squared = 0.959

t-value (P) = 18.2

t-value (G) = 4.2

t-value (P*P) = 3.6

t-value (P*G) = 4.2

Torrefied biomass biochar yield model:

$$Biochar\ yield\ (wt.\%) = 0.769 - 0.0012P + 4.35 \times 10^{-5}(T - 215)^2$$

R-squared = 0.752

t-value (P) = 5.8

t-value (T*T) = 4.5

Key:

P – Pyrolysis temperature, °C

G – Grind size, mm

M – Moisture content, % water dry basis

T – Torrefaction temperature, °C

Figure 29: Biochar yield models for each major biomass pretreatment.

4.3.2.2 Biochar ultimate analysis

Each biochar sample from the tests was analyzed for composition of carbon, hydrogen, and nitrogen. Samples were tested for sulfur to confirm the concentrations were below a quantitative limit. The data is available in **Appendix D** under **D.2 Biochar analysis data**.

The hydrogen content in biochar decreased steadily with increasing pyrolysis temperature (Figure 30). The magnitude of this change was almost two percent for the 118˚C temperature difference and was a thirty percent decrease of the total hydrogen in the biochar. The higher pyrolysis temperatures volatilized more hydrogen containing compounds from the biomass. The major pretreatments showed small differences in hydrogen content, but the differences were minimal when compared to temperature effects.

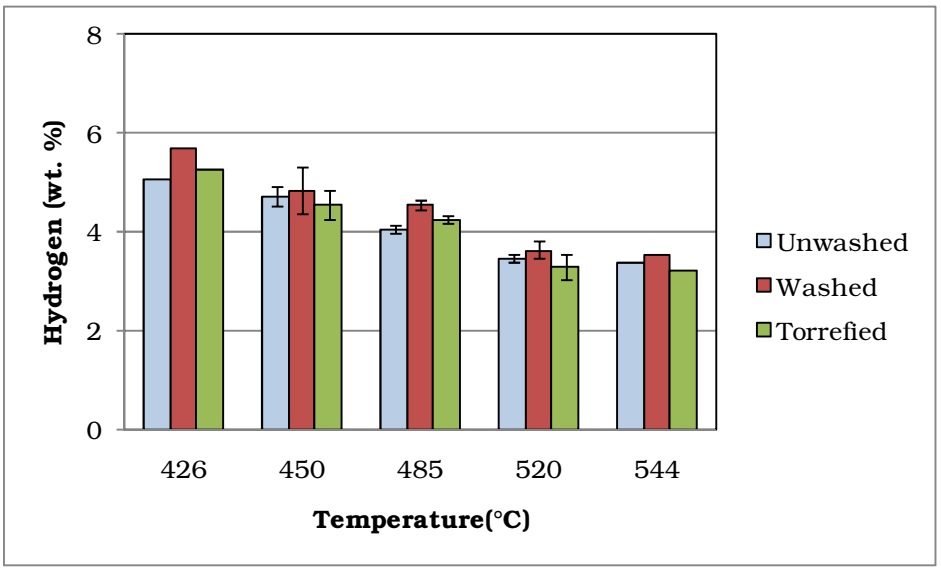

Figure 30: Average hydrogen content in biochar at each pyrolysis temperatures for each pretreatment type as a weight percent of biochar. Samples at 426°C and 544°C are only performed once with the specified middle grind size and moisture content or torrefaction temperature from the design of experiments. Samples at 450°C and 520°C are averaged from four runs of each high and low value of grind size and moisture content or torrefaction temperature. Samples at 485°C are averaged from the six replicated center conditions and one run at each high and low variable with all other variables at the center.

The average carbon content measured in the biochar as a function of temperature is shown in Figure 31. The carbon content steadily increased as the pyrolysis temperature increased. The values increased 5-10% for total carbon weight percent over the temperature range studied. The higher pyrolysis temperatures volatilized less carbon containing compounds and acted to fix carbon in the biochar rather than volatilize it. The similarity in the carbon content averages between major pretreatments showed that the pretreatments did not affect the carbon content in produced biochar. The error bars widened significantly only for washed biomass in the two peripheral averages. The variance in the data points showed that the other varied treatments had some significance on this biomass type only.

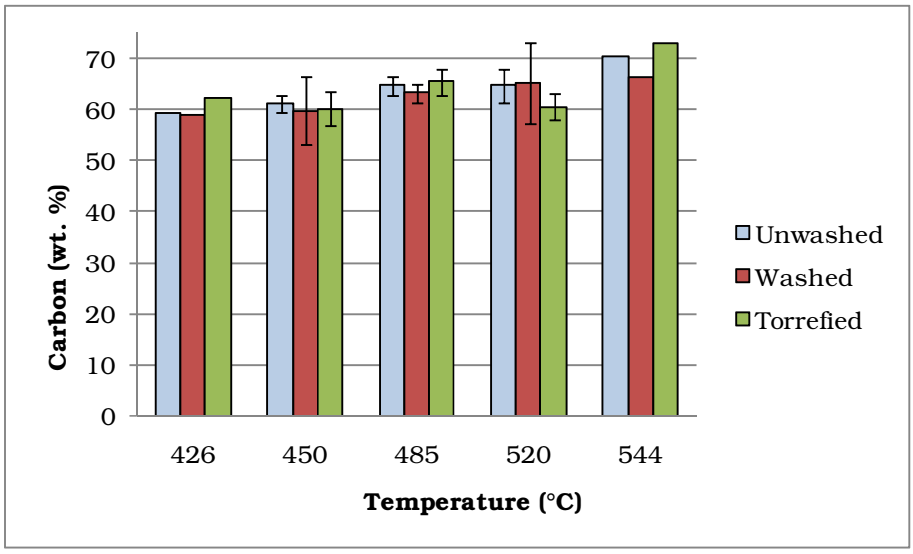

Figure 31: Average carbon content in biochar at each pyrolysis temperature for each pretreatment type as a weight percent of biochar. Samples at 426°C and 544°C are only performed once with the specified middle grind size and moisture content or torrefaction temperature from the design of experiments. Samples at 450°C and 520°C are averaged from four runs of each high and low value of grind size and moisture content or torrefaction temperature. Samples at 485°C are averaged from the six replicated center conditions and one run at each high and low variable with all other variables at the center.

The measured nitrogen content in the biochar was very low (Figure 32). The measured values were each less than one percent of the total biochar composition. No trends were visible due to pyrolysis temperature. Since the biochar yield was shown to decrease with higher pyrolysis temperatures, the nitrogen was volatilized equally with temperature so that the percent weight in the biochar remained the

same. The nitrogen content trended with the major pretreatment. Unwashed biomass had the highest average nitrogen content, and torrefied biomass had the lowest. Although the difference was less than 0.1%, it was repeated at each temperature. The reactions that occurred during torrefaction reduced the nitrogen content in the solid product during the pretreatment.

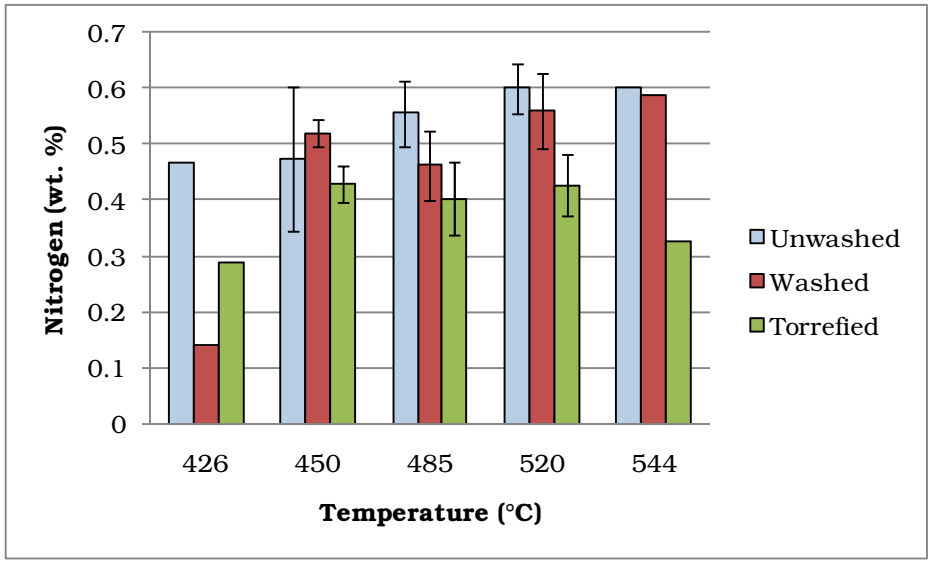

Figure 32: Average nitrogen content in biochar at each pyrolysis temperatures for each pretreatment type as a weight percent of biochar. Samples at 426°C and 544°C are only performed once with the specified middle grind size and moisture content or torrefaction temperature from the design of experiments. Samples at 450°C and 520°C are averaged from four runs of each high and low value of grind size and moisture content or torrefaction temperature. Samples at 485°C are averaged from the six replicated center conditions and one run at each high and low variable with all other variables at the center.

The sulfur concentrations were also very low. The analysis equipment did not register a value on for many of the tests. The resulting sulfur composition in biochar was valued at below 0.01% for all samples.

The oxygen content in the biochar was calculated by difference assuming it was the percent mass remaining after adding together the other measured components (Figure 33). The oxygen content had no significant trends for any of the parameters. The similarity in the averaged data points showed the oxygen content did not vary between major pretreatments.

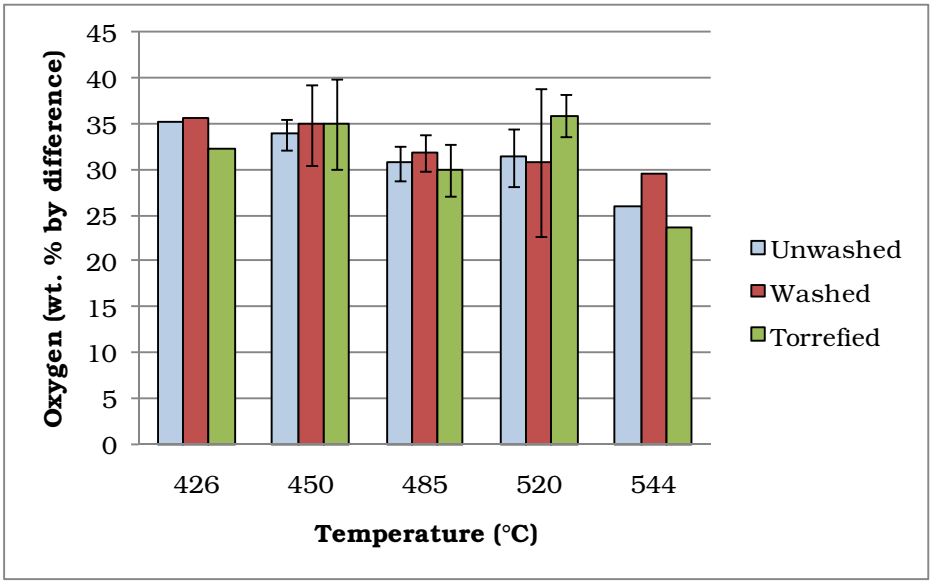

Figure 33: Average oxygen content by difference in biochar at each pyrolysis temperature for each pretreatment type as a weight percent of biochar. Samples at 426°C and 544°C are only performed once with the specified middle grind size and moisture content or torrefaction temperature from the design of experiments. Samples at 450°C and 520°C are averaged from four runs of each high and low value of grind size and moisture content or torrefaction temperature. Samples at 485°C are averaged from the six replicated center conditions and one run at each high and low variable with all other variables at the center.

Statistical response surface models were derived from the elemental analysis of the biochar. The statistical data for the model equations are available in **Appendix E**. A model to determine the hydrogen content in biochar was derived for all the three major biomass groups with relatively high r-squared values (Figure 34). The carbon content models had lower high r-squared values (Figure 35). Therefore the models were not very precise, but showed the carbon content dependence on the varied parameters. Nitrogen and oxygen content were not able to be modeled with any of the experimental parameters. This was due to the limited accuracy of either of the measurements in relation to the variance of the samples or the variance being due to other unmeasured parameters.

Figure 34 contains the three derived models for percent hydrogen in biochar. For the three models, pyrolysis temperature and grind size were the most significant parameters for each. Torrefaction temperature was also significant for the torrefied biomass model. The models showed that the amount of physical

degradation had an effect on biochar hydrogen content. Higher pyrolysis temperatures lowered the biochar hydrogen content due to biochar reacting more completely. This was similar to what was found with biochar yield. Higher temperatures volatilized more hydrogen compounds from the biochar. This agreed with hydrogen content decreasing with increasing temperature discussed earlier and shown in Figure 30.

Increasing the grind size decreased the hydrogen content in biochar for each model. The total effect of grind size was much less in washed biomass when compared to the other two models. Similar to biochar yield, larger particles remain in the reactor longer due to their increases weight and are able to volatilize more completely with the added time.

As the level of torrefaction increased, the hydrogen content in the biochar also increased. The torrefaction temperatures were low enough to drive off carbon compounds from the biomass, like CO_2 and CO, which in turn concentrated hydrogen in the biomass with increasing torrefaction temperature (Bergman, et al., 2005). This also agreed with the fact the torrefaction does not remove much of the total biomass energy carried in the hydrogen (Bergman, et al., 2005 b).

Unwashed biomass biochar hydrogen content model:

$$Biochar\ hydrogen\ (wt.\%) = 12.25 - 0.0165P - 0.355G$$

R-squared = 0.949

t-value (P) = 17.6

t-value (G) = 2.3

Washed biomass biochar hydrogen content model:

$$Biochar\ hydrogen\ (wt.\%) = 14.32 - 0.02P - 3.65(G - 0.5)^2 + 0.018(P - 485)(G - 0.5)$$

R-squared = 0.939

t-value (P) = 15.8

t-value (G*G) = 3.0

t-value (P*G) = 2.6

Torrefied biomass biochar hydrogen content model:

$$Biochar\ hydrogen\ (wt.\%) = 12.39 + 0.0041T - 0.0184P - 0.547G$$

R-squared = 0.901

t-value (T) = 2.2

t-value (P) = 11.9

t-value (G) = 2.2

Key:

P – Pyrolysis temperature, °C

G – Grind size, mm

T – Torrefaction temperature, °C

Figure 34: Hydrogen content in biochar models for each major biomass pretreatment.

In Figure 35, the models of carbon content in biochar are shown. The washed and unwashed models correlated to the actual data better than torrefied biomass shown by their higher r-squared values. The pyrolysis temperature and

grind size were the parameters in the washed and unwashed biomass models and each was relatively significant having similar t-values. The pyrolysis temperature had different affects on the two equations. Increased pyrolysis temperature

Unwashed biomass biochar carbon content model:

$$Biochar\ carbon\ (wt.\%) = 27.3 - 0.0679P + 7.33G$$

R-squared = 0.496

t-value (P) = 3.42

t-value (G) = 2.25

Washed biomass biochar carbon content model:

$$Biochar\ carbon\ (wt.\%) = 24.4.5 + 0.0623P + 16.6G$$

R-squared = 0.593

t-value (P) = 2.17

t-value (G) = 4.5

Torrefied biomass biochar carbon content model:

$$Biochar\ carbon\ (wt.\%) = 65.8 - 0.00378(T - 215)^2$$

R-squared = 0.220

t-value (T*T) = 2.3

Key:

P – Pyrolysis temperature, °C

G – Grind size, mm

T – Torrefaction temperature, °C

Figure 35: Carbon content in biochar models for each major biomass pretreatment.

decreased the carbon in unwashed biomass, and increased it for washed biomass. This was evidence of the wash pretreatment having an effect on the reactions taking place at higher pyrolysis temperatures that fix carbon in the biochar.

Increasing the grind size increased the carbon in both models. This was related to the decreased yield and hydrogen contents the larger particles had

shown. The larger particles remained in the reactor longer to completely devolatilize. Increased devolatilization in the absence of oxygen increased the fixed carbon content in the solid yield.

The models for biochar composition show how the pretreatments affected biochar formation. Pyrolysis temperature and grind size were the most significant parameters. Grind size regulated how biomass was devolatilized by how long it remained in the reactor before being elutriated. Pyrolysis temperature controlled many of the reactions taking place creating or eliminating biochar. Moisture content was not a significant factor in modeling the components of biochar. This verifies the water was completely removed from the biochar during pyrolysis, and that the biomass water content did not have an impact on the biochar composition. Torrefaction had an effect on the hydrogen content of biochar only. This was due to the removal of other compounds in the biomass during torrefaction increasing the hydrogen content in the feedstock.

4.3.3 Bio-oil

4.3.3.1 Bio-oil yield

The bio-oil collected as fraction one (SF1), fraction two (SF2), fraction three (SF3), and fraction four (SF4) were collected and stored separately after each test. Each fraction was weighed to provide a yield of each fraction from a test as a weight percent of the biomass fed. The complete sample masses and yields from each experiment are shown in **Appendix D** under the heading **D.1 Test mass balance data**.

The yield of each bio-oil fraction as a percent of biomass feedstock is illustrated in Figure 36 as a function of pyrolysis temperature for each of the three pretreatments. The first two fractions (SF1 and SF2) had a lower yield compared to the last two fractions (SF3 and SF4). The first two condensers only collected bio-oil compounds that condensed on the heat exchanger walls. The third fraction was collected by the ESP. This showed the aerosols are a large portion of the total bio-oil weight. The third fraction also showed a maximum yield at the center

temperature value in the three biomass types. The fourth bio-oil fraction was composed of the condensable liquids remaining after the ESP. The plot showed that the water and lightweight compounds collected at this final stage makes up the second largest mass of total bio-oil. A notable decrease in the yield was found from the torrefied biomass in SF4. This confirmed the removal of water and volatiles during torrefaction was realized as a bio-oil reduction. The error in other biomass treatments showed the varied parameters had some affect on bio-oil yield, but were minimal.

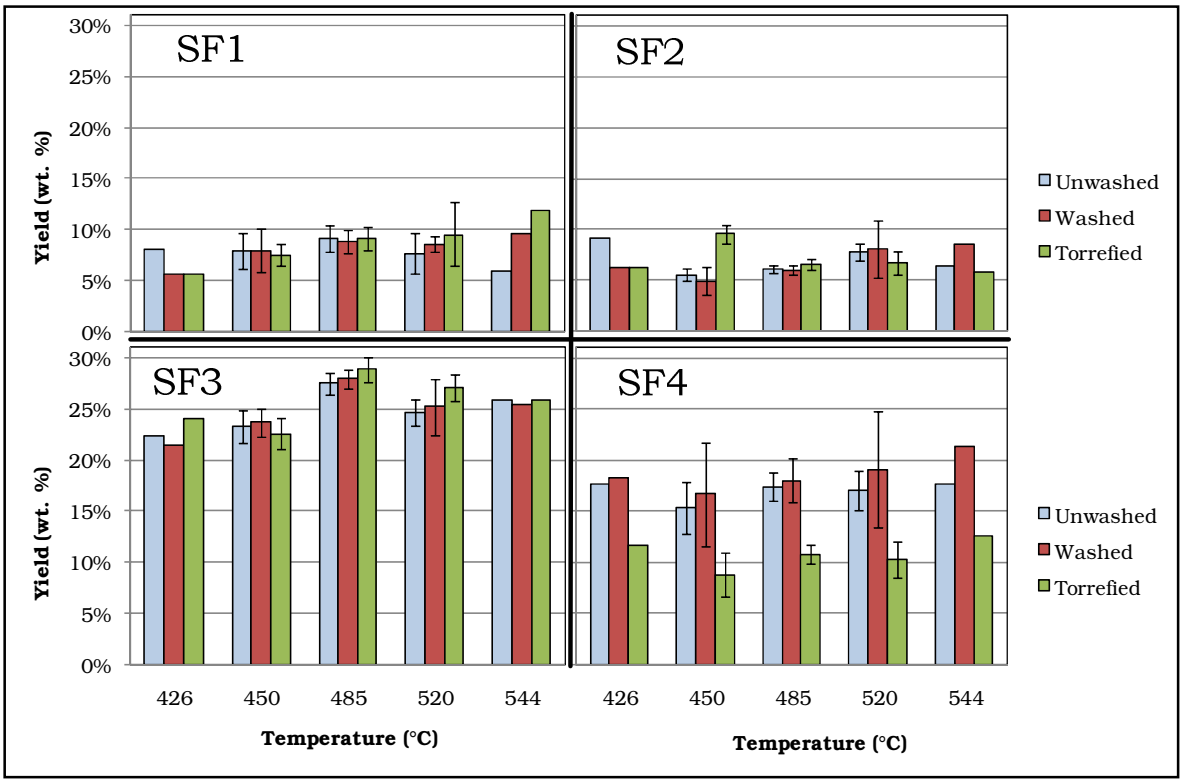

Figure 36: Average bio-oil yield for each pyrolysis temperature for fraction one (SF1), fraction two (SF2), fraction three (SF3), and fraction four (SF4) as a weight percent of biomass fed. Samples at 426°C and 544°C are only performed once with the specified middle grind size and moisture content or torrefaction temperature from the design of experiments. Samples at 450°C and 520°C are averaged from four runs of each high and low value of grind size and moisture content or torrefaction temperature. Samples at 485°C are averaged from the six replicated center conditions and one run at each high and low variable with all other variables at the center.

The total bio-oil yield was calculated by adding the four fraction yields from each test together (Figure 37). The plot shows a bio-oil increase with respect to pyrolysis temperature. The difference in the total bio-oil yield at different pyrolysis

temperatures and biomass pretreatments were not larger than the average value errors for each.

The error in the samples could not confirm any difference in yield due to the water wash pretreatment. Washed and unwashed biomass both had similar yields in each averaged bio-oil yield. The torrefied biomass did show a reduced bio-oil yield when compared to the other types. This is likely due to the fourth bio-oil fraction yield reduction that was evident in torrefied biomass only. The difference although was not beyond the error in the measurements.

The bio-oil products were analyzed for several other properties that describe important qualities of the bio-oil. Bio-oil analyses techniques became available during this study and were used to characterize the bio-oil in order to provide a baseline for modeling how the pyrolysis reactions occurred and for comparisons of the loblolly pine slash bio-oil fractions with previously published data.

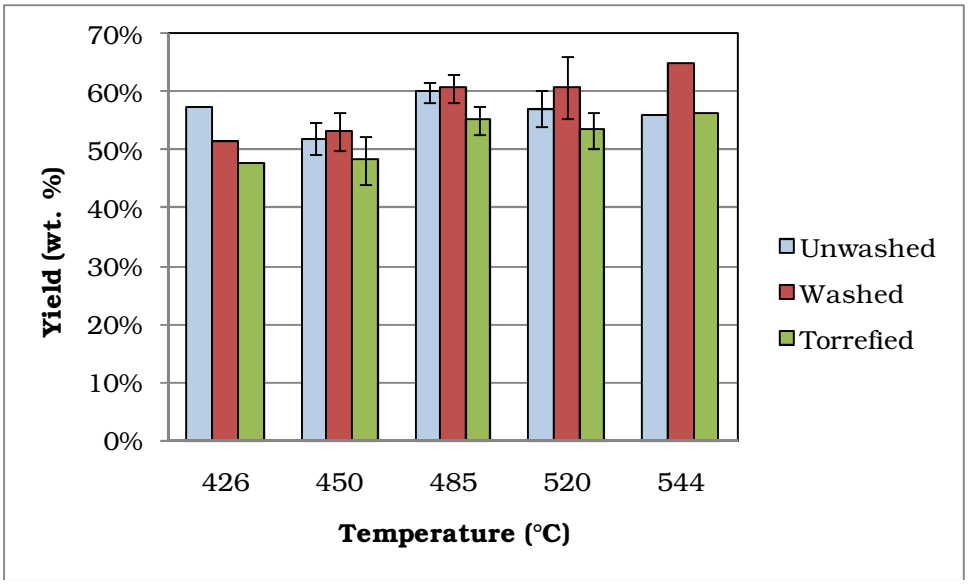

Figure 37: Average total bio-oil yeield at each pyrolysis temperature for each pretreatment type as a weight percent of biomass fed. Samples at 426°C and 544°C are only performed once with the specified middle grind size and moisture content or torrefaction temperature from the design of experiments. Samples at 450°C and 520°C are averaged from four runs of each high and low value of grind size and moisture content or torrefaction temperature. Samples at 485°C are averaged from the six replicated center conditions and one run at each high and low variable with all other variables at the center.

Models were derived for each of the four bio-oil fraction yields. The statistical data for the model equations are available in **Appendix E**. In some cases the recorded parameters could not significantly fit a model and remained undefined. In the SF1 models (Figure 38) washed biomass could not be modeled. Unwashed biomass showed a low r-squared value, but showed a dependence simply on the product of grind size and moisture content. This confirmed the yield of these two types was not solely dependant on the pyrolysis temperature. The model for torrefied biomass had a higher correlation with an r-squared value of 0.827. The model required a large number of significant parameters. The model showed the bio-oil yield to increase with increasing pyrolysis temperature. Increasing torrefaction temperature decreased bio-oil yield. This was expected from the increased volatiles released during higher torrefaction temperatures. Increasing the grind size has a small effect in increasing bio-oil yield at low temperatures and decreasing bio-oil yields at higher temperatures. The first bio-oil fraction was large

compounds with high dew point temperatures. The large compounds were more difficult to be vaporized form larger particles. The compounds had to degrade into smaller compounds to be removed from the particles. At low temperatures less compounds vaporized resulting in lower yield. At low pyrolysis temperatures the speed of compound vaporization was not limited by the small particle size. At high pyrolysis temperatures, the particle size began to limit bio-oil production as more compounds were formed.

Unwashed biomass SF1 bio-oil yield model:

$$Fraction\ one\ bio-oil\ yield\ (wt.\%) = 0.031 + 3.44(G - 0.5)(M - 0.1)$$

R-squared = 0.200

t-value (G*M) = 2.1

Washed biomass SF1 bio-oil yield model: Undefined

Torrefied biomass SF1 bio-oil yield model:

$$Fraction\ one\ bio-oil\ yield\ (wt.\%) = -0.0475 - 0.00055T + 0.000534P + 0.00188(T - 215)(G - 0.5) - 0.277(G - 0.5)^2 - 0.00178(G - 0.5)(P - 485)$$

R-squared = 0.827

t-value (T) = 5.3

t-value (P) = 6.2

t-value (T*G) = 3.9

t-value (G*G) = 3.5

t-value (G*P) = 3.9

Key:

P – Pyrolysis temperature, °C

G – Grind size, mm

M – Moisture content, % water dry basis

T – Torrefaction temperature, °C

Figure 38: Bio-oil fraction one yield models for each major biomass pretreatment.

The bio-oil fraction two yield models could only be determined for washed and torrefied biomass (Figure 39). The unwashed biomass could not correlate the yields with any of the control parameters which showed other unmeasured factors may have influenced the specific fraction yield. The r-squared value for washed biomass was much higher than for torrefied biomass. Torrefied and unwashed biomass had higher ash content when compared to washed biomass. Since the

torrefied model r-squared was low and the unwashed model was undefined the ash content may have a significant impact on the modeling abilities of the second bio-oil fraction yield.

The two models for washed and torrefied biomass were dependant primarily on pyrolysis temperature. Pyrolysis temperature controlled the rate of reactions during fast pyrolysis and was expected to have a significant role on bio-oil forming processes. The biomass moisture content was significant in the washed bio-oil yield model. The moisture content from the biomass was collected into the second fraction of bio-oil. Higher water weight in the biomass would increase the yield of water containing product such as the second bio-oil fraction.

Unwashed biomass SF2 bio-oil yield model: Undefined

Washed biomass SF2 bio-oil yield model:

$$Fraction\ two\ bio-oil\ yield\ (wt.\%) = -0.062 + 0.000255P + 0.00583(P - 485)(M - 0.1)$$

R-squared = 0.646

t-value (P) = 2.9

t-value (P*M) = 4.0

Torrefied biomass SF2 bio-oil yield model:

$$Fraction\ two\ bio-oil\ yield\ (wt.\%) = 0.186 - 0.000252P + 0.241(G - 0.5)^2$$

R-squared = 0.243

t-value (P) = 2.4

t-value (G) = 3.0

Key:

P – Pyrolysis temperature, °C

M – Moisture content, % water dry basis

G – Grind size, mm

Figure 39: Bio-oil fraction two yield models for each major biomass pretreatment.

The third bio-oil fraction yield was modeled for each major pretreatment (Figure 40). In each model the pyrolysis temperature was the most significant variable. In each case specifically, the pyrolysis temperature squared term was used. This term showed the bio-oil yield was maximized at the center temperature as was seen in the yield plots. The third fraction was the bio-oil was collected with the ESP and was the aerosol compounds contained in the gas stream after the first two condensers. The fraction three bio-oil yield models showed the aerosol portions of bio-oil were highly dependent on the pyrolysis temperature and maximized within the temperature range studied.

The correlation of the models were 0.325, 0.707, and 0.469 for unwashed, washed, and torrefied biomass respectively. A similar pattern to fraction two showed ash content may have influenced the prediction ability of the models. The reduced ash in the washed biomass had the best correlated model. The washed biomass model was the only model to include moisture content. Some moisture was collected in the bio-oil fraction and the increased purity of washed biomass allowed moisture to become a significant variable in the model.

The fourth bio-oil fraction yield model equations were derived for the unwashed and washed biomass groups (Figure 41). The bio-oil from torrefied biomass did not correlate to any of the controlled parameters. The decreased yield in the fourth bio-oil fraction due to the torrefaction pretreatment showed the torrefaction temperature alone was not significant enough to correlate the reduced product yields.

Unwashed biomass SF3 bio-oil yield model:

$$Fraction\ three\ bio-oil\ yield\ (wt.\%) = 0.0268 - 1.27 \times 10^{-5}(P - 485)^2$$

R-squared = 0.325

t-value (P*P) = 3.0

Washed biomass SF3 bio-oil yield model:

$$Fraction\ three\ bio-oil\ yield\ (wt.\%) = 0.082 + 0.000432P - 1.76 \times 10^{-5}(P - 485)^2 - 3.79(M - 0.1)^2$$

R-squared = 0.707

t-value (P) = 3.6

t-value (P*P) = 5.3

t-value (M*M) – 3.4

Torrefied biomass SF3 bio-oil yield model:

$$Fraction\ three\ bio-oil\ yield\ (wt.\%) = 0.0789 + 0.000436P - 1.35 \times 10^{-5}(P - 485)^2 - 0.33(G - 0.5)^2$$

R-squared = 0.591

t-value (P) = 2.7

t-value (P*P) = 3.0

t-value (G*G) = 2.2

Key:

P – Pyrolysis temperature, °C

M – Moisture content, wt. % db

G – Grind size, mm

Figure 40: Bio-oil fraction three yield models for each major biomass pretreatment.

The fraction four bio-oil yield models for the washed and unwashed biomass were functions of the biomass grind size and moisture content. The significance of moisture content was expected because the fourth fraction collected the compounds that condensed at lower temperatures including water from the

Unwashed biomass SF4 bio-oil yield model:

$$Fraction\ four\ bio-oil\ yield\ (wt.\%) = 0.093 + 0.036G + 0.624M$$

R-squared = 0.856

t-value (G) = 2.2

t-value (M) = 5.3

Washed biomass SF4 bio-oil yield model:

$$Fraction\ four\ bio-oil\ yield\ (wt.\%) = 0.071 + 0.0634G + 0.574M$$

R-squared = 0.856

t-value (G) = 3.0

t-value (M) = 9.8

Torrefied biomass SF4 bio-oil yield model: Undefined

Key:

G – Grind size, mm

M – Moisture content, % water dry basis

Figure 41: Bio-oil fraction four yield models for each major biomass pretreatment.

biomass. Additional moisture content in the biomass would directly affect the fourth bio-oil fraction yield by increasing the amount of water or water derived compounds collected in it, thus increasing the yield. Increasing grind size also had a significant impact on increasing the fourth fraction bio-oil yield. The larger grind size trapped the larger volatile compounds within the biomass particle. The compounds were further deconstructed before they could escape from the particle as smaller compounds. These smaller compounds are not condensed at high temperatures and are collected in the fourth fraction of bio-oil or as non-condensable gas. The significance of grind size relative to the moisture content was less for both models, shown by lower t-values for the grind size parameter.

The model equations for total bio-oil yield was influenced by the pyrolysis temperature, grind size, and moisture content as shown in Figure 42. The pyrolysis

temperature was expected to influence the bio-oil yield (Bridgwater, et al., 2001). The models show that bio-oil yield also increased with increases in grind size and moisture content. Moisture content effects were from water in original biomass that was collected into the bio-oil. Larger grind sizes allowed biomass to remain in the reactor longer allowing for complete devolatilization of the biomass to occur, increasing the bio-oil yield. The reduction in biochar yield due to grind size was realized as an increase in the bio-oil yield.

The total bio-oil yield models are in effect the sum of each fraction yield model. Each fraction model equation affected the total model with a magnitude equal to the specific fraction yield. The fractions with the highest yield, SF3 and SF4, affected the total bio-oil yield the greatest.

Unwashed biomass total bio-oil yield model:

$Total\ bio-oil\ yield\ (wt.\%) = 0.539 + 0.603M - 0.656(G - 0.5)^2$

R-squared = 0.486

t-value (M) = 2.2

t-value (G*G) = 3.0

Washed biomass total bio-oil yield model:

$Total\ bio-oil\ yield\ (wt.\%) = -0.54 + 0.00114P + 0.0942G + 0.406M - 1.67 \times 10^{-5}(P-485)^2$

R-squared = 0.804

t-value (P) = 5.1

t-value (G) = 2.8

t-value (M) = 4.4

t-value (P*P) = 2.8

Torrefied biomass total bio-oil yield model:

$Total\ bio-oil\ yield\ (wt.\%) = 0.177 + 0.000771P - 3.33 \times 10^{-5}(T-215)^2$

R-squared = 0.442

t-value (P) = 2.8

t-value (T*T) = 2.5

Key:

P – Pyrolysis temperature, °C

G – Grind size, mm

M – Moisture content, % water dry basis

Figure 42: Total bio-oil yield models for each major biomass pretreatment.

Model equations of total bio-oil yield for unwashed and torrefied biomass were not as accurate as washed biomass. The washed biomass model for total bio-oil yield was the most accurate with an r-squared value above 0.8. This further

developed the hypothesis that mineral content had a significant impact on the bio-oil yield model's prediction ability. Since the mineral content was not directly recorded for each biomass sample used in the experiments, this variable could have caused the data to become unpredictable. Although the modeling accuracy was decreased, the actual yields were relatively similar. The models show the reaction pathways changed for bio-oil production, but the differences did not change the magnitude of the yield substantially.

4.3.3.2 Bio-oil moisture

A table of data for bio-oil moisture content analysis is shown in **Appendix D** under the heading **D.3.1 Moisture analysis**. The fraction four (SF4) samples exhibited the highest water content and varied between treatment types (Figure 43). The first three fractions did not show any variance or dependency on the tested variables. The high viscosity and slow dissolution time also made the analysis of the moisture content of the first three bio-oil fractions difficult.

The moisture content of each bio-oil fraction showed why torrefaction yielded less bio-oil than the other types, particularly in the fourth fraction (Figure 36). The moisture analyses showed that torrefaction played a significant role in reducing the bio-oil moisture content. It was known that the torrefied biomass feedstock had very low moisture content and had experienced some thermal decomposition prior to fast pyrolysis. The water content and the volatiles removed during torrefaction also reduced the bio-oil yield from torrefied biomass.

Figure 43 showed how the moisture content of the bio-oil was concentrated into the final fourth bio-oil fraction and that torrefaction significantly reduced the moisture content of the bio-oil.

To calculate the total bio-oil moisture content the bio-oil moisture content of each fraction was added together, weighted by the particular fraction's yield. The total moisture content was still low. An average of published total bio-oil moisture content is 20% (Oasmaa, et al., 2005). The total moisture content of the bio-oil collected was much lower: 15% for washed and unwashed biomass and 5% for

torrefied biomass. The moisture content for unwashed and washed biomass was almost identical, while torrefied biomass produced far less moisture in the bio-oil.

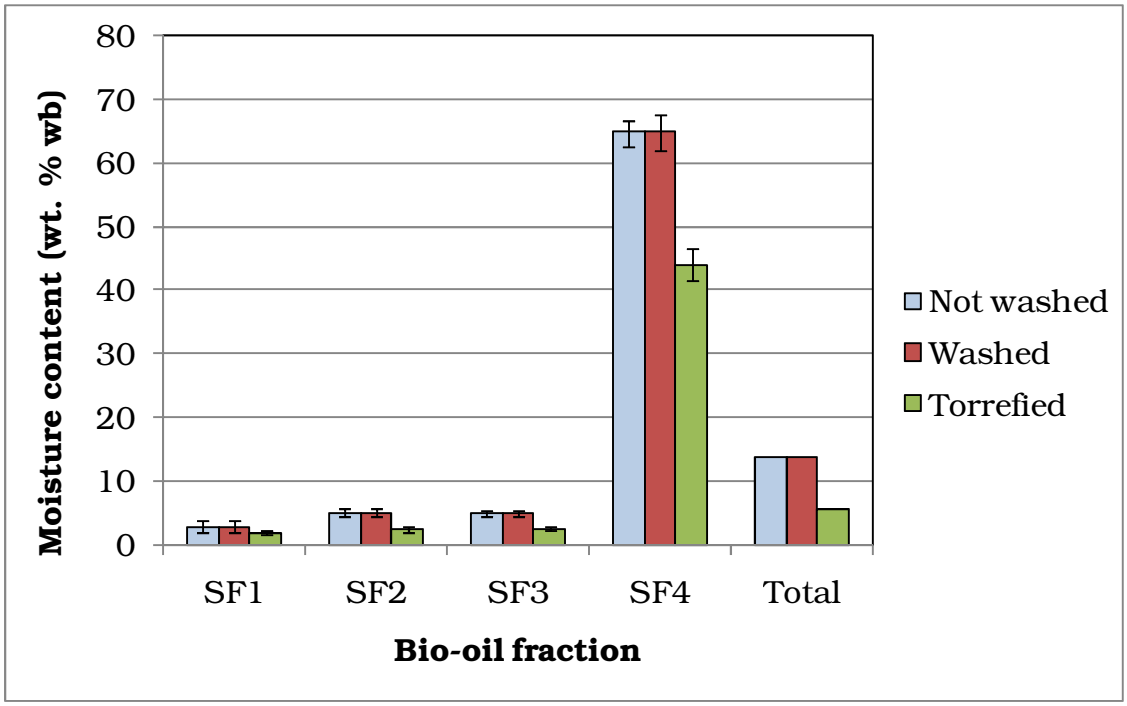

Figure 43: Average moisture content of each analyzed bio-oil fraction and a calculated total for each major pretreatment type as a weight percent of bio-oil on a wet basis.

Model equations for bio-oil moisture content were developed for the bio-oil fraction number four (Figure 44). The statistical data for the model equations are available in **Appendix E**. The other fractions' moisture content was low and irrelevant when compared to the fourth fraction. The first three fractions could not be successfully modeled with the experiment variables. It was desired to have the collected water concentrated into the fourth bio-oil fraction. A model of this was most appropriate and was successfully derived for each biomass type. The fraction four bio-oil moisture content models depended on the moisture content and grind size of the biomass. Pyrolysis temperature was a factor included in the unwashed biomass model and had a lower r-squared value compared to washed biomass. The SF4 moisture content model for torrefied biomass was a factor of torrefaction temperature and grind size. Torrefaction temperature simulated the moisture

content in the torrefied biomass type. This showed the volatiles removed during torrefaction did affect the moisture content in the fourth bio-oil fraction like water content affected the other biomass types. The r-squared for torrefied biomass was also low showing the high ash content in torrefied and unwashed biomass affected the model prediction ability for each compared to washed biomass model.

The grind size in each model had different affects. Both small and large grind sizes reduced the bio-oil moisture content from unwashed biomass showing a polynomial effect rather than linear. The larger grind size trapped more water in the biomass forcing pyrolysis reactions to convert the water into other compounds. The elimination of water would reduce the moisture content collected in the bio-oil. Small grind sizes have been previously identified to elutriate from the reactor before complete devolatilization occurred. Small grind size reduced the moisture content in the bio-oil by not completely vaporizing the water from biomass. The bio-oil moisture content from washed biomass increased with grind size. The overall impact of grind size was small when compared to the magnitude of the other factors visible by the reduced t-value for grind size in the well correlated model for washed biomass.

The bio-oil fraction four had the largest water content. The variable affects found in the fourth fraction would have the most influence on the total bio-oil moisture content as well. The moisture content in the other fractions was minimal and constant when compared to the fourth fraction. No models could be derived from the calculated total bio-oil moisture content. The models for SF4 moisture content were most relevant to the bio-oil product characterization.

Unwashed biomass SF4 bio-oil moisture content model:

$$Fraction\ four\ moisture\ (wt.\%) = 55.94 + 86.94M - 0.357(P - 485)(G - 0.5) - 693(G - 0.5)(M - 0.1)$$

R-squared = 0.516

t-value (M) = 2.7

t-value (P*G) = 2.5

t-value (G*M) = 2.2

Washed biomass SF4 bio-oil moisture content model:

$$Fraction\ four\ moisture\ (wt.\%) = 50.45 + 7.19G + 79.7M - 221(G - 0.5)(M - 0.13)$$

R-squared = 0.811

t-value (G) = 2.0

t-value (M) = 7.8

t-value (G*M) = 4.0

Torrefied biomass SF4 bio-oil moisture content model:

$$Fraction\ four\ moisture\ (wt.\%) = 44.5 - 0.57(T - 215)(G - 0.5)$$

R-squared = 0.301

t-value (T*G) = 2.8

Key:

P – Pyrolysis temperature, °C

G – Grind size, mm

M – Moisture content, % water dry basis

T – Torrefaction temperature, °C

Figure 44: Fraction four bio-oil moisture content models for each major biomass pretreatment.

4.3.3.3 Bio-oil ultimate analysis

The ultimate analysis for bio-oil was done to determine the carbon, hydrogen, and nitrogen composition in each sample. The complete data is included in **Appendix D** under the heading **D.3.2 Bio-oil analysis**. Sulfur was also tested to quantify the appropriate fuel qualities of the bio-oil fractions. The sulfur content was low enough to be excluded from a mineral balance, but did show that sulfur was available in the bio-oil and would create harmful emissions if burned (Table 11) (Oasmaa, et al., 2005). Only the positive values generated from the measurement instrument were used to obtain the overall average sulfur content.

Table 11: Average sulfur concentration of each bio-oil fraction as a weight percent of bio-oil on a wet basis.

	SF1	SF2	SF3	SF4
Sulfur (wt. %)	0.0097 ± 0.0034	0.0081 ± 0.0034	0.0081 ± 0.0024	0.0207 ± 0.0093

Other elements analyzed in the bio-oil were hydrogen (H), carbon (C), and nitrogen (N) shown in Figure 45. The nitrogen content was very low compared to the other elements. Assuming a perfect mass balance, the oxygen (O) content was calculated by difference from the other measured elements and ash. The elements are calculated by the instrument as a weight percent of the sample on a wet basis. The bio-oil moisture content altered the values of hydrogen (H) and oxygen (O) equal to the amount of water (H_2O) in the bio-oil. The data was recalculated on a dry basis to account for the effects of water on the tests.

There was no correlation with the biomass pretreatments or operation conditions affecting the mineral composition of the bio-oil. It was determined that the variation in the data was insignificant. The elemental concentration data from each bio-oil elemental analysis was significantly dependent on the particular fraction (Figure 45). The elemental concentration data from all the samples were averaged together for each fraction. The error in each of these averages was very small, reinforcing how the results were independent of pretreatment variables or pyrolysis operational variables. The large variance in the fourth fraction was due to the high moisture content of the sample.

The results concluded that although carbon and oxygen were relatively constant in each of the first three fractions, in the fourth fraction carbon decreased and oxygen increased. The fourth fraction was lighter in color and less viscous than the other bio-oil fractions. The carbon is most responsible for the large bio-oil compounds that increase the viscosity and color of the first three fractions. Increased acidic compounds in the fourth fraction increased oxygen elements in relation to carbon. The first three fractions are higher in hydrocarbon compounds bonding more carbon elements with hydrogen elements in relation to bonding with oxygen.

The values for each fraction were added together weighted by each bio-oil fraction yield to calculate a total elemental composition for the bio-oil. The values were similar to the first three fraction values. The values compared very well with other bio-oil types from literature shown in Table 12 in section **4.3.3.11 Summary**.

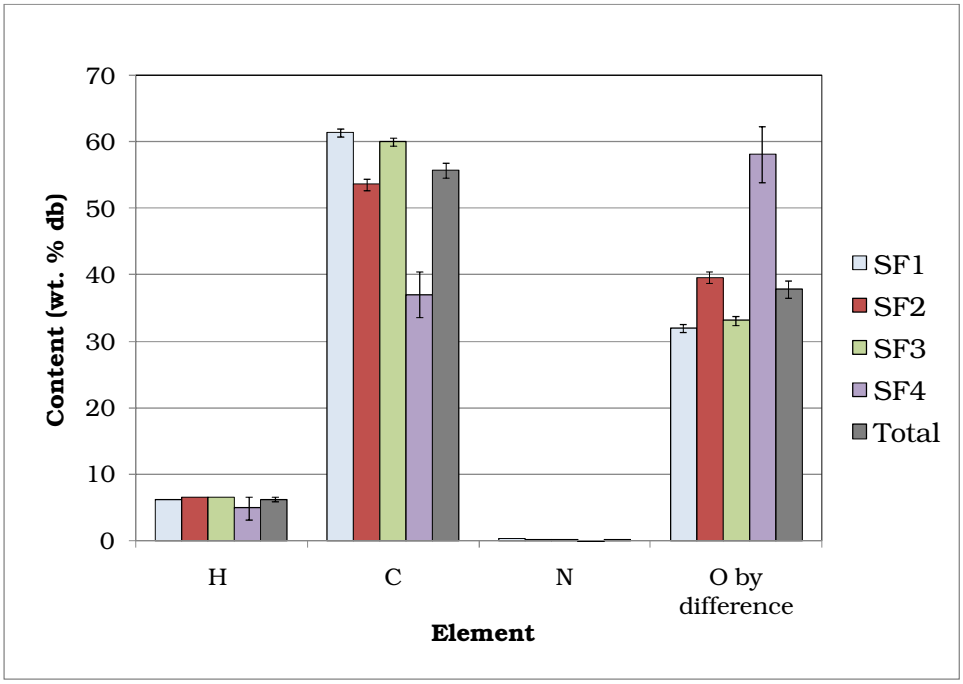

Figure 45: Total average elemental analysis of each bio-oil fraction and a total as a weight percent of bio-oil on a dry basis.

4.3.3.4 Bio-oil GC-MS

The information from the GC-MS analysis gave the weight percent composition of the volatile compounds in the bio-oil samples. The actual number of compounds was likely in the hundreds, and only particular compounds were identified and measured in this study according to the calibration capability of the instrument (Figure 46). The information was shown on an “as received” basis since all samples could not be analyzed for moisture or ash content.

Mass balance for the bio-oil compounds was not achieved due to the high number of low concentration unidentifiable compounds and the undetermined non-volatile weight percent of bio-oil. In the future, more sophisticated equipment and methods may be tried to improve the resolution of the GC-MS as well as quantify the other compounds in the bio-oil that are not precisely measured.

Three specific compounds were of greater interest from the GC-MS data: levoglucosan, furfural, and acetic acid. These compounds were signals to how the pyrolysis reactions occurred (Demirbaş, 2000). Cellulose degrades into levoglucosan in pyrolysis conditions. Other reaction pathways, possibly involving mineral contaminants, further degrades the levoglucosan into other compounds such as furfural and acetic acid (Kawamoto, et al., 2003). Hemicellulose, another biomass compound, also tends to produce lightweight compounds such as acetic acid.

The highest percentage of any one compound in a bio-oil fraction was found with levoglucosan at 6% in the first bio-oil fraction (SF1). The levoglucosan composition was also the highest for the second and the third bio-oil fractions. The fourth bio-oil fraction did not contain any levoglucosan. This showed that the levoglucosan was only present in the initially condensed compounds and the aerosols collected in the first three fractions. The same is true for the smaller concentrations of 5-hydroxy-methyl-furfural and hydroquinone.

The concentration of levoglucosan in each fraction varied between samples, but the variations could not be correlated to a model equation using the experimental parameters. Since no accurate models could be derived, the controlled variables were not significant in determining the concentration of levoglucosan in the bio-oil. This was also true for furfural and acidic acid

concentrations measured by the GC-MS. Since it was expected these compounds would be affected by the pretreatments, other unmeasured factors impacted the reactions. The alternate reactions did not allow for model equations to be derived from the known variables.

The bio-oil collection system attempted to concentrate the acetic acid into the final fraction, SF4. This was achieved, but acetic acid was also collected in each of the first three fractions. Acetic acid was the largest component measured in the fourth fraction at 2.8%. Since the acetic acid increased with each lower temperature bio-oil condenser (SF1 was the hottest, and SF4 was the coldest), it was shown acetic acid only condensed from the gas phase and was not in the aerosols. The acetic acid in the third bio-oil fraction either condensed into the ESP tube or condensed onto the aerosol droplets prior to collection in the ESP. Since no large increase was evident in the third fraction, it was assumed the aerosols did not contain large concentrations of acetic acid.

The large confidence interval in the acetic acid content is due to the low detection ability of the equipment for the lightweight compound. The concentration of acetic acid in the fourth fraction and levoglucosan in the first fraction could not be correlated with any of the controlled parameters. The GC-MS analysis data showed that the particular method of collecting bio-oil had a much more significant role on altering the bio-oil compound concentrations in a predictable way.

To determine the accuracy of the GC-MS within a single sample, a statistical analysis was done on one bio-oil sample. The analysis was repeated three times on a single bio-oil sample. The variance in the measured concentrations within the single sample was comparable in magnitude to the variance between total averages of all the bio-oil samples. This confirmed that no measureable variance of the bio-oil compound concentrations was due to the biomass pretreatments. The complete GC-MS analysis data, a sample GC-MS profile, and the statistical analysis plot are included in **Appendix D** under the heading **D.3.5 Gas chromatograph mass spectroscopy information**. Since no differences in the compounds were apparent, no model equations could be derived describing the formations of compounds in each bio-oil fraction.

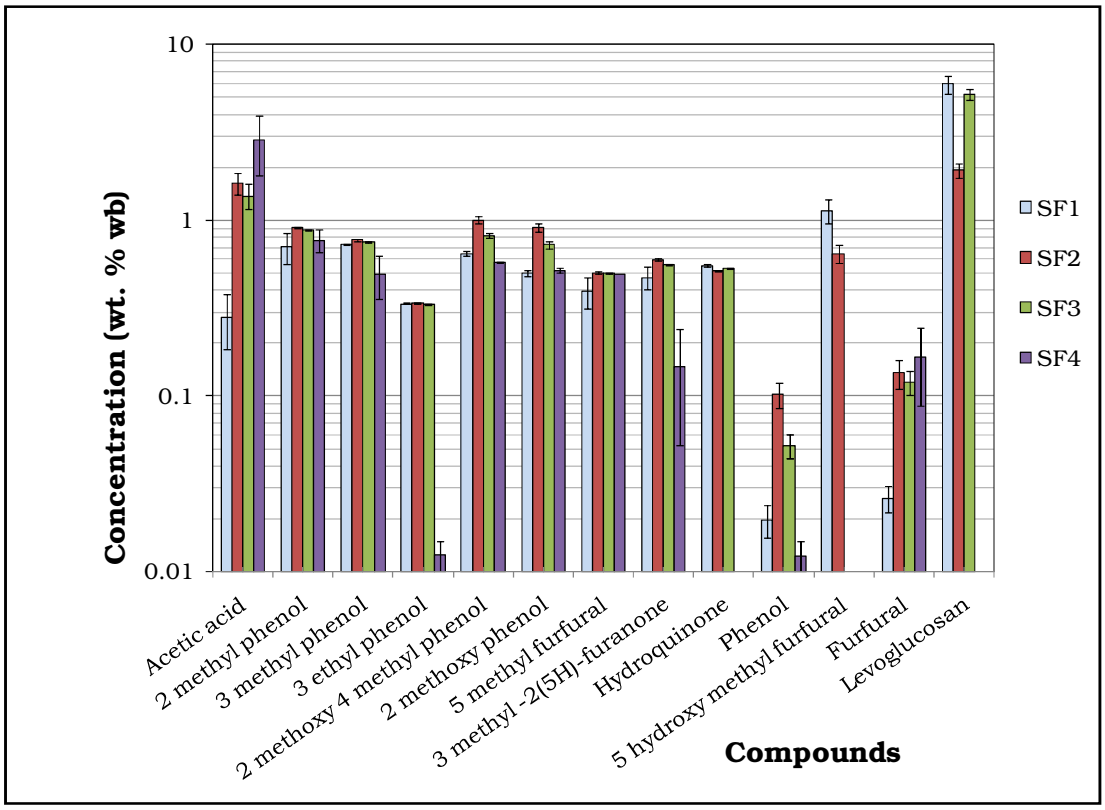

Figure 46: Average volatile compound composition in bio-oil fraction one (SF1), fraction two (SF2), fraction three (SF3), and fraction four (SF4) samples. Identified by gas chromatograph mass-spectrometer as weight percent of bio-oil.

4.3.3.5 Bio-oil solids

The solids in several bio-oil samples were measured as methanol insoluble solids (Figure 47). All bio-oil liquid components from pine wood were solubalized by methanol (Oasmaa, et al., 2001). The analysis data is shown in **Appendix D** under **D.3.4 Bio-oil characteristics**. Solids content in bio-oil can be reduced through optimized biochar collection and proper gas temperature management to eliminate the formation of secondary biochar. The solids were highest in the first bio-oil fraction and decreased with each following fraction. This was evidence of solids entrained in the gas stream passing through the cyclone or formed by secondary reactions occurring after the cyclone producing biochar from volatiles. The theoretical gas flow in the first three collectors was laminar, and the flow in the

final condenser, SF4, was turbulent. The turbulent flow collected the small amount of biochar that remained elutriated passed the ESP.

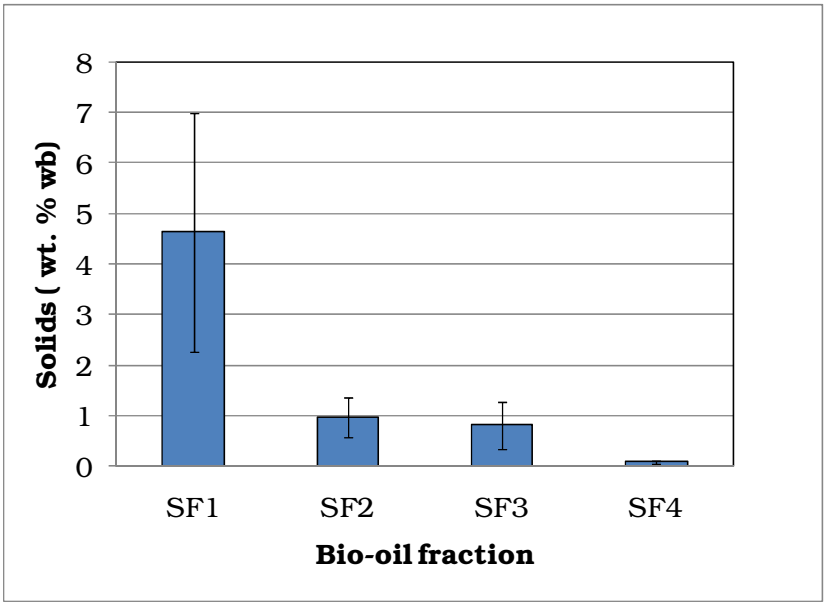

Figure 47: Average solids content in of each bio-oil fraction as a weight percent of the bio-oil on a wet basis.

4.3.3.6 Bio-oil ash

The ash content of bio-oil samples from the four bio-oil fractions were tested for and shown in Figure 48. The data is shown in **Appendix D** under **D.3.4 Bio-oil characteristics**. When evaluating bio-oil as a fuel, ash can become a major problem. Any solids and mineral content in the liquid also causes wear on piping and fluid transfer equipment (Oasmaa, et al., 2005). An increase was found in the third fraction, SF3. This fraction was collected by the ESP. The ESP collected a large portion of the aerosols as bio-oil. The chart shows that either a portion of the ash was contained with the aerosols or it was entrained in the gas stream and collected by the ESP. The wide variance in the data also showed that the ash varied between samples. The ash content was not a function of only the solid content in the bio-oil. More solids were measured in the bio-oil compared to ash for the first three fractions: 10:1 for SF1, 2:1 for SF2, and 1:1 for SF3. Fewer solids were measured compared to ash in the fourth fraction: 1:2 (solids:ash). This showed that ash may have formed from a fraction of the solids in the bio-oil in the first

fractions, and precipitated as various salts from the acidic bio-oil liquids in the fourth fraction.

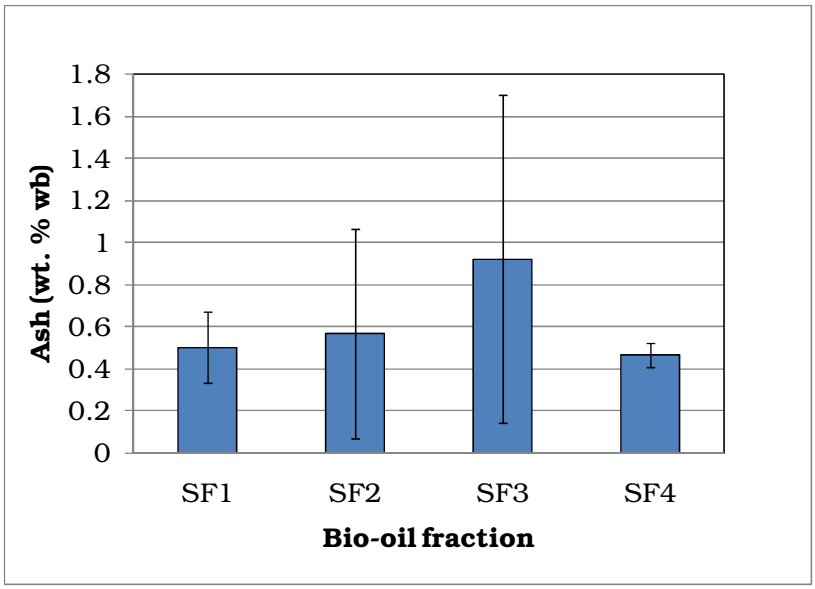

Figure 48: Average ash content in bio-oil as a weight percent of bio-oil on a wet basis.

4.3.3.7 Bio-oil water insolubles

The bio-oil water insoluble portion is thought to consist mostly of lignin oligomers and is sometimes referred to as "pyrolytic lignin" although it likely contains other insoluble compounds as well. The bio-oil collection method used for this research was able to concentrate a large portion of the water insolubles into the first three fractions of bio-oil shown in Figure 49. The total weighted average water insolubles collected as a percent of biomass fed was 30.1 ± 1.3%. Less than 1% of water insolubles content was measured for the fourth bio-oil fraction. The data from the analysis is shown in **Appendix D** under **D.3.4 Bio-oil characteristics**.

The water insolubles were condensed at higher temperatures in the first two bio-oil fractions and collected in the aerosols in the third bio-oil fraction. The analysis measured the water insoluble ash, solids, and any other water insoluble compounds present in the liquid bio-oil. The largest insoluble compound in bio-oil was expected to be pyrolytic lignin, but this was not confirmed. The compounds

collected in the first two fractions were expected to be large compounds with the highest dew point temperatures. It was undetermined whether the insoluble portion of the bio-oil was pyrolytic lignin or another compound. Due to the difficult physical properties of pyrolytic lignin, this method only provided a close approximation of the pyrolytic lignin content.

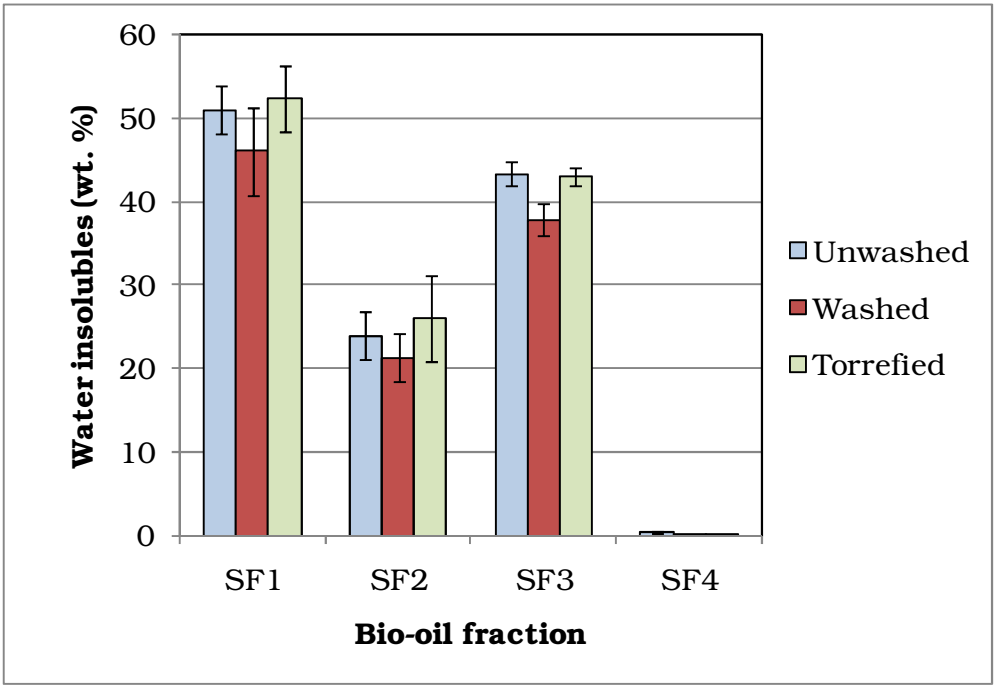

Figure 49: Average bio-oil water insoluble content for each bio-oil fraction as a percent of bio-oil on a wet basis.

The water insoluble fraction in the second and third bio-oil fractions remained relatively constant when compared to the experimental variables. The insolubles in the third fraction showed the water insoluble content produced as aerosols were reduced for washed biomass. The second fraction was collected as carryover from the first fraction and was an irrelevant measurement compared to fraction one. The water insoluble content of the first fraction varied with the experimental parameters for each major biomass type. This allowed model equations to be derived to represent the results which are shown in Figure 50. Increasing the pyrolysis temperature had the most significant effect on the water insolubles collected into the first fraction bio-oil compounds. The statistical data and contour plots for each model are included in **Appendix E**.

It was determined for unwashed biomass that the water insoluble content increased with pyrolysis temperature for the SF1 bio-oil samples. Increased pyrolysis temperature had previously been shown to affect the bio-char yield, biochar composition, and bio-oil yields. Higher temperatures also increased the amount of pyrolytic lignin volatilizing from the feedstock.

Strangely, the water insoluble content for washed biomass decreased with increased pyrolysis temperature and decreased with larger grind size. This was opposite to the unwashed biomass model. Torrefied biomass showed that water insoluble content decreased with increasing pyrolysis temperature up to 500°C. The water insoluble content then increased for torrefied biomass with pyrolysis temperatures above 500°C. Like washed biomass larger grind size in torrefied biomass also decreased the water insoluble content of the bio-oil.

The increased ash content and light volatiles of the unwashed biomass was likely the reason for increased insoluble content was found with increased pyrolysis temperature. The degradation of soluble compounds was enhanced by the presence of the ash at higher temperatures. The torrefied biomass had reduced light compounds and high ash content. The parabolic model of torrefied biomass showed that for low pyrolysis temperatures, the absence of light compounds allowed water insolubles to decrease for increasing temperature. The ash and light compounds together were not available in washed biomass or from torrefied biomass at low pyrolysis temperatures. When temperatures became significantly high, degradation of volatile compounds occurred, which formed light compounds. The presence of light compounds and ash then caused insoluble content to increase with temperature. Unwashed biomass contained high levels of ash and produced light compounds during all temperatures of fast pyrolysis. The constant availability of light compounds and ash in untreated biomass allowed insoluble content to increases for all temperatures.

The grind size also effected unwashed and torrefied biomass types but not the unwashed type. Reduced water insoluble content was due to increased volatile degradation. The actual changes in water insoluble content did not change by a large amount. The base water insoluble content for each biomass type was similar and likely due to the major biomass constituent: lignin. The major pathway for

producing elevated water insolubles was the light compounds and ash in biomass. The pathway was eliminated for washed and torrefied biomass. Therefore, in the water insoluble models, grind size became significant in modeling the product formation. Overall the magnitude of insolubles content of each biomass type remained similar and the relative decreases or increases in water insolubles due to pretreatment were very small. The major water insoluble component was most likely pyrolytic lignin from the original lignin in the biomass. The other biomass properties did effect the water insoluble content, but to a far less degree to the consistent biomass lignin content.

Unwashed biomass SF1 bio-oil water insoluble content model:

$$Fraction\ one\ water\ insolubles\ (wt.\%) = -0.205 + 0.00147P$$

R-squared = 0.421

t-value (P) = 3.4

Washed biomass SF1 bio-oil water insoluble content model:

$$Fraction\ one\ water\ insolubles\ (wt.\%) = 184.2 - 0.0256P - 29.1G$$

R-squared = 0.493

t-value (P) = 3.6

t-value (G) = 2.5

Torrefied biomass SF1 bio-oil water insoluble content model:

$$Fraction\ one\ water\ insolubles\ (wt.\%) = 109.5 - 0.101P - 23.12G + 0.0042P^2$$

R-squared = 0.595

t-value (P) = 2.1

t-value (G) = 3.0

t-value (P*P) = 3.2

Key:

P – Pyrolysis temperature, °C

G – Grind size, mm

Figure 50: Water insoluble content models for each major biomass pretreatment.

4.3.3.8 Bio-oil higher heating value

The first three bio-oil fractions each had elevated higher heating values as shown in Figure 51. The analysis data is included in **Appendix D** under **D.3.4 Bio-oil characteristics**. The higher heating value of commercial bio-oil is 17 to 20 MJ/kg (Oasmaa, et al., 2001). The SF1 and SF3 fractions were near 25% above this level. The SF2 fraction was just above the maximum value. The SF4 fraction was less than half the commercial values. This was due to the water and lightweight compounds being concentrated in the SF4 fraction. The cumulative average heating value of the bio-oil if the fractions were mixed was 20 MJ/kg. This is still high when compared to other bio-oil types, but also reflects that the bio-oil produced in this study had significantly less moisture than other bio-oil types.

The higher heating values followed very similar trends to the carbon content and the water insoluble content information. The first and third fractions were the largest, with fraction two also being high, but notably less than the other two. The fourth fraction was far less than any of the other fractions. The carbon, water insoluble, and higher heating value were linked by assuming the water insoluble compounds contained the largest percentage of the available energy in the bio-oil and are composed of the majority of the carbon in the bio-oil.

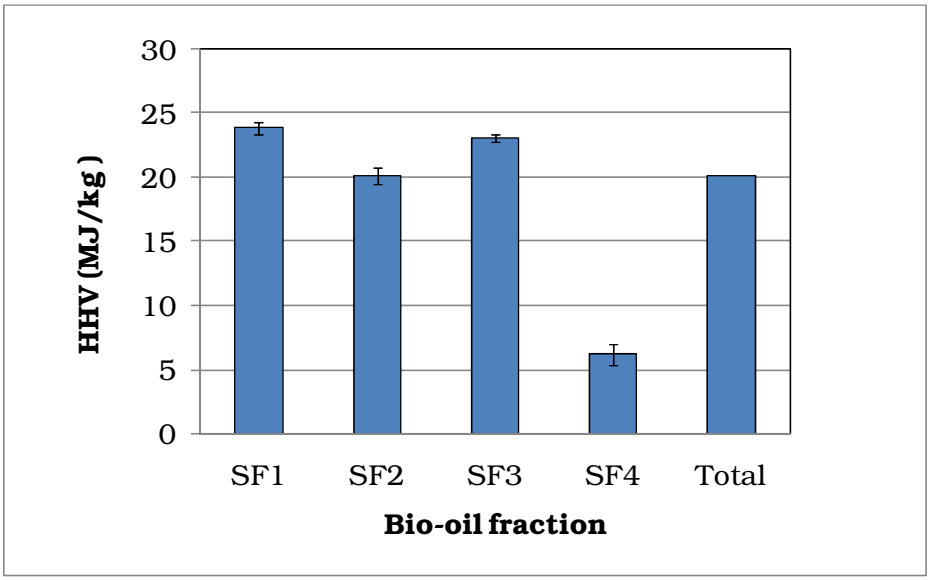

Figure 51: Average higher heating value of each bio-oil fraction and a total on a wet basis.

4.3.3.9 Bio-oil viscosity

The SF3 and SF4 fractions were analyzed for viscosity shown in Table 12. The data is available in **Appendix D** under **D.3.4 Bio-oil characteristics**. The viscosities of each bio-oil fraction varied from commercially available bio-oil (Oasmaa, et al., 2001). The bio-oil SF3 fraction had an extremely high viscosity at 20°C of 270,000 cP. The viscosity decreased when heated to 50°C to 4,643 cP. The bio-oil SF4 fraction had a very low viscosity, likely due to the high water content it also exhibited. This viscosity decreased with temperature from 2.3 cP at 20°C to 0.78 cP at 50°C. This proved the aerosols were much higher in viscosity than the other condensed compounds in the fourth fraction.

The SF1 bio-oil fraction was solid at room temperature and could not be analyzed. SF2 did not produce a sufficient volume of bio-oil to be analyzed properly. The first three fractions were notably very viscous and sticky in nature. This was linked to the high water insolubles content and the low moisture content. In each case the bio-oil from the first three fractions had a high viscosity, were sticky in nature, had elevated higher heating values, had high amounts of water insolubles, and had lower moisture content compared to the last bio-oil fraction.

4.3.3.10 Bio-oil pH

The pH of the bio-oil was measured with an electronic pH meter. The analysis could only be done on the low viscosity SF4 bio-oil fraction. The data is shown in **Appendix D** under **D.3.4 Bio-oil characteristics**. An average pH of the SF4 bio-oil was 1.8. It was expected that the acid concentration would create a very low pH. The first three fractions, SF1, SF2, and SF3, could not be analyzed due to their high viscosities.

4.3.3.11 Summary

Tests for several characteristics were performed on selected samples of the four fractions of bio-oil, including the solids content, higher heating value, and ash content of the bio-oil. This information is presented in Table 12. The staged

collection method was able to greatly reduce the water content of the first three fractions.

The higher heating value (HHV) showed promise to the capabilities of the bio-oil collection method. Energy content of traditional bio-oil is rather low (less than 20 MJ/kg) due to the high water content present. The methods used in this research reduced the water content of the first three fractions and in turn greatly increased the energy content. The energy content of the last fraction was low due to the high water content. The higher energy in the first three also came with higher viscosities and higher percentages of water insoluble compounds.

The ash content of each fraction was higher than commercially available bio-oil types. The increased bio-oil ash content in this study may have been due to the biomass used or the bio-oil collection methods used when compared to the other referenced bio-oils.

Table 12: Bio-oil properties of each fraction as a complete average from all tests compared with other documeted bio-oil.

Source	ISU	ISU	ISU	ISU	ISU	VTT[1]	VTT[1]	Ensyn[1]	NREL[1]
Feedstock	Loblolly pine slash	Loblolly pine slash	Loblolly pine slash	Loblolly pine slash	Loblolly pine slash	Pine	Forest residue	Mixed hardwood	Poplar
Fraction (% total)	SF1 (17.6)	SF2 (12.8)	SF3 (53.3)	SF4 (16.3)	Composite	N/A	N/A[2]	N/A	N/A[3]
Property									
Water, wt%	2.8	4.4	4.3	58	11.1	16.6	24.1	22	18.9
Elementals (dry), wt%:									
C	61.4	53.6	60.1	37.9	55.9	55.8	56.36	56.4	57.3
H	6.23	6.62	5.64	5.64	5.9	5.8	6.2	6.2	6.3
O (by diff.)	31.4	39.1	33.1	56.0	37.3	38.2	36.9	37.1	36.2
N	0.52	0.17	0.21	0	0.2	0.1	0.1	0.2	0.18
S	<0.01	<0.01	<0.01	<0.01	<0.01	0.02	0.03	<0.01	0.02
Ash	0.50	0.56	0.92	0.46	0.7	0.03	0.08	0.01	<.01
HHV, MJ/kg	23.8	20.1	23.1	6.2	20.1	19.1	17.4	17	18.7
HHV (dry), MJ/kg	24.5	21.1	24.1	19.7	23.0	22.9	23	23.1	22.3
Viscosity, cP									
20°C	n.d.	n.d.	>270,000	2.3	n.d.	n.d.	18.5	n.d.	15.36
50°C	n.d.	n.d.	4,643	0.78	n.d.	3.844	3.5 (40°C)	5.9	1.62
Solids wt %[4]	4.64	0.97	0.82	0.09	1.4	n.d.	0.02	n.d.	n.d.

1. Oasmaa & Peacocke, A guide to pysical property characterisation of biomass-derived fast pyrolysis liquids, 2001. VTT Technical Research Centre of Finland
2: Bottom phase (90% of total liquid)
3: Hot gas filtered
4: As wt. % insolubles in methanol

The analysis showed that the solids content of the oil was relatively high compared to commercial bio-oil types. Fraction one experienced the highest percentage of solids. The solids were biochar that passed the cyclone and collected on the wetted walls of the first condenser or from secondary reactions forming biochar from volatiles. The solids in the rest of the fractions were very low, less than one percent.

The values of each bio-oil fraction were added together by the weight percent of the average dry bio-oil fraction yield (Table 12). The calculated composite bio-oil values were similar to the other referenced values. The table showed that the bio-oil had many of the same qualities as bio-oil collected as one fraction with reduced water content.

4.3.4 Non-condensable gas

4.3.4.1 Non-condensable gas yield

The gas yield, expressed as a percentage of the biomass fed into the reactor on a wet basis, was recorded with the particular test's feedstock and reactor conditions. Gas yield was found to increase as a function of pyrolysis temperature shown in Figure 52. This was due to increased secondary reactions occurring when the pyrolysis temperature increased (Di Blasi, 2002).

The micro-GC resolution was not fast enough to provide precise gas analysis during a test. Only an average value of the gas composition was available to relate back for the mass balance. Any variation to the gas composition between the three minute sample increments was unidentifiable. This caused the accuracy of the gas yield measurement to be reduced, visible as the large error in the data points.

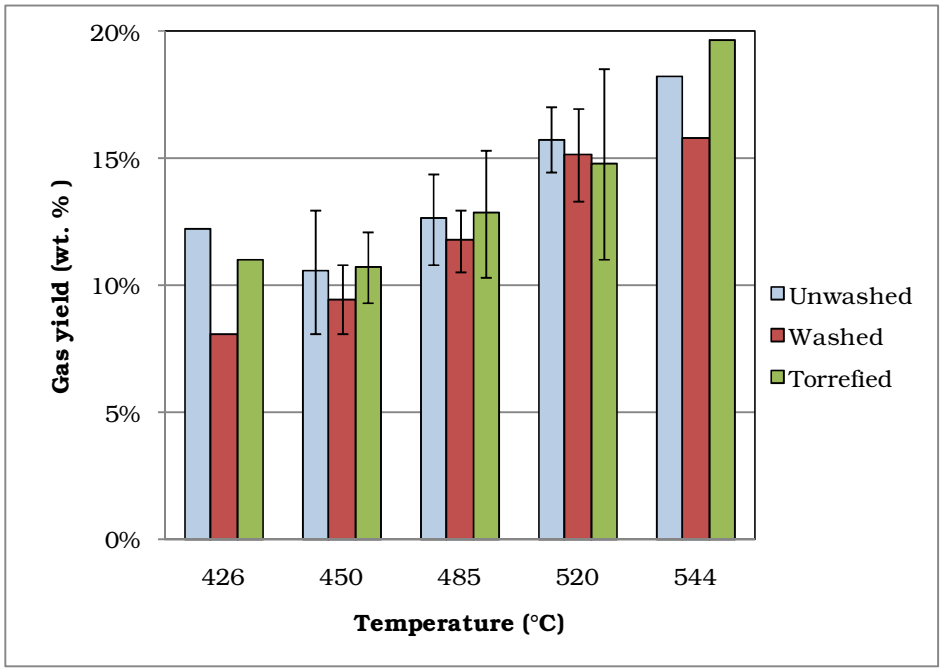

Figure 52: Average non-condensable gas yield at each pyrolysis temperature for each pretreatment type as a percent of fed biomass. Samples at 426°C and 544°C are only performed once with the specified middle grind size and moisture content or torrefaction temperature from the design of experiments. Samples at 450°C and 520°C are averaged from four runs of each high and low value of grind size and moisture content or torrefaction temperature. Samples at 485°C are averaged from the six replicated center conditions and one run at each high and low variable with all other variables at the center.

The derived models for the non-condensable gas yield are shown in Figure 53. The statistical data for the model equations are available in **Appendix E**. The models for unwashed and washed biomass are functions of pyrolysis temperature only, and the torrefied biomass model was a function of grind size and pyrolysis temperature. The reduced r-squared values for the models reflect the limited resolution of the micro GC reducing the sensitivity of the yield measurement. The models showed that the non-condensable gas yield relied heavily on the pyrolysis temperature. Increasing temperature increased the gas yield. This was because higher temperatures completely devolatilized biochar into more gas, as well as caused secondary reactions to react bio-oil compounds into gas.

For torrefied biomass, the larger grind sizes also caused increased non-condensable gas yield independent of torrefaction temperature. Larger grind sizes

allowed biomass to remain in the reactor longer before being elutriated out, this allowed more compounds to be volatilized out of the biomass creating more non-condensable gas. The impact of torrefaction was linked to the increased grindability that torrefied biomass exhibited. When torrefied biomass was ground to small diameters, much of the biomass was ground very fine. The biomass ground too fine elutriated from the fluidized bed before it could completely react reducing the gas yield for small grind sizes. This issue was less significant in the other biomass types for the non-condensable gas yield.

Unwashed biomass non-condensable gas yield model:

$$Non-condensable\ gas\ yield\ (wt.\%) = -0.1823 + 0.0006455P$$

R-squared = 0.509

t-value (P) = 4.3

Washed biomass non-condensable gas yield model:

$$Non-condensable\ gas\ yield\ (wt.\%) = -0.242 + 0.000747P$$

R-squared = 0.741

t-value (P) = 7.4

Torrefied biomass non-condensable gas yield model:

$$Non-condensable\ gas\ yield\ (wt.\%) = -0.227 + 0.0892G + 0.000645P$$

R-squared = 0.624

t-value (G) = 3.4

t-value (P) = 4.1

Key:

P – Pyrolysis temperature, °C

G – Grind size, mm

Figure 53: Non-condensable gas yield models for each major biomass pretreatment.

4.3.4.2 Non-condensable gas compositions

The micro gas chromatograph (Micro-GC) was capable of measuring the concentrations of a wide array of gases. The gases measured by the Micro-GC were nitrogen, carbon monoxide, carbon dioxide, hydrogen, methane, and propane. The complete gas analysis data for each test is included in **Appendix D** under the heading **D.4 Non-condensable gas data**. The relative concentrations of four major gas constituents plotted against pyrolysis temperature are shown in Figure 54. They are plotted as a percentage of the non-condensable gas produced from fast pyrolysis with the nitrogen fraction removed. As expected, carbon monoxide concentration increased and carbon dioxide decreased with increased pyrolysis temperature (Luo, et al., 2004). Methane and hydrogen concentrations were small and showed little change over the varying temperature range. Propane measurement was not plotted as it varied widely due to other unidentified higher molecular weight compounds in the gas possibly affecting the reading. The trends shown in Figure 54 agree with those in literature (Prins, et al., 2006 b). Carbon monoxide was a direct product of secondary reactions cracking volatiles into biochar and non-condensable gas, the concentration of CO increases with increasing pyrolysis temperature. This confirmed that more secondary reaction occur at higher pyrolysis temperatures.

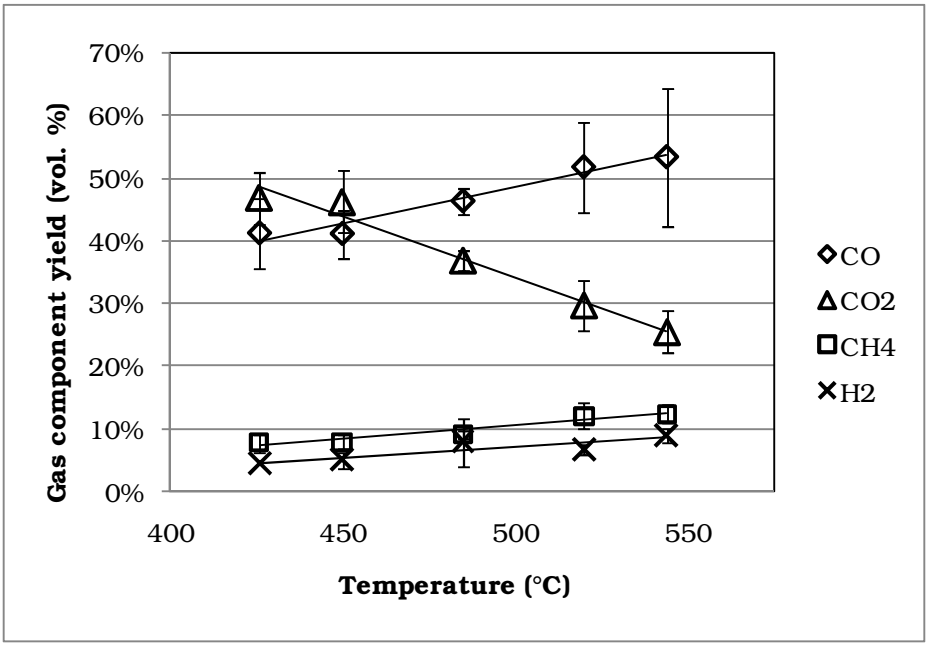

Figure 54: Non-condensable gas concentrations of measured compounds for increasing pyrolysis temperature as a percent of non-condensable gas produced. The points at each temperature are average values for unwashed, washed, and torrefeid biomass. Samples at 426°C and 544°C are only performed once with the specified middle grind size and moisture content or torrefaction temperature from the design of experiments. Samples at 450°C and 520°C are averaged from four runs of each high and low value of grind size and moisture content or torrefaction temperature. Samples at 485°C are averaged from the six replicated center conditions and one run at each high and low variable with all other variables at the center.

The non-condensable gas composition data was modeled with each pretreatment type. The statistical data for the model equations are available in **Appendix E**. The models for carbon monoxide composition in the non-condensable gas are shown in Figure 55. Each model was significantly represented by pyrolysis temperature. In addition: unwashed biomass depended on the grind size and moisture content; washed biomass on the moisture content; and torrefied biomass on the torrefaction temperature and grind size.

The parameters used in the models determined how biomass reacted during pyrolysis. Increased pyrolysis temperature increased the heat energy available for the reactions to occur in all cases. Increased grind size trapped more volatiles within the larger particle leading to increased secondary reactions in the unwashed biomass case. The larger torrefaction temperature started many of the initial

pyrolysis reactions during the pretreatment, allowing them to continue faster when introduced to the fast pyrolysis conditions after torrefaction. Decreased grind size created more surface area available on the biomass and biochar for surface reactions to occur. The results for unwashed and torrefied biomass also likely relied on a function of the ash content of the biomass, since CO producing reactions are catalyzed by ash in biomass (Agblevor, et al., 1994).

The models showed that the CO concentration increased with grind size and torrefaction temperatures in biomass were ash was available as a catalyst. When ash content was reduced in the washed biomass, only the moisture content was relevant in modeling CO concentration. This showed that moisture was a factor in CO production but was less significant than ash catalyzed reactions occurring inside larger particles of washed and unwashed biomass.

In all three cases the measured CO concentrations were similar, so in each case the different reaction pathways to produce CO were similar in magnitude. The non-condensable gas models showed that the pretreatments changed the pathways CO was formed, but the overall weight percent and yield were not significantly altered as they were according to pyrolysis temperature

The models for the carbon dioxide concentration in non-condensable gas are shown in Figure 56. The carbon dioxide decreased with temperature for each of the models studied. The concentration between the major biomass types was also similar. The major variable in each of the models was pyrolysis temperature. The models also include several other parameters that improve the r-squared values of each.

Biomass moisture content was important to the washed biomass model for CO_2 concentration. The reduction in mineral content influenced the importance of moisture content in the model. The torrefied biomass model included torrefaction temperature and grind size. The torrefied biomass exhausted CO_2 during the pretreatment, which caused the torrefaction pretreatment to influence the CO_2 gas produced during pyrolysis. The grind size was also an important variable, due to the reduction in devolatilization with lower grind sizes discussed previously.

Unwashed biomass CO concentration model:

$$CO\ (vol.\%) = -0.347 + 3.11 \times 10^{-5}(P-485)^2 - 0.0904(P-485)(M-0.1)$$

R-squared = 0.483

t-value (P*P) = 3.0

t-value (P*M) = 3.8

Washed biomass CO concentration model:

$$CO\ (vol.\%) = -0.530 + 0.00196P - 0.483M + 0.0704G - 0.471(G-0.5)^2$$

R-squared = 0.886

t-value (P) = 9.9

t-value (M) = 5.4

t-value (G) = 2.2

t-value (G*G) = 2.5

Torrefied biomass CO concentration model:

$$CO\ (vol.\%) = -0.255 + 0.00123P - 0.00517(T-215)(G-0.5)$$

R-squared = 0.869

t-value (P) = 7.8

t-value (T*G) = 5.6

Key:

P – Pyrolysis temperature, °C

G – Grind size, mm

M – Moisture content, % water dry basis

T – Torrefaction temperature, °C

Figure 55: Non-condensable gas carbon monoxide concentration models for each major biomass pretreatment.

Unwashed biomass CO_2 concentration model:

$$CO_2\ (vol.\%) = 1.063 - 0.00154P$$

R-squared = 0.457

t-value (P) = 3.9

Washed biomass CO_2 concentration model:

$$CO_2\ (vol.\%) = 1.03 - 0.00143P - 0.392G - 0.00358(P - 485)(G - 0.5)$$

R-squared = 0.670

t-value (P) = 4.4

t-value (M) = 2.7

t-value (P*G) = 2.1

Torrefied biomass CO_2 concentration model:

$$CO_2\ (vol.\%) = 0.978 - 0.00115P - 0.000611T - 0.00320(T - 215)(G - 0.5)$$

R-squared = 0.812

t-value (P) = 6.7

t-value (T) = 3.1

t-value (T*G) = 3.5

Key:

P – Pyrolysis temperature, °C

G – Grind size, mm

M – Moisture content, % water dry basis

T – Torrefaction temperature, °C

Figure 56: Non-condensable gas carbon dioxide concentration models for each major biomass pretreatment.

The hydrogen gas concentration models for each biomass type are shown in Figure 57. The hydrogen content in the non-condensable gas was low and did not change significantly compared to carbon monoxide or carbon dioxide. The small variance did not allow a model to be derived for unwashed biomass. The model for washed biomass had low significance and was a function of the grind size and pyrolysis temperature. The torrefied biomass fit model was only a function of pyrolysis temperature. The severe pretreatments that torrefied biomass experienced relative to the other types did not affect the hydrogen production in the non-condensable gas.

Unwashed biomass H_2 concentration model: Undefined

Washed biomass H_2 concentration model:

$$H_2\ (vol.\%) = 0.0544 + 0.00249(P - 485)(G - 0.5)$$

R-squared = 0.203

t-value (P*G) = 2.2

Torrefied biomass H_2 concentration model:

$$H_2\ (vol.\%) = -0.0733 + 0.000241P$$

R-squared = 0.222

t-value (P) = 7.2

Key:

P – Pyrolysis temperature, °C

G – Grind size, mm

Figure 57: Non-condensable gas hydrogen gas concentration models for each major biomass pretreatment.

The methane concentration in the non-condensable gas did not vary significantly similar to hydrogen gas. The models for methane concentration were included in Figure 58. Like the hydrogen content models, unwashed biomass could not be fit to a model. Torrefied biomass also developed a well fit model relative to the washed biomass model. The torrefied biomass model was a function of several parameters for the methane concentration.

The low concentration of methane made it difficult to distinguish a difference in the measured values. The models show that torrefaction temperature and moisture content each had significant impacts on the methane concentration in the non-condensable gas. Like several other models the grind size of torrefied biomass was important for the torrefied biomass model. Due to the amount of devolatilization that was able to occur to the ground biomass before it was elutriated from the pyrolysis reactor.

Unwashed biomass CH_4 concentration model: Undefined

Washed biomass CH_4 concentration model:

$$CH_4\ (vol.\%) = -0.143 + 0.000424P + 3.51(M - 0.1)^2$$

R-squared = 0.519

t-value (P) = 2.9

t-value (M*M) = 2.6

Torrefied biomass CH_4 concentration model:

$$CH_4\ (vol.\%) = -0.234 + 0.000403T + 0.0522G + 0.0004P + 1.86 \times 10^{-5}(T - 215)^2 + 5.66 \times 10^{-6}(P - 485)^2$$

R-squared = 0.864

t-value (T) = 3.6

t-value (G) = 3.4

t-value (P) = 4.3

t-value (T*T) = 4.2

t-value (P*P) = 2.2

Key:

P – Pyrolysis temperature, °C

M – Moisture content, % water dry basis

G – Grind size, mm

T – Torrefaction temperature, °C

Figure 58: Non-condensable gas methane concentration models for each major biomass pretreatment.

CHAPTER 5: CONCLUSION

The effects of biomass pretreatments were investigated to identify how each impacted the three major products of fast pyrolysis. Product yields and compositions were studied and modeled with response surface equations and the experimental variables. The surface equation models can be used to predict product formation from known pretreatments, but only for those cases with adequate correlation. In many cases, the biomass pretreatments were identified to affect the pyrolysis reaction models, but changes in yield or composition were insignificant. The torrefied biomass exhibited very low moisture content and visual thermal decomposition prior to being pyrolyzed. Torrefaction did not affect the first three bio-oil fractions or non-condensable gas yields compared to other biomass types. The torrefaction pretreatment reduced the bio-oil yield in the fourth fraction and increased the biochar yield. These results are attributed to the mass loss experienced during the torrefaction pretreatment. The water wash pretreatment showed no significant difference when compared to unwashed biomass in terms of product yields.

The effect of pyrolysis temperature on pyrolysis products was most significant in the experiments for this study. The biochar yield steadily decreased as temperature increased. Higher pyrolysis temperatures decreased the hydrogen content in all biochar. This showed that more hydrogen volatilized at higher temperatures. Bio-oil yield was not greatly affected by temperature, but maximized at 485°C. The total bio-oil yield was dependant on the third bio-oil fraction that came from aerosol collection in the ESP. The third fraction was most reliant on pyrolysis temperature. The non-condensable gas yield increased for increasing temperatures consistent with the loss of biochar yield.

The grind size and moisture content of the biomass affected only the biochar yield and the SF4 bio-oil yield considerably. The two variables had only minimal affects on product yields and properties. The effects of these two parameters were far less than the effect of pyrolysis temperature for each product yield. Grind size most commonly affected the degree of devolatilization that occurred from the feedstock. Larger particles devolatilized more completely, reducing the biochar

yield, and increasing the SF4 bio-oil yield. Moisture content in the biomass altered the yields of biochar and SF4 bio-oil because biochar was a dry yield and the SF4 bio-oil was very high in water content.

The washed biomass produced the best model for bio-oil yield. The model was dependant on pyrolysis temperature, grind size, and moisture content of the biomass. The yield also reached a maximum at the center temperature in the experiments, 485°C. The r-squared value was 0.804 for the washed biomass. This was better than the unwashed and torrefied models with 0.486 and 0.422 respectively. The unknown inorganic content such as ash in the other biomass types affected the bio-oil yields too significantly to be correctly modeled with the controlled parameters. Although the effects of the ash may have caused the models to fit poorly, the actual yield of bio-oil between washed and unwashed biomass was indistinguishable. This showed that although reaction pathways were changed the product yield magnitudes were not significantly affected.

A fractionating bio-oil collection system was used with the fast pyrolysis reactor. It was designed to collect the lightweight compounds and water separate from other bio-oil compounds. The bio-oil collection method was able to concentrate a large majority of water into the fourth fraction. The total water collected as a percentage of bio-oil was lower than other published values. The high percent of water content in the fourth fraction (58%) caused it to have a low higher heating value (6.2MJ/kg). In contrast, the first three fractions had elevated higher heating values due to the removed water (higher heating values of 23.8 MJ/kg, 20.1 MJ/kg, and 23.1 MJ/kg and water contents of 2.8%, 4.4%, and 4.3% respectively for SF1, SF2, and SF3). The first three fractions were also more viscous, contained higher amounts of water insolubles, and contained more elemental carbon and less oxygen compared to bio-oil collected as the fourth fraction (elemental carbon contents of 61.4%, 53.6%, 60.1%, and 37.9% and oxygen contents of 31.4%, 39.1%, 33.1%, and 56.0% respectively for SF1, SF2, SF3, and SF4). The ultimate analysis and volatile compound analysis of the bio-oil showed noticeable differences between each fraction, but no differences in bio-oil due to the pretreatments studied. Hydrogen content was constant between samples at 6%, nitrogen content was below 1%, and sulfur was below 0.1%. The biomass

pretreatments did not have a significant impact on the bio-oil compounds formed during fast pyrolysis.

The non-condensable gas yield increased with temperature. The non-condensable gas yield models were most dependant on pyrolysis temperature alone. The concentration of major compounds in the gas also changed with temperature. Carbon monoxide concentration increased while carbon dioxide decreased for increased pyrolysis temperature. Carbon monoxide concentration increased significantly with biomass pyrolysis temperature for each biomass tested. This confirmed that carbon monoxide is a product of secondary reactions producing biochar and non-condensable gas from volatiles at higher temperatures. Other reaction pathways were found in the models for each pretreatment type, but the overall yields were unaffected.

5.1 Water wash effects

The water wash successfully reduced the mineral content in the biomass. The ash content in the raw treated biomass was reduced from 2.72% to 0.74%. Some of the removed minerals were dissolved in the water used for the wash. A much higher amount was suspended in the water as it was washed off the biomass. Some minerals were still present in the biomass after the wash.

The washed biomass was able to be more accurately modeled for the bio-oil yield models. The reduction of foreign material during the wash increased the predictability of the process with the controlled variables. Washed biomass also caused a significant effect in forming water insolubles content in the bio-oil stage fraction one. This was attributed to the mineral content reduction that occurred during the water wash. Minerals in ash and light volatiles together were found to increase water insolubles. Reducing either of the two parts would reduce water insolubles content.

5.2 Torrefaction effects

Torrefaction was an extreme pretreatment for biomass prior to fast pyrolysis. Currently, the most promising benefit of torrefaction is the improved grindability

and energy densification of biomass. Torrefaction for fast pyrolysis showed reduced bio-oil yields. The bio-oil from torrefaction also had lower water content. This showed the moisture content of the bio-oil is highly dependent on the moisture content of the biomass used as a feedstock. The reduced bio-oil yields were due to both the water removed and volatiles removed during torrefaction.

The reduced moisture content of bio-oil was the only recorded improvement from the pretreatment for pyrolysis. The biomass still caused reactions similar to untreated biomass at the pyrolysis conditions studied.

5.3 Future work

The field of fast pyrolysis is wide open for scientific study and analysis. One significant problem observed from this study was the inability to correctly and efficiently analyze all of the pyrolysis products. The ability to accurately measure the specific compounds in the bio-oil is critical to forming intelligent conclusions of what was studied. Stemming directly from this research project are several more areas that can be explored to further develop the conclusions made. From the results of this project, it is recommended to keep grind size constant and at a size large enough to allow for complete devolatilization before elutriation from the reactor. Also to keep moisture content constant when studying other parameters. The effects of water content are only evident on products that are free of water or have high water content.

Pyrolyzing several model compounds to represent biomass and mixtures of model compounds in the 100 g/hr reactor may give insight into what reactions are occurring during fast pyrolysis from each specific compound in biomass. The actual reactions occurring during fast pyrolysis are very complex and need to be further defined in this way. The wide range of compounds in biomass slash may have skewed the results of this study.

Biomass that underwent torrefaction showed a wide differential in mineral composition. The method of removing all extractives from biomass using two-stage Soxhlet extraction might be a more complete way to further analyze how inorganic compounds affect biomass pyrolysis reactions. A follow-up study of washed and

washed-torrefied biomass could complete this research by confirming many of the models developed during this research.

Advanced development or optimization of the water wash used in this project using elevated water temperatures, acid concentrations, or longer washing times could aid in the ability to purify the biomass. Washing could be used in an industrial processing facility, and the most effective methods for purifying the biomass should be determined.

This project was designed to use the most realistic feedstock possible. The large variables found in the feedstock composition may have been amplified when processing with such a small scale reactor. The wide array of ash content, biomass purity, particle size distributions, and moisture content could be investigated individually to determine the magnitude that each variable has on the overall process. Reactor variables could also be explored in this same fashion. The reactor freeboard size, condenser lengths, and all temperatures in the system could be altered to determine the critical component for the operation of the system.

In commercial fast pyrolysis with a fluidized bed, the fluidization gas cannot be nitrogen. Using the non-condensable gas as a fluidizing gas however requires additional equipment and control. This is practiced in industry and should be studied in the laboratory. The gas compounds may affect the production kinetics during fast pyrolysis which is critical to the operation of a large facility. The gas-solid-liquid interactions in the reactor and the following condensers could become significant at the high temperatures and concentrations.

At the time of this research, a real-time gas analyzer was unavailable for the gas concentration levels produced. Since the completion of this research, De Jaye Technologies, LLC, has provided CSET with a first-of-its-kind on-line gas analyzer for gas concentrations less than 1% in a nitrogen environment. For this project, the producer gas was assumed to have the overall average composition measured by the Micro GC during a test. The average composition then was used to calculate the total non-condensable gases produced during a specific test. The Micro-GC sampled the gas every three minutes. The on-line gas analyzer measures the gas composition every second. This increased resolution should allow for more complete gas analysis and tracking for future tests.

The flow rates of the exhaust were calculated using the concentration of the nitrogen at the exit equal to what was fed into the reactor. For future tests, a low pressure wet-test meter should be used with the new gas analyzer to give a much more accurate on-line analysis of the produced gas composition at the exhaust of the reactor.

BIBLIOGRAPHY

Advantech Manufacturing [Online] // www.advantechmfg.com. - 2001. - November 10, 2008. - http://www.advantechmfg.com/pdf/Principles_Procedures_Manual_with_Tables.pdf.

Agblevor F. A., Besler S. and Evans R. J. Inorganic compounds in biomass feedstocks: Their role in char formation and effect on the quality of fast pyrolysis oils [Conference] // Biomass Pyrolysis Oil Properties and Combusiton Meeting. - Estes Park, CO : U.S. Department of energy, NREL, Natural Resources Canada, VTT energy Finland., 1994. - pp. 76-89.

Agblevor F. A., Besler S. and Wiselogel A. E. Fast Pyrolysis of Stored Biomass Feedstocks [Journal] // Energy and Fuels. - 1995. - 4 : Vol. 9. - pp. 635-640. - DOI: 10.1021/ef00052a010.

Antal M. J., Varhegyi G. and Jakab E. Cellulose Pyrolysis Kinetics: Revised [Journal] // Industrial & Engineering Chemical Research. - 1998. - pp. 1267-1275.

Arias B., Pevida C., Fermoso J., Plaza M. G., Rubiera F. and Pis J. J. Influence of torrefaction on the grindability and reactivity of woody biomass [Journal] // Fuel Processing Technology. - 2008. - 2 : Vol. 89. - pp. 169-175.

Asadullah M., Ali M. A., Rahman M. S., Motin M. A., Sultan M. B. and Alam M. R. Production of bio-oil from fixed bed pyrolysis of bagasse [Journal] // Fuel. - 2007.

Babu B.V. and Chaurasia A. S. Dominant design variables in pyrolysis of biomass particles of different geometries in thermally thick regime [Journal] // Chemical Engineering Science. - 2004. - pp. 611-622.

Baker James B. and Langdon O. Gordon US Forest Service [Online] // Silvics of North America, Volume 1: Conifers. - December 1990. - Feb 8, 2008. - http://www.na.fs.fed.us/pubs/silvics_manual/Volume_1/pinus/taeda.htm.

Ball R., McIntosh A. C. and Brindley J. The role of char-forming processes in the thermal decomposition of cellulose [Journal] // Phys. Chem. Chem. Phys.. - 1999. - pp. 5035-5043, DOI: 10.1039/a905867b.

Bergman P. C. A., Boersma A. R., Zwart R. W. R. and Kiel J. H. A. Torrefaction for biomass co-firing in existing coal-fired power stations [Report] / ECN Biomass. - [s.l.] : ECN-C--05-013, 2005. - pp. 1-72.

Bergman Patrick C. A. and Kiel Jacob H. A. Torrefaction for biomass upgrading [Conference] // 14th European Biomass Conference. - Paris, France : ECN Biomass, ECN-RX--05-180, 2005 b.

Boateng Akwasi, Daugaard Daren E, Goldberg Neil M, and Hicks Kevin B Bench-Scale Fluidized-Bed Pyrolysis of Switchgrass for Bio-Oil Priduction [Journal] // Industrial & Engineering Chemical Research. - [s.l.] : American Chemical Society, 2007. - 46. - pp. 1891-1897.

Bonelli P. R., Della Rocca P. A., Cerrella E. G. and Cukierman A. L. Effect of pyrolysis temperature on composition, surface properties and thermal degradation rates of Brazil Nut shells [Journal] // Bioresource Technology. - 2001. - Vol. 76. - pp. 15-22.

Bridgwater A. V. Fast Pyrolysis of biomass: a handbook [Book]. - [s.l.] : CPL Press, 1999.

Bridgwater A. V. Production of high grade fuels and chemicals from catalytic pyrolysis of biomass [Journal] // Catalysis Today. - 1996. - 1-4 : Vol. 29. - pp. 285-295.

Bridgwater A. V., Meier D. and Radlein D. An overview of fast pyrolysis of biomass [Journal] // Organic Geochemistry. - 1999 b. - 12 : Vol. 30. - pp. 1479-1493.

Bridgwater A.V. and Peacocke G. V. C. An overview of Fast Pyrolysis [Journal] // Progress in Thermochemical Biomass Conversion. - [s.l.] : Blackwell Science Ltd., 2001. - Vol. 2. - pp. 977-997.

Brown Robert C. and Holmgren Jenifer Fast Pyrolysis and Bio-Oil Upgrading [Online] // United States Department of Agriculture. - 2006. - May 22, 2008. - http://www.ars.usda.gov/sp2UserFiles/Program/307/biomasstoDiesel/RobertBrown&JenniferHolmgrenpresentationslides.pdf.

Brown Robert C. Biorenewable Resources: Engineering New Products From Agriculture [Book]. - Ames, IA : Iowa State Press, 2003.

Brue Greg Six Sigma for Small Business [Book]. - Madison, Wisconsin : Entrepreneur Press, 2006.

Coulson M. and Bridgwater A.V. Fast Pyrolysis of annually harvested crops for bioenergy applications [Report]. - Birmingham, UK : Aston Universiy, Bio-Energy Reserch Group, 2003.

Czernik S. and Bridgwater A. V. Overview of Applications of Biomass Fast Pyrolysis Oil [Journal] // Energy and Fuels. - 2004. - 18. - pp. 590-598.

Daugaard Daren E. and Brown Robert C. Enthalpy for Pyrolysis for Several Types of Biomass [Journal] // Energy and Fuels. - 2003. - Vol. 17. - pp. 934-939.

Davidsson K. O., Korsgren J. G., Pettersson J. B. C. and Jaglid U. The effects of fuel washing techniques on alkali release from biomass [Journal] // Fuel. - 2002. - 2 : Vol. 81. - pp. 137-142.

de Jonga W., Pironea A and Wójtowicz M.A. Pyrolysis of Miscanthus Giganteus and wood pellets: TG-FTIR [Journal] // Fuel. - 2003. - pp. 1139-1147.

Della Rocca P. A., Cerrella E. G., Bonelli P. R. and Cukierman A. L. Pyrolysis of hardwood residues: on kinetics and chars characterization [Journal] // Biomass and Bioenergy. - 1999. - pp. 79-88.

Demirbaş A. Mechanisms of liquefaction and pyrolysis reactions of biomass [Journal] // Energy Conversion and Management. - 2000. - 6 : Vol. 41. - pp. 633-646.

Di Blasi Colomba Modeling chemical and physical processes of wood and biomass pyrolysis [Journal] // Progress in Energy and Combusiton Science. - [s.l.] : Elsevier, 2008. - 1 : Vol. 34. - pp. 47-*90.

Di Blasi Colomba Modeling Intra- and Extra-Particle Processes of Wood Fast Pyrolysis [Journal] // AIChE Journal. - 2002. - 10 : Vol. 48. - pp. 2386-2397.

Encarta Encyclopedia Microsoft Encarta Online Fossil Fuels [Online]. - Microsoft Corporation, 2008. - 1997-2008 all rights reserved. - 04 08, 2009. - http://encarta.msn.com.

Ergudenler A., Ghaly A. E., Hamdullahpur F. and Al-Taweel A. M. Mathematical Modeling of a Fluidized Bed Straw Gasifier: Part III - Model Verification [Journal] // Energy Sources. - 1997. - Vol. 19. - pp. 1099-1121.

Fagbemi L., Khezami L. and Capart R. Pyrolysis products from different biomasses: application for the thermal cracking of tar [Journal] // Applied Energy. - 2001. - 69. - pp. 293-306.

Fransham Peter [Patent] : 2351892. - Canada, 2001.

Geldart D Gas Fluidization Technology [Book]. - New York : Wiley, 1986.

Gerdes C., Simon C. M., Ollesch T., Meier D. and Kaminsky W. Design, Construction, and Operation of a Fast Pyrolysis Plant for Biomass [Journal] // Engineering Life Sciences. - 2002. - 6 : Vol. 2. - pp. 167-174.

Goyal H.B., Diptendu S. and Saxena R. C. Biofuels from thermochemical conversion of renewable resources: A review [Journal] // Renewable and Sustainable Energy Reviews. - 2006. - p. doi:10.1016/j.rser.2006.07.014.

Holmgren Jennifer, Marinangeli Richard, Elliot Doug and Bain Richard. Converting Pyrolysis Oils to renewable Transport Fuels: Processing Challenges & Opportunities // National Petrochemical & Refiners Association. - San Diego : UOP LLC, March 9-11, 2008.

Hottle Ryan Comments by Dr. R. K. Pachauri, Chairman of the IPCC, on James Hansen and Biochar [Online] // Global Climate Solutions. - 10 10, 2008. - 02 28, 2009. - http://globalclimatesolutions.org/2008/10/10/comments-by-dr-r-k-pachauri-chairman-of-the-ipcc-on-james-hansen-and-biochar/.

Kawamoto Haruo, Murayama Masaru and Saka Shiro Pyrolysis behavior of levoglucosan as an intermediate in cellulose pyrolysis: polymerization into polysaccharide as key readtion to carbonized product formation [Journal] // Journal of wood science. - [s.l.] : Springer Japan, 2003. - 5 : Vol. 49. - pp. 469-473.

Kersten S. R., Wang X., Prins W. and van Swaaij W. P. Biomass Pyrolysis in a Fluidized Bed Reactor. Part1: Literature Review and Model Simulations [Journal] // Industial & Engineering Chemical Research. - 2005. - pp. 8773-8785.

Kock Peter and McKenzie Dan Machine to Harvest Slash, Brush, and Thinnings for fuel and fiber - A Concept [Journal] // Journal of Forestry. - [s.l.] : Society of American Foresters, December 1, 1976. - 12 : Vol. 74. - pp. 809-812.

Leonard Ingram Dinesh Mohan, Mark Bricka, Philip Steele, David Strobel, David Crocker, Brian Mitchell, Javeed Mohammad, Kelly Cantrell and Charles U. Pittman Jr. Pyrolysis of Wood and Bark in an Auger Reactor: Physical Properties and Chemical Analysis of the Produced Bio-oils [Journal] // Energy & Fuels. - 2008. - pp. 614-625.

Li Shiguang, Xu Shaoping, Liu Shuqin, Yang Chen and Lu Qinghua. Fast pyrolysis of biomass in free-fall reactor for hydrogen-rich gas [Journal] // Fuel Processing Technology. - 2004. - 8-10 : Vol. 85. - pp. 1201-1211.

Luo Z., Wang S., Liao Y., Zhou J., Gu Y. and Cen K. Research on biomass fast pyrolysis for liquid fuel [Journal] // Biomass and Bioenergy. - 2004. - pp. 455-462.

Mahfud Farchad Exploratory Studies on Fast Pyrolysis Oil Upgrading [Book]. - Netherlands : RUG Groningen, 2007.

Mason R. L., F. Gunst. R. and Hess J. L. Statistical Design and Analysis of Experiments [Book]. - Hoboken, New Jersey : Wiley & Sons, 2003. - Vol. 2.

McHenry Mark P. Agricultural bio-char production, renewable energy generation and farm carbon sequestration in Western Australia: Certainly uncertainty and risk [Journal] // Agriculture, Ecosystems & Environment. - 2009. - 1-3 : Vol. 129. - pp. 1-7.

Minkova V., Razvigorova M., Bjornbom E., Zanzi R. and Petrov, N. Effect of water vapour and biomass nature on the yield and quality of the pyrolysis products from biomass [Journal] // Fuel Processing Technology. - 2001. - 1 : Vol. 70. - pp. 53-61.

Mohan Dinesh, Pittman Charles U. Jr. and Steele Philip H. Pyrolysis of Wood/Biomass for Bio-oil: A Critical Review [Journal] // Energy & Fuels. - 2006. - 3 : Vol. 20. - pp. 848-889.

Morris E. Putting the carbon back: black is the new green [Journal] // Nature. - 2006. - Vol. 442. - pp. 624-626.

Mosier Nathan, Wyman Charles, Dale Bruce, Elander Richard, Lee Y. Y., Holtzapple Mark and Ladisch Michael. Features of promising technologies for pretreatment of lignocellulosic biomass [Journal] // Bioresource Technology. - 2005. - 6 : Vol. 96. - pp. 673-686.

NREL Determination of Extractives in Biomass [Report] : Technical Report / U.S DOE and Office of Energy Efficiency and Renewable Energy. - [s.l.] : NREL/TP-510-42619, 2008. - p. http://www.nrel.gov/biomass/pdfs/42619.pdf.

Oasmaa Anja, Peacocke C., Gust S., Meier D. and McLellan R. Norms and Standards for Pyrolysis Liquids. End-User Requirements and Specifications [Journal] // Energy and Fuels. - 2005. - 5 : Vol. 19. - pp. 2155-2163.

Oasmaa Anja, Sipilä Kai, Solantausta Yrjo and Kuoppala Eva. Quality Improvement of Pyrolysis Liquid: Effect of Light Volatiles on the Stability of Pyrolysis Liquids [Journal] // Energy & Fuels. - 2005 b. - 19. - pp. 2556-2561.

Oasmaa Anja and Peacocke Cordner A guide to pysical property characterisation of biomass-derived fast pyrolysis liquids [Book]. - Technical Research Centre of Finland : VTT Publications, 2001.

Onay O. and Kockar O. M. Fixed-bed pyrolysis of rapeseed (Brassica napus L.) [Journal] // Biomass and Bioenergy. - 2004. - Vol. 26. - pp. 289-299.

Prins Mark J., Ptasinski Krzysztof J. and Janssen Frans J. J. G Torrefaction of wood Part 2. Analysis of products [Journal] // Journal of Analytical and Applied Pyrolysis. - 2006 b. - pp. 35-40.

Prins Mark J., Ptasinski Krzysztof J. and Janssen Frans J. J. G. Torrefaction of wood Part1. Weight loss kinetics [Journal] // Journal of Analytical and Applied Pyrolysis. - 2006. - pp. 28-34.

Qiang Lu, Wen-Shi Li and Xi-Feng Zhu Overview of fuel properties of biomass fast pyrolysis oils [Journal] // Energy Conservation Management. - 2009. - p. doi: 10.1016/j.enconman.2009.01.001.

Raveendran K., Ganesh Anuradda and Khilar Kartic C. Influence of mineral matter on biomass pyrolysis characteristics [Journal] // Fuel. - [s.l.] : Elseveier Science Ltd., 1995. - 12 : Vol. 74. - pp. 1812-1822.

Scahill J., Diebold J. P. and Feik C. Removal of residual char fines from pyrolysis vapors by hot gas filtration [Book Section] // Developments in thermochemical biomass conversion / book auth. Bridgwater A. V. and Boocock D. G. B.. - 1997. - Vol. 1.

Scholze B and Meier D. Characterization of the water-insoluble fraction from pyrolysis oil (pyrolytic lignin). Part I. PY-GC/MS, FTIR, and functional groups [Journal] // Journal of Analytical and Applied Pyrolysis. - 2001. - 1 : Vol. 60. - pp. 41-54.

Scott Donald S., Paterson Lachlan, Piskorz Jan and Radlein Desmond Pretreatment of poplar wood for fast pyrolysis: rate of cation removal [Journal] // Journal of Analytical and Applied Pyrolysis. - 2001. - 2 : Vol. 57. - pp. 169-176.

Suarez J. A., Beaton P. A., Zani R. and Grimm A. Autothermal Fluidized Bed Pyrolysis of Cuban Pine Sawdust. Energy Sources Part A:Recovery, Utilization and Environmental Effects [Journal]. - 2006. - Vol. 28. - pp. 695-704.

The American Coal Foundation Glossary [Online] // American Coal Foundation. - 2007. - February 21, 2009. - http://www.teachcoal.org/glossary.html.

U.S. DOE Breaking the Biological Barriers to Cellulosic Ethanol: A Joint Research Agenda, DOE/SC-0095 [(www.doeegenomestolife.org/biofuels/)]. - Rockville, MD : U.S. Department of energy Office of Science and Office of Energy Efficiency and Renewable Energy, 2006.

Uslu Ayla, Faaij Andre P. C. and Bergman P. C. A. Pre-treatment technologies, and their effect on international bio-energy supply chain logistics. Techno-economic evaluation of torrefaction, fast pyrolysis and pelletisation [Journal] // Energy. - [s.l.] : Elsevier, 2008. - 8 : Vol. 33. - pp. 1206-1223.

Venderbosch R. H. and Prins W. Entrained flow gasification of bio-oil for synthesis gas [Online]. - BTG biomass technology group b.v., 2008. - February 12, 2009. - http://www.p2pays.org/ref/35/34029.pdf.

Wang X., Kersten S. R., Prins W., and van Swaaij W. P. Biomass Pyrolysis in a Fluidized bed Reactor. Part 2: Experimental Validation of Model Results [Journal] // Industrial and Engineering Chemical Research. - 2005. - 44. - pp. 8786-8795.

Wei L., Xu S., Zhang L., Zhang H., Liu C., Zhu H. and Liu S. Characteristics of fast pyrolysis of biomass in a free fall reactor [Journal] // Fuel Processing Technology. - 2006. - pp. 863-871.

Williams Christopher, Satrio Justinus, Rover Marjorie, Brown Robert, Shropshire Ryan, and Teng Sheng Utilization of Bio-Oil Fractions as an Asphalt Additive [Online] // Bioeconomy Conference. - September 9, 2008. - 02 10, 2009. - http://www.bioeconomyconference.org/08%20Presentations%20approved/Breakouts/Utilization%20of%20Biobased%20Products/williams,%20chris.pdf.

Wright Mark M., Brown Robert C. and Boateng Akwasi A. Distributed processing of biomass to bio-oil for subsequent production of Fischer-Tropsch liquids [Journal] // Biofuels, Bioproducts and Biorefining. - 2008. - 3 : Vol. 2. - pp. 229-238.

Yang H., Yan R., Chen H., Lee D. H. and Zheng C. Characteristcs of hemicellulose, cellulose and lignin pyrolysis [Journal] // Fuel. - 2007. - p. doi:10.1016/j.fuel.2006.12.013..

Yang H., In-Depth Investigation of Biomass Pyrolysis Based on Three Major Components: Hemicellulose, Cellulose and Lignin [Journal] // Energy and fuels. - 2006. - pp. 388-393.

Zanzi R., Yan R., Chen H., Zheng C. and Lee D. H. Biomass Torrefaction [Online] // Transnational Technologies LLC. - 2008. - 7 20, 2008. - http://www.techtp.com/recent%20papers/Biomass%20Torrefaction.pdf.

Zwart Robin W. R., Boerrigter Harold and van der Drift Abraham The Impact of Biomass Pretreatment on the Feasability of Overseas Biomass Conversion to Fischer-Tropsch Products [Journal] // Energy and Fuels. - 2006. - 5 : Vol. 20. - pp. 2192-2197.

APPENDIX A: DESIGN AND ANALYSIS OF EXPERIMENTS

Adapted from Daren Daugaard, ConocoPhillips, 2008.

Purpose – The purpose of this design and analysis of experiments is to determine the response surface of bio-oil yield and other responses compared to three continuous factors: pyrolysis temperature, moisture content or level of torrefaction, and biomass particle size. Three resulting sets of surfaces responses will result based on the pretreatment received (categorical factor). In addition to the yield response, it is also conceivable to determine other responses such as carbon content of the bio-oil, char yield, etc.

Initially, the strategy will be to study one reactor and one biomass type and perform a statistical analysis on the results to determine the regressed relationship. If successful, it is anticipated that the remaining two reactor designs would be investigated in a similar manner.

Systems and Feedstocks

Reactors – Fluidized Bed (FB)

Biomass –Loblolly Pine slash (LP)

Factors:

Biomass **M**oisture – 3 level (5%, 10%, 15%), Continuous Factor or
or **T**orrefaction – 3 Level (180, 215, 250 ºC), Continuous Factor

Particle **S**ize – 3 level (100, 300, 750, 1500, 4000 μm)*, Continuous Factor

Pyrolysis Temperature – 3 levels (450 ºC, 485 ºC, 520 ºC), Continuous Factor

* Only three levels would be selected from the list for each reactor type, defining the size in terms of hammer mill screen, volumetric diameter, or sieved screen is yet to be determined. It is anticipated that the particle size will be simply defined as the screen size used in the reduction process. Particle size characterization may be required such as sieving.

The anticipated results from this study include relating the bio-oil yield to various factor levels. In addition, the ultimate analysis and HHV will be determined for each reactor feedstock and all products produced for each test. The bio-oil will undergo chemical analysis to determine chemicals present. A governing relationship for each measured result of interest will be established with primary importance placed on bio-oil yield.

For the selected case of pyrolyzing loblolly pine in a fluid bed (**FB-LP**), three continuous factors and one categorical factor are utilized. Because of the categorical factor, three sets of equations (one for each pretreatment) will result with independent variables of temperature (**P**), moisture (**M**), and particle size (**S**). The most likely dependent variable will be bio-oil yield. Again, other dependent variables could be analyzed such as carbon content of bio-oil, char yield, etc.

The primary method considered is a design of experiments utilizing Central Composite design similar in concept to the Box-Behnken with the disadvantage of a few more tests at 60 runs per Reactor – Biomass (R-B) pair (Mason, et al., 2003). This method does test “corner points” as well as “face-centered” points. The design also has replication (6) of the “center” point. The result of this methodology is a quadratic surface regressed from the experimental data. This method has a Resolution IV characteristic which implies that no main effect (single factor) is aliased with any other single factor or with any two factor interaction. However,

main effects are aliased with three factor interactions and two factor interactions are aliased with each other.

Proposed Approach:

The approach proposed is a slightly modified central composite design for **one** R-B case, specifically a fluidized bed processing loblolly pine slash. The central composite design requires 60 runs (Table A1, A2, and A3) for determining the response surface. A modification of the temperature factor occurs for runs 7 and 14 in order to provide additional data at alternative temperatures (Table A5 and A6). In addition to these 60 runs, 10 additional runs (Table A4) are proposed for the remaining R-B cases to determine general relationships to that of the detailed FB-LP case. 5 of these 10 will be at the "center point", while the remaining five will be determined later likely at the best yield case of the FB-LP runs.

The pretreating of the biomass will be conducted internally at COP. For the central composite design, 53 kg of finished loblolly pine is required. With the consideration of non-steady biomass consumption, failed tests, and other miscellaneous issues, this amount is conservatively tripled to 160 kg of pine minimum. A 50% factor plus moisture content should be added for the raw material before pretreatment.

200 kg dry (400 kg wet) will first undergo pretreatment with 1/3 torrefied, 1/3 water washed, and 1/3 receiving no treatment. The biomass will be dried or torrefied in a convection oven in ~10 kg batches under a nitrogen environment.

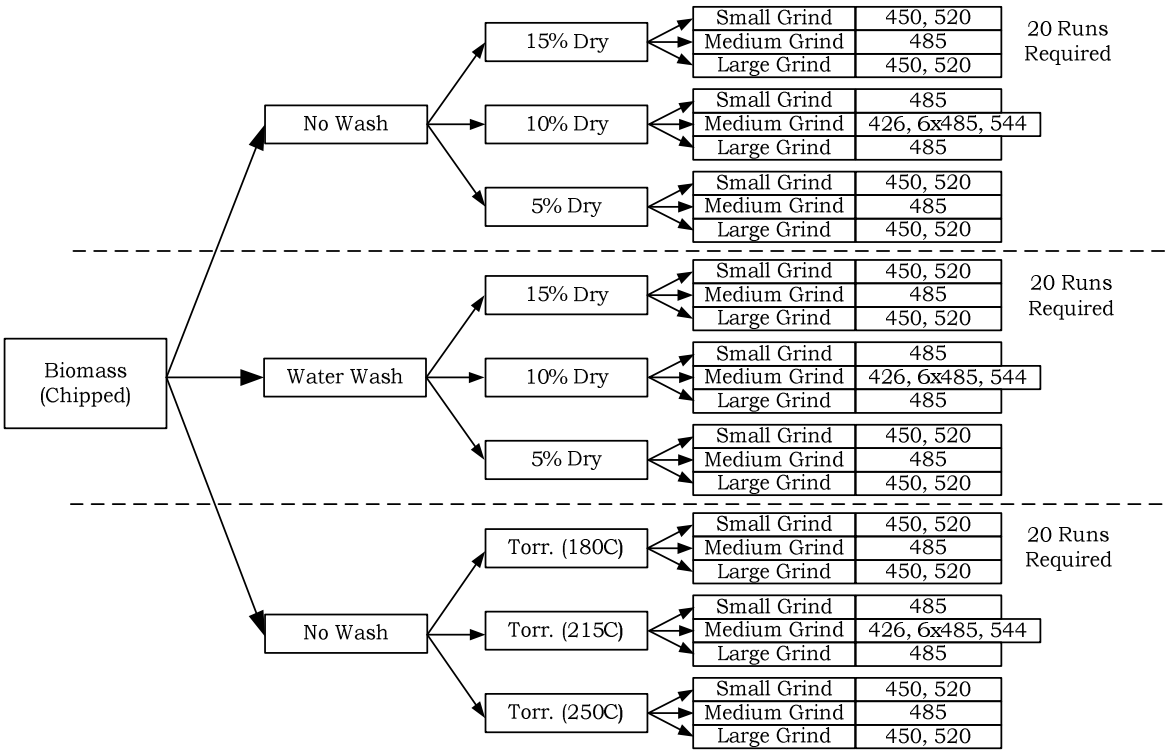

The pretreatment/preprocessing should be performed one pretreatment at a time. All water washed material should be processed at one time as should all acid washed material. ISU will pyrolyze the biomass in a pseudo-random fashion. While the pretreatment will not occur in a random order, all other variables will in an effort to minimize time between runs for the same pretreatment. Note than in addition to determining products yield, a characterization of the biomass and the pyrolyzed products will be performed in order to determine carbon balance and other pertinent information.

The results gained from this design of experiments can be applied to the conceptual design task of the characterization plan. Specially, any response equations such as a function of pretreatment, temperature, moisture content, and particle size can be applied in Aspen Plus for modeling considerations.

Central composite design for wahsed and unwashed loblolly pine slash

Run	Moisture contetnt	Grind size	Pyrolysis temperature
1	-1	-1	-1
2	-1	-1	1
3	-1	0	0
4	-1	1	-1
5	-1	1	1
6	0	-1	0
7	0	0	-1.68
8	0	0	0
9	0	0	0
10	0	0	0
11	0	0	0
12	0	0	0
13	0	0	0
14	0	0	1.68
15	0	1	0
16	1	-1	-1
17	1	-1	1
18	1	0	0
19	1	1	-1
20	1	1	1

Central composite design for torrefied loblolly pine slash

Run	Torrefaction temperature	Grind size	Pyrolysis temperature
1	-1	-1	-1
2	-1	-1	1
3	-1	0	0
4	-1	1	-1
5	-1	1	1
6	0	-1	0
7	0	0	-1.68
8	0	0	0
9	0	0	0
10	0	0	0
11	0	0	0
12	0	0	0
13	0	0	0
14	0	0	1.68
15	0	1	0
16	1	-1	-1
17	1	-1	1
18	1	0	0
19	1	1	-1
20	1	1	1

APPENDIX B: DESIGN CALCULATIONS

Nomenclature

Ar - Archimedes number
C_d - Gas flow factor for tube diameter
C_{or} - Gas flow factor for distributor orifice
d_{bed} - Diameter of bed
d_{bubble} - Diameter of gas bubble
d_c - Char diameter
d_p - Feedstock particle diameter
d_{or} - Orifice diameter
f_{or} - Orifice restriction factor
g - Gravitational acceleration
L_f - Length of fluidized bed
P_{atm} - Atmospheric pressure
s - Distance between orifice centers
T_{bed} - Temperature of fluidized bed
T_{atm} - Temperature of environment
U_{mf} - Minimum fluidization gas velocity
U_f - Actual fluidization velocity
V_c - Char elutriation velocity
ΔP_{bed} - Pressure drop across sand bed
ΔP_d - Pressure drop across distributor plate
ρ_p - Feedstock particle density
ρ_g - Gas density
ρ_c - Char density
μ - Gas viscosity
ε_{mf} - Voidance in sand bed

B.1 Reactor design

The reactor was designed to pyrolyze 100 g/hr of finely ground biomass with nitrogen as the fluidizing gas, and sand as the bed media. The residence time for the gas was designed to remain less than 1 second from leaving the bed, to the time they were cooled down to 100ºC.

The proper gas velocity in a bubbling fluidized bed was determined to fluidize the bed at 2 – 3 times the velocity required for minimum fluidization (Geldart, 1986).

$$U_f = [2 \text{ to } 3] \cdot U_{mf}$$

The minimum fluidization velocity is determined through a standard equation that uses geometric and quantitative properties of the system.

$$U_{mf} = \frac{\mu}{\rho_g d_p}\left[\left(1135.7 + 0.0408Ar\right)^{0.5} - 33.7\right]$$

The equation to determine the minimum fluidization velocity uses a dimensionless Archimedes number to correlate the regime where the sand particles will become suspended in the gas flow stream.

$$Ar = \frac{\rho_g d_p^3 \left(\rho_p - \rho_g\right) g}{\mu^2}$$

The gas velocity within the reactor was determined to properly elutriate char from the bed when it had completely volatilized as well as be sufficiently fluidized. 50 μm char was used for this model shown below.

$$V_c = \left[\frac{4 g d_c \left(\rho_p - \rho_g\right)}{3 \rho_g C_d}\right]^{0.5}$$

This equation required an iteration to be solved. This is done using the following two equations.

$$C_d = \frac{10}{\text{Re}} \text{ for } 0.5 < \text{Re} < 500$$

$$\text{Re} = \frac{d_c V_c \rho_c}{\mu}$$

These equations defined the gas velocity that is required for the reactor. This in turn set a correlation between the diameter of the reactor and the nitrogen flow rate to achieve the proper gas velocity rates. The total reactor height is based on the fact that the residence time is to be kept below 1.0 seconds.

The bed is surrounded by a 900 W electric ceramic shell heater that radiates heat into the bed to minimize any heat loss. The freeboard is surrounded by an 1800W electric ceramic shell heater to preheat and minimize any heat loss from the reactor.

The sand bed will create a pressure differential between the bottom and top of the bed. This pressure differential is a function of the bed properties and dimensions.

$$\Delta P_{bed} = \rho_p g L_f \left(1 - \varepsilon_{mf}\right)$$

The fluidized bed reactor was manufactured out of 38.1mm schedule 40, 316 stainless steel tubing and standard flanges. Biomass is fed into the reactor pneumatically through a 6.53mm diameter thin wall stainless steel tube. Biomass is fed into the tube by an electronically controlled metering auger. Nitrogen gas at room temperature is used for the pneumatic fluid. The flow is controlled by an electronic mass flow controller. The biomass is fed directly into the bottom of the fluidized bed through the side of the reactor. The bed is fluidized by heated nitrogen gas. The gas flow is controlled by an electronic mass flow controller, and fed into the bottom the reactor. A plenum section is fixed below the fluidized bed. The nitrogen is first heated in the plenum while flowing through a packed bed of hot steel beads. The plenum is heated by a 900 W electric ceramic shell heater surrounding the plenum section. The gas flows from the plenum to the bed through a perforated distributor plate. The distributor plate is designed to have a pressure drop correctly related to the pressure drop in the bed.

$$\frac{\Delta P_d}{\Delta P_{bed}} = 0.01 + 2\left(1 - e^{-\frac{d_{bed}}{2L_f}}\right)$$

To properly determine the pressure drop across the distributor, the orifice size and instance must be known. Using an equation to verify correct the velocity through the orifice along with an equation to determine the drag through an orifice, the correct fractional area can be solved for from varying the diameter of the orifice.

$$\frac{U_f}{U_{mf}} > 1 + \left(1 - \frac{2}{\pi}\right)\frac{2\rho_p g\left(1-\varepsilon_{mf}\right)L_f}{\rho_g}\left(\frac{C_d f_{or}}{U_{mf}}\right)^2$$

$$C_d = 0.82\left(\frac{t_d}{d_{or}}\right)^{0.13}$$

$$f_{or} = \frac{U_f}{C_d}\sqrt{\frac{\rho_g}{2\Delta P_d}}$$

$$U_{or} = C_{or}\sqrt{\frac{2\Delta P_d}{\rho_g}} = \frac{U_f}{f_{or}}$$

The distributor plate also needed to be drilled so that the entering gas was evenly distributed across the entire bed. It was chosen to use an equilateral triangle geometric spacing to fit the proper number of holes into the limited area. The correct distance between holes is calculated to eliminate premature bubble coagulation.

$$\frac{s}{d_{or}} = \frac{0.9523}{\sqrt{f_{or}}}$$

The reactor then incorporated a 304.8 mm freeboard above the bed. The freeboard section is heated by a ceramic electric guard heater to eliminate heat loss from the small scale reactor. Glass wool is used for insulation on all exposed steel areas that are not heated to reduce the amount of heat loss from the reactor.

Design constraints		
Operating temperatere	500	°C
Feed rate	100	g/hr
Gravity	9.81	m/s^2
Pressure	1	atm
Biomass type	Loblolly pine slash	
Fluidizing gas	N_2	
Gas constant	0.0821	(L*atm)/(K*mol)
Bed media	sand	
Reactor material	316SS	
Wall thickness	2.8	mm

Distributor plate information

Bed diameter	3.81	mm
Length of bed	7.62	mm
Orofice diameter	1.8	mm
Pressure drop over bed	1011	Pa
Pressure drop over plate	54.8	Pa
Thickness of plate	4.76	mm
Number of orifices	25	
Center hole spacing	7.20	mm

Material Properties

Biomass

Molar mass	17.85	kg/kmol
Pyrolysis entropy	1.8	kJ/kg
Maximum size	0.8	mm

Sand

Diameter	8.0E-04	m
Density	2600	kg/m^3
Spherocity	0.75	
Voidance	0.4	

Char

Density	400	kg/m^3
Diameter max	750	μm
Diameter min	25	μm

Nitrogen

Viscocity at 25°C	1.8E-05	kg/m^2
Viscocity at 500°C	3.4E-05	kg/m^2
Molar mass	28	kg/kmol
Inlet temperature	25	°C
Process temperature	500	°C
Specific heat	1081	J/(kg*K)
Temperature in cyclone	400	°C
Temperature at ESP inlet	80	°C
Temperature at exhaust	10	°C

Flow Rates

Nitrogen into reactor	18	lpm
Gas out of reactor	52	lpm
Gas into initial condenser	43	lpm
Gas into ESP	23	lpm
Gas out of final condenser	18	lpm

B.2 Cyclone design

The cyclone is a basic piece of equipment that is used to separate particulate matter from a gas stream. The cyclone works best with unlimited pressure drop allowances and with very high gas flow rates. The cyclone used for this reactor was required to be small enough to accommodate for the flow rates that are expected during normal operation.

It was desired that the pressure drop in the cyclone be minimized to reduce the pressure required in the reactor. The particle diameters to be filtered are set at 5μm. This is rather arbitrary, but used as a basis for vary fine particulate that may elutriate from the bed. This is only a theoretical cut rate based on the geometry of the cyclone. The dimensioned parameters were calculated based on Figure B1. The dimensions were changed until a proper operating efficiency was achieved, and resulted in a size that was still able to be manufactured. The data is shown in Table that was used in the design of the cyclone used for the experimentation.

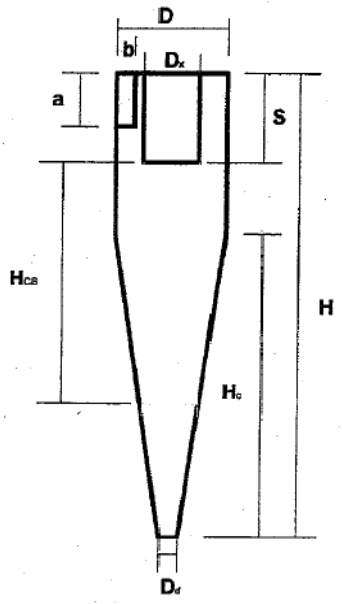

Figure B1: Cyclone dimentioning

The cyclone operated as expected. The cyclone that was used for the reactor used circular entrance geometry rather than a rectangular as shown in the picture. The hydraulic diameter of the circle was the same as what would have been used with the designed rectangle. It was suspected that this geometrical change did have an effect on the overall efficiency and operation of the small cyclonic filter.

Table B1: Cyclone operational values

Operational values

Description	Symbol	Calculations	Value	
Dimension	a		0.0127	m
Dimension	b		0.005588	m
Dimension	D		0.0381	m
Dimension	Dx		0.0127	m
Dimension	Dd		0.0127	m
Dimension	S		0.01905	m
Dimension	H		0.0762	m
Dimension	Hc		0.0508	m
Particle size	dp		5	µm
Standard flow	Qs		**20**	liters/min
Ambient temperature	Ts		298.15	K
Ambient temperature	Ps		101325	Pa
Char/Cyclone temperature	Tc	~450degrees C	748.15	K
Char pressure	Pc		101325	Pa
Volume flow	Q	Qs*(Tc/Ts)*(Ps/Pc)	50.186148	L/min
Volume flow	Q		0.0008364	M^3/sec
Roughness coefficient	co		0.056	
Density	ρ		400	kg/m^3
viscosity	µ N2		0.0000351	Ns/m^2
Dimension	R	D/2	0.01905	m
Dimension	Rx	Dx/2	0.00635	m
Dimension	Rd	Dd/2	0.00635	m
Inlet velocity	Vin	Q/(a*b)	11.786	m/s
Eq. inlet radius	Rin	R-b/2	0.01626	m
Height of imaginary cylinder surface	Hcs	(H-S)-Hc*((Rx-Rd)/(R-Rd))	0.05715	m
Radial Velocity	VrCS	Q/(pi*Dx*Hcs	0.36681	m/s
constriction coeff.	alph	1.04(b/R)^.5	0.56327	
Tangent wall velocity	Vsw	Vin*Rin/(alph*R)	17.855	m/s
Friction factor	f	.005(1+3*co^.5)	0.00855	
tangent cylinder surface velocity	Vscs	Vsw*(R/Rx)/(1+Hcs*R*pi*f*Vsw/Q)	32.978	m/s
cut diameter	dp50	((VrCS*9*mu N2*Dx)/(Ro p*Vscs^2))^.5	0.00000184	m
eff curve	N(dp)	1/(1+(dp50*10^6/dp)^6.4)	0.99834	

B.3 Condenser design

After char particulate was filtered using the cyclone the gas stream entered the condensing system. The first condenser inlet temperature is kept between 400°C and 420°C. This is done with a high wattage heat tape controlled by LabView and a thermocouple on the outer wall of the process tube after the cyclone and before the first condenser inlet. The wall temperature was monitored so that heat loss from the pipe was kept to a minimum.

The first two condensers were constructed from stainless steel quick-connect sanitary piping. The size and shape of the condensers were modeled directly from a glass condenser that was used during condenser development. The first two condensers form an "H" shape with two collection cups at each direction. The condenser set-up has an inlet at the top left, exit at the top right, and two collection ports at the bottom left and right corners. The left half of the condenser (condenser 1) was kept warm with a copper tube wrapped tightly around the entire surface with hot tap water circulating through it at 45˚C. This was done to allow the walls of the condenser high enough to allow for the thick bio-oil to run down the walls, but not so hot that bio-oil was cooked into secondary char. The tube ID was 2.25cm. The gas traveled 30cm through condenser 1, and an additional 30cm through condenser 2. The gas flow rate can be assumed to be the nitrogen plus any gases volatilized from the reactor. The volatile gases mass flow should account for 85% of the biomass that is fed into the reactor. Using the ideal gas law and average molecular weights of bio-oil and gas, this gives a standard correlation of 20 liters per minute of pyrolysis gas for every kilogram of biomass fed per hour. This is also assuming the gases are at 450-500°C.

Initially the gas will be this sum together to shown the volumetric flow rate of gas through the reactor. The small fluidized bed reactor feeds 100grams per hour. As shown in Equation 16

$$20\frac{lpm}{\frac{kg}{hr}} * 0.1\frac{kg}{hr} = 2\ lpm_{pyrolysis\ gas}$$

The nitrogen in the exit steam is eighteen standard liters per minute and must be calculated for 450°C for when it enters the condenser. This flow rate is fifty liters per minute at the elevated temperature. The total gas flow entering into the condenser is fifty two liters per minute.

$$Q_{Nitorgen} + Q_{Pyrolysis\ gas} = 50_{l\ pm} + 2_{l\ pm} = 52_{lpm}$$

The right side of the condenser (condenser 2) was operated in the same manner but rather circulated cold tap water to reduce the gas vapor to a manageable temperature. The exiting vapors are kept between 70 and 85˚C depending on the operating conditions. The dimensions of condenser 2 was the exact same as condenser 1.

The dimensions were originally based on mimicking the size and heat transfer area of small glass impingers. The plow through the condensers was designed to remain laminar.

After exiting condenser 2 the gas entered an electrostatic precipitator (ESP). The ESP was designed to have flow at Reynolds number less than 1, an operating voltage of -20kV, and a theoretical efficiency above 99.99%. The diameter of the tube is 38.1mm. It was constructed out of stainless steel sanitary tubing. The ESP has a collection port at the bottom of the tube for bio-oil collection. Some heat loss occurred in the ESP resulting in small amount of condensable compounds being collected.

The gas flow then enters a final heat exchanger to collect any remaining condensable bio-oil. The gas enters a 9.525mm OD stainless steel thin wall tube that is coiled in a salt-ice bath. Approximately 2.5m of tube length is coiled into the ice bath. The collected liquid flowed into a collection port under the ice bath. The gas exited at a temperature around 5˚C.

B.4 Part drawings

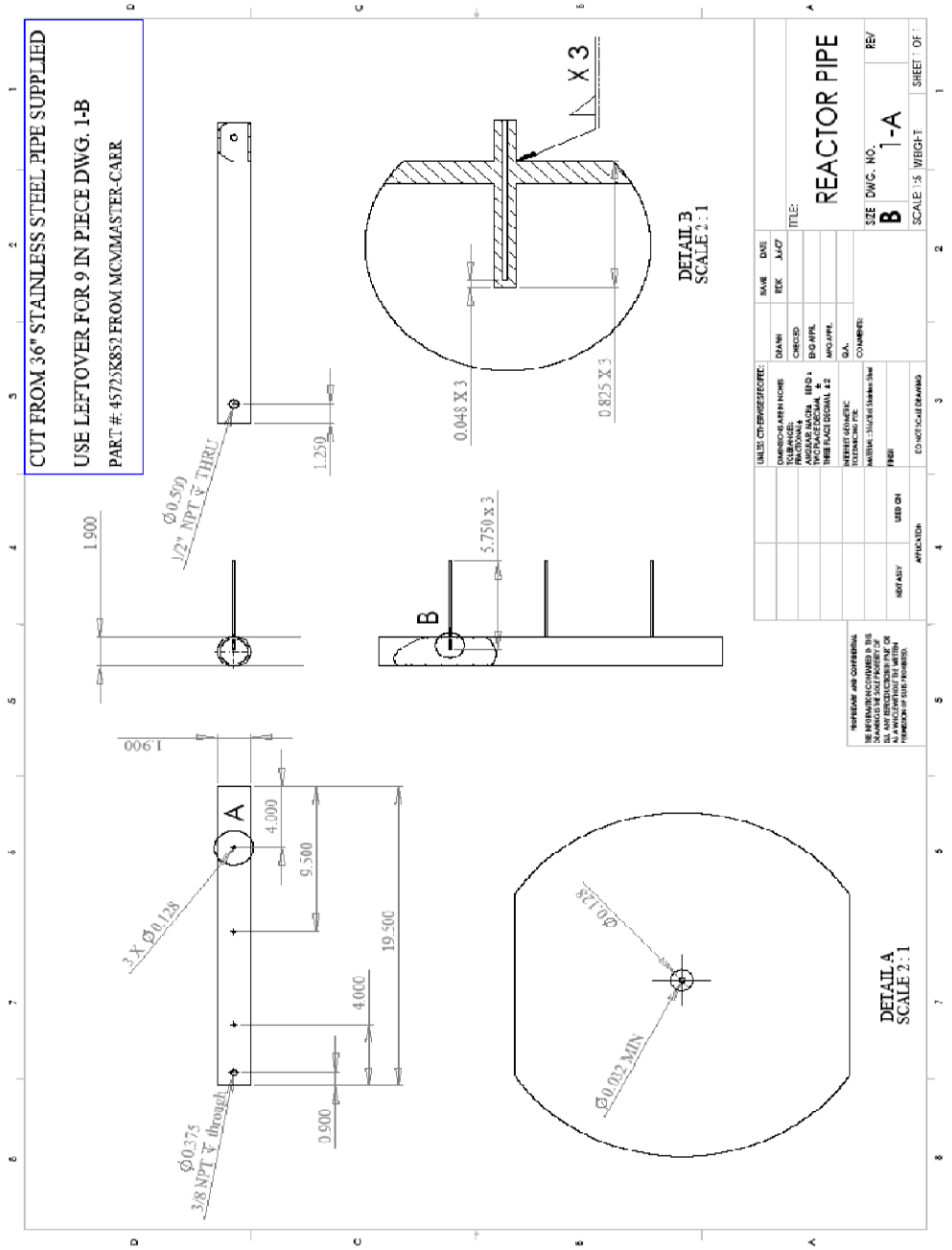

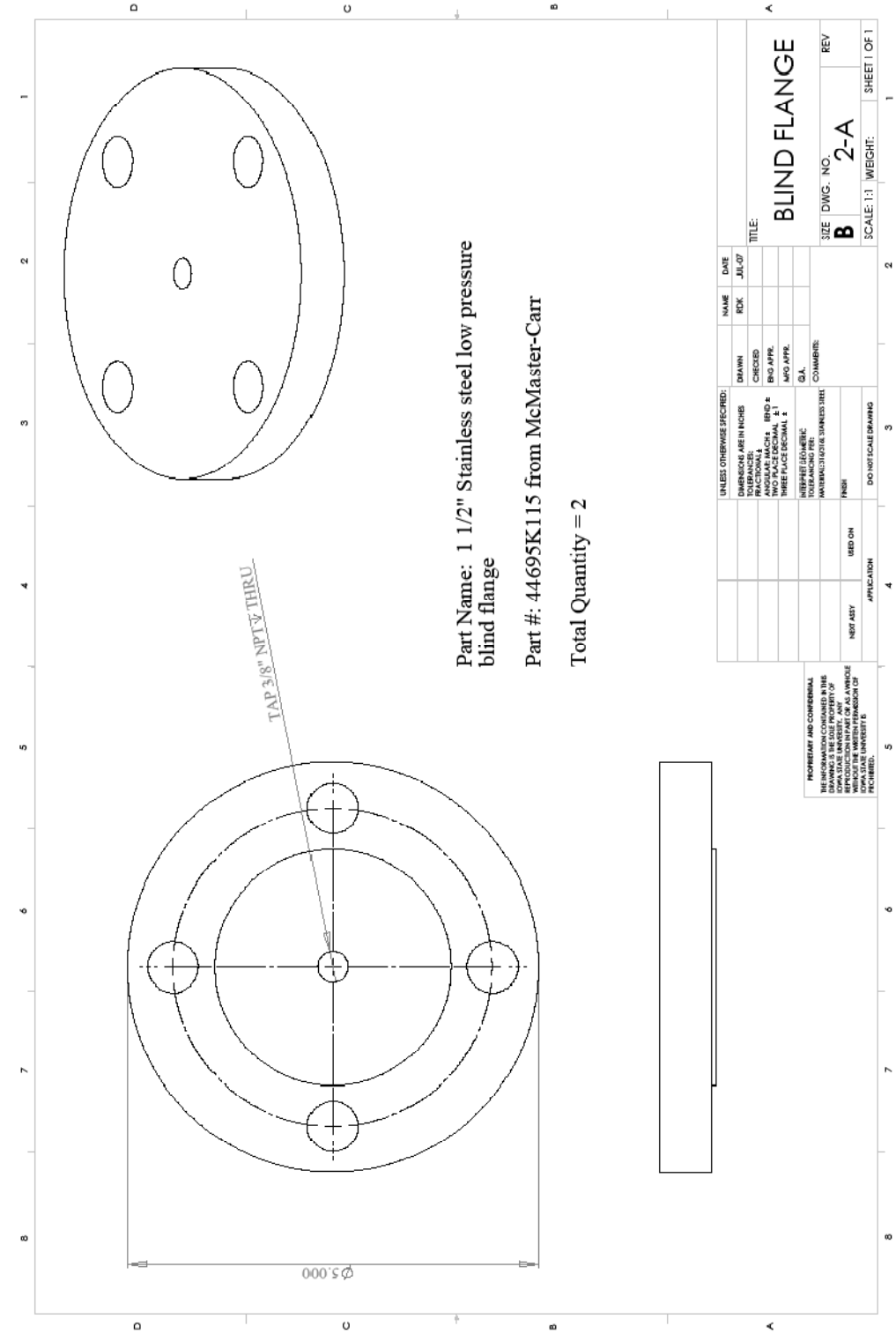
TAP 3/8" NPT ↧ THRU
Ø5.000
Part Name: 1 1/2" Stainless steel low pressure blind flange
Part #: 44695K115 from McMaster-Carr
Total Quantity = 2
BLIND FLANGE
2-A
B
SCALE: 1:1
WEIGHT:
SHEET 1 OF 1
DRAWN
CHECKED
ENG APPR.
MFG APPR.
Q.A.
COMMENTS:
NAME
DATE
RDK
JUL-07
UNLESS OTHERWISE SPECIFIED:
DIMENSIONS ARE IN INCHES
TOLERANCES:
FRACTIONAL ±
ANGULAR: MACH ± BEND ±
TWO PLACE DECIMAL ± 1
THREE PLACE DECIMAL ±
INTERPRET GEOMETRIC
TOLERANCING PER:
MATERIAL
FINISH
NEXT ASSY
USED ON
APPLICATION
DO NOT SCALE DRAWING
PROPRIETARY AND CONFIDENTIAL
THE INFORMATION CONTAINED IN THIS DRAWING IS THE SOLE PROPERTY OF IOWA STATE UNIVERSITY. ANY REPRODUCTION IN PART OR AS A WHOLE WITHOUT THE WRITTEN PERMISSION OF IOWA STATE UNIVERSITY IS PROHIBITED.

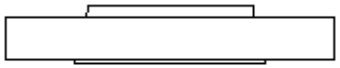

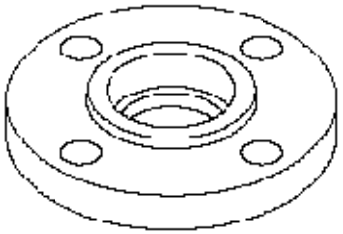

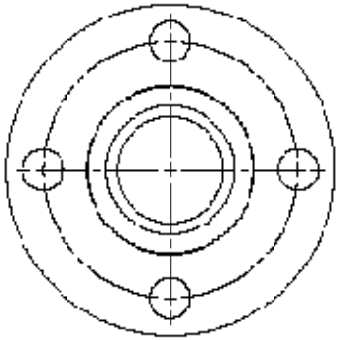

NO MODIFICATION NECESSARY

PART #:44695K55 MCMASTER-CARR

		UNLESS OTHERWISE SPECIFIED:		NAME	DATE
		DIMENSIONS ARE IN INCHES TOLERANCES: FRACTIONAL ± ANGULAR: MACH ± BEND ± TWO PLACE DECIMAL ± THREE PLACE DECIMAL ±	DRAWN		
			CHECKED		
			ENG APPR.		
			MFG APPR.		
		INTERPRET GEOMETRIC TOLERANCING PER:	Q.A.		
		MATERIAL 316L STAINLESS STEEL	COMMENTS:		
NEXT ASSY	USED ON	FINISH			
APPLICATION		DO NOT SCALE DRAWING			

TITLE:

WELD FLANGE

SIZE	DWG. NO.	REV
A	2-B	
SCALE: 1:2	WEIGHT:	SHEET 1 OF 1

5 4 3 2 1

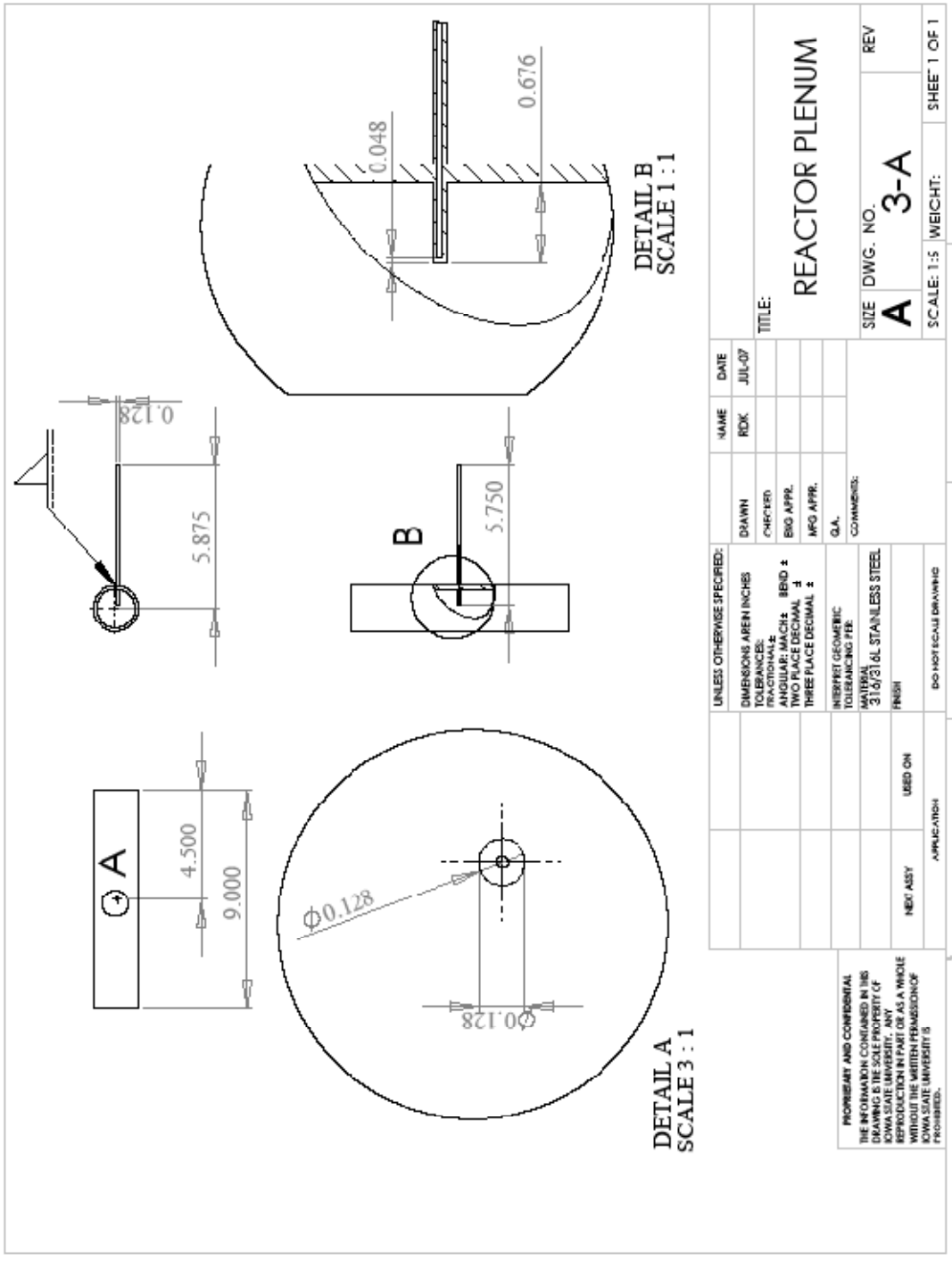
A
4.500
9.000
ϕ0.128
ϕ0.128
DETAIL A
SCALE 3 : 1
0.128
5.875
B
5.750
0.048
0.676
DETAIL B
SCALE 1 : 1
UNLESS OTHERWISE SPECIFIED:
DIMENSIONS ARE IN INCHES
TOLERANCES:
FRACTIONAL ±
ANGULAR: MACH ± BEND ±
TWO PLACE DECIMAL ±
THREE PLACE DECIMAL ±
INTERPRET GEOMETRIC TOLERANCING PER:
MATERIAL
316/316L STAINLESS STEEL
FINISH
DO NOT SCALE DRAWING
NAME
DATE
DRAWN
RDK
JUL-07
CHECKED
ENG APPR.
MFG APPR.
Q.A.
COMMENTS:
TITLE:
REACTOR PLENUM
SIZE
A
DWG. NO.
3-A
REV
SCALE: 1:5
WEIGHT:
SHEET 1 OF 1
NEXT ASSY
USED ON
APPLICATION
PROPRIETARY AND CONFIDENTIAL
THE INFORMATION CONTAINED IN THIS DRAWING IS THE SOLE PROPERTY OF IOWA STATE UNIVERSITY. ANY REPRODUCTION IN PART OR AS A WHOLE WITHOUT THE WRITTEN PERMISSION OF IOWA STATE UNIVERSITY IS PROHIBITED.

EACH PART DWG. NUMBER IS SPECIFIED

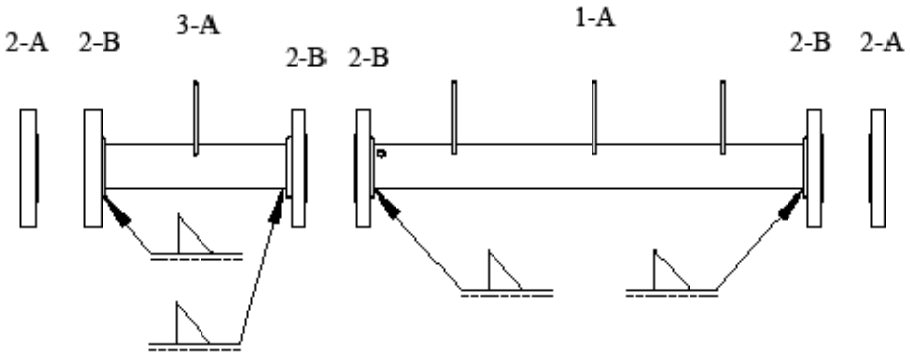

UNLESS OTHERWISE SPECIFIED:		NAME	DATE		
DIMENSIONS ARE IN INCHES TOLERANCES: FRACTIONAL ± ANGULAR: MACH ± BEND ± TWO PLACE DECIMAL ± THREE PLACE DECIMAL ±	DRAWN	RDK	JUL-07	TITLE: ASSEMBLY	
	CHECKED				
	ENG APPR.				
	MFG APPR.				
INTERPRET GEOMETRIC TOLERANCING PER:	Q.A.				
MATERIAL 316L STAINLESS STEEL	COMMENTS:			SIZE A	DWG. NO. 1-B
FINISH					REV
NEXT ASSY / USED ON				SCALE: 1:10	WEIGHT:
APPLICATION					SHEET 1 OF 1
DO NOT SCALE DRAWING					

5 4 3 2 1

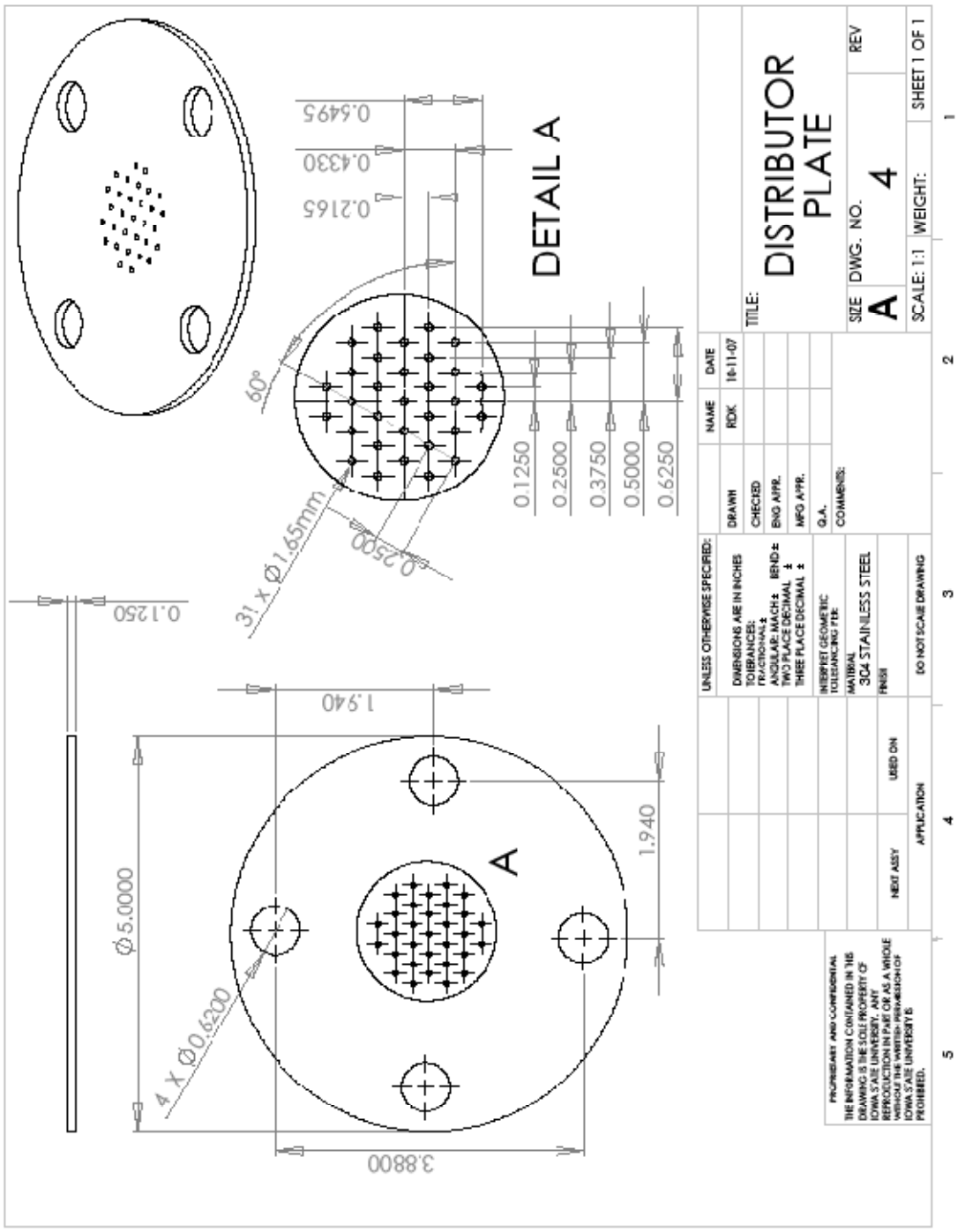
DETAIL A
DISTRIBUTOR PLATE
A
4
SCALE: 1:1
WEIGHT:
SHEET 1 OF 1
DRAWN
RDK
16-11-07
CHECKED
ENG APPR.
MFG APPR.
Q.A.
COMMENTS:
304 STAINLESS STEEL
DO NOT SCALE DRAWING
0.1250
0.2500
0.3750
0.5000
0.6250
0.2165
0.4330
0.6495
60°
31 X Ø1.65mm
0.2500
1.940
3.8800
Ø5.0000
4 X Ø0.6200
PROPRIETARY AND CONFIDENTIAL
THE INFORMATION CONTAINED IN THIS DRAWING IS THE SOLE PROPERTY OF IOWA STATE UNIVERSITY. ANY REPRODUCTION IN PART OR AS A WHOLE WITHOUT THE WRITTEN PERMISSION OF IOWA STATE UNIVERSITY IS PROHIBITED.

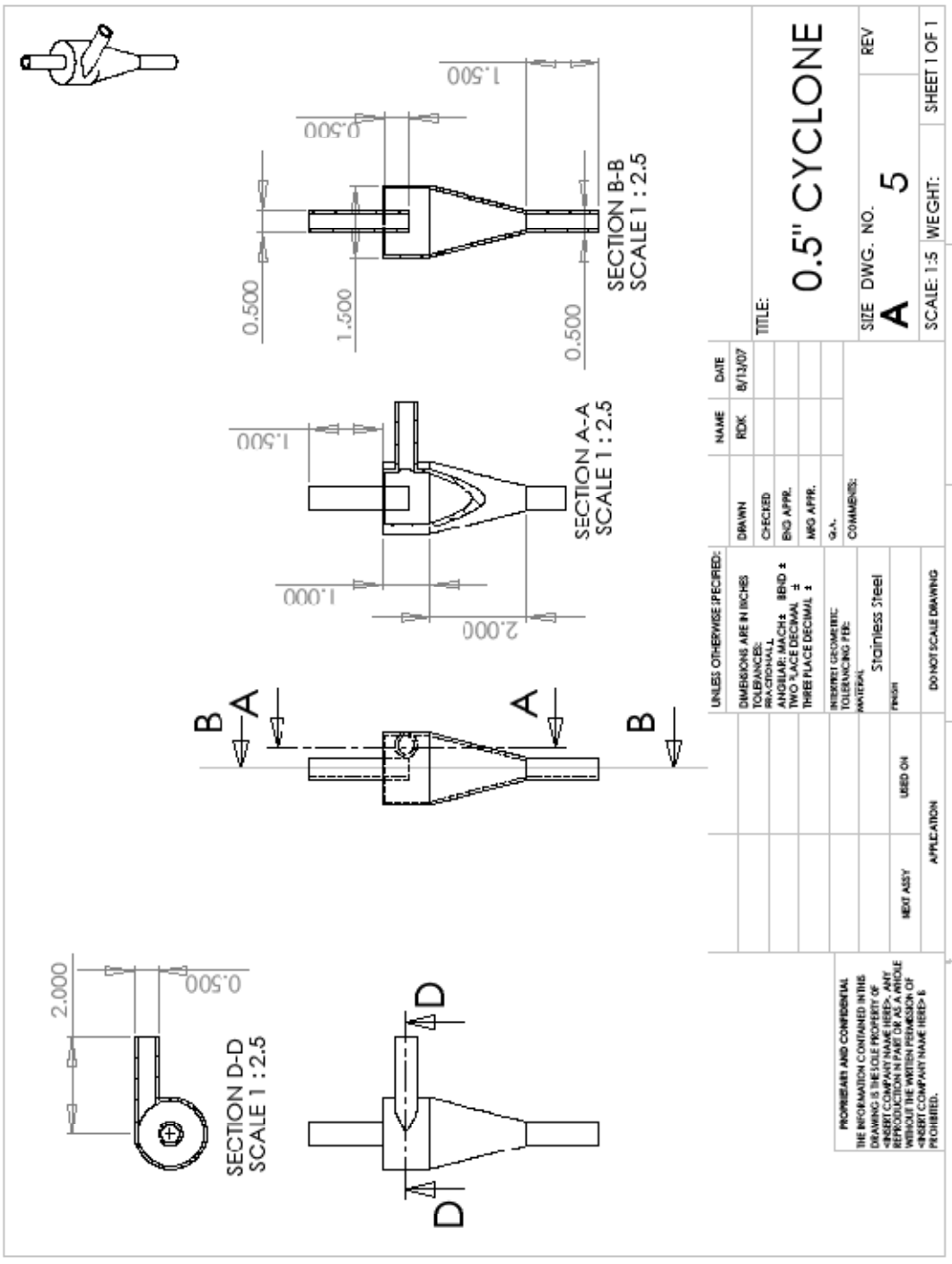
0.5" CYCLONE
SECTION A-A
SCALE 1 : 2.5
SECTION B-B
SCALE 1 : 2.5
SECTION D-D
SCALE 1 : 2.5
Stainless Steel
SIZE DWG. NO.
A 5
REV
SCALE: 1:5
WEIGHT:
SHEET 1 OF 1
DRAWN
RDK
8/13/07
CHECKED
ENG APPR.
MFG APPR.
COMMENTS:
DO NOT SCALE DRAWING
PROPRIETARY AND CONFIDENTIAL

APPENDIX C: MINI PYROLYSIS REACTOR STANDARD OPERATING PROCEDURE

Mini Pyrolysis Reactor

Standard Operating Procedure

2nd Edition

CSET – ISU

Location: 278 Metals Development

Emergency Contacts:

Responsible Student/Post Doc: Randy Kasparbauer

Lab Supervisors: Randy Kasparbauer
Pedro Ortiz

Group Leader: Samuel Jones
Robert C. Brown

Description

The Mini Pyrolysis Reactor is an experimental device for the thermochemical fast pyrolysis of organic matter. Ground biomass is fed with an auger from a sealed hopper. The particles are transported pneumatically, using nitrogen gas from a compressed nitrogen cylinder. When in operation, the biomass is fed into a fluidized sand bed that is operated at an elevated temperature less than 1000°C and above 300° C. The heaters, motor, and data acquisition system are all powered by 120VAC. This apparatus is designed, used, and maintained by the Center for Sustainable Environmental Technologies (CSET). The equipment will be used to produce crude bio-oil, char, and product gases. Each product will be analyzed for content and production levels. Figure 1 & 2 denote a rendered model and actual photo of the apparatus located in a hood vent in 278 Metals Development.

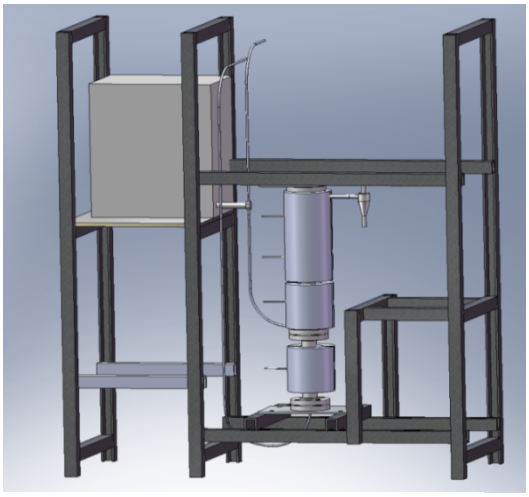

Figure C1: Model of mini pyrolysis reactor

Figure C2: Photo of mini pyrolysis reactor

Potential Hazards

Electrical Shock: This lab utilizes 120, and 24 V power to energize the heaters, motors, and all other equipment associated with the pyrolyzer. When working with or around high voltage caution is required from the operator to ensure safety. Examples of 120 V power include heat tapes and most of the power outlets in the lab. Examples of 24 V power can be found in the data acquisition system. Always disconnect power and follow proper lock out tag out procedure during maintenance.

The electrostatic precipitator (ESP) is an industrial device that uses static charge to clean the incoming gas stream. The ESP is operated at 20kV and should be used with extreme caution to protect other sensitive electronic devices. The ability for the ESP to create a painful spark is very real. Although the power source is not strong enough to cause death from a short exposure, extreme pain, burning, or death could result from an extended short.

Burns: The reactor will be heated by ceramic haters and heat tape when in operation. These may be in excess of 500°C. Keep vent sash closed whenever possible, and always avoid direct contact to the ceramic heaters or the reactor cyclone during or after a test. Heat will be held in the steel parts for up to 3 hours after a test has been completed. Always assume the parts are hot unless confirmed otherwise by at least two sources. An example of two sources are a hand held thermometer and the thermocouple sensors in the Lab View program.

The fumes exiting the reactor can be very hot. Do not put any unprotected body part near an exit gas stream. Proper personal safety equipment includes ceramic heat gloves and long sleeves.

Mechanical Hazards: The biomass feeder contains a motorized auger. Never run the auger unless the cover is on the feeder and the auger is connected to the reactor feed tube or the calibration tube.

Poisonous Gas: The gas being exhausted from the reactor can contain gases poisonous to inhale. The gas is oxygen free and can cause asphyxiation if concentrations become too high. Be sure gas is exhausted only into the vent hood, and only with the vent hood fan at full velocity.

Dust: The biomass and char produced from the reactor can cause respiratory irritation if inhaled. Use proper respiratory protection when working with either material in large quantities.

Chemical: The bio-oil produced during pyrolysis will stain the skin and clothing if contacted. Always wear proper protective equipment when handling bio-oil and during the experiment tests.

Required Personal Protective Equipment (PPE)

Safety Glasses: Regardless of the task being completed, anyone entering the lab must wear safety glasses.

Face Shield: Whenever extra protection is required for the face, eyes, or neck a face shield should be worn. Examples of use include grinding or cutting operations. The face shield is not a substitute for safety glasses and both should be used if the face shield is required.

Respiratory Protection: Inhalation hazards have potential to cause harm in the lab. Always wear appropriate respiratory protection whenever handling biomass, char, sand, limestone, or any other fine particulate matter which could become airborne and pose an inhalation threat. Respiratory PPE should be labeled with the operators name or initials and stored in a sealed Ziploc bag in the media preparation room.

Hearing Protection: Hearing hazards are a potential problem in the lab. Always wear appropriate hearing protection when working in a loud environment. Examples of this include grinding, cutting, or anything else that causes excessive noise.

Hand/Arm Protection: Skin contact hazards can come from particulate, high temperatures, or chemicals in this lab. When working with chemicals appropriate chemically resistant gloves (e.g. latex or nitride) must be worn. Be sure to read MSDS for the chemical in question before using to help in glove selection. When working with particulate matter or splintering materials use appropriate glove (e.g. leather). When working with hot surfaces, use heat resistant gloves and attempt to

use tools rather than directly touching the hot equipment. Lastly, in all situations when it appears handling these dangerous materials is necessary, try to find safer alternatives.

Foot Protection: Closed toed shoes are required at all times while in the lab (e.g. no sandals or perforated shoes). Steel toed footwear is recommended for doing heavy lifting and moving compressed gas cylinders.

Head Protection: A hard hat should be worn whenever work is occurring over your head, regardless of whether it is you or another operator performing the work.

Handling and Storage

A typical pyrolysis experiment includes operator contact with materials being introduced into the reactor and samples being produced by it. There is a proper way to prepare for, handle, and store all of these materials.

Biomass: Biomass is required for every pyrolysis experiment regardless of the simplicity or complexity. There are some simple procedures which can be followed to ensure that handling biomass leads to a safe and successful test. Before biomass can be used with the feed system in the lab, it must be finely ground. For this reason, in addition to safety glasses, proper respiratory protection is required whenever handling biomass. Biomass is to be stored in sealed labeled containers and small amounts may be stored in the lab. When loading the hopper, be careful to limit the amount of dust produced. A portion of the biomass from each test should be saved in a 1 pint Ziploc bag and labeled with a unique sample ID as depicted in Figure 3.

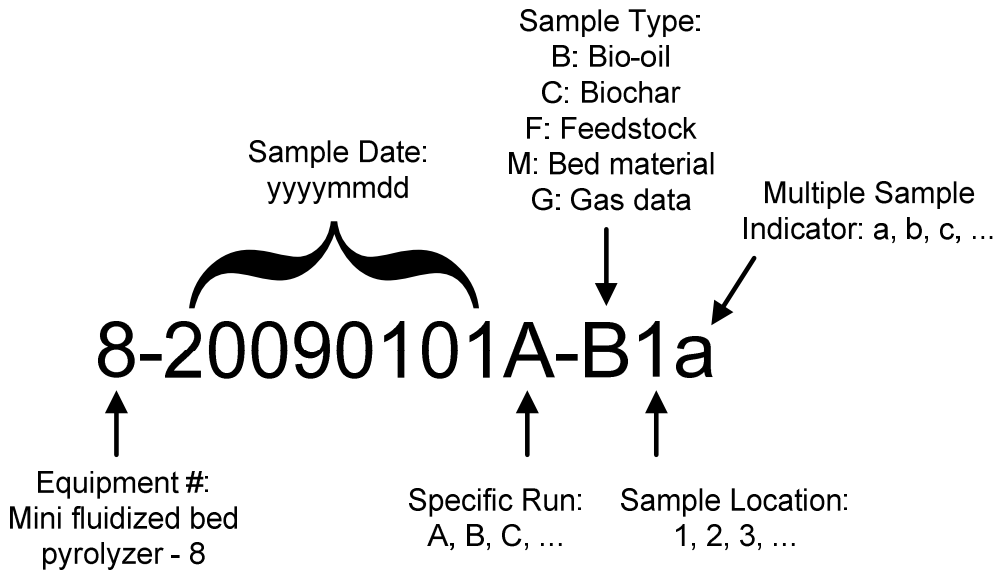

Figure C3: Sample ID procedure

Bed Material: Bed material can be very dusty. For this reason, in addition to safety glasses, proper respiratory protection is required whenever handling bed material. Some experiments require bed material to be collected and analyzed at a later date. If this is necessary, be sure that the bed is cool enough for removal before vacuuming out contents. When the bed is changed, a sample of the old material is stored in a pint Ziploc bag (once cool enough) and labeled in the same fashion as biomass.

Biochar: Char exits the system in two places. The particulate cyclone and the thimble filter. Char is very dusty. For this reason, in addition to safety glasses, proper respiratory protection is required whenever handling char. The char catch on the producer gas line particulate cyclone will need to be changed after each test. The char must be allowed to cool for a minimum of 30 minutes before handling. A one pint zip-top bag can then be filled and labeled with the same sample ID, but properly labeled for char. In terms of sample location, char from the cyclone and thimble filter can be combined in the temporary char storage container.

Bio-Oil: Oil is collected in the two metal condensers, ESP, and cooling tube. The oil from the experiment is to be put into a 50ml centrifuge tube and labeled with the same sample ID format, but for bio-oil. Bio-oil from each collection location is

to be kept separate and labeled accordingly. B1 and B2 are from the first and second condenser collection cups respectively. B3 is the oil that is collected from the ESP. B4 is the oil that is collected from the cooling tubes. After a test the oil from each location is scraped out of the reactor to attain a proper mass balance every run with the oil that derived from that particular test. The condensers and ESP should be cleaned between each test.

Pre-Experiment Checklist

- The following checklist is to be performed each time before energizing any pyrolysis equipment in preparation for an experiment. A copy of this list is also found in the log book and should be filled out for every experiment. A detailed floor plan to aid in this checklist is found at the end of this section.
- Operator 1 Name: Operator 2 Name:
- Date & Time:
- No tools, trash, or unused parts are in the vent hood area.
- All proper shields and guards are in place and working properly
- Check all electrical wires for damage or excessive wear
- Locate information for amount and size of sand in bed
- Check that the pressure regulator on nitrogen cylinder is attached properly
- Inspect nitrogen gas lines from cylinder to the reactor
- Turn on nitrogen gas cylinder
- Check that tank has enough pressure to supply the full experiment.
- Check that line pressure is below 50psi
- Turn on ball valve to feed gas to flow controllers
- Power on the data acquisition equipment with the red switch in the control box, open the Lab View software; load the program “Pyrolysis5.VI”.
- Input proper run information into Tab 1
- Start the VI
- Monitor and control the system in Tab 2

- Do not turn gas flow on to the bed without sealing off the tube to the feeder. Either: 1. Have it plugged or 2. Have the feeder connected with nitrogen flowing to it
- Be sure gas can flow through the bed properly before installing char catch and condensers for a test.
- Power on gas analysis instruments and ready to operate
- Pre-weigh char catch and properly connect to reactor with heat tape addition
- Attach condensers properly with water supply connected properly
- ESP is correctly mounted and ready to be powered on
- Attach clear tube between condenser and ESP
- Place new centrifuge tubes on the ESP and cooling tube collection ports
- Weigh biomass sample to be used for the experiment
- Perform a moisture analysis of the biomass being used
- Fill hopper with pre-weighed biomass for entire experiment
- Place acrylic lid on hopper, place clamp over acrylic lid, and secure tightly with latches on the side of the feeder
- Be sure hopper discharge is properly attached to the feeding plenum
- Turn on each heater control power supply: 3 on Watlow enclosure, 1 for heat tape
- Check that each control thermocouple is reading a proper signal
- Set each “Zone” set point to desired temperature for the test. Refer to the Watlow controller manuals for proper operation
- In Lab View, set desired heat tape temperature. (Normally 30-50°C below the operating temperature or proper temperature to keep gas flow into condenser above 400°C and below 450°C)
- Confirm that after a short time, the temperature in each zone begins to rise.
- Set flow controllers to proper levels
- Set feeder gas line to desired level (3-4 SLPM)
- Set fluidize gas stream desired level (15 SLPM)
- Check that each controller is working properly
- Check that there are no leaks in the system
- Fill ice bath with ice and salt mixture

- Wait for steady state to begin experiment constant zone temperatures
- Before starting to feed turn on the data recorder to save all the information from the experiment
- Enter the desired feeding rate voltage for the feeder. (Dependant on biomass type, size, and moisture content normally a value of 0.6-0.8 is sufficient for 100g/hr)

Equipment Operation

Pre-Test Setup/Material & Equipment Prep:

Biomass

The biomass samples that have been used to date are corn stover ground in a cutting mill to a maximum 0.75mm diameter. The biomass must be air dry at a minimum (~20% moisture). Moisture content can be recorded using the Omniark moisture analyzer in 279 Metals Development

* The amount of biomass put into the feeder must be weighed immediately before the experiment. The total amount of biomass in the feeder should not be forced or packed down in any way.

Nitrogen

The nitrogen will be used directly from a compressed cylinder. The cylinder will be leased from the ISU Chemistry Stores, and will be returned as soon as possible after all usable pressure has been utilized. Using standing order, nitrogen can be delivered at request and charged to the proper account corresponding to the standing order.

Chemistry Stores Contact:

Counter/Orders: 294-0203

Office/account set up: 294-4413

Condensers

Stainless steel condensers are used to condense fractions of oil as reduce the temperature of the gas stream. 1" standard sanitary flange fittings are used as the pipe. Soft copper pipe is used to wrap around the tubing. The copper pipe has either hot or cold water flowing through it, depending on the set up, and is regulated with a manual flow liquid rotameters. The tube unions use PTFE gaskets to seal the gap along with quick connection clamps. After the ESP a separate condenser is used that is a coil of 3/8" stainless steel tubing in an ice bath.

Electrostatic Precipitator (ESP)

The ESP can be powered on before a run begins but it cannot be turned to full power until the reactor is in operation. Meaning a flow of aerosols must be entering the ESP or it must be coated with a layer of oil on the inside to prevent premature sparking of the electrode

Ice bath

The liquid used to cool the tube condenser will be a mixture of water, ice and salt. The mixture will be held by a sealed container and will allow the condenser to contact the ice slurry.

Char

After each experiment run the car catch must be emptied. If a thimble filter is used the same must be done for it. This is done only after the system has cooled down to room temperature. The char catch can be removed by loosening the Swagelok connection at the bottom of the cyclone. The ash should be treated as volatile until it has completely cooled. Store the char in a covered metal container until it has had a chance to cool. A minimum of 15 minutes of cooling time is required for each 100g of biomass run for the experiment.

Sand

When it is necessary to change the bed material, the sand can be replaced. This can be done only when the bed has cooled completely to room temperature.

Remove the insulation cap from the top of the reactor. The (4) bolts that hold the blank flange in the top of the reactor are then removed. The sand it removed by use of the shop vacuum and a ½ tube fitting that can fit down the reactor. Check that the reactor is empty with a flash light. The bed can then be refilled. A bucket of pre-sieved clean sand is located under the workbench. Weigh out the amount it requires to fill the bed to the desired height:
Sieve between Sieve size #16 and #40 for proper sand particle sizes:
175g – 3.125" bed
150g – 2.625" bed
2 operators must be present in the lab area at all times for operation of the Mini Fast Pyrolysis Reactor. One of these must be a CSET graduate student, post-doctorate, or supervisor.
The operation of each subsystem is now covered more in depth.

Biomass:

Biomass that will be used for any experiment needs to be ground to a small enough diameter to be fed through the feeding system. A screen size of 0.75mm on the cutting mill has been verified to feed corn stover properly. Calibration of any biomass sample needs to be done before each experiment. The biomass should be as dry as possible to reduce any water vapor in the outlet gas stream as well as proper feeding from the feeder box. For most experiments the moisture level will be defined in the experiment set up.

Nitrogen gas:

A constant supply of N2 is required for operation of the reactor. The maximum capacity of the reactor is 50 L/min for the entire duration of the experiment.
The flow of nitrogen will be controlled with two Alicat Flow controllers. One will control the flow to the plenum that will fluidize the bed, while the other will control the carrier gas to the feeder that will carry the biomass into the fluidized bed.
The Alicat controllers are controlled with a computer program.
The Nitrogen is contained in a compressed cylinder. Cylinder safety training must be done before any work can be done using or handling any gas cylinder.

When not in use be sure both cylinder valve and ball valve are both in their respected OFF positions.

A pressure regulator attaches directly to the gas cylinder. This can only be removed or attached when the gas cylinder is turned off. Turning the valve to the right (clockwise) turns off the cylinder. When the pressure regulator is securely attached the gas from the cylinder can be slowly turned on. This is done by turning the valve to the left (counterclockwise). (On/Off directions are imprinted on the cylinder valve knob for reference)

If a leak is audible from the pressure regulator, immediately turn off the cylinder valve and tighten all threaded joints on the pressure regulator.

If no leak is audible from the pressure regulator, the ball valve can be turned on when a nitrogen supply to the reactor is needed.

Nitrogen gas must be supplied to the Alicat controllers before they are powered on.

Electrical power supply:

In case of emergency, the breakers for each outlet are marked. The location of the breaker control panel is in the hallway just south of the door to the lab.

The Accurate feeder control box, a 24V power supply, the heat tape power box, the Compaq DAQ™ data sampler , and the computer each have a separate power supply connected to outlets with standard plug-in cords. The heater control box is powered by two separate 20 amp plugs that must be plugged into two outlets that are on separate breakers.

The lights for the vent hood are also powered from the same control box as the outlets. The vent fan is controlled by a control panel that is located on the right hand side of the vent hood enclosure.

Heater Control:

2 - 20amp 120VAC plug chord that control the thermocouples, and heaters.

One is plugged into the West outlet; the other is plugged into the East outlet.

If both are plugged into the same outlet, it will eventually trip the outlet over current protection.

The control box will be powered on when it is plugged in. To open the control panel; all electrical plugs must be unplugged and locked out. The display will show many various pieces of information. A good understanding of the Watlow controllers is needed to operate them properly. The operation manual is available in the Fast Pyrolysis file cabinet drawer.

When operational the heater will control the current going to each heater. The power is transmitted with 12AWG THHN. The wire is covered with a protective plastic wrap. The wire must still be inspected for damage every time before use. The wire has quick detachable plugs near the heater terminal. The plugs must be disengaged to remove the heaters during disassembly.

Thermocouples are also supplied to the heater control. These wires carry a low but precision voltage. Do to the required accuracy of the wire signal; the wires must be inspected for any damage or wear. The thermocouple wire terminates at a ceramic thermocouple quick connector. This connecter connects directly to the thermocouple probe that sets in the reactor.

Feeder Control:

1 - 10amp 120VAC plug chord that will power the Accurate feeder

The controller is always powered on when the cord is plugged in. To open the control panel; all electrical plugs must be unplugged and locked out. The Accurate feeder control specifies the voltage that is supplied to the motor, determining the RPM of the DC motor. The operation manual is located in the Fast Pyrolysis file cabinet drawer. The number on the display corresponds to the rpm of the motor. After a step down the auger turns at a slightly slower rate. The feeder is turned on and off by pressing the I/O button on the controller. A green light turns on in the digital screen to signify that it is running. A calibration is required for each new type of biomass going to be run in an experiment. See Feeder Calibration.

Cyclone:

The cyclone char collector should be emptied before each experiment to keep the container from overfilling. During a test the cyclone will get very hot. Never touch or attempt to touch any part of the filter or the insulation surrounding them. A

thermocouple will monitor the wall temperature of it. Use the thermocouple to verify is has cooled to room temperature if maintenance is required. Only when the filter is at room temperature can it be disassembled and cleaned.

During a test, monitor the thermocouples for abnormal temperature gradients in the filter. The filter needs to remain above 400°C to prevent premature condensing of bio-oil in it.

During a test, carefully watch the pressure transducer across the cyclone. If ever the pressure becomes too high, the filter has become plugged, and the test must be aborted.

Before a test, pre-weigh the biochar collector to record the total amount of char that will be collected.

Condenser:

The condenser system should be clean and free from debris before the start of and during any experiment. Before starting an experiment, be sure all condensers are arranged correctly with the hot water flowing in counter current fashion up the first section of the condenser. The cool water then flows down the second half of the condenser that has gas flowing up it. Water is controlled with liquid rotameters located underneath the condenser table

Sufficient ice and rock salt should be on hand before starting any experiment. The operator should monitor the ice level periodically during the experiment to keep the ice level high enough to keep the cooling tube at the correct temperature.

Ventilation:

The vent hood containing the mini pyrolyzer has a flow monitor and warning alarm. During an experiment be sure the vent is performing properly and take appropriate action if ever the alarm sounds.

Water Disposal:

A drain located in the vent hood area will be used to drain the water that is used for heat exchange in the first condensers. Do not pour anything other than water down this drain.

Instrument Calibration:

Feeder Calibration for each specific biomass type:

- The correct feed rate is necessary to achieving proper heat transfer in the bed, as well as properly producing pyrolysis products. Since grams are the major unit used for the experiments the calibration is done for the range of 30-150 grams/hour. This allows for only 0.5 – 2.5g/min feeding rates for calibration.
- To begin calibration, have a sample of the biomass, or material that is going to be run in the experiment. 100g should be sufficient for complete calibration. Loosely fill it into the feeder and seal down the hopper lid as if a test was going to be done.
- Load the Lab View program "Claibration.VI" from the Lab View programs folder
- The feed tube to the reactor is disconnected from the tee connected to the feeder.
- The calibration tube is then connected to the tee and directed to the biomass receiver.
- Turn on the gas stream to the feed line as if an experiment is going to be ran.
- Set feeder to the setting desired to test.
- Make sure gas is flowing properly out of the tube end.
- Turn on the feeder while simultaneously starting a stopwatch timer.
- Wait until biomass begins to flow from the outlet of the calibration tube.
- Turn Off the feeder and record the time for biomass to begin to flow. Reset the stop watch.
- Turn ON the feeder while simultaneously starting a stopwatch timer.
- After 10 minutes, stop the feeder.
- Measure the mass of the biomass that had been fed out of the feeder.
- Plot the results for grams/minute.
- Repeat steps 4-11 for different settings until a range around the desired feed rate has been plotted.
- Note steps 6, 7, 8 are only required when the feeding auger is completely empty of biomass.

- Use the plot to determine the appropriate feeder setting to achieve the desired bulk feeding rate.
- Save the calibration plot for future reference.

Pressure transducer Calibration:

The pressure transducers require calibration to verify the voltage output correctly corresponds to the pressure drop across it. Use the standard procedure using the drop tube manometers available in the lab for calibration

Flow controller calibration:

The nitrogen flow controllers are originally calibrated by Alicat, and should be sent in for re-calibration every year. Follow the schedule in each controller manual. The flow controllers can also be calibrated in the lab using the standard procedure for the wet-test flow meters.

Equipment Operation

Normal Equipment Operation/Test Method/Sampling:

Procedures

- After all set-ups are completed, the set can begin.
- Gas should be flowing from the nitrogen cylinder through the Alicat flow controllers
- The heat of each zone should be steady and near the desired set point for the experiment
- The pressure drop across the bed as well as the filter should be relatively stable and within the desired operational range of each
- Begin to record the data in the LabView program and start the Micro GC program.
- Start the test by setting the feeder to the desired set point, and turning the feeder ON.
- Note: The feeder must be powered on ant have the green light visible on the digital screen. This is turned on by pressing the I/O button.

- Start the gas sampling
- While running, monitor the temperature, pressure, gas flow throughout the system, and ESP operation. If any parameter exceeds or drops below the desired range, record the issue, and if necessary abort the test
- After the desired test length has passed. Turn the feeder control OFF
- Turn the water off to the condensers
- Wait until all pyrolysis vapor has exited the system
- Turn the gas flow off. First to the bed, then the feeder
- Stop recording data in the LabView program
- Stop the Micro GC equipment and save all data
- Save and backup all data acquisition data from test
- Using proper safety equipment, remove the condensers collect all oil from them and begin to soak them in alkaline-soap water. The cooling water connection must be taken apart and the quick clamp connections are disconnected to remove the condensers. The inlet to the first condenser will be very hot. Use extreme caution when removing the condenser from the system.
- The oil in condenser 1 should be collected first. It is very viscous and will need to be scraped out with a steel weighing spoon. This can only be done when the oil is above 80°C.
- Oil in condenser 2 is much less viscous and can be easily scrapped out at any temperature.
- Bio-oil from the ESP is also very viscous but can be collected at any temperature. A weighing spatula works best to effectively scrape out all oil from the walls of the collection tube.
- Remove char collector weigh, and empty char into a proper storage container. Caution: Top portion of char collector will be very hot.
- Label all collected samples and properly store them for later analysis
- Equipment Shutdown:
- Allow the system to completely cool down before attempting to examine or touch any part of the reactor system. Cool down may require several hours.
- Turn heaters off

- If a sample of the bed material is required, monitor the thermocouple reading s to verify when the reactor has cooled to room temperature.
- Check all gaskets for abnormal wear. Replace if excess wear is found.
- If required, weigh Drierite and/or glass wool filters to determine any mass collected. Discard old glass wool properly. Drierite can be regenerated if spoiling has occurred.
- Note the gas level in the nitrogen cylinder. Order a refilled cylinder if levels are below 50%.
- Remove unfed biomass from the feeder to complete the mass balance. Disconnect the feeder from the feeding tube. Most of the biomass can be removed by hand when the feeder is OFF. Turn the feeder ON to remove the small amount that is inaccessible by hand. Weigh the biomass from after the test to determine the mass that was fed.

Cleanup

Feeder Cleanup:

The vacuum, hand broom, and a dust pan are to be used to clean up all dry particulate that may have accumulated in the area. Do not use any body part of clean up due to the possibility of sharp fragments and rough surfaces. Clean the feeder surfaces as well as the cement floor below the entire apparatus.

Condenser Cleanup:

The condensers can be cleaned of left over bio-oil with hot water and cleaning solvents. Proper precaution must be taken for each chemical when in use. The sonicator or methanol can be used to speed the cleaning process of the parts if required.

Area Cleanup:

Pick up any debris that may have accumulated around during the experiment. Throw away all trash. If no more tests will be done for some time, put away all tools and materials that were used for the test.

Maintenance

Maintenance on all parts should be done before running a test. Check all electrical connections and gas lines for wear or abnormalities.
Lubricate feeder according to maintenance schedule in the owner's manual.

Required ISU Safety Training Courses

[Example items populate or depopulate the list as needed – delete this text when done]
Lockout-Tagout
Electrical Training for Researchers
Management of Unwanted Materials for Laboratory Personnel (Replaces Hazardous Waste Generator)
Chemical Waste Communication Training
Safeguarding Mechanical Hazards
Gas Cylinder Training
PPE
Ladder training
Strains and Sprains Prevention
Fire Safety and Extinguisher Training

Emergency Contacts

In case of emergency, the following people should be contacted.

Randy Kasparbauer, Graduate Research Assistant
Office: 2043 Black Engineering; 515-294-9451
Cell: 712-269-4658 Email: kasparbauer@gmail.com

Sam Jones, Lab Supervisor
Office: 515-294-6904
Cell: 515-450-2044

Robert Brown, Director BEI/CSET Office: (515)-294-8733

Department of Public Safety: 515-294-4428 or 911

If the emergency is minor, please contact responsible graduate student or lab supervisor. If there is a serious emergency or life threatening emergency please contact 911 followed immediately by contacting [lab supervisor] and/or Robert Brown. If there is a chemical spill too large to be cleaned using a typical spill kit contact Environmental Health and Safety.

APPENDIX D: EXPERIMENTAL DATA

The data logs for each test were recorded into an Excel file. Table shows each parameter that was saved into the data file along with its respective unit of measurement. Each of the measurements was taken using the Compaq DAQ™ data acquisition hardware and the Lab View software interface. A data point was saved ever second the program was operating in record mode. The data is used to find overall overages of values that were experienced during a particular test.

Table D1: Data log recorded information and units

Measurement	Units
Pressure difference across bed	in. H_2O
Pressure difference across cyclone	in. H_2O
Plenum temperature	°C
Bed temperature	°C
Lower freeboard temperature	°C
Upper freeboard temperature	°C
Cyclone filter wall temperature	°C
SF1 inlet temperature	°C
SF2 outlet temperature	°C
SF1 cooling water in temperature	°C
SF1 cooling water outlet temperature	°C
SF3 ice temperature	°C
SF3 outlet temperature	°C
Gas flow to plenum	SLPM
Gas flow to feeder	SLPM
Feeder set point	V

Table D2: Mass balance data for all tests

Date/ Sample name	Pretreatment[1]	Pyrolysis temperature	Screen size	Moisture	Biomass fed	Biochar		Total bio-oil		Non-condensable gas		Closure
		°C	mm	% dry basis	g	g	wt. %	g	wt. %	g	wt. %	%
9/18/2008 A	T (215)	485	0.5	2.0%	194.97	37.09	19.0%	108.9	55.9%	21.127	10.8%	85.7%
10/9/2008 A	T (215)	485	0.75	2.0%	173.71	30.32	17.5%	94.5	54.4%	27.9	16.1%	87.9%
10/10/2008 A	T (215)	544	0.5	2.0%	199.68	21.71	10.9%	112.3	56.2%	39.244	19.7%	86.7%
10/21/2008 B	T (215)	426	0.5	0.1%	186.13	57.14	30.7%	88.6	47.6%	20.515	11.0%	89.3%
10/27/2008 A	T (215)	485	0.25	2.7%	162.73	32.84	20.2%	83.8	51.5%	15.914	9.8%	81.4%
10/27/2008 B	T (215)	485	0.5	2.3%	166.73	28.57	17.1%	101.0	60.6%	22.524	13.5%	91.2%
10/28/2008 A	T (215)	485	0.5	2.3%	180.49	32.02	17.7%	98.0	54.3%	23.789	13.2%	85.2%
10/29/2008 A	T (215)	485	0.5	2.2%	197.3	36.21	18.4%	113.5	57.5%	34.683	17.6%	93.4%
10/30/2008 A	T (250)	450	0.75	1.5%	129.6	38.84	30.0%	58.4	45.0%	16.243	12.5%	87.5%
10/31/2008 A	T (250)	520	0.75	1.5%	178.79	40.6	22.7%	90.9	50.9%	32.548	18.2%	91.8%
10/31/2008 B	T (250)	485	0.5	1.5%	169.12	45.38	26.8%	84.3	49.8%	21.901	12.9%	89.6%
11/5/2008 A	T (250)	520	0.25	1.8%	150.22	31.87	21.2%	80.2	53.4%	14.404	9.6%	84.2%
11/6/2008 A	T (180)	450	0.75	1.7%	115.47	24.75	21.4%	61.2	53.0%	12.907	11.2%	85.6%
11/6/2008 B	T (180)	520	0.75	1.7%	138.78	25.66	18.5%	71.8	51.7%	23.757	17.1%	87.3%
11/7/2008 A	T (180)	485	0.5	2.0%	169.7	33.02	19.5%	97.3	57.3%	20.354	12.0%	88.8%
11/11/2008 A	T (180)	520	0.25	2.0%	159.45	37.29	23.4%	92.2	57.8%	22.648	14.2%	95.4%
11/13/2008 A	T (180)	450	0.25	1.9%	111.42	32.13	28.8%	49.6	44.5%	10.882	9.8%	83.1%
11/14/2008 A	T (215)	485	0.5	2.2%	151	27.06	17.9%	91.2	60.4%	19.176	12.7%	91.0%
11/18/2008 A	T (180)	450	0.25	1.9%	138.6	37.9	27.3%	70.0	50.5%	13.08	9.4%	87.3%
1/30/2009 A	T (215)	485	0.5	1.6%	226.9	50.6	22.3%	114.2	50.3%	21.892	9.6%	82.3%
7/25/2008 A	N	450	0.75	7.1%	159.6	34.67	21.7%	82.8	51.9%	16.34	10.2%	83.8%
8/7/2008 A	N	485	0.5	8.3%	191.9	31.99	16.7%	117.6	61.3%	22.826	11.9%	89.9%
8/12/2008 A	N	485	0.75	10.3%	213.84	31.71	14.8%	122.4	57.2%	31.638	14.8%	86.9%
8/19/2008 A	N	450	0.75	10.2%	187.87	31.84	16.9%	104.9	55.8%	20.345	10.8%	83.6%
8/20/2008 A	N	450	0.25	10.2%	196.75	53.03	27.0%	96.7	49.1%	14.792	7.5%	83.6%
8/22/2008 A	N	520	0.75	10.0%	148.17	18.94	12.8%	89.0	60.1%	25.653	17.3%	90.2%
8/22/2008 B	N	520	0.25	9.2%	156.33	22.56	14.4%	83.6	53.5%	22.996	14.7%	82.6%
8/25/2008 A	N	485	0.5	9.2%	173	26.27	15.2%	104.7	60.5%	25.16	14.5%	90.2%
8/26/2008 A	N	485	0.5	6.8%	197.6	31.49	15.9%	110.9	56.1%	28.145	14.2%	86.3%
8/26/2008 B	N	520	0.75	7.3%	172.36	23.29	13.5%	95.1	55.2%	28.159	16.3%	85.0%
8/27/2008 A	N	520	0.25	7.6%	133.33	18.27	13.7%	79.0	59.3%	19.461	14.6%	87.6%
9/2/2008 B	N	485	0.25	10.2%	161.84	28.62	17.7%	94.5	58.4%	19.311	11.9%	88.0%
9/4/2008 A	N	426	0.5	7.0%	127.56	32.62	25.6%	73.0	57.2%	15.572	12.2%	95.0%
9/10/2008 A	N	485	0.5	7.1%	186.2	33.78	18.1%	108.0	58.0%	24.145	13.0%	89.1%
9/11/2008 B	N	485	0.5	7.0%	204.68	34.97	17.1%	124.2	60.7%	17.598	8.6%	86.4%
9/16/2008 B	N	485	0.5	16.1%	175.21	25.14	14.3%	114.5	65.3%	20.194	11.5%	91.2%
9/30/2008 A	N	544	0.5	10.0%	181.05	18.66	10.3%	101.2	55.9%	32.994	18.2%	84.4%
10/17/2008 A	N	450	0.25	7.2%	191.95	51.79	27.0%	97.9	51.0%	26.078	13.6%	91.6%
10/24/2008 A	N	485	0.5	10.1%	192.45	30.43	15.8%	116.5	60.6%	23.774	12.4%	88.7%
11/10/2008 A	N	485	0.5	15.1%	178.1	28.28	15.9%	109.4	61.4%	23.728	13.3%	90.6%

1. Nomenclature: T = Torrefied (temperature in parentheses °C); N = Not washed; W = Washed.

Table D2: (Continued)

Date/ Sample name	Pretreatment[1]	Pyrolysis temperature	Screen size	Moisture	Biomass fed	Biochar		Total bio-oil		Non-condensable gas		Closure
		°C	mm	% dry basis	g	g	wt. %	g	wt. %	g	wt. %	%
7/23/2008 A	W	450	0.75	7.7%	220.53	50.17	22.7%	118.9	53.9%	18.863	8.6%	85.2%
7/30/2008 A	W	450	0.75	7.2%	233.87	46.92	20.1%	125.6	53.7%	23.56	10.1%	83.8%
8/1/2008 B	W	520	0.75	6.8%	204.5	24.33	11.9%	117.2	57.3%	31.244	15.3%	84.5%
8/8/2008 A	W	485	0.5	6.4%	223.17	37.79	16.9%	126.7	56.8%	22.203	9.9%	83.7%
8/11/2008 A	W	485	0.5	6.4%	228.28	38.2	16.7%	127.8	56.0%	23.207	10.2%	82.9%
8/13/2008 A	W	485	0.5	7.4%	168.45	30.43	18.1%	91.7	54.4%	23.252	13.8%	86.3%
8/13/2008 B	W	485	0.75	7.3%	231.65	33.67	14.5%	150.1	64.8%	29.472	12.7%	92.1%
8/26/2008 C	W	520	0.75	25.6%	96.3	11.85	12.3%	65.9	68.4%	14.769	15.3%	96.0%
9/2/2008 A	W	485	0.25	7.6%	183.96	35.57	19.3%	107.2	58.3%	21.505	11.7%	89.3%
9/3/2008 A	W	520	0.25	7.6%	181.53	23.84	13.1%	102.3	56.3%	31.404	17.3%	86.8%
9/12/2008 A	W	450	0.25	7.8%	163.09	46.89	28.8%	82.6	50.7%	15.552	9.5%	89.0%
9/15/2008 A	W	485	0.5	23.7%	177.63	27.92	15.7%	115.0	64.7%	22.958	12.9%	93.4%
9/16/2008 A	W	520	0.25	19.7%	149.6	13.92	9.3%	91.7	61.3%	19.113	12.8%	83.4%
9/16/2008 C	W	485	0.5	20.7%	182.57	26.87	14.7%	116.9	64.0%	20.589	11.3%	90.0%
9/19/2008 A	W	485	0.5	19.0%	194.16	31.86	16.4%	122.5	63.1%	23.823	12.3%	91.8%
9/30/2008 B	W	544	0.5	17.3%	136.85	9.55	7.0%	88.8	64.9%	21.647	15.8%	87.7%
10/6/2008 A	W	485	0.5	11.4%	179.2	26.72	14.9%	111.5	62.2%	21.817	12.2%	89.3%
10/21/2008 A	W	426	0.5	17.0%	189.13	63.29	33.5%	97.4	51.5%	15.249	8.1%	93.0%
10/23/2008 A	W	485	0.5	16.0%	211.31	37.53	17.8%	132.5	62.7%	22.351	10.6%	91.1%
1/21/2009 A	W	450	0.75	21.32%	145.2	28.5	19.6%	85.0	58.5%	16.535	11.4%	89.5%
1/23/2009 A	W	450	0.25	18.4%	188.9	51.3	27.16%	92.9	49.19%	14.592	7.7%	84.1%

Table D3: Mass balance for bio-oil fractions

Date/ Sample name	Pretreatment[1]	Pyrolysis temperature	Screen size	Moisture	Biomass fed	SF1		SF2		SF3		SF4		Total bio-oil
		°C	mm	% dry basis	g	g	wt. %	g	wt. %	g	wt. %	g	wt. %	wt. %
9/18/2008 A	T (215)	485	0.5	2.0%	194.97	19.24	9.87%	11.67	5.99%	55.69	28.6%	22.32	11.4%	55.9%
10/9/2008 A	T (215)	485	0.75	2.0%	173.71	14.78	8.51%	11.67	6.72%	47.76	27.5%	20.27	11.7%	54.4%
10/10/2008 A	T (215)	544	0.5	2.0%	199.68	23.72	11.88%	11.67	5.84%	51.59	25.8%	25.28	12.7%	56.2%
10/21/2008 B	T (215)	426	0.5	0.1%	186.13	10.50	5.64%	11.67	6.27%	44.79	24.1%	21.59	11.6%	47.6%
10/27/2008 A	T (215)	485	0.25	2.7%	162.73	10.60	6.51%	11.67	7.17%	49.21	30.2%	12.29	7.6%	51.5%
10/27/2008 B	T (215)	485	0.5	2.3%	166.73	17.94	10.76%	11.67	7.00%	51.58	30.9%	19.81	11.9%	60.6%
10/28/2008 A	T (215)	485	0.5	2.3%	180.49	14.45	8.01%	11.67	6.47%	55.38	30.7%	16.48	9.1%	54.3%
10/29/2008 A	T (215)	485	0.5	2.2%	197.3	20.95	10.62%	11.67	5.91%	58.68	29.7%	22.15	11.2%	57.5%
10/30/2008 A	T (250)	450	0.75	1.5%	129.6	7.92	6.11%	11.67	9.00%	29.29	22.6%	9.48	7.3%	45.0%
10/31/2008 A	T (250)	520	0.75	1.5%	178.79	16.44	9.20%	11.67	6.53%	45.48	25.4%	17.35	9.7%	50.9%
10/31/2008 B	T (250)	485	0.5	1.5%	169.12	11.13	6.58%	11.67	6.90%	44.15	26.1%	17.3	10.2%	49.8%
11/5/2008 A	T (250)	520	0.25	1.8%	150.22	11.59	7.72%	11.67	7.77%	42.93	28.6%	13.96	9.3%	53.4%
11/6/2008 A	T (180)	450	0.75	1.7%	115.47	10.16	8.80%	11.67	10.11%	26.91	23.3%	12.46	10.8%	53.0%
11/6/2008 B	T (180)	520	0.75	1.7%	138.78	9.74	7.02%	6.98	5.03%	37.07	26.7%	17.97	12.9%	51.7%
11/7/2008 A	T (180)	485	0.5	2.0%	169.7	20.10	11.84%	11.67	6.88%	46.84	27.6%	18.7	11.0%	57.3%
11/11/2008 A	T (180)	520	0.25	2.0%	159.45	22.42	14.06%	11.67	7.32%	43.53	27.3%	14.53	9.1%	57.8%
11/13/2008 A	T (180)	450	0.25	1.9%	111.42	8.17	7.33%	11.67	10.47%	22.6	20.3%	7.17	6.4%	44.5%
11/14/2008 A	T (215)	485	0.5	2.2%	151	13.13	8.70%	11.67	7.73%	46.92	31.1%	19.52	12.9%	60.4%
11/18/2008 A	T (180)	450	0.25	1.9%	138.6	10.87	7.84%	11.67	8.42%	32.99	23.8%	14.51	10.5%	50.5%
1/30/2009 A	T (215)	485	0.5	1.6%	226.9	21.22	9.35%	10.13	4.46%	58.03	25.58%	24.8	10.93%	50.3%
7/25/2008 A	N	450	0.75	7.1%	159.6	11.12	6.97%	9.70	6.08%	40.2	25.2%	21.76	13.6%	51.9%
8/7/2008 A	N	485	0.5	8.3%	191.9	25.50	13.29%	11.67	6.08%	48.75	25.4%	31.71	16.5%	61.3%
8/12/2008 A	N	485	0.75	10.3%	213.84	18.69	8.74%	11.67	5.46%	53.94	25.2%	38.12	17.8%	57.2%
8/19/2008 A	N	450	0.75	10.2%	187.87	17.66	9.40%	9.70	5.16%	42.36	22.5%	35.13	18.7%	55.8%
8/20/2008 A	N	450	0.25	10.2%	196.75	11.39	5.79%	11.67	5.93%	42.22	21.5%	31.38	15.9%	49.1%
8/22/2008 A	N	520	0.75	10.0%	148.17	13.26	8.95%	11.67	7.88%	35.85	24.2%	28.23	19.1%	60.1%
8/22/2008 B	N	520	0.25	9.2%	156.33	9.06	5.80%	11.67	7.46%	36.37	23.3%	26.54	17.0%	53.5%
8/25/2008 A	N	485	0.5	9.2%	173	18.37	10.62%	11.67	6.75%	44.13	25.5%	30.48	17.6%	60.5%
8/26/2008 A	N	485	0.5	6.8%	197.6	14.61	7.39%	9.70	4.91%	53.41	27.0%	33.2	16.8%	56.1%
8/26/2008 B	N	520	0.75	7.3%	172.36	10.52	6.10%	11.67	6.77%	42.76	24.8%	30.17	17.5%	55.2%
8/27/2008 A	N	520	0.25	7.6%	133.33	13.05	9.79%	11.67	8.75%	35.04	26.3%	19.24	14.4%	59.3%
9/2/2008 B	N	485	0.25	10.2%	161.84	10.47	6.47%	9.60	5.93%	46.79	28.9%	27.66	17.1%	58.4%
9/4/2008 A	N	426	0.5	7.0%	127.56	10.30	8.07%	11.67	9.15%	28.59	22.4%	22.45	17.6%	57.2%
9/10/2008 A	N	485	0.5	7.1%	186.2	18.37	9.87%	11.67	6.27%	53.29	28.6%	24.7	13.3%	58.0%
9/11/2008 B	N	485	0.5	7.0%	204.68	22.36	10.92%	11.67	5.70%	56.09	27.4%	34.06	16.6%	60.7%
9/16/2008 B	N	485	0.5	16.1%	175.21	14.31	8.17%	11.67	6.66%	51.08	29.2%	37.39	21.3%	65.3%
9/30/2008 A	N	544	0.5	10.0%	181.05	10.81	5.97%	11.67	6.45%	46.88	25.9%	31.85	17.6%	55.9%
10/17/2008 A	N	450	0.25	7.2%	191.95	17.66	9.20%	9.16	4.77%	46.1	24.0%	24.97	13.0%	51.0%
10/24/2008 A	N	485	0.5	10.1%	192.45	14.10	7.33%	11.67	6.06%	58.55	30.4%	32.22	16.7%	60.6%
11/10/2008 A	N	485	0.5	15.1%	178.1	13.97	7.84%	11.67	6.55%	48.17	27.0%	35.6	20.0%	61.4%

1. Nomenclature: T = Torrefied (temperature in parentheses, °C); N = Not washed; W = Washed.

Table D3: (Continued)

Date/ Sample name	Pretreatment[1]	Pyrolysis temperature	Screen size	Moisture	Biomass fed	SF1		SF2		SF3		SF4		Total oil
		°C	mm	% dry basis	g	g	wt. %	g	wt. %	g	wt. %	g	wt. %	wt. %
7/23/2008 A	W	450	0.75	7.7%	220.53	23.08	10.47%	11.67	5.29%	53.63	24.3%	30.52	13.8%	53.9%
7/30/2008 A	W	450	0.75	7.2%	233.87	22.87	9.78%	11.67	4.99%	60.54	25.9%	30.47	13.0%	53.7%
8/1/2008 B	W	520	0.75	6.8%	204.5	16.82	8.22%	11.67	5.71%	56.08	27.4%	32.61	15.9%	57.3%
8/8/2008 A	W	485	0.5	6.4%	223.17	20.39	9.14%	11.67	5.23%	65.38	29.3%	29.26	13.1%	56.8%
8/11/2008 A	W	485	0.5	6.4%	228.28	20.21	8.85%	11.67	5.11%	61.89	27.1%	33.98	14.9%	56.0%
8/13/2008 A	W	485	0.5	7.4%	168.45	12.98	7.71%	11.67	6.93%	42.87	25.4%	24.19	14.4%	54.4%
8/13/2008 B	W	485	0.75	7.3%	231.65	30.46	13.15%	11.67	5.04%	61.52	26.6%	46.45	20.1%	64.8%
8/26/2008 C	W	520	0.75	25.6%	96.3	8.05	8.36%	11.67	12.12%	20.39	21.2%	25.74	26.7%	68.4%
9/2/2008 A	W	485	0.25	7.6%	183.96	12.98	7.06%	11.67	6.34%	54.42	29.6%	28.11	15.3%	58.3%
9/3/2008 A	W	520	0.25	7.6%	181.53	17.75	9.78%	11.67	6.43%	48.46	26.7%	24.41	13.4%	56.3%
9/12/2008 A	W	450	0.25	7.8%	163.09	14.50	8.89%	11.67	7.16%	36.96	22.7%	19.5	12.0%	50.7%
9/15/2008 A	W	485	0.5	23.7%	177.63	13.02	7.33%	11.67	6.57%	47.95	27.0%	42.31	23.8%	64.7%
9/16/2008 A	W	520	0.25	19.7%	149.6	11.75	7.85%	11.67	7.80%	38.11	25.5%	30.17	20.2%	61.3%
9/16/2008 C	W	485	0.5	20.7%	182.57	12.21	6.69%	11.67	6.39%	52.4	28.7%	40.64	22.3%	64.0%
9/19/2008 A	W	485	0.5	19.0%	194.16	18.89	9.73%	11.67	6.01%	52.65	27.1%	39.26	20.2%	63.1%
9/30/2008 B	W	544	0.5	17.3%	136.85	13.08	9.56%	11.67	8.53%	34.81	25.4%	29.24	21.4%	64.9%
10/6/2008 A	W	485	0.5	11.4%	179.2	15.09	8.42%	11.67	6.51%	52.06	29.1%	32.69	18.2%	62.2%
10/21/2008 A	W	426	0.5	17.0%	189.13	10.69	5.65%	11.67	6.17%	40.5	21.4%	34.5	18.2%	51.5%
10/23/2008 A	W	485	0.5	16.0%	211.31	20.66	9.78%	11.67	5.52%	62.31	29.5%	37.88	17.9%	62.7%
1/21/2009 A	W	450	0.75	21.32%	145.2	8.08	5.56%	4.92	3.39%	34.1	23.5%	37.85	26.1%	58.5%
1/23/2009 A	W	450	0.25	18.4%	188.9	9.74	5.16%	6.81	3.61%	41.45	21.94%	34.92	18.49%	49.19%

D.2 Biochar analysis data

Table D4: Elemental analysis of char samples from each test

Date/ Sample name	Pretreatment[1]	Pyrolysis temperature	Screen size	Moisture content	Biochar elemental content				95% Confidence interval		
					H	C	N	O	H	C	N
		°C	mm	% dry basis	wt. %	wt. %	wt. %	wt. % by difference	wt. %	wt. %	wt. %
9/18/2008 A	T (215)	485	0.50	2.0%	4.28	63.69	0.52	31.51	0.55	0.04	0.03
10/9/2008 A	T (215)	485	0.75	2.0%	4.10	72.03	0.29	23.58	0.07	1.66	0.05
10/10/2008 A	T (215)	544	0.50	2.0%	3.20	72.74	0.33	23.74	0.08	0.34	0.02
10/21/2008 B	T (215)	426	0.50	0.1%	5.25	62.26	0.29	32.20	1.01	0.08	0.03
10/27/2008 A	T (215)	485	0.25	2.7%	4.39	66.62	0.30	28.69	0.98	0.05	0.05
10/27/2008 B	T (215)	485	0.50	2.3%	4.26	70.33	0.24	25.18	0.77	0.01	0.03
10/28/2008 A	T (215)	485	0.50	2.3%	4.27	70.01	0.41	25.31	0.42	0.06	0.01
10/29/2008 A	T (215)	485	0.50	2.2%	4.38	67.12	0.42	28.07	1.10	0.09	0.00
10/30/2008 A	T (250)	450	0.75	1.5%	4.66	65.58	0.47	29.28	0.63	0.05	0.01
10/31/2008 A	T (250)	520	0.75	1.5%	3.34	63.35	0.46	32.84	2.16	0.08	0.01
10/31/2008 B	T (250)	485	0.50	1.5%	4.12	62.27	0.45	33.15	0.54	0.06	0.00
11/5/2008 A	T (250)	520	0.25	1.8%	3.51	60.94	0.37	35.19	1.00	0.09	0.01
11/6/2008 A	T (180)	450	0.75	1.7%	4.24	60.62	0.45	34.70	0.60	0.01	0.03
11/6/2008 B	T (180)	520	0.75	1.7%	3.06	58.86	0.43	37.66	8.20	0.37	0.05
11/7/2008 A	T (180)	485	0.50	2.0%	4.06	63.37	0.47	32.10	1.20	0.04	0.00
11/11/2008 A	T (180)	520	0.25	2.0%	3.26	58.56	0.44	37.73	1.19	0.08	0.02
11/13/2008 A	T (180)	450	0.25	1.9%	4.63	53.63	0.39	41.35	0.60	0.06	0.02
11/14/2008 A	T (215)	485	0.50	2.2%	4.16	59.70	0.40	35.73	1.77	0.10	0.02
11/18/2008 A	T (180)	450	0.25	1.9%	4.69	60.33	0.41	34.57	0.71	0.09	0.06
1/30/2009 A	T (215)	485	0.50	1.6%	3.71	58.64	0.30	37.34	0.06	0.84	0.07
7/25/2008 A	N	450	0.75	7.1%	4.57	59.62	0.56	35.26	0.04	0.68	0.05
8/7/2008 A	N	485	0.50	8.3%	4.06	63.86	0.63	31.44	0.05	0.53	0.01
8/12/2008 A	N	485	0.75	10.3%	4.15	66.56	0.59	28.71	0.02	0.42	0.02
8/19/2008 A	N	450	0.75	10.2%	4.50	63.16	0.53	31.81	0.02	0.87	0.01
8/20/2008 A	N	450	0.25	10.2%	4.87	59.43	0.53	35.17	0.08	1.05	0.03
8/22/2008 A	N	520	0.75	10.0%	3.40	67.53	0.55	28.52	0.09	1.71	0.01
8/22/2008 B	N	520	0.25	9.2%	3.55	63.18	0.65	32.62	0.06	0.98	0.01
8/25/2008 A	N	485	0.50	9.2%	4.00	62.29	0.57	33.14	0.03	0.78	0.03
8/26/2008 A	N	485	0.50	6.8%	3.84	63.39	0.55	32.22	0.07	1.15	0.01
8/26/2008 B	N	520	0.75	7.3%	3.40	66.97	0.58	29.04	0.05	1.01	0.04
8/27/2008 A	N	520	0.25	7.6%	3.48	60.55	0.61	35.36	0.04	0.44	0.02
9/2/2008 B	N	485	0.25	10.2%	4.10	60.63	0.66	34.61	0.10	1.25	0.03
9/4/2008 A	N	426	0.50	7.0%	5.08	59.27	0.47	35.19	0.04	0.61	0.04
9/10/2008 A	N	485	0.50	7.1%	4.05	64.50	0.59	30.86	0.10	0.60	0.07
9/11/2008 B	N	485	0.50	7.0%	3.96	62.05	0.56	33.43	0.09	1.00	0.03
9/16/2008 B	N	485	0.50	16.1%	4.03	65.13	0.59	30.24	0.02	0.46	0.02
9/30/2008 A	N	544	0.50	10.0%	3.37	70.10	0.60	25.94	0.07	1.75	0.05
10/17/2008 A	N	450	0.25	7.2%	4.90	61.73	0.27	33.10	0.05	0.33	0.00
10/24/2008 A	N	485	0.50	10.1%	4.15	70.02	0.32	25.51	0.04	0.93	0.03
11/10/2008 A	N	485	0.50	15.1%	4.17	68.63	0.49	26.71	0.01	1.10	0.04

1. Nomenclature: T = Torrefied (temperature in parentheses, °C); N = Not washed; W = Washed.

Table D4: (Continued)

Date/ Sample name	Pretreatment[1]	Pyrolysis temperature	Screen size	Moisture content	Biochar elemental content				95% Confidence interval		
					H	C	N	O	H	C	N
		°C	mm	% dry basis	wt. %	wt. %	wt. %	wt. % by difference	wt. %	wt. %	wt. %
7/23/2008 A	W	450	0.75	7.7%	4.75	59.02	0.57	35.66	0.01	0.00	0.00
7/30/2008 A	W	450	0.75	7.2%	4.61	63.10	0.51	31.79	0.00	0.68	0.03
8/1/2008 B	W	520	0.75	6.8%	3.88	74.27	0.58	21.28	0.24	4.99	0.11
8/8/2008 A	W	485	0.50	6.4%	4.40	62.91	0.50	32.19	0.02	0.18	0.02
8/11/2008 A	W	485	0.50	6.4%	4.52	62.45	0.51	32.52	0.05	0.16	0.02
8/13/2008 A	W	485	0.50	7.4%	4.58	62.84	0.51	32.08	0.06	0.17	0.03
8/13/2008 B	W	485	0.75	7.3%	4.23	67.43	0.54	27.79	0.05	0.14	0.06
8/26/2008 C	W	520	0.75	25.6%	3.58	69.41	0.51	26.50	0.09	0.97	0.04
9/2/2008 A	W	485	0.25	7.6%	4.55	61.28	0.61	33.57	0.03	0.20	0.04
9/3/2008 A	W	520	0.25	7.6%	3.45	58.50	0.65	37.40	0.12	1.56	0.05
9/12/2008 A	W	450	0.25	7.8%	5.08	56.35	0.53	38.04	0.04	0.22	0.03
9/15/2008 A	W	485	0.50	23.7%	4.63	59.69	0.44	35.24	0.12	0.93	0.01
9/16/2008 A	W	520	0.25	19.7%	3.59	58.01	0.50	37.90	0.08	0.89	0.02
9/16/2008 C	W	485	0.50	20.7%	4.70	61.13	0.47	33.71	0.01	0.17	0.02
9/19/2008 A	W	485	0.50	19.0%	4.80	61.30	0.45	33.45	0.02	0.23	0.02
9/30/2008 B	W	544	0.50	17.3%	3.53	66.34	0.59	29.55	0.02	0.36	0.00
10/6/2008 A	W	485	0.50	11.4%	4.45	68.26	0.32	26.97	0.02	0.05	0.05
10/21/2008 A	W	426	0.50	17.0%	5.69	58.65	0.14	35.52	0.04	0.52	0.02
10/23/2008 A	W	485	0.50	16.0%	4.72	63.96	0.28	31.04	0.05	1.13	0.03
1/21/2009 A	W	450	0.75	21.3%	5.06	68.57	0.23	26.14	0.46	5.89	0.08
1/23/2009 A	W	450	0.25	18.4%	5.57	61.22	0.18	33.03	0.04	0.45	0.03

Table D5: Sulfur analysis of char samples

Date/ Sample name	Pretreatment[1]	Pyrolysis temperature	Screen size	Moisture	Sulfur
		°C	mm	% dry basis	wt. %
9/18/2008 A	T (215)	485	0.5	2.0%	0.0071
8/25/2008 A	N	485	0.5	9.2%	0.0041
9/2/2008 A	W	485	0.25	7.6%	0.0125

1. Nomenclature: T = Torrefied (temperature in parentheses, °C); N = Not washed; W = Washed.

D.3 Bio-oil analysis data

D.3.1 Moisture analysis for bio-oil fractions

Table D6: Moisture analysis data of bio oil fractions

Date/ Sample name	Pretreatment[1]	Pyrolysis temperature °C	Moisure[2] (wt. % wb)				95% Confidence interval			
			SF1	SF2	SF3	SF4	SF1	SF2	SF3	SF4
7/25/2008 A	N	450	6.77	5.99	5.07	70.32	1.55	0.18	0.46	0.62
8/7/2008 A	N	485	6.13	5.82	4.21	63.92	2.05	0.14	0.48	0.25
8/12/2008 A	N	485	5.30	6.10	6.02	66.76	1.50	0.54	0.26	2.34
8/19/2008 A	N	450	1.62	4.93	4.68	66.06	0.16	0.20	0.39	0.91
8/20/2008 A	N	450	1.97	4.87	4.89	65.55	0.31	0.27	0.02	2.93
8/22/2008 B	N	520	1.39	3.63	2.88	61.17	0.30	0.39	0.11	2.67
8/22/2008 A	N	520	1.75	4.22	4.14	68.58	0.45	0.28	0.33	0.14
8/25/2008 A	N	485	6.60	7.72	4.87	63.88	0.15	0.86	0.21	0.60
8/26/2008 A	N	485	1.88	3.72	3.35	58.85	0.26	0.12	0.42	1.18
8/26/2008 B	N	520	5.23	4.65	4.13	60.22	5.32	0.14	0.26	1.10
8/27/2008 A	N	520	1.69	3.31	3.29	59.36	0.15	0.13	0.13	0.22
9/2/2008 B	N	485	2.30	4.69	8.09	61.07	-	0.05	-	1.15
9/4/2008 A	N	426	1.92	6.60	5.26	66.93	0.16	0.18	0.53	2.40
9/10/2008 A	N	485	1.67	4.11	3.40	63.42	0.62	0.23	0.89	5.26
9/11/2008 B	N	485	2.82	3.74	3.45	60.36	0.82	0.19	0.11	3.58
9/16/2008 B	N	485	1.54	6.43	5.63	74.94	0.05	0.12	0.22	0.89
9/30/2008 A	N	544	-	-	-	67.17	-	-	-	2.14
10/17/2008 A	N	450	-	-	-	53.97	-	-	-	1.20
10/24/2008 A	N	485	-	-	-	65.84	-	-	-	1.32
11/10/2008 A	N	485	-	-	-	61.31	-	-	-	2.22
9/18/2008 A	T (215)	485	-	-	-	52.20	-	-	-	3.45
10/9/2008 A	T (215)	485	-	-	-	40.24	-	-	-	1.28
10/10/2008 A	T (215)	544	-	-	-	45.51	-	-	-	3.11
10/21/2008 B	T (215)	426	-	-	-	52.33	-	-	-	2.11
10/27/2008 A	T (215)	485	-	-	-	51.28	-	-	-	2.07
10/27/2008 B	T (215)	485	-	-	-	45.82	-	-	-	2.51
10/28/2008 A	T (215)	485	-	-	-	44.06	-	-	-	2.46
10/29/2008 A	T (215)	485	3.66	2.56	3.52	44.32	0.90	0.30	0.49	1.14
10/30/2008 A	T (250)	450	1.98	2.20	2.77	37.87	0.62	0.25	0.65	1.01
10/31/2008 B	T (250)	485	2.24	1.91	1.85	36.60	0.07	0.08	0.38	0.22
10/31/2008 A	T (250)	520	1.80	2.41	2.79	40.88	0.17	0.37	0.90	1.69
11/5/2008 A	T (250)	520	1.52	4.24	2.81	48.05	0.48	0.13	0.42	1.53
11/6/2008 A	T (180)	450	1.50	2.18	2.29	41.78	0.22	0.10	0.17	0.72
11/6/2008 B	T (180)	520	-	-	-	46.28	-	-	-	3.07
11/7/2008 A	T (180)	485	-	-	-	47.51	-	-	-	1.51
11/11/2008 A	T (180)	520	-	-	-	42.39	-	-	-	0.91
11/13/2008 A	T (180)	450	-	-	-	28.01	-	-	-	1.29
11/14/2008 A	T (215)	485	1.51	1.55	2.06	46.83	0.24	0.27	0.04	1.22
11/18/2008 A	T (180)	450	1.82	2.35	2.30	42.83	0.44	0.44	0.68	0.63
1/30/2009 A	T (215)	485	-	-	-	45.54	-	-	-	1.01

1. Nomenclature: T = Torrefied (temperature in parentheses, °C); N = Not washed; W = Washed.
2. Blank data points not analyzed due to insignificance

Table D6: (Continued)

Date/ Sample name	Pretreatment[1]	Pyrolysis temperature °C	Moisure[2] (wt. % wb) SF1	SF2	SF3	SF4	95% Confidence interval SF1	SF2	SF3	SF4
7/23/2008 A	W	450	8.01	8.31	4.87	69.33	2.75	0.33	0.27	0.72
7/30/2008 A	W	450	4.57	5.08	4.99	67.90	0.43	0.65	0.66	1.15
8/1/2008 B	W	520	4.53	5.00	4.66	60.26	2.54	0.65	0.45	1.68
8/8/2008 A	W	485	2.25	4.46	4.19	56.70	0.15	0.18	0.40	1.49
8/11/2008 A	W	485	2.59	3.11	3.74	53.85	0.08	0.06	0.44	1.22
8/13/2008 A	W	485	1.67	4.79	4.84	60.28	0.55	0.24	0.70	0.14
8/13/2008 B	W	485	1.63	4.05	3.53	64.64	0.01	0.20	0.15	0.11
8/26/2008 C	W	520	2.11	6.02	5.75	69.92	0.51	0.24	0.68	3.72
9/2/2008 A	W	485	2.16	4.25	5.39	50.29	0.57	0.84	1.53	9.53
9/3/2008 A	W	520	1.53	4.15	7.49	58.62	0.12	0.59	0.80	1.71
9/12/2008 A	W	450	-	-	-	58.70	-	-	-	0.81
9/15/2008 A	W	485	-	-	-	70.79	-	-	-	1.25
9/16/2008 C	W	485	-	-	-	72.35	-	-	-	1.55
9/16/2008 A	W	520	-	-	-	70.22	-	-	-	1.57
9/19/2008 A	W	485	-	-	-	68.29	-	-	-	3.16
9/30/2008 B	W	544	1.54	6.43	5.63	68.04	0.02	0.19	0.55	2.54
10/6/2008 A	W	485	-	-	-	64.42	-	-	-	1.94
10/21/2008 A	W	426	-	-	-	70.97	-	-	-	4.90
10/23/2008 A	W	485	-	-	-	68.01	-	-	-	1.95
1/21/2009 A	W	450	-	-	-	68.47	-	-	-	1.05
1/23/2009 A	W	450	-	-	-	68.91	-	-	-	1.82

D.3.2 Bio-oil elemental analysis

Table D7: Elemental analysis for bio-oil fractions SF1 and SF2

Date/ Sample name	Pretreatment[1]	Pyrolysis temperature	Screen size	Moisture content	SF1[2]				SF2[2]			
					H	C	N	O	H	C	N	O
		°C	mm	% dry basis	wt. %	wt. %	wt. %	wt. % by difference	wt. %	wt. %	wt. %	wt. % by difference
9/18/2008 A	T (215)	485	0.5	2.0%	6.29	59.06	0.40	34.24	6.64	50.32	0.18	42.86
10/9/2008 A	T (215)	485	0.75	2.0%	6.20	57.35	0.38	36.07	6.39	50.41	0.18	43.02
10/27/2008 A	T (215)	485	0.25	2.7%	6.81	58.24	0.27	34.68	7.21	60.60	0.17	32.03
10/27/2008 B	T (215)	485	0.5	2.3%	6.41	58.49	0.22	34.89	6.81	53.35	0.10	39.74
10/28/2008 A	T (215)	485	0.5	2.3%	6.60	64.55	0.23	28.62	7.07	55.75	0.05	37.13
10/29/2008 A	T (215)	485	0.5	2.2%	6.84	61.11	0.17	31.88	-	-	-	-
10/30/2008 A	T (250)	450	0.75	1.5%	6.23	57.41	0.30	36.06	-	-	-	-
10/31/2008 A	T (250)	520	0.75	1.5%	6.24	61.12	0.31	32.33	-	-	-	-
11/5/2008 A	T (250)	520	0.25	1.8%	-	-	-	-	6.66	54.42	0.10	38.81
11/6/2008 A	T (180)	450	0.75	1.7%	-	-	-	-	6.60	54.10	0.11	39.19
11/18/2008 A	T (180)	450	0.25	1.9%	6.31	62.86	0.18	30.64	-	-	-	-
7/25/2008 A	N	450	0.75	7.1%	6.7459	60.314	0.4842	32.455887	7.4009	57.212	0.1918	35.19501
8/7/2008 A	N	485	0.5	8.3%	6.6443	57.28	0.4124	35.66326	6.8655	51.882	0.2048	41.04775
8/19/2008 A	N	450	0.75	10.2%	6.3423	57.212	0.4792	35.966567	6.463	45.872	0.1896	47.474972
8/20/2008 A	N	450	0.25	10.2%	6.2405	58.23	0.6976	34.83241	6.5037	48.493	0.3619	44.64175
8/22/2008 A	N	520	0.75	10.0%	6.9097	64.775	0.4384	27.87692	7.1163	57.176	0.229	35.478383
8/25/2008 A	N	485	0.5	9.2%	6.2896	57.152	0.5465	36.011557	6.7468	46.937	0.1869	46.12964
8/26/2008 A	N	485	0.5	6.8%	6.3612	57.431	0.4721	35.73569	6.6189	50.29	0.2504	42.840667
8/26/2008 B	N	520	0.75	7.3%	6.507	56.917	0.4882	36.087737	6.6692	53.265	0.2168	39.84927
8/27/2008 A	N	520	0.25	7.6%	6.3991	62.587	0.5621	30.451783	6.8032	52.495	0.3043	40.39749
9/4/2008 A	N	426	0.5	7.0%	6.4832	59.704	0.4718	33.340673	6.7851	49.506	0.1896	43.51933
9/10/2008 A	N	485	0.5	7.1%	6.5082	59.474	0.4991	33.518697	6.8325	50.846	0.2327	42.088835
9/16/2008 B	N	485	0.5	16.1%	6.4492	60.251	0.4568	32.842707	6.7198	50.013	0.2384	43.028453
9/30/2008 A	N	544	0.5	10.0%	6.5252	61.932	0.4465	31.096253	7.0888	52.889	0.1461	39.876457
10/17/2008 A	N	450	0.25	7.2%	6.4786	60.382	0.4587	32.68104	6.9915	52.872	0.1074	40.029457
10/24/2008 A	N	485	0.5	10.1%	6.6083	62.711	0.3681	30.312267	7.1802	53.473	0.1045	39.242247
7/23/2008 A	W	450	0.75	7.7%	6.3576	56.245	0.4943	36.903083	6.9371	47.235	0.1595	45.668337
8/1/2008 B	W	520	0.75	6.8%	6.7145	61.585	0.2491	31.45174	6.8779	53.884	0.1086	39.129517
8/11/2008 A	W	485	0.5	6.4%	6.7401	62.526	0.2866	30.4473	7.1352	54.035	0.0863	38.743103
8/13/2008 A	W	485	0.5	7.4%	6.13	56.71	0.38	36.78	6.53	50.74	0.20	42.54
8/13/2008 B	W	485	0.75	7.3%	6.328	57.119	0.4693	36.084043	6.7335	48.545	0.1293	44.592213
8/26/2008 C	W	520	0.75	25.6%	6.1687	57.825	0.4064	35.599563	6.8522	49.702	0.0534	43.392787
9/2/2008 A	W	485	0.25	7.6%	6.3197	59.952	0.5495	33.178483	6.7348	51.684	0.3031	41.277797
9/12/2008 A	W	450	0.25	7.8%	6.2837	60.414	0.6059	32.69667	6.6419	50.32	0.2746	42.763807
9/15/2008 A	W	485	0.5	23.7%	6.068	62.288	0.4159	31.22839	6.7336	46.236	0.1404	46.89037
9/16/2008 A	W	520	0.25	19.7%	6.2864	58.127	0.4157	35.170587	6.8356	47.243	0.1884	45.733043
9/16/2008 C	W	485	0.5	20.7%	5.9815	62.259	0.4219	31.3377	6.9337	46.554	0.0852	46.427555
9/19/2008 A	W	485	0.5	19.0%	6.1533	58.757	0.2967	34.79296	6.6	48.145	0.1126	45.142123
9/30/2008 B	W	544	0.5	17.3%	6.3269	60.452	0.2823	32.93881	7.0015	49.637	0.0218	43.340275
10/6/2008 A	W	485	0.5	11.4%	6.2692	57.956	0.3512	35.423903	6.6109	49.824	0.1348	43.430677
10/21/2008 A	W	426	0.5	17.0%	6.042	62.267	0.4045	31.28685	6.5374	50.185	0.1362	43.141777
10/23/2008 A	W	485	0.5	16.0%	6.4254	59.428	0.3243	33.822313	6.936	51.685	0.1251	41.25361
1/21/2009 A	W	450	0.75	21.32%	6.3624	58.102	0.4465	35.08906	-	-	-	-
1/23/2009 A	W	450	0.25	18.4%	6.2337	56.735	0.477	36.553887	7.0866	50.004	0.0837	42.82567

1. Nomenclature: T = Torrefied (temperature in parentheses, °C); N = Not washed; W = Washed.
2. Blank data points are undetermined

Table D8: Elemental analysis for bio-oil fractions SF3 and SF4

Date/ Sample name	Pretreatment[1]	Pyrolysis temperature	Screen size	Moisture content	SF3[2]				SF4[2]			
					H	C	N	O	H	C	N	O
		°C	mm	% dry basis	wt. %	wt. %	wt. %	wt. % by difference	wt. %	wt. %	wt. %	wt. % by difference
9/18/2008 A	T (215)	485	0.5	2.0%	6.8585	59.044	0.1221	33.975653	-	-	-	-
10/9/2008 A	T (215)	485	0.75	2.0%	6.4111	56.445	0.24	36.903567	8.3596	24.69	-0.031	66.981537
10/27/2008 A	T (215)	485	0.25	2.7%	6.6154	55.386	0.1973	37.801687	-	-	-	-
10/27/2008 B	T (215)	485	0.5	2.3%	6.7177	58.439	0.1265	34.716797	-	-	-	-
10/28/2008 A	T (215)	485	0.5	2.3%	7.0271	62.944	0.0941	29.934433	-	-	-	-
10/29/2008 A	T (215)	485	0.5	2.2%	6.9758	62.67	0.0974	30.25706	8.2464	24.54	0.0745	67.139437
11/5/2008 A	T (250)	520	0.25	1.8%	6.6769	59.66	0.0863	33.57639	-	-	-	-
11/6/2008 A	T (180)	450	0.75	1.7%	6.6121	58.774	0.1454	34.468163	-	-	-	-
7/25/2008 A	N	450	0.75	7.1%	7.2154	59.007	0.2356	33.542297	9.6283	13.07	-0.025	77.32678
8/7/2008 A	N	485	0.5	8.3%	6.7967	57.508	0.2774	35.418167	9.1268	14.617	0.0183	76.237923
8/19/2008 A	N	450	0.75	10.2%	6.6971	54.918	0.2631	38.121393	9.1683	13.48	-0.019	77.369903
8/20/2008 A	N	450	0.25	10.2%	6.7959	55.34	0.3902	37.474223	4.563	13.24	-0.034	82.231343
8/22/2008 A	N	520	0.75	10.0%	7.1579	62.763	0.1871	29.89231	-	-	-	-
8/22/2008 B	N	520	0.25	9.2%	-	-	-	-	9.086	17.777	0.0059	73.131507
8/25/2008 A	N	485	0.5	9.2%	6.5183	54.671	0.2939	38.516803	4.2956	12.706	-0.028	83.0263
8/26/2008 A	N	485	0.5	6.8%	6.7225	55.748	0.2358	37.293323	9.0858	15.988	-0.054	74.980837
8/26/2008 B	N	520	0.75	7.3%	6.8117	59.531	0.1887	33.468917	9.1311	17.257	-0.124	73.736647
8/27/2008 A	N	520	0.25	7.6%	6.8838	59.032	0.3192	33.764997	9.1336	17.12	0.0087	73.737637
9/4/2008 A	N	426	0.5	7.0%	6.8946	57.654	0.2631	35.188673	-	-	-	-
9/10/2008 A	N	485	0.5	7.1%	6.7752	57.924	0.2695	35.0313	9.0112	16.665	-0.015	74.338627
9/16/2008 B	N	485	0.5	16.1%	6.907	54.572	0.2024	38.318323	9.5162	12.34	-0.018	78.16213
9/30/2008 A	N	544	0.5	10.0%	6.9702	60.571	0.2341	32.224393	8.9185	15.232	-0.011	75.860847
10/17/2008 A	N	450	0.25	7.2%	7.0121	58.312	0.2628	34.413183	-	-	-	-
10/24/2008 A	N	485	0.5	10.1%	7.1887	60.328	0.1429	32.340057	9.2264	14.675	0.0118	76.08713
7/23/2008 A	W	450	0.75	7.7%	6.9544	56.422	0.3093	36.314337	8.6375	12.392	-0.012	78.982587
8/1/2008 B	W	520	0.75	6.8%	7.002	60.185	0.1023	32.71104	9.3887	17.143	-0.103	73.571473
8/8/2008 A	W	485	0.5	6.4%	6.7843	59.48	0.0744	33.661347	-	-	-	-
8/13/2008 A	W	485	0.5	7.4%	6.5324	55.339	0.168	37.960263	-	-	-	-
8/13/2008 B	W	485	0.75	7.3%	6.5982	54.29	0.2323	38.87978	9.2871	14.857	-0.035	75.89121
8/26/2008 C	W	520	0.75	25.6%	6.4039	54.993	0.152	38.451093	9.512	11.985	-0.016	78.519027
9/2/2008 A	W	485	0.25	7.6%	6.7543	56.912	0.313	36.02031	9.0754	19.608	0.0055	71.311463
9/12/2008 A	W	450	0.25	7.8%	6.7275	57.591	0.3293	35.351827	-	-	-	-
9/15/2008 A	W	485	0.5	23.7%	6.6609	54.676	0.1813	38.481463	-	-	-	-
9/19/2008 A	W	485	0.5	19.0%	6.519	55.842	0.1711	37.4679	-	-	-	-
9/30/2008 B	W	544	0.5	17.3%	6.7511	58.567	0.0925	34.589073	-	-	-	-
10/6/2008 A	W	485	0.5	11.4%	6.6255	56.096	0.1875	37.091257	-	-	-	-
10/21/2008 A	W	426	0.5	17.0%	6.66	54.363	0.1665	38.81096	-	-	-	-
10/23/2008 A	W	485	0.5	16.0%	6.7974	56.446	0.2494	36.50722	-	-	-	-
1/21/2009 A	W	450	0.75	21.32%	6.6619	57.047	0.2017	36.089677	-	-	-	-
1/23/2009 A	W	450	0.25	18.4%	6.9532	53.886	0.126	39.0351	-	-	-	-

1. Nomenclature: T = Torrefied (temperature in parentheses, °C); N = Not washed; W = Washed.
2. Blank data points not analyzed due to insignificance

Table D9: Characteristics analysis for bio-oil fractions

Date/ Sample Name	Pretreatment[1]	Pyrolysis temperature	Screen size	Moisture content	SF1[2]			SF2[2]			SF3[2]			SF4[2]			
					Solids	HHV	Ash	Solids	HHV	Ash	Solids	HHV	Ash	Solids	HHV	Ash	pH
		°C	mm	% dry basis	wt. %	Btu/lb	wt. %	wt. %	Btu/lb	wt. %	wt. %	Btu/lb	wt. %	wt. %	Btu/lb	wt. %	
11/13/2008 A	T (180)	450	0.25	1.9%	-	-	-	-	8909.5	-	0.350	10028.2	0.271	0.009	2261.4	0.5386	-
11/18/2008 A	T (180)	450	0.25	1.9%	-	-	-	-	-	-	-	10290.7	-	-	2782.3	-	-
11/11/2008 A	T (180)	520	0.25	2.0%	-	-	-	-	-	-	-	-	-	-	2960.2	-	-
10/27/2008 B	T (215)	485	0.5	2.3%	-	-	0.795	-	-	1.255	-	-	2.519	-	-	-	-
8/20/2008 A	N	450	0.25	10.2%	-	10564.6	-	-	-	-	-	-	-	-	-	-	-
10/17/2008 A	N	450	0.25	7.2%	-	-	-	-	-	-	-	-	-	-	-	-	-
7/25/2008 A	N	450	0.75	7.1%	5.017	10172.8	0.345	-	-	0.054	-	-	0.267	-	-	-	-
10/21/2008 A	W	426	0.5	17.0%	-	-	-	-	8297.3	-	0.421	9898.4	-	0.117	2334.3	-	-
9/12/2008 A	W	450	0.25	7.8%	-	-	-	0.762	9054.7	-	1.524	10066.6	-	0.102	2395.7	-	-
1/23/2009 A	W	450	0.25	18.4%	-	-	-	1.546	-	-	0.173	9876.1	-	0.080	3115.9	-	-
7/23/2008 A	W	450	0.75	7.7%	7.397	9946.0	0.525	-	8524.3	-	-	9829.6	0.338	-	3171.4	0.4954	-
7/30/2008 A	W	450	0.75	7.2%	-	10082.0	-	-	-	-	-	-	-	-	-	-	-
8/13/2008 B	W	485	0.75	7.3%	-	-	-	0.610	-	-	1.143	-	-	0.042	2017.9	-	-
8/1/2008 B	W	520	0.75	6.8%	-	10249.8	-	-	-	-	-	-	-	-	-	-	-
9/30/2008 B	W	544	0.5	17.3%	1.511	10500.4	-	-	-	-	-	-	-	-	-	-	-
9/3/2008 A	W	520	0.25	7.6%	-	-	-	-	-	-	-	-	-	-	-	-	1.83
9/4/2008 A	N	426	0.5	7.0%	-	-	-	-	-	-	-	-	-	-	-	-	1.74
9/10/2008 A	N	485	0.5	7.1%	-	-	-	-	-	-	-	-	-	-	-	-	2.05
9/11/2008 B	N	485	0.5	7.0%	-	-	-	-	-	-	-	-	-	-	-	-	1.75
9/2/2008 A	W	485	0.25	7.6%	-	-	-	-	-	-	-	-	-	-	-	-	2.00
8/25/2008 A	N	485	0.5	9.2%	-	-	0.341	-	-	0.387	-	-	0.570	-	-	0.4357	-

1. Nomenclature: T = Torrefied (temperature in parentheses, °C); N = Not washed; W = Washed.
2. Blank data points not analyzed due to insignificance

Table D10: Insoluble analysis for bio-oil fractions

Date/ Sample name	Pretreatment[1]	Pyrolysis temperature	Screen size	Moisture content	Water insoluble content[2]			
					SF1	SF2	SF3	SF4
		°C	mm	% dry basis	wt. %	wt. %	wt. %	wt. %
9/18/2008 A	T (215)	485	0.5	2.0%	51.1	-	-	-
10/9/2008 A	T (215)	485	0.75	2.0%	48.2	-	42.0	-
10/10/2008 A	T (215)	544	0.5	2.0%	55.9	-	46.6	-
10/21/2008 B	T (215)	426	0.5	0.1%	71.3	-	-	-
10/27/2008 A	T (215)	485	0.25	2.7%	54.8	21.3	42.3	0.1
10/27/2008 B	T (215)	485	0.5	2.3%	45.4	-	-	-
10/28/2008 A	T (215)	485	0.5	2.3%	44.8	9.8	37.8	0.4
10/29/2008 A	T (215)	485	0.5	2.2%	41.5	-	-	-
10/30/2008 A	T (250)	450	0.75	1.5%	47.7	32.2	43.6	0.2
10/31/2008 A	T (250)	520	0.75	1.5%	47.3	24.5	47.0	0.4
10/31/2008 B	T (250)	485	0.5	1.5%	48.2	21.5	44.2	0.6
11/5/2008 A	T (250)	520	0.25	1.8%	55.1	22.0	44.4	0.3
11/6/2008 A	T (180)	450	0.75	1.7%	44.3	26.7	39.7	0.2
11/6/2008 B	T (180)	520	0.75	1.7%	49.9	22.1	43.2	0.4
11/7/2008 A	T (180)	485	0.5	2.0%	41.2	16.8	44.9	0.3
11/11/2008 A	T (180)	520	0.25	2.0%	51.2	-	42.4	-
11/13/2008 A	T (180)	450	0.25	1.9%	71.4	55.2	43.8	-
11/14/2008 A	T (215)	485	0.5	2.2%	49.0	-	-	-
11/18/2008 A	T (180)	450	0.25	1.9%	62.7	34.2	41.1	-
1/30/2009 A	T (215)	485	0.5	1.6%	64.1	-	-	-
7/25/2008 A	N	450	0.75	7.1%	49.6	37.1	41.1	0.0
8/7/2008 A	N	485	0.5	8.3%	40.6	29.4	49.6	0.2
8/12/2008 A	N	485	0.75	10.3%	47.6	24.0	42.5	0.2
8/19/2008 A	N	450	0.75	10.2%	40.4	21.9	46.6	0.4
8/22/2008 A	N	520	0.75	10.0%	65.4	21.8	46.7	0.4
8/22/2008 B	N	520	0.25	9.2%	56.2	28.5	47.2	0.0
8/25/2008 A	N	485	0.5	9.2%	49.7	-	45.5	0.4
8/26/2008 A	N	485	0.5	6.8%	51.9	25.4	42.8	0.3
8/26/2008 B	N	520	0.75	7.3%	60.4	24.8	44.6	0.8
8/27/2008 A	N	520	0.25	7.6%	53.2	35.8	45.7	1.0
9/2/2008 B	N	485	0.25	10.2%	51.3	14.6	44.1	0.4
9/4/2008 A	N	426	0.5	7.0%	48.7	-	40.0	0.1
9/10/2008 A	N	485	0.5	7.1%	53.0	16.1	42.0	1.0
9/11/2008 B	N	485	0.5	7.0%	42.7	21.3	39.8	0.3
9/16/2008 B	N	485	0.5	16.1%	59.5	18.1	37.4	0.1
9/30/2008 A	N	544	0.5	10.0%	57.5	18.3	42.4	0.6
10/17/2008 A	N	450	0.25	7.2%	45.2	21.0	42.1	1.1
10/24/2008 A	N	485	0.5	10.1%	48.5	-	39.2	0.1
11/10/2008 A	N	485	0.5	15.1%	48.0	-	43.7	-
7/23/2008 A	W	450	0.75	7.7%	45.8	-	-	-
7/30/2008 A	W	450	0.75	7.2%	34.7	-	38.0	-
8/1/2008 B	W	520	0.75	6.8%	38.9	-	38.3	-
8/8/2008 A	W	485	0.5	6.4%	38.5	-	36.1	-
8/11/2008 A	W	485	0.5	6.4%	41.4	20.9	39.4	0.3
8/13/2008 A	W	485	0.5	7.4%	42.7	-	41.0	-
8/13/2008 B	W	485	0.75	7.3%	39.7	-	41.3	-
8/26/2008 C	W	520	0.75	25.6%	-	17.2	43.2	0.2
9/2/2008 A	W	485	0.25	7.6%	48.4	-	41.5	-
9/3/2008 A	W	520	0.25	7.6%	41.2	-	42.6	-
9/12/2008 A	W	450	0.25	7.8%	57.2	33.0	38.6	0.3
9/15/2008 A	W	485	0.5	23.7%	45.0	-	34.5	-
9/16/2008 A	W	520	0.25	19.7%	42.2	19.1	39.4	0.2
9/16/2008 C	W	485	0.5	20.7%	46.6	-	35.6	-
9/19/2008 A	W	485	0.5	19.0%	36.8	-	37.7	-
9/30/2008 B	W	544	0.5	17.3%	44.7	-	38.5	-
10/6/2008 A	W	485	0.5	11.4%	39.5	-	33.5	-
10/21/2008 A	W	426	0.5	17.0%	83.2	14.8	30.5	0.1
10/23/2008 A	W	485	0.5	16.0%	35.8	-	33.7	-
1/21/2009 A	W	450	0.75	21.3%	46.8	22.9	36.0	0.2
1/23/2009 A	W	450	0.25	18.4%	71.6	-	35.5	-

1. Nomenclature: T = Torrefied (temperature in parentheses, °C); N = Not washed; W = Washed.
2. Blank data points are undetermined

D.3.4 Gas chromatograph mass spectroscopy information

Table D11: GC/MS volatile compound analysis for bio-oil SF1

Date/ Sample name	Pretreatment[1]	Moisture	Screen size	Pyrolysis temperature	Compound wt. % in bio-oil SF1[2]												
		% db	mm	°C	Acetic Acid	2 methyl phenol	3 methyl phenol	3 ethyl phenol	2 methoxy 4 methyl phenol	2 methoxy phenol	5 methyl furfural	3 methyl - 2(5H)- furanone	Hydroquinone	Phenol	5 hydroxy methyl furfural	Furfural	Levoglucosan
9/18/2008 A	T (215)	2.0%	0.5	485	0.535	0.869	0.713	0.334	0.713	0.557	0.490	0.535	0.535	0.027	0.676	0.045	3.124
10/10/2008 A	T (215)	2.0%	0.5	544	0.267	0.868	0.734	0.334	0.601	0.467	0.490	0.534	0.556	0.035	1.002	0.022	6.495
10/21/2008 B	T (215)	0.1%	0.5	426	0.269	0.000	0.719	0.337	0.629	0.472	0.000	0.539	0.584	0.010	1.011	0.022	5.539
10/27/2008 A	T (215)	2.7%	0.25	485	0.312	0.868	0.735	0.334	0.735	0.601	0.490	0.534	0.534	0.028	1.136	0.067	3.376
10/27/2008 B	T (215)	2.3%	0.5	485	0.000	0.871	0.737	0.335	0.692	0.514	0.491	0.536	0.581	0.020	1.946	0.022	7.119
10/28/2008 A	T (215)	2.3%	0.5	485	0.000	0.000	0.719	0.315	0.562	0.427	0.000	0.000	0.539	0.003	0.651	0	8.862
10/29/2008 A	T (215)	2.2%	0.5	485	-	-	-	-	-	-	-	-	-	-	-	0.046	4.573
10/30/2008 A	T (250)	1.5%	0.75	450	-	-	-	-	-	-	-	-	-	-	-	0.023	7.6
10/31/2008 A	T (250)	1.5%	0.75	520	-	-	-	-	-	-	-	-	-	-	-	0.022	6.835
10/31/2008 B	T (250)	1.5%	0.5	485	-	-	-	-	-	-	-	-	-	-	-	0	9.867
11/5/2008 A	T (250)	1.8%	0.25	520	-	-	-	-	-	-	-	-	-	-	-	0.023	11.94
11/6/2008 A	T (180)	1.7%	0.75	450	-	-	-	-	-	-	-	-	-	-	-	0.03	7.081
11/6/2008 B	T (180)	1.7%	0.75	520	-	-	-	-	-	-	-	-	-	-	-	0	10.03
11/7/2008 A	T (180)	2.0%	0.5	485	-	-	-	-	-	-	-	-	-	-	-	0	7.686
7/25/2008 A	N	7.1%	0.75	450	-	-	-	-	-	-	-	-	-	-	-	0.04	6.183
8/7/2008 A	N	8.3%	0.5	485	-	-	-	-	-	-	-	-	-	-	-	0.044	3.034
8/19/2008 A	N	10.2%	0.75	450	0.334	0.868	0.735	0.334	0.668	0.534	0.490	0.534	0.601	0.026	1.115	0.022	6.596
8/20/2008 A	N	10.2%	0.25	450	0.378	0.867	0.711	0.333	0.600	0.489	0.489	0.533	0.578	0.015	1.324	0.022	3.334
8/22/2008 A	N	10.0%	0.75	520	0.468	0.891	0.757	0.334	0.691	0.557	0.490	0.557	0.601	0.049	1.211	0.022	6.922
8/25/2008 A	N	9.2%	0.5	485	-	-	-	-	-	-	-	-	-	-	-	0.042	6.101
8/26/2008 A	N	6.8%	0.5	485	-	-	-	-	-	-	-	-	-	-	-	0.022	7.979
8/26/2008 B	N	7.3%	0.75	520	-	-	-	-	-	-	-	-	-	-	-	0.022	7.778
8/27/2008 A	N	7.6%	0.25	520	0.000	0.907	0.767	0.349	0.651	0.512	0.512	0.535	0.581	0.022	1.402	0.023	7.837
9/2/2008 B	N	10.2%	0.25	485	0.760	0.872	0.715	0.335	0.693	0.559	0.492	0.536	0.514	0.028	0.919	0.045	3.472
9/4/2008 A	N	7.0%	0.5	426	0.510	0.000	0.709	0.332	0.620	0.487	0.487	0.554	0.554	0.014	0.807	0.022	5.838
9/10/2008 A	N	7.1%	0.5	485	0.422	0.866	0.711	0.333	0.622	0.466	0.489	0.533	0.533	0.015	0.727	0.022	5.453
9/11/2008 B	N	7.0%	0.5	485	0.646	0.869	0.736	0.334	0.713	0.580	0.490	0.535	0.557	0.032	1.071	0.045	4.6
10/24/2008 A	N	10.1%	0.5	485	0.000	0.885	0.749	0.318	0.658	0.545	0.499	0.545	0.545	0.020	0.794	0.045	5.722
11/10/2008 A	N	15.1%	0.5	485	-	-	-	-	-	-	-	-	-	-	-	-	8.438
7/23/2008 A	W	7.7%	0.75	450	0.561	0.875	0.718	0.336	0.695	0.538	0.493	0.538	0.538	0.022	0.957	0.022	6.175
7/30/2008 A	W	7.2%	0.75	450	-	-	-	-	-	-	-	-	-	-	-	0.046	5.811
8/1/2008 B	W	6.8%	0.75	520	-	-	-	-	-	-	-	-	-	-	-	0.044	5.247
8/8/2008 A	W	6.4%	0.5	485	-	-	-	-	-	-	-	-	-	-	-	0.025	4.164
8/11/2008 A	W	6.4%	0.5	485	-	-	-	-	-	-	-	-	-	-	-	0.022	4.589
8/13/2008 A	W	7.4%	0.5	485	0.000	0.869	0.735	0.334	0.713	0.512	0.490	0.535	0.557	0.028	1.518	0.022	7.58
8/26/2008 C	W	25.6%	0.75	520	0.000	0.869	0.736	0.334	0.646	0.468	0.490	0.535	0.557	0.024	1.988	0.022	8.732
9/2/2008 A	W	7.6%	0.25	485	0.514	0.871	0.737	0.335	0.647	0.491	0.491	0.514	0.514	0.016	0.931	0.045	6.099
9/3/2008 A	W	7.6%	0.25	520	0.000	0.869	0.735	0.334	0.624	0.468	0.490	0.512	0.535	0.021	1.408	0.022	6.886
9/12/2008 A	W	7.8%	0.25	450	0.356	0.000	0.713	0.334	0.579	0.423	0.490	0.512	0.534	0.008	1.477	0.022	4.562
9/15/2008 A	W	23.7%	0.5	485	0.512	0.868	0.712	0.334	0.623	0.467	0.490	0.512	0.512	0.011	0.009	0.022	2.834
9/16/2008 A	W	19.7%	0.25	520	0.000	0.868	0.712	0.334	0.556	0.423	0.000	0.000	0.534	0.007	1.083	0	6.435
9/16/2008 C	W	20.7%	0.5	485	0.156	0.000	0.711	0.333	0.578	0.422	0.000	0.000	0.533	0.005	1.115	0	6.756
10/23/2008 A	W	16.0%	0.5	485	0.000	0.881	0.723	0.339	0.610	0.452	0.000	0.520	0.542	0.007	2.003	0.023	7.814

1. Nomenclature: T = Torrefied (temperature in parentheses, °C); N = Not washed; W = Washed.
2. Blank data points are undetermined

Table D12: GC/MS volatile compound analysis for bio-oil SF2

Date/ Sample name	Pretreatment[1]	Moisture	Screen size	Pyrolysis temperature	Compound wt. % in bio-oil SF2[2]											
		% db	mm	°C	Acetic Acid	2 methyl phenol	3 methyl phenol	3 ethyl phenol	2 methoxy 4 methyl phenol	2 methoxy phenol	5 methyl furfural	3 methyl -2(5H) furanone	Hydroquinone	Phenol	5 hydroxy methyl furfural	Furfural	Levoglucosan
9/18/2008 A	T (215)	2.0%	0.5	485	1.988	0.916	0.737	0.335	1.117	1.028	0.491	0.603	0.514	0.112	0.332	0.112	1.734
10/21/2008 B	T (215)	0.1%	0.5	426	1.926	0.896	0.739	0.336	1.120	0.985	0.493	0.582	0.515	0.081	0.365	0.09	1.388
10/27/2008 A	T (215)	2.7%	0.25	485	1.535	0.890	0.801	0.334	1.068	0.957	0.512	0.601	0.512	0.084	0.718	0.133	1.764
10/27/2008 B	T (215)	2.3%	0.5	485	1.675	0.941	0.780	0.344	1.216	1.102	0.528	0.620	0.528	0.195	0.706	0.138	2.424
10/28/2008 A	T (215)	2.3%	0.5	485	1.470	0.927	0.769	0.339	1.244	1.085	0.520	0.633	0.520	0.118	0.705	0.136	2.105
10/29/2008 A	T (215)	2.2%	0.5	485	-	-	-	-	-	-	-	-	-	-	-	0.067	1.754
10/30/2008 A	T (250)	1.5%	0.75	450	-	-	-	-	-	-	-	-	-	-	-	0.022	3.397
10/31/2008 A	T (250)	1.5%	0.75	520	-	-	-	-	-	-	-	-	-	-	-	0.067	3.511
10/31/2008 B	T (250)	1.5%	0.5	485	-	-	-	-	-	-	-	-	-	-	-	0.067	2.977
11/5/2008 A	T (250)	1.8%	0.25	520	-	-	-	-	-	-	-	-	-	-	-	0.09	4.306
11/6/2008 A	T (180)	1.7%	0.75	450	-	-	-	-	-	-	-	-	-	-	-	0.116	2.102
11/6/2008 B	T (180)	1.7%	0.75	520	-	-	-	-	-	-	-	-	-	-	-	0.334	3.906
11/7/2008 A	T (180)	2.0%	0.5	485	-	-	-	-	-	-	-	-	-	-	-	0.423	3.006
11/11/2008 A	T (180)	2.0%	0.25	520	-	-	-	-	-	-	-	-	-	-	-	0.267	-
11/13/2008 A	T (180)	1.9%	0.25	450	-	-	-	-	-	-	-	-	-	-	-	0.25	-
11/14/2008 A	T (215)	2.2%	0.5	485	-	-	-	-	-	-	-	-	-	-	-	0.067	-
7/25/2008 A	N	7.1%	0.75	450	-	-	-	-	-	-	-	-	-	-	-	0.224	1.616
8/19/2008 A	N	10.2%	0.75	450	1.449	0.914	0.758	0.334	1.137	1.114	0.513	0.624	0.535	0.135	0.370	0.156	2.098
8/20/2008 A	N	10.2%	0.25	450	1.892	0.890	0.779	0.334	0.890	0.868	0.490	0.601	0.512	0.083	0.427	0.111	1.423
8/22/2008 A	N	10.0%	0.75	520	1.627	0.958	0.802	0.334	1.025	0.981	0.513	0.646	0.535	0.216	0.374	0.111	1.966
8/25/2008 A	N	9.2%	0.5	485	-	-	-	-	-	-	-	-	-	-	-	0.192	1.602
8/26/2008 A	N	6.8%	0.5	485	-	-	-	-	-	-	-	-	-	-	-	0.135	2.458
8/26/2008 B	N	7.3%	0.75	520	-	-	-	-	-	-	-	-	-	-	-	0.112	3.196
8/27/2008 A	N	7.6%	0.25	520	1.826	0.913	0.757	0.334	0.891	0.869	0.512	0.601	0.512	0.132	0.605	0.134	2.315
9/2/2008 B	N	10.2%	0.25	485	0.490	0.891	0.802	0.334	0.958	0.958	0.512	0.601	0.512	0.102	0.460	0.156	1.614
9/4/2008 A	N	7.0%	0.5	426	1.944	0.872	0.760	0.335	0.894	0.872	0.492	0.559	0.514	0.062	0.231	0.089	1.11
9/10/2008 A	N	7.1%	0.5	485	2.089	0.889	0.800	0.333	1.022	0.978	0.489	0.600	0.511	0.109	0.306	0.111	1.464
9/11/2008 B	N	7.0%	0.5	485	1.915	0.891	0.735	0.334	0.980	0.935	0.490	0.579	0.512	0.101	0.273	0.089	1.644
10/24/2008 A	N	10.1%	0.5	485	2.133	0.889	0.733	0.333	1.000	0.977	0.511	0.600	0.511	0.097	0.571	0.156	1.591
11/10/2008 A	N	15.1%	0.5	485	-	-	-	-	-	-	-	-	-	-	-	0.222	-
7/23/2008 A	W	7.7%	0.75	450	2.410	0.892	0.781	0.335	0.982	0.870	0.491	0.580	0.513	0.062	0.112	0.089	1.779
8/13/2008 A	W	7.4%	0.5	485	2.315	0.913	0.779	0.334	1.224	1.024	0.512	0.623	0.512	0.143	0.413	0.178	2.914
8/26/2008 C	W	25.6%	0.75	520	0.560	0.918	0.828	0.336	0.963	0.828	0.515	0.627	0.515	0.130	0.570	0.112	2.629
9/2/2008 A	W	7.6%	0.25	485	0.646	0.891	0.802	0.334	0.957	0.779	0.490	0.579	0.512	0.072	0.628	0.089	2.391
9/3/2008 A	W	7.6%	0.25	520	1.959	0.912	0.734	0.334	0.912	0.801	0.512	0.579	0.512	0.110	0.357	0.111	2.191
9/12/2008 A	W	7.8%	0.25	450	0.735	0.869	0.780	0.334	0.913	0.735	0.490	0.557	0.512	0.062	0.379	0.089	1.978
9/15/2008 A	W	23.7%	0.5	485	0.971	0.881	0.768	0.339	0.858	0.723	0.497	0.565	0.519	0.050	0.434	0.068	1.85
9/16/2008 A	W	19.7%	0.25	520	1.741	0.893	0.736	0.335	0.803	0.692	0.491	0.558	0.513	0.083	0.374	0.067	2.587
9/16/2008 C	W	20.7%	0.5	485	1.359	0.869	0.758	0.312	0.825	0.713	0.490	0.557	0.513	0.049	0.020	0.067	1.371
10/23/2008 A	W	16.0%	0.5	485	2.075	0.870	0.759	0.335	0.937	0.803	0.491	0.580	0.513	0.061	0.548	0.134	1.853

1. Nomenclature: T = Torrefied (temperature in parentheses, °C); N = Not washed; W = Washed.
2. Blank data points are undetermined

Table D13: GC/MS volatile compound analysis for bio-oil SF3

Date/ Sample name	Pretreatment[1]	Moisture	Screen size	Pyrolysis temperature	Compound wt. % in bio-oil SF3[2]												
		% db	mm	°C	Acetic Acid	2 methyl phenol	3 methyl phenol	3 ethyl phenol	2 methoxy 4 methyl phenol	2 methoxy phenol	5 methyl furfural	3 methyl -2(5H)-furanone	Hydroquinone	Phenol	5 hydroxy methyl furfural	Furfural	Levoglucosan
9/18/2008 A	T (215)	2.0%	0.5	485	1.293	0.891	0.735	0.334	0.869	0.758	0.490	0.557	0.535	0.050	0.552	0.08915	4.91082
10/21/2008 B	T (215)	0.1%	0.5	426	0.941	0.874	0.717	0.336	0.874	0.762	0.493	0.560	0.538	0.041	0.553	0.0672	4.34988
10/27/2008 A	T (215)	2.7%	0.25	485	0.512	0.868	0.756	0.311	0.845	0.756	0.512	0.556	0.534	0.047	0.877	0.13346	4.05789
10/27/2008 B	T (215)	2.3%	0.5	485	1.760	0.891	0.757	0.334	0.936	0.847	0.512	0.557	0.535	0.061	0.852	0.15594	5.05107
10/28/2008 A	T (215)	2.3%	0.5	485	1.249	0.892	0.736	0.334	0.914	0.803	0.491	0.557	0.535	0.059	0.987	0.1115	5.62452
10/29/2008 A	T (215)	2.2%	0.5	485	-	-	-	-	-	-	-	-	-	-	-	0.06746	4.76821
10/30/2008 A	T (250)	1.5%	0.75	450	-	-	-	-	-	-	-	-	-	-	-	0.04476	6.97482
10/31/2008 A	T (250)	1.5%	0.75	520	-	-	-	-	-	-	-	-	-	-	-	0.0444	8.23535
10/31/2008 B	T (250)	1.5%	0.5	485	-	-	-	-	-	-	-	-	-	-	-	0.04442	7.13428
11/5/2008 A	T (250)	1.8%	0.25	520	-	-	-	-	-	-	-	-	-	-	-	0.06773	6.98591
11/6/2008 A	T (180)	1.7%	0.75	450	-	-	-	-	-	-	-	-	-	-	-	0.09337	5.48909
11/6/2008 B	T (180)	1.7%	0.75	520	-	-	-	-	-	-	-	-	-	-	-	0.24468	10.0726
11/7/2008 A	T (180)	2.0%	0.5	485	-	-	-	-	-	-	-	-	-	-	-	0.31151	5.37247
11/11/2008 A	T (180)	2.0%	0.25	520	-	-	-	-	-	-	-	-	-	-	-	0.2666	-
11/13/2008 A	T (180)	1.9%	0.25	450	-	-	-	-	-	-	-	-	-	-	-	0.17857	-
11/14/2008 A	T (215)	2.2%	0.5	485	-	-	-	-	-	-	-	-	-	-	-	0.15648	-
7/25/2008 A	N	7.1%	0.75	450	-	-	-	-	-	-	-	-	-	-	-	0.20145	5.11142
8/7/2008 A	N	8.3%	0.5	485	-	-	-	-	-	-	-	-	-	-	-	0.11111	3.13932
8/19/2008 A	N	10.2%	0.75	450	2.289	0.889	0.756	0.333	0.911	0.889	0.511	0.578	0.556	0.069	0.551	0.15559	5.65329
8/20/2008 A	N	10.2%	0.25	450	2.088	0.866	0.755	0.333	0.778	0.755	0.489	0.555	0.533	0.052	0.569	0.1333	4.42391
8/22/2008 A	N	10.0%	0.75	520	2.219	0.932	0.777	0.333	0.865	0.843	0.510	0.599	0.555	0.127	0.582	0.15532	6.61285
8/25/2008 A	N	9.2%	0.5	485	-	-	-	-	-	-	-	-	-	-	-	0.14123	5.27754
8/26/2008 A	N	6.8%	0.5	485	-	-	-	-	-	-	-	-	-	-	-	0.13539	5.92724
8/26/2008 B	N	7.3%	0.75	520	-	-	-	-	-	-	-	-	-	-	-	0.13412	7.56154
8/27/2008 A	N	7.6%	0.25	520	0.801	0.890	0.756	0.334	0.779	0.734	0.512	0.556	0.534	0.069	0.782	0.13349	5.63119
9/2/2008 B	N	10.2%	0.25	485	1.836	0.873	0.761	0.336	0.806	0.739	0.515	0.560	0.538	0.052	0.780	0.13438	5.4443
9/4/2008 A	N	7.0%	0.5	426	1.288	0.866	0.733	0.311	0.755	0.688	0.489	0.533	0.533	0.032	0.497	0.08884	4.16183
9/10/2008 A	N	7.1%	0.5	485	1.266	0.866	0.755	0.333	0.800	0.733	0.489	0.555	0.533	0.053	0.550	0.06665	4.21709
9/11/2008 B	N	7.0%	0.5	485	1.450	0.892	0.758	0.335	0.803	0.736	0.491	0.558	0.513	0.049	0.415	0.06691	3.77999
10/24/2008 A	N	10.1%	0.5	485	2.364	0.892	0.758	0.335	0.825	0.781	0.513	0.558	0.535	0.050	0.684	0.15611	4.2671
11/10/2008 A	N	15.1%	0.5	485	-	-	-	-	-	-	-	-	-	-	-	0.17778	-
7/23/2008 A	W	7.7%	0.75	450	2.039	0.874	0.762	0.336	0.807	0.672	0.493	0.560	0.515	0.046	0.436	0.08962	6.35106
7/30/2008 A	W	7.2%	0.75	450	-	-	-	-	-	-	-	-	-	-	-	0.11126	5.71539
8/1/2008 B	W	6.8%	0.75	520	-	-	-	-	-	-	-	-	-	-	-	0.15545	4.89681
8/8/2008 A	W	6.4%	0.5	485	-	-	-	-	-	-	-	-	-	-	-	0.11095	4.3994
8/11/2008 A	W	6.4%	0.5	485	-	-	-	-	-	-	-	-	-	-	-	0.06657	4.40799
8/13/2008 A	W	7.4%	0.5	485	1.717	0.892	0.780	0.334	0.959	0.780	0.513	0.580	0.535	0.070	0.838	0.15608	7.57027
8/26/2008 C	W	25.6%	0.75	520	1.067	0.889	0.756	0.333	0.800	0.667	0.489	0.578	0.534	0.065	0.709	0.08892	6.9283
9/2/2008 A	W	7.6%	0.25	485	0.444	0.865	0.754	0.311	0.776	0.643	0.488	0.532	0.510	0.038	0.759	0.08873	5.30361
9/3/2008 A	W	7.6%	0.25	520	1.388	0.896	0.761	0.336	0.761	0.627	0.493	0.560	0.515	0.055	0.684	0.08956	6.19602
9/12/2008 A	W	7.8%	0.25	450	1.219	0.865	0.732	0.333	0.732	0.599	0.488	0.532	0.510	0.028	0.694	0.06651	4.93564
9/15/2008 A	W	23.7%	0.5	485	1.045	0.867	0.733	0.311	0.733	0.600	0.489	0.533	0.511	0.025	0.692	0.04445	5.41661
9/16/2008 A	W	19.7%	0.25	520	0.512	0.890	0.757	0.334	0.734	0.623	0.490	0.534	0.512	0.049	0.517	0.06676	4.85611
9/16/2008 C	W	20.7%	0.5	485	1.420	0.865	0.732	0.311	0.732	0.621	0.488	0.533	0.510	0.029	0.018	0.06657	4.06923
10/23/2008 A	W	16.0%	0.5	485	0.732	0.866	0.732	0.333	0.777	0.666	0.488	0.533	0.511	0.032	0.853	0.13318	4.63637

1. Nomenclature: T = Torrefied (temperature in parentheses, °C); N = Not washed; W = Washed.
2. Blank data points are undetermined

Table D14: GC/MS volatile compound analysis for bio-oil SF4

Date/ Sample name	Pretreatment[1]	Moisture	Screen size	Pyrolysis temperature	Compound wt. % in bio-oil SF4[2]												
		% db	mm	°C	Acetic Acid	2 methyl phenol	3 methyl phenol	3 ethyl phenol	2 methoxy 4 methyl phenol	2 methoxy phenol	5 methyl furfural	3 methyl - 2(5H)-furanone	Hydroquinone	Phenol	5 hydroxy methyl furfural	Furfural	Levoglucosan
9/18/2008 A	T (215)	2.0%	0.5	485	1.601	0.867	0.712	0.000	0.578	0.556	0.489	0.000	0.000	0.011	0.000	0.089	0.000
10/10/2008 A	T (215)	2.0%	0.5	544	0.356	0.867	0.711	0.311	0.600	0.578	0.489	0.533	0.000	0.038	0.000	0.067	0.000
10/21/2008 B	T (215)	0.1%	0.5	426	8.124	0.868	0.000	0.000	0.579	0.512	0.490	0.000	0.000	0.010	0.000	0.089	0.000
10/27/2008 A	T (215)	2.7%	0.25	485	8.145	0.875	0.718	0.000	0.561	0.516	0.494	0.000	0.000	0.008	0.000	0.224	0.000
10/27/2008 B	T (215)	2.3%	0.5	485	4.543	0.909	0.745	0.000	0.629	0.606	0.513	0.536	0.000	0.016	0.000	0.186	0.000
10/28/2008 A	T (215)	2.3%	0.5	485	7.940	0.872	0.716	0.000	0.604	0.626	0.514	0.514	0.000	0.018	0.000	0.201	0.000
10/29/2008 A	T (215)	2.2%	0.5	485	2.271	-	-	-	-	-	-	-	-	-	-	0.089	0.000
10/30/2008 A	T (250)	1.5%	0.75	450	3.965	-	-	-	-	-	-	-	-	-	-	0.069	0.000
10/31/2008 A	T (250)	1.5%	0.75	520	0.553	-	-	-	-	-	-	-	-	-	-	0.066	0.000
10/31/2008 B	T (250)	1.5%	0.5	485	7.297	-	-	-	-	-	-	-	-	-	-	0.067	0.000
11/5/2008 A	T (250)	1.8%	0.25	520	1.696	-	-	-	-	-	-	-	-	-	-	0.07	0.000
11/6/2008 A	T (180)	1.7%	0.75	450	1.062	-	-	-	-	-	-	-	-	-	-	0.097	0.000
11/6/2008 B	T (180)	1.7%	0.75	520	10.89	-	-	-	-	-	-	-	-	-	-	1.645	0.000
11/7/2008 A	T (180)	2.0%	0.5	485	0.378	-	-	-	-	-	-	-	-	-	-	0.423	0.000
11/11/2008 A	T (180)	2.0%	0.25	520	1.333	-	-	-	-	-	-	-	-	-	-	0.467	0.000
11/13/2008 A	T (180)	1.9%	0.25	450	0.133	-	-	-	-	-	-	-	-	-	-	0.2	0.000
11/14/2008 A	T (215)	2.2%	0.5	485	0.422	-	-	-	-	-	-	-	-	-	-	0.156	0.000
7/25/2008 A	N	7.1%	0.75	450	0.569	-	-	-	-	-	-	-	-	-	-	0.237	0.000
8/7/2008 A	N	8.3%	0.5	485	3.245	-	-	-	-	-	-	-	-	-	-	0.133	0.000
8/19/2008 A	N	10.2%	0.75	450	0.782	0.871	0.000	0.000	0.558	0.491	0.491	0.000	0.000	0.008	0.000	0.112	0.000
8/20/2008 A	N	10.2%	0.25	450	1.281	0.000	0.719	0.000	0.562	0.517	0.494	0.517	0.000	0.010	0.000	0.09	0.000
8/22/2008 A	N	10.0%	0.75	520	3.651	0.863	0.000	0.000	0.553	0.465	0.487	0.000	0.000	0.012	0.000	0.089	0.000
8/25/2008 A	N	9.2%	0.5	485	-	-	-	-	-	-	-	-	-	-	-	0.222	0.000
8/26/2008 A	N	6.8%	0.5	485	4.752	-	-	-	-	-	-	-	-	-	-	0.137	0.000
8/26/2008 B	N	7.3%	0.75	520	5.107	-	-	-	-	-	-	-	-	-	-	0.089	0.000
8/27/2008 A	N	7.6%	0.25	520	0.557	0.870	0.713	0.000	0.557	0.513	0.491	0.000	0.000	0.016	0.000	0.134	0.000
9/2/2008 B	N	10.2%	0.25	485	0.808	0.876	0.719	0.000	0.584	0.539	0.494	0.517	0.000	0.014	0.000	0.112	0.000
9/4/2008 A	N	7.0%	0.5	426	1.225	0.869	0.713	0.000	0.557	0.490	0.490	0.000	0.000	0.010	0.000	0.067	0.000
9/10/2008 A	N	7.1%	0.5	485	1.740	0.870	0.714	0.000	0.558	0.513	0.491	0.000	0.000	0.010	0.000	0.067	0.000
9/11/2008 B	N	7.0%	0.5	485	1.252	0.872	0.000	0.000	0.581	0.536	0.492	0.000	0.000	0.011	0.000	0.067	0.000
10/17/2008 A	N	7.2%	0.25	450	3.107	-	-	-	-	-	-	-	-	-	-	0.044	0.000
10/24/2008 A	N	10.1%	0.5	485	3.725	0.870	0.000	0.000	0.558	0.491	0.513	0.513	0.000	0.008	0.000	0.223	0.000
11/10/2008 A	N	15.1%	0.5	485	8.735	-	-	-	-	-	-	-	-	-	-	0.155	0.000
7/23/2008 A	W	7.7%	0.75	450	6.891	0.000	0.000	0.000	0.535	0.424	0.491	0.000	0.000	0.004	0.000	0.089	0.000
7/30/2008 A	W	7.2%	0.75	450	0.711	-	-	-	-	-	-	-	-	-	-	0.2	0.000
8/1/2008 B	W	6.8%	0.75	520	0.716	-	-	-	-	-	-	-	-	-	-	0.134	0.000
8/8/2008 A	W	6.4%	0.5	485	2.705	-	-	-	-	-	-	-	-	-	-	0.229	0.000
8/11/2008 A	W	6.4%	0.5	485	0.845	-	-	-	-	-	-	-	-	-	-	0.2	0.000
8/13/2008 A	W	7.4%	0.5	485	-	0.869	0.713	0.000	0.579	0.513	0.490	0.000	0.000	0.013	0.000	0.111	0.000
8/13/2008 B	W	7.3%	0.75	485	1.471	-	-	-	-	-	-	-	-	-	-	-	-
8/26/2008 C	W	25.6%	0.75	520	0.405	0.878	0.720	0.000	0.563	0.495	0.495	0.518	0.000	0.019	0.000	0.135	0.000
9/2/2008 A	W	7.6%	0.25	485	1.867	0.867	0.711	0.000	0.578	0.556	0.489	0.000	0.000	0.015	0.000	0.089	0.000
9/3/2008 A	W	7.6%	0.25	520	3.230	0.869	0.713	0.000	0.579	0.512	0.490	0.000	0.000	0.016	0.000	0.067	0.000
9/12/2008 A	W	7.8%	0.25	450	0.795	0.886	0.727	0.000	0.591	0.522	0.500	0.000	0.000	0.010	0.000	0.068	0.000
9/15/2008 A	W	23.7%	0.5	485	3.180	0.867	0.000	0.000	0.578	0.467	0.489	0.000	0.000	0.008	0.000	0.044	0.000
9/16/2008 A	W	19.7%	0.25	520	3.947	0.869	0.713	0.000	0.557	0.468	0.490	0.000	0.000	0.010	0.000	0.045	0.000
9/16/2008 C	W	20.7%	0.5	485	2.561	0.000	0.000	0.000	0.561	0.471	0.493	0.000	0.000	0.003	0.000	0.045	0.000
10/23/2008 A	W	16.0%	0.5	485	0.488	0.865	0.710	0.000	0.577	0.510	0.488	0.000	0.000	0.010	0.000	0.111	0.000

1. Nomenclature: T = Torrefied (temperature in parentheses, °C); N = Not washed; W = Washed.
2. Blank data points are undetermined

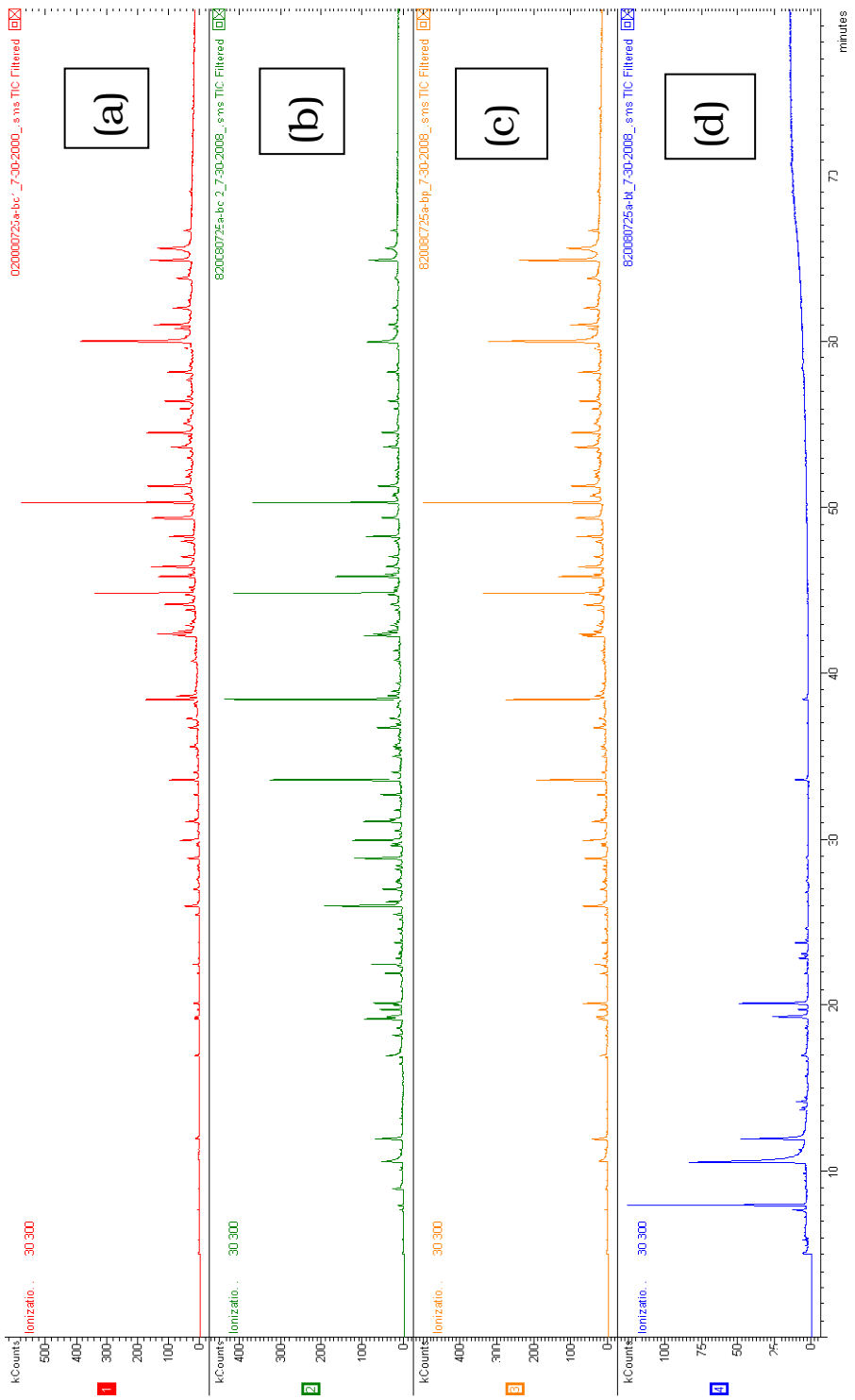

Figure D1: Sample GC-MS profile plots for each bio-oil fraction (a) SF1, (b) SF2, (c) SF3, (d) SF4

Sample run: 7/25/2008 A, pyrolysis temperature = 450°C,

grind size = 0.75mm, moisture content = 7.2% db

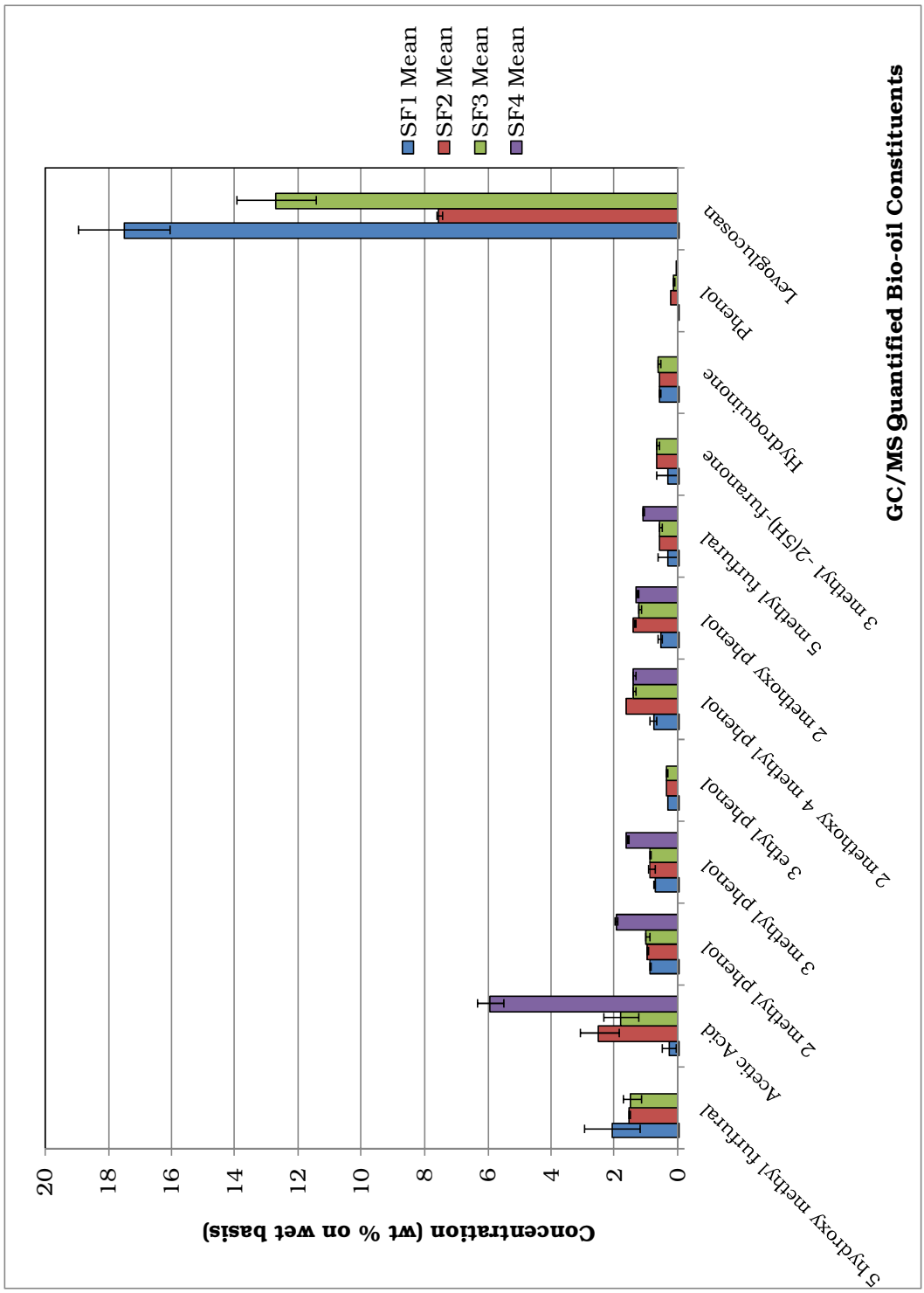

Figure D2: Average compound concentrations with 95% confidence intervals from three repeated tests on the same bio-oil sample: 11/5/2008A

Table D15: Micro-gas chromatograph gas concentration data

	Sample gas data								95% Confidence Interval									
Date/Run	Nitrogen flow rate SLPM	Run time Minutes	Nitrogen Vol. %	Hydrogen Vol. %	Carbon Monoxide Vol. %	Methane Vol. %	Propane Vol. %	Carbon Dioxide Vol. %	Nitrogen Vol. %	Hydrogen Vol. %	Carbon Monoxide Vol. %	Methane Vol. %	Propane Vol. %	Carbon Dioxide Vol. %	Total gas Liters	Ave. density g/L	Gas Produced g total	± g
Unwashed biomass tests																		
7/25/2008 A	18.3897	67.6	92.76	0.0148	0.2811	0.0529	0.1410	0.3516	0.092	0.0022	0.0245	0.0039	0.0120	0.0429	1242.5	0.0132	16.34	1.71
8/7/2008 A	18.1350	95.2	94.12	0.0300	0.3400	0.0762	0.1692	0.2854	0.115	0.0022	0.0368	0.0052	0.0015	0.0378	1726.2	0.0132	22.83	2.14
8/12/2008 A	18.0893	102.5	80.97	0.6200	0.3782	0.0618	0.3138	0.2753	0.492	0.0133	0.0345	0.0050	0.0148	0.0205	1854.2	0.0171	31.64	2.10
8/19/2008 A	18.1345	100.8	94.32	0.0200	0.3238	0.0586	0.0186	0.3357	0.035	0.0000	0.0090	0.0010	0.0023	0.0104	1827.3	0.0111	20.35	0.65
8/20/2008 A	18.1292	129.6	94.75	0.0120	0.1640	0.0367	0.0214	0.1893	0.163	0.0026	0.0281	0.0077	0.0023	0.0384	2349.8	0.0063	14.79	2.77
8/22/2008 A	18.1974	87.5	93.86	0.0821	0.5393	0.1314	0.1021	0.3536	0.094	0.0044	0.0376	0.0052	0.0158	0.0237	1592.6	0.0161	25.65	1.96
8/22/2008 B	18.2130	101.5	94.21	0.0563	0.3744	0.0975	0.1444	0.2388	0.111	0.0064	0.0555	0.0162	0.0205	0.0326	1848.9	0.0124	23.00	3.29
8/25/2008 A	18.1542	106.3	93.91	0.0311	0.3144	0.0589	0.1794	0.2872	0.149	0.0032	0.0454	0.0046	0.0111	0.0443	1930.4	0.0130	25.16	3.16
8/26/2008 A	18.1824	101.5	94.00	0.0372	0.4065	0.0867	0.1717	0.3428	0.078	0.0051	0.0344	0.0091	0.0034	0.0300	1845.5	0.0153	28.15	2.07
8/26/2008 B	18.1938	93.3	93.81	0.0788	0.5206	0.1181	0.1675	0.3338	0.100	0.0075	0.0500	0.0179	0.0036	0.0298	1696.6	0.0166	28.16	2.32
8/27/2008 A	18.2671	77.9	97.41	0.0592	0.4442	0.0867	0.1425	0.2667	1.070	0.0072	0.0594	0.0168	0.0414	0.0446	1422.7	0.0137	19.46	3.49
9/2/2008 B	18.1707	85.2	98.46	0.0385	0.2969	0.0483	0.1733	0.2777	0.729	0.0045	0.0525	0.0058	0.0091	0.0425	1548.4	0.0125	19.31	2.57
9/4/2008 A	18.1779	73.5	97.78	0.0211	0.2320	0.0400	0.2060	0.2480	1.603	0.0039	0.0305	0.0098	0.0055	0.0362	1336.7	0.0116	15.57	1.66
9/10/2008 A	18.3891	85.3	98.44	0.0388	0.3881	0.0569	0.1944	0.3506	0.183	0.0058	0.0642	0.0080	0.0196	0.0612	1567.7	0.0154	24.14	3.71
9/11/2008 B	18.0869	94.5	98.43	0.0320	0.2145	0.0264	0.2073	0.1927	0.283	0.0049	0.0578	0.0031	0.0139	0.0396	1708.3	0.0103	17.60	2.95
9/16/2008 B	18.1221	77.1	98.89	0.0312	0.3547	0.0641	0.2000	0.3153	0.095	0.0016	0.0374	0.0058	0.0064	0.0351	1396.3	0.0145	20.19	1.79
9/30/2008 A	18.1134	89.0	98.34	0.1106	0.6356	0.1550	0.2850	0.3383	0.111	0.0123	0.0830	0.0157	0.0200	0.0435	1611.8	0.0205	32.99	3.72
10/17/2008 A	19.5201	123.3	100.20	0.0209	0.1982	0.0100	0.2158	0.2282	0.806	0.0018	0.0328	0.0065	0.0092	0.0425	2406.5	0.0108	26.08	3.45
10/24/2008 A	18.9474	80.9	99.21	0.0488	0.3700	0.0713	0.2219	0.3350	0.134	0.0048	0.0427	0.0071	0.0120	0.0377	1532.8	0.0155	23.77	2.32
11/10/2008 A	18.9982	91.3	99.62	0.0381	0.2729	0.0719	0.2714	0.2538	0.119	0.0033	0.0262	0.0049	0.0353	0.0256	1733.6	0.0137	23.73	2.59
Washed biomass tests																		
7/23/2008 A	17.6000	110.0	92.86	0.0121	0.2136	0.0447	0.0727	0.2847	0.1134	0.0022	0.0476	0.0079	0.0125	0.0342	1936.0	0.0097	18.86	2.92
7/30/2008 A	18.3222	99.3	93.09	0.0136	0.2805	0.0473	0.1299	0.3545	0.1451	0.0035	0.0441	0.0066	0.0355	0.0753	1818.5	0.0130	23.56	4.91
8/1/2008 B	17.5763	101.1	102.58	0.0800	0.6046	0.1432	0.1693	0.3243	0.1274	0.0040	0.0398	0.0098	0.0014	0.0203	1777.0	0.0176	31.24	1.70
8/8/2008 A	19.6715	124.2	94.03	0.0286	0.2972	0.0533	0.0300	0.2383	0.1770	0.0067	0.0465	0.0048	0.0078	0.0382	2442.5	0.0091	22.20	3.60
8/11/2008 A	20.0206	123.3	93.38	0.0569	0.2606	0.0553	0.0506	0.2529	2.3407	0.0438	0.0313	0.0042	0.0406	0.0823	2467.9	0.0094	23.21	7.01
8/13/2008 A	18.1312	104.4	91.11	0.0317	0.4064	0.0658	0.1333	0.2367	0.0233	0.0026	0.0176	0.0041	0.0016	0.0118	1892.3	0.0123	23.25	0.94
8/13/2008 B	18.1623	146.4	91.18	0.0293	0.3293	0.0747	0.1767	0.1773	0.0200	0.0005	0.0048	0.0015	0.0045	0.0043	2658.4	0.0111	29.47	0.62
8/26/2008 C	18.0114	82.6	94.36	0.0585	0.2792	0.0777	0.1654	0.1546	0.0715	0.0048	0.0266	0.0050	0.0112	0.0151	1486.8	0.0099	14.77	1.27
9/2/2008 A	18.1710	99.8	98.59	0.0373	0.3036	0.0418	0.1691	0.2491	0.2062	0.0068	0.0822	0.0091	0.0043	0.0706	1814.1	0.0119	21.51	4.52
9/3/2008 A	18.1980	99.5	97.79	0.0664	0.5582	0.0936	0.2291	0.3027	0.8371	0.0101	0.1356	0.0220	0.0299	0.0800	1811.0	0.0173	31.40	6.98
9/12/2008 A	18.0745	115.0	99.20	0.0167	0.1217	0.0117	0.1917	0.1250	0.0441	0.0045	0.0401	0.0036	0.0179	0.0350	2078.3	0.0075	15.55	3.14
9/15/2008 A	18.1356	105.5	102.41	0.0336	0.2882	0.1220	0.2155	0.1936	2.3146	0.0050	0.0738	0.0845	0.0305	0.0517	1913.6	0.0120	22.96	5.81
9/16/2008 A	18.1362	90.9	98.89	0.0531	0.3394	0.0613	0.1981	0.1800	0.1825	0.0110	0.0949	0.0128	0.0217	0.0465	1648.6	0.0116	19.11	4.14
9/16/2008 C	17.5530	101.2	99.20	0.0276	0.2812	0.0641	0.2071	0.2065	0.1278	0.0028	0.0515	0.0171	0.0023	0.0406	1776.1	0.0116	20.59	2.77
9/19/2008 A	18.1193	108.7	100.26	0.0353	0.2865	0.0772	0.2190	0.2124	0.8562	0.0047	0.0628	0.0359	0.0149	0.0497	1969.6	0.0121	23.82	4.41
9/30/2008 B	18.1103	56.6	98.30	0.1254	0.7923	0.1731	0.2069	0.3454	0.2476	0.0142	0.1234	0.0211	0.0049	0.0488	1024.7	0.0211	21.65	2.70
10/6/2008 A	18.0843	86.6	98.75	0.0447	0.3729	0.0600	0.1941	0.2835	0.1224	0.0049	0.0537	0.0052	0.0130	0.0385	1566.4	0.0139	21.82	2.60
10/21/2008 A	19.1932	92.1	100.36	0.0219	0.1506	0.0263	0.1550	0.1944	0.3289	0.0020	0.0237	0.0052	0.0203	0.0382	1767.1	0.0086	15.25	2.54
10/23/2008 A	19.1245	92.1	99.18	0.0445	0.2900	0.0455	0.2345	0.2370	0.1264	0.0063	0.0631	0.0061	0.0119	0.0569	1760.4	0.0127	22.35	3.73
1/21/2009 A	18.7860	117.9	99.65	0.0207	0.1448	0.0259	0.1397	0.1534	0.0825	0.0011	0.0123	0.0020	0.0093	0.0083	2214.2	0.0075	16.54	1.09
1/23/2009 A	19.1728	94.9	97.58	0.1013	0.1370	0.0413	0.1490	0.1641	1.4938	0.0568	0.0342	0.0128	0.0113	0.0307	1820.1	0.0080	14.59	2.55

Table D15: (Continued)

			Sample run data						95% Confidence Interval									
RunDate	Nitrogen flow rate SLPM	Run time Minutes	Nitrogen Vol. %	Hydrogen Vol. %	Carbon Monoxide Vol. %	Methane Vol. %	Propane Vol. %	Carbon Dioxide Vol. %	Nitrogen Vol. %	Hydrogen Vol. %	Carbon Monoxide Vol. %	Methane Vol. %	Propane Vol. %	Carbon Dioxide Vol. %	Total gas Liters	Ave. density g/L	Gas Produced g total	± g
Torrefied biomass tests																		
9/18/2008 A	18.1400	79.5	98.48	0.0325	0.3994	0.0544	0.1925	0.3094	0.0816	0.0023	0.0163	0.0026	0.0166	0.0161	1442.1	0.0146	21.13	1.20
10/9/2008 A	18.6700	125.0	98.85	0.0335	0.2971	0.0529	0.1947	0.2306	0.0661	0.0039	0.0285	0.0034	0.0097	0.0225	2333.8	0.0120	27.90	2.28
10/10/2008 A	18.8300	115.4	98.49	0.1071	0.6141	0.1471	0.2218	0.2906	0.1087	0.0069	0.0567	0.0180	0.0241	0.0216	2173.0	0.0181	39.24	3.60
10/21/2008 B	19.1400	88.6	100.07	0.0225	0.2388	0.0513	0.2025	0.2656	0.1592	0.0023	0.0411	0.0055	0.0129	0.0338	1696.2	0.0121	20.52	2.40
10/27/2008 A	19.2900	70.8	99.36	0.0281	0.2973	0.0494	0.1650	0.2444	0.0692	0.0067	0.0302	0.0129	0.0190	0.0228	1365.7	0.0117	15.91	1.70
10/27/2008 B	19.4884	88.5	99.43	0.0235	0.3429	0.0665	0.1876	0.2624	0.0903	0.0073	0.0254	0.0042	0.0075	0.0147	1725.1	0.0131	22.52	1.31
10/28/2008 A	19.2445	102.9	98.81	0.0269	0.2956	0.0531	0.1863	0.2425	0.4600	0.0102	0.0474	0.0044	0.0139	0.0212	1980.9	0.0120	23.79	2.51
10/29/2008 A	19.1690	103.9	100.20	0.0600	0.5094	0.1125	0.2269	0.3306	1.0620	0.0826	0.3669	0.0595	0.0202	0.1345	1991.0	0.0174	34.68	15.51
10/30/2008 A	18.9911	99.7	99.63	0.0268	0.1805	0.0642	0.1584	0.1574	0.2069	0.0116	0.0247	0.0064	0.0188	0.0095	1892.8	0.0086	16.24	1.66
10/31/2008 A	19.2456	121.9	99.72	0.0600	0.4024	0.1438	0.2029	0.2238	0.0854	0.0046	0.0266	0.0132	0.0171	0.0135	2346.7	0.0139	32.55	2.32
10/31/2008 B	19.2151	108.2	99.58	0.0305	0.2614	0.0809	0.1773	0.1855	0.0803	0.0031	0.0222	0.0042	0.0066	0.0153	2079.7	0.0105	21.90	1.48
11/5/2008 A	20.1245	34.5	98.78	0.0311	0.6878	0.1875	0.2156	0.3833	0.4994	0.0197	0.2751	0.0530	0.0180	0.1611	693.3	0.0208	14.40	4.90
11/6/2008 A	18.5803	77.7	100.22	0.0213	0.2525	0.0575	0.0347	0.2513	0.0979	0.0017	0.0325	0.0135	0.0063	0.0169	1444.0	0.0089	12.91	1.33
11/6/2008 B	19.5676	73.3	99.47	0.0745	0.6518	0.1455	0.0791	0.3291	0.1417	0.0059	0.1300	0.0307	0.0135	0.0347	1433.7	0.0166	23.76	3.80
11/7/2008 A	18.7513	77.2	99.53	0.0429	0.3690	0.0619	0.1671	0.3171	0.0850	0.0037	0.0337	0.0038	0.0269	0.0337	1447.0	0.0141	20.35	2.28
11/11/2008 A	18.8226	75.5	99.46	0.0550	0.4750	0.0850	0.2267	0.2867	0.5803	0.0121	0.1450	0.0121	0.0575	0.0759	1420.2	0.0159	22.65	6.13
11/13/2008 A	18.2820	120.0	100.13	0.0132	0.0882	0.0133	0.1068	0.0950	0.0623	0.0020	0.0136	0.0025	0.0084	0.0226	2193.8	0.0050	10.88	1.71
11/14/2008 A	18.7926	88.9	99.41	0.0343	0.2977	0.0400	0.1705	0.2333	0.0735	0.0026	0.0313	0.0030	0.0083	0.0209	1670.0	0.0115	19.18	1.58
11/18/2008 A	19.0710	75.3	100.49	0.0178	0.1700	0.0278	0.1763	0.1878	0.6553	0.0031	0.0372	0.0058	0.0036	0.0463	1435.4	0.0091	13.08	2.09
1/30/2009 A	20.1629	88.6	99.02	0.0674	0.3131	0.0641	0.1441	0.2763	0.3009	0.0758	0.0448	0.0098	0.0151	0.0306	1786.1	0.0123	21.89	2.86

APPENDIX E: STATISTICAL MODEL DATA

Response Biochar Yield (wt. %) unwashed biomass

Key:
Pyro – Pyrolysis temperature
M – Moisture content
G – Grind size
Char % = Biochar wt. % yield

Actual by Predicted Plot

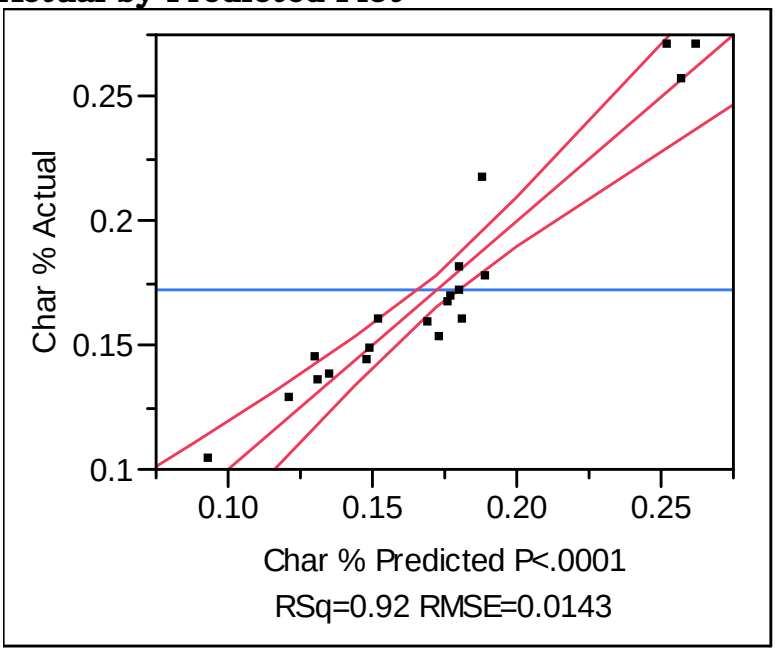

Summary of Fit

RSquare	0.924709
RSquare Adj	0.904632
Root Mean Square Error	0.01432
Mean of Response	0.1722
Observations (or Sum Wgts)	20

Parameter Estimates

Term	Estimate	Std Error	t Ratio	Prob>|t|
Intercept	0.8768658	0.054835	15.99	<.0001
Pyro	-0.001304	0.000111	-11.72	<.0001
G	-0.079699	0.018116	-4.40	0.0005
M	-0.350387	0.129522	-2.71	0.0163
(Pyro-485)*(G-0.5)	0.0019729	0.000579	3.41	0.0039

Residual by Predicted Plot

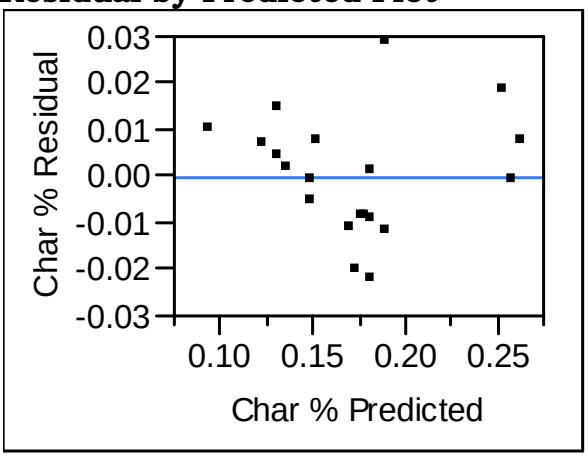

Contour Profiler

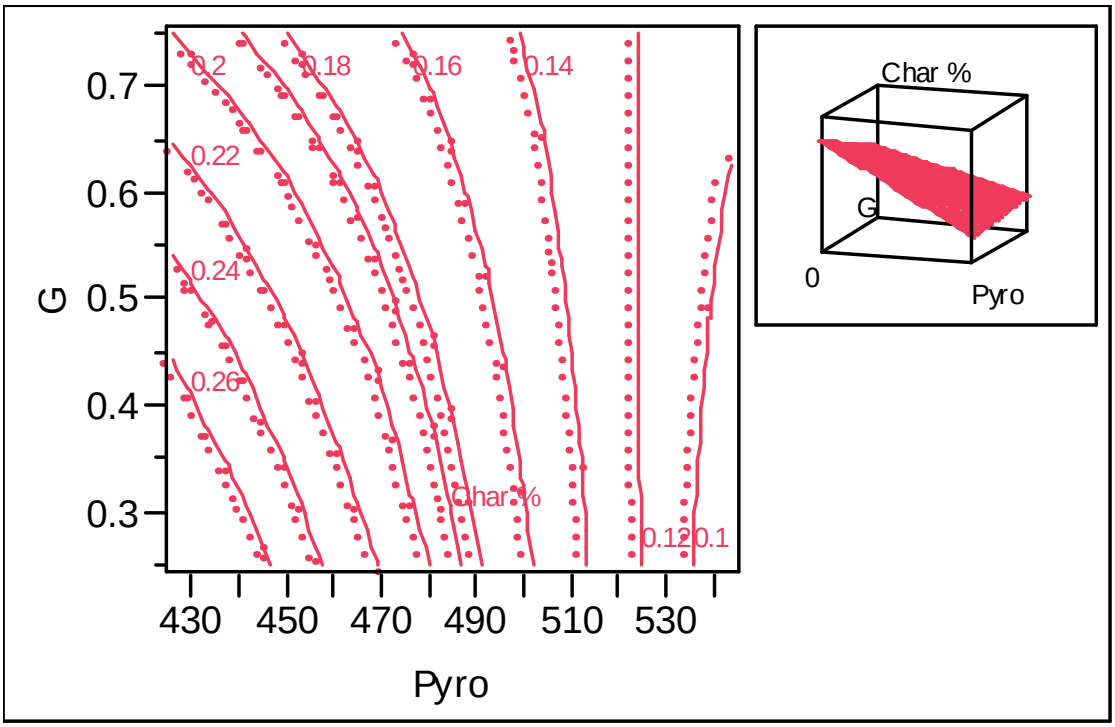

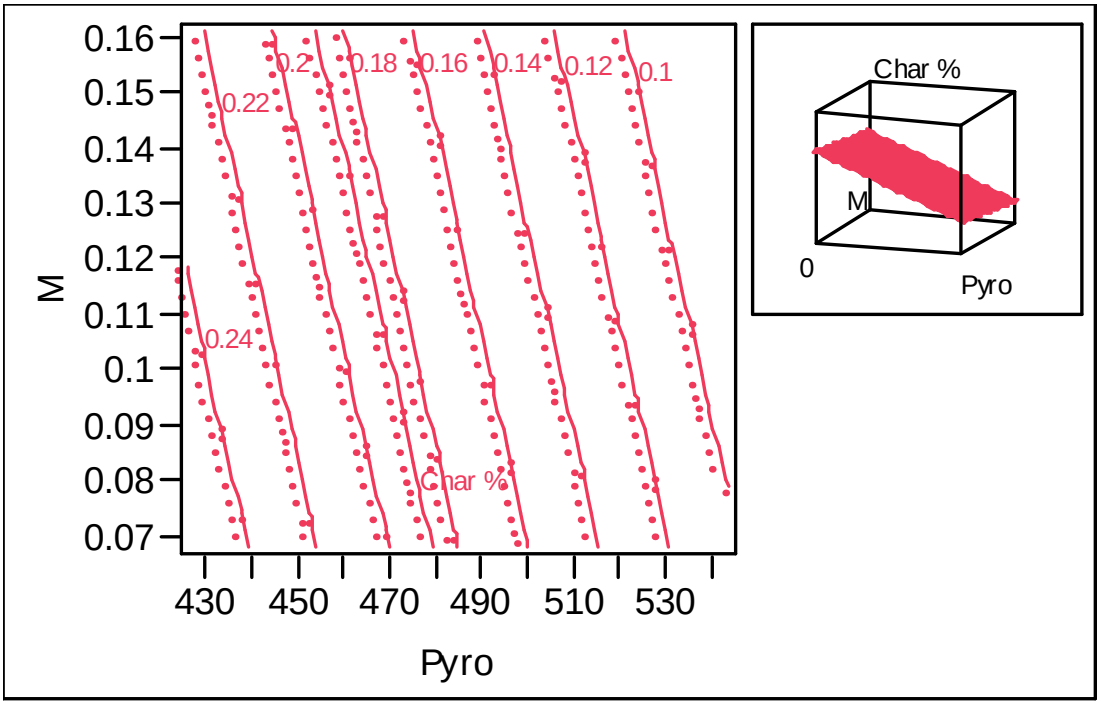
0.16
0.15
0.14
0.13
0.12
0.11
0.1
0.09
0.08
0.07
M
0.22
0.2
0.18
0.16
0.14
0.12
0.1
0.24
Char %
430
450
470
490
510
530
Pyro
Char %
M
0
Pyro

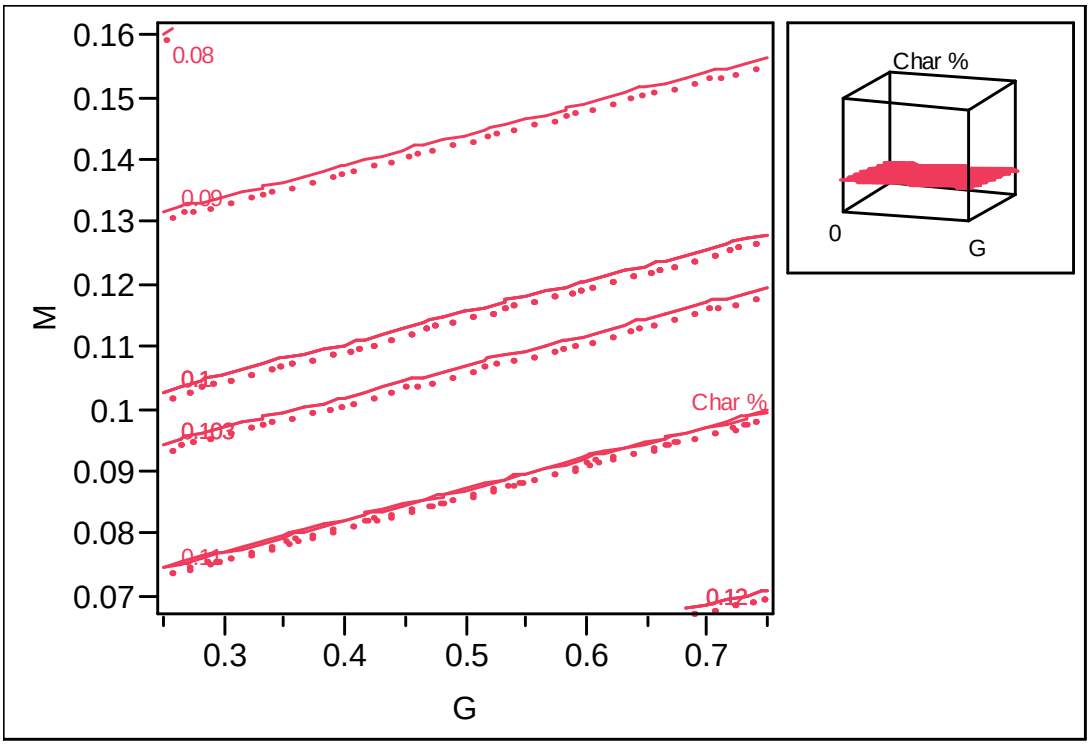
0.16
0.15
0.14
0.13
0.12
0.11
0.1
0.09
0.08
0.07
M
0.08
0.09
0.1
0.103
0.11
0.12
Char %
0.3
0.4
0.5
0.6
0.7
G
Char %
0
G

Response biochar yield (wt. %) washed biomass

Key:

Pyro – Pyrolysis temperature
G – Grind size
Char % = Biochar wt. % yield

Actual by Predicted Plot

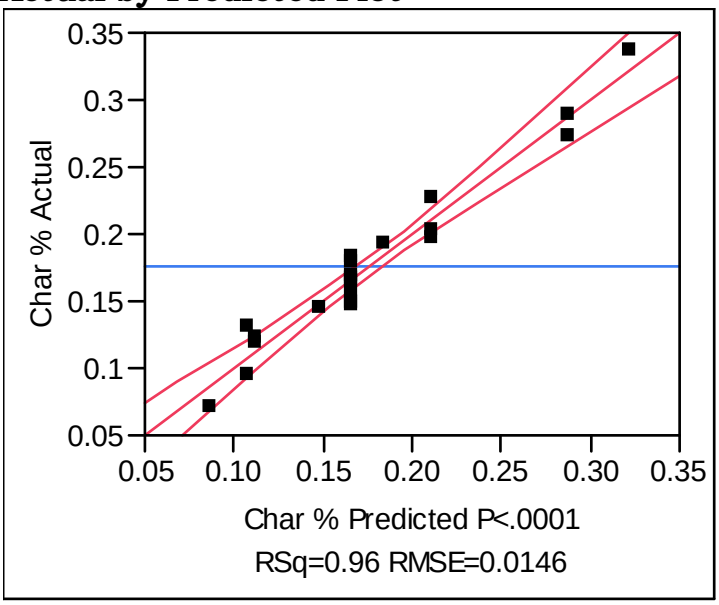

Summary of Fit

RSquare	0.957463
RSquare Adj	0.946829
Root Mean Square Error	0.014609
Mean of Response	0.17641
Observations (or Sum Wgts)	21

Parameter Estimates

Term	Estimate	Std Error	t Ratio	Prob>|t|
Intercept	1.1728309	0.054444	21.54	<.0001
Pyro	-0.002	0.00011	-18.23	<.0001
G	-0.074362	0.017724	-4.20	0.0007
(Pyro-483.333)*(Pyro-483.333)	0.000011	3.093e-6	3.56	0.0026
(Pyro-483.333)*(G-0.5119)	0.0023448	0.000562	4.17	0.0007

Residual by Predicted Plot

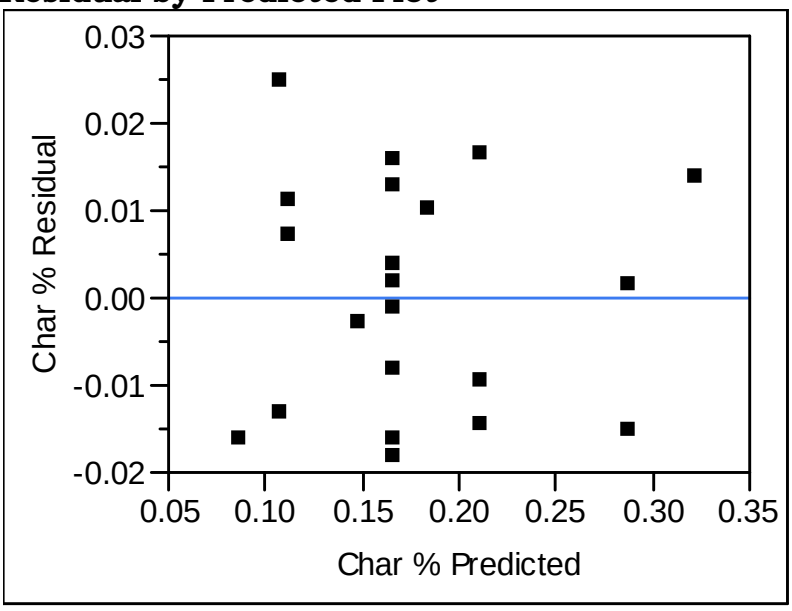

Contour Profiler

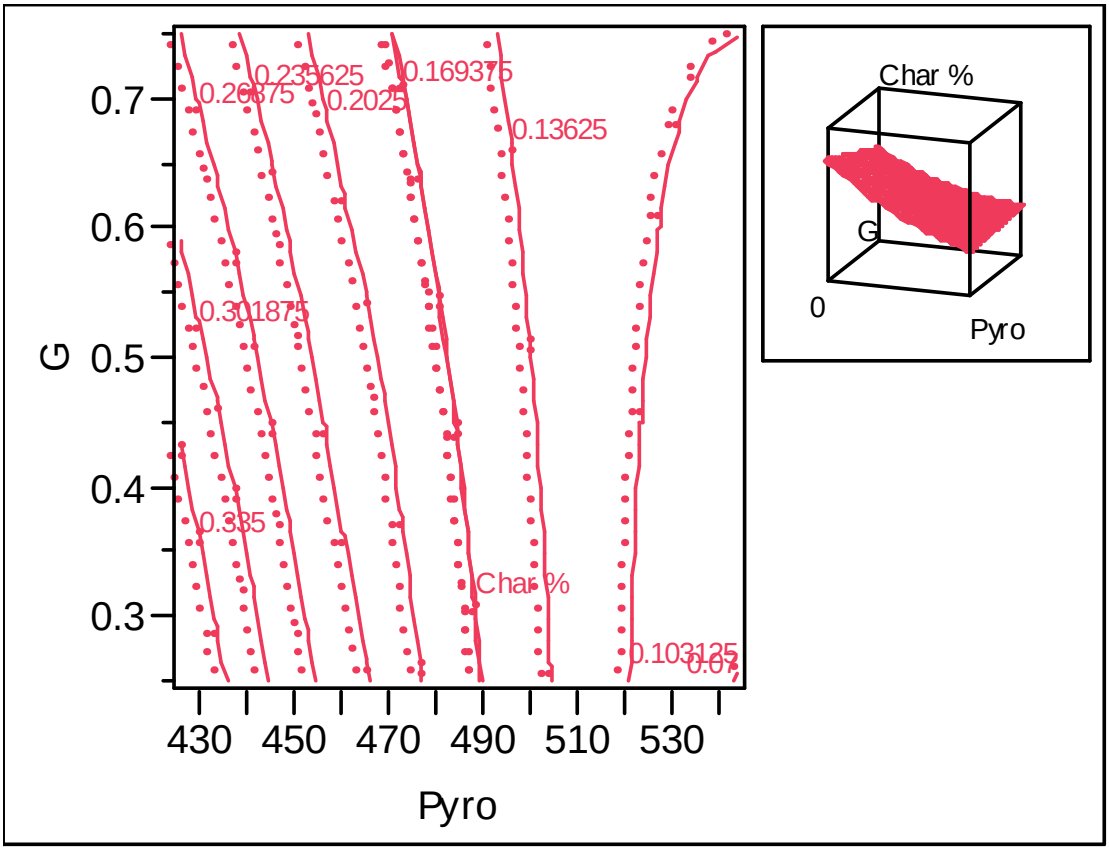

Response biochar yield (wt. %) torrefied biomass

Key:
Pyro – Pyrolysis temperature
Tor – Torrefaction temperature
Char % = Biochar wt. % yield

Actual by Predicted Plot

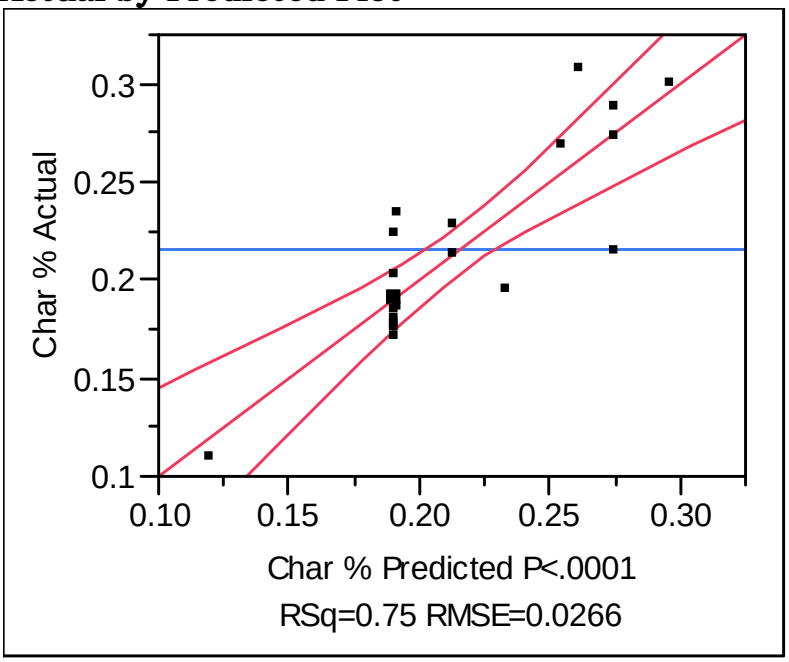

Summary of Fit

RSquare	0.751501
RSquare Adj	0.722266
Root Mean Square Error	0.026579
Mean of Response	0.21565
Observations (or Sum Wgts)	20

Parameter Estimates

Term	Estimate	Std Error	t Ratio	Prob>|t|
Intercept	0.768894	0.09975	7.71	<.0001
Pyro	-0.001195	0.000206	-5.81	<.0001
(Tor-211.5)*(Tor-211.5)	4.3512e-5	9.722e-6	4.48	0.0003

Residual by Predicted Plot

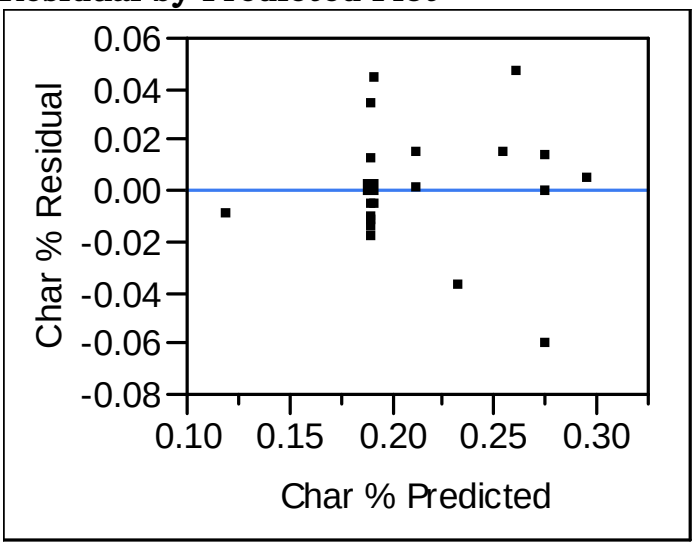

Contour Profiler

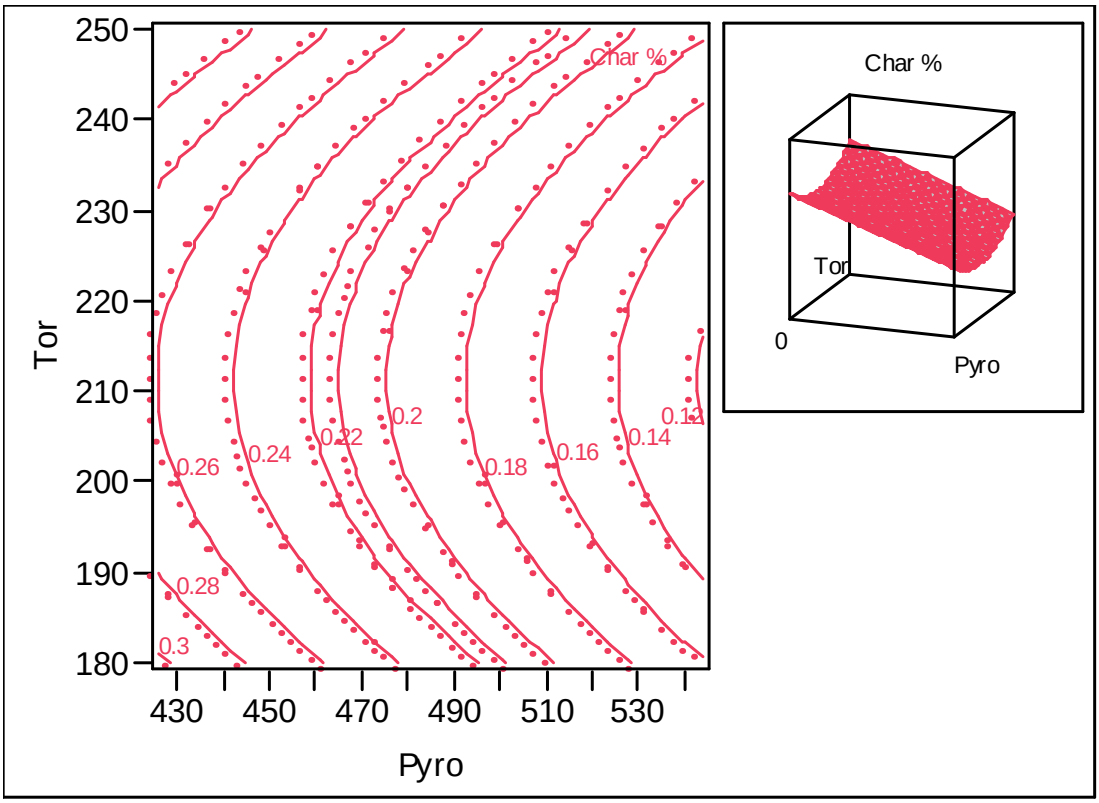

Response wt. % hydrogen in biochar for unwashed biomass

Key:
Pyro – Pyrolysis temperature
G – Grind size
Char H – Hydrogen wt. % in biochar

Actual by Predicted Plot

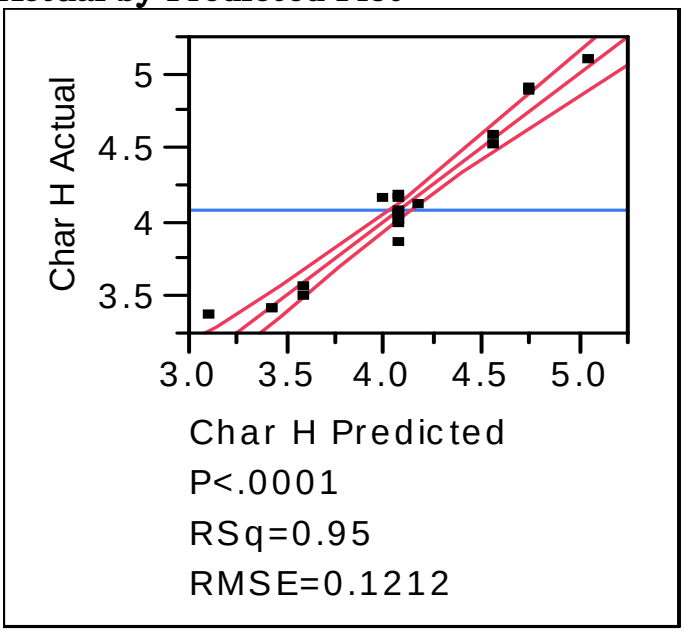

Summary of Fit

RSquare	0.948815
RSquare Adj	0.942793
Root Mean Square Error	0.121167
Mean of Response	4.081433
Observations (or Sum Wgts)	20

Parameter Estimates

Term	Estimate	Std Error	t Ratio	Prob>|t|
Intercept	12.247671	0.461124	26.56	<.0001
Pyro	-0.016472	0.000936	-17.60	<.0001
G	-0.35476	0.153266	-2.31	0.0334

Residual by Predicted Plot

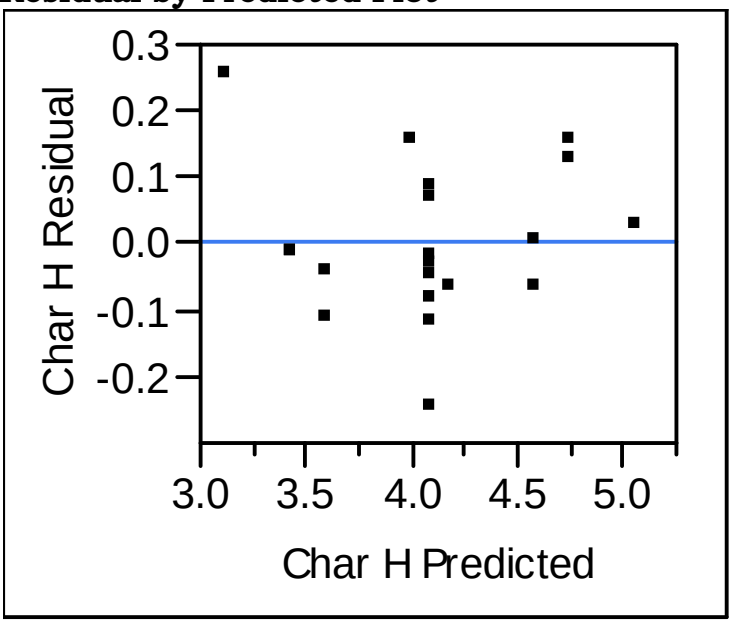

Contour Profiler

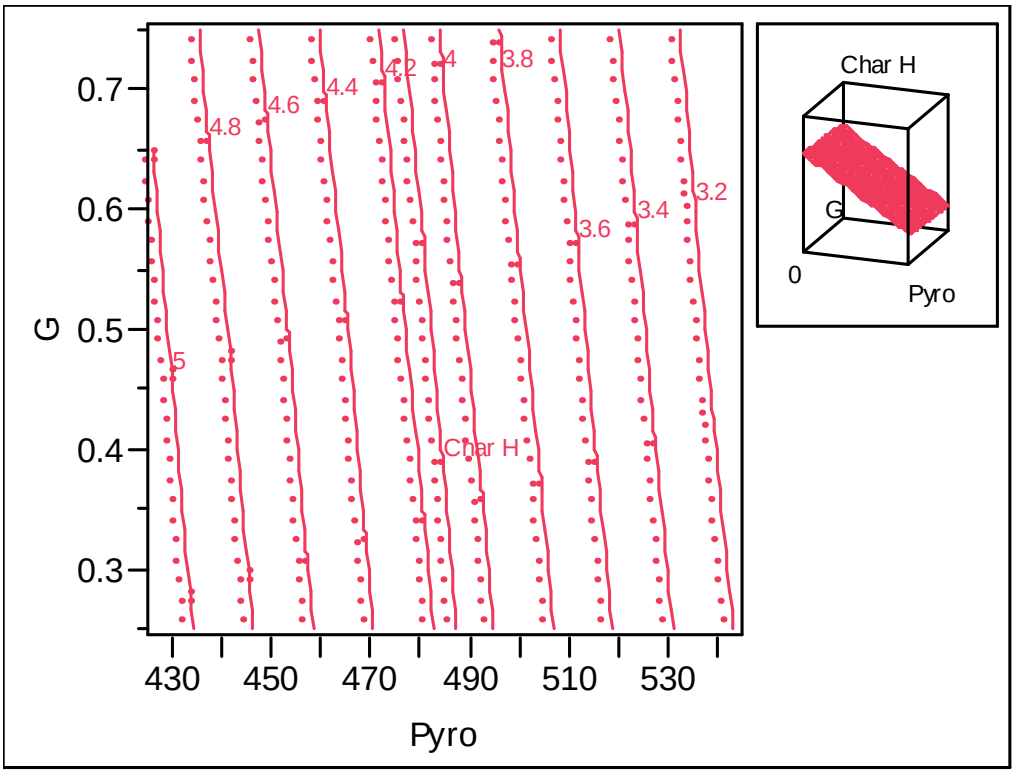

Response wt. % hydrogen in biochar for washed biomass

Key:
Pyro – Pyrolysis temperature
M – Moisture content
G – Grind size
Char H – Hydrogen wt. % in biochar

Actual by Predicted Plot

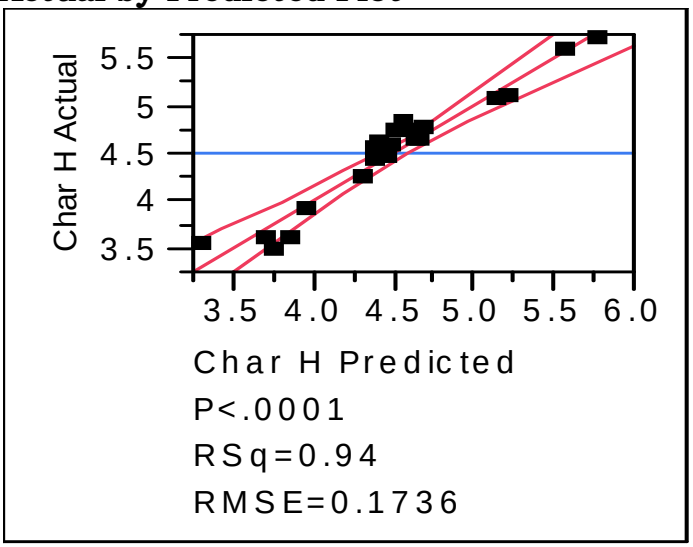

Summary of Fit

RSquare	0.941127
RSquare Adj	0.921503
Root Mean Square Error	0.173585
Mean of Response	4.49381
Observations (or Sum Wgts)	21

Parameter Estimates

Term	Estimate	Std Error	t Ratio	Prob>|t|
Intercept	13.538073	0.674696	20.07	<.0001
Pyro	-0.018679	0.001353	-13.80	<.0001
M	1.4680821	0.594043	2.47	0.0259
G	-0.381186	0.212376	-1.79	0.0928
(Pyro-483.333)*(M-0.13444)	-0.05438	0.022632	-2.40	0.0297
(Pyro-483.333)*(G-0.5119)	0.0206391	0.006709	3.08	0.0077

Residual by Predicted Plot

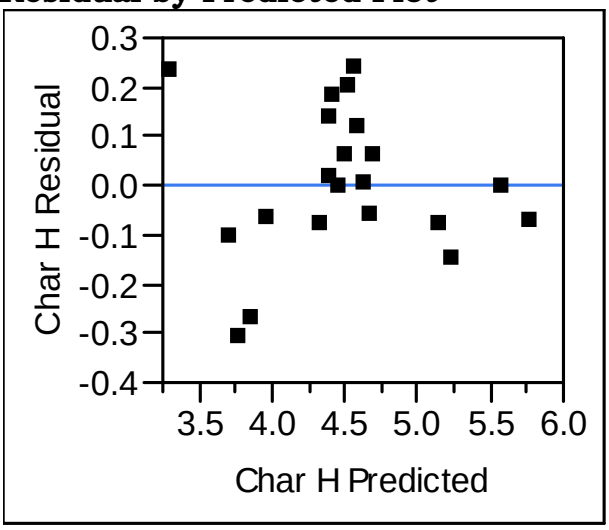

Contour Profiler

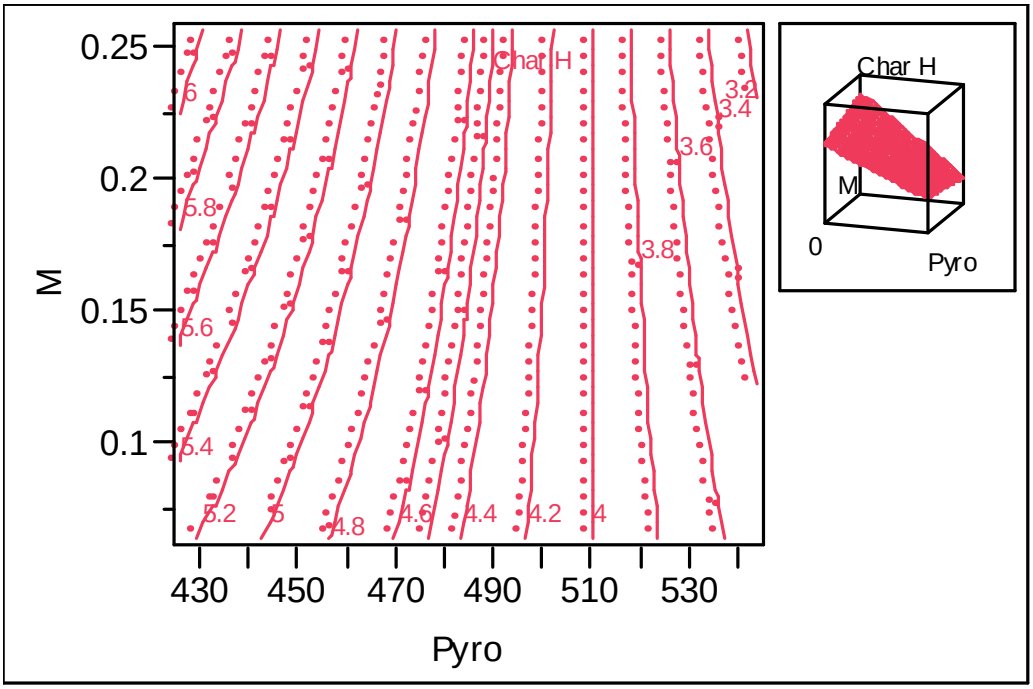

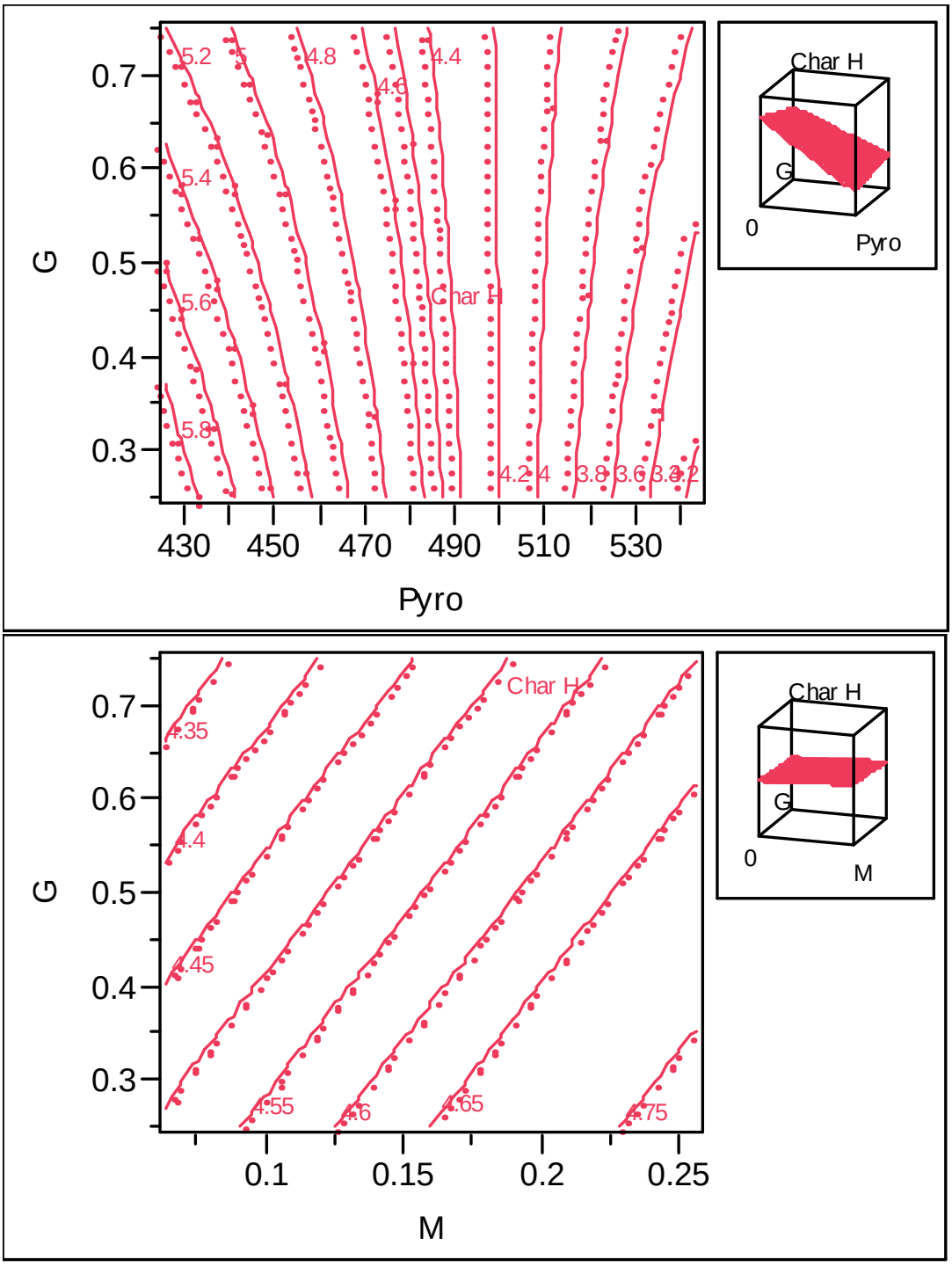
G
0.7
0.6
0.5
0.4
0.3
5.2
5
4.8
4.6
4.4
5.4
5.6
5.8
Char H
4.2
4
3.8
3.6
3.4
3.2
430
450
470
490
510
530
Pyro
Char H
G
0
Pyro
G
0.7
0.6
0.5
0.4
0.3
Char H
4.35
4.4
4.45
4.55
4.6
4.65
4.75
0.1
0.15
0.2
0.25
M
Char H
G
0
M

Response wt. % hydrogen in biochar for torrefied biomass

Key:
Pyro – Pyrolysis temperature
G – Grind size
Tor – Torrefaction temperature
Char H – Hydrogen wt. % in biochar

Actual by Predicted Plot

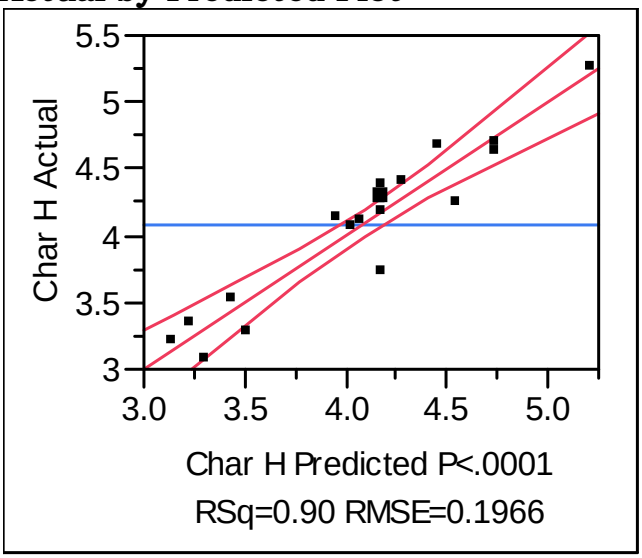

Summary of Fit

RSquare	0.900361
RSquare Adj	0.881679
Root Mean Square Error	0.196581
Mean of Response	4.0785
Observations (or Sum Wgts)	20

Parameter Estimates

Term	Estimate	Std Error	t Ratio	Prob>|t|
Intercept	12.909244	0.748124	17.26	<.0001
Pyro	-0.0176	0.00152	-11.58	<.0001
G	-0.40126	0.249057	-1.61	0.1267
(Tor-211.5)*(Tor-211.5)	-0.000157	0.000072	-2.18	0.0448

Residual by Predicted Plot

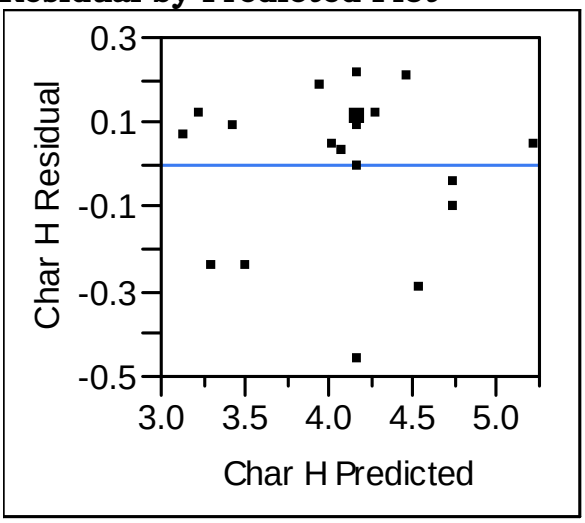

Contour Profiler

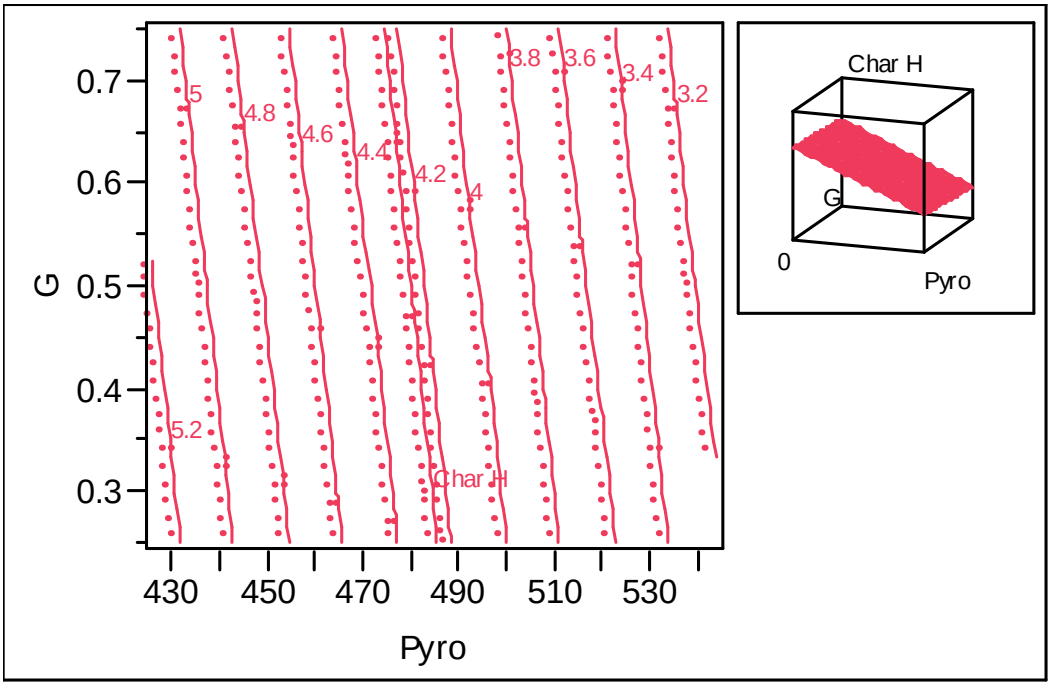

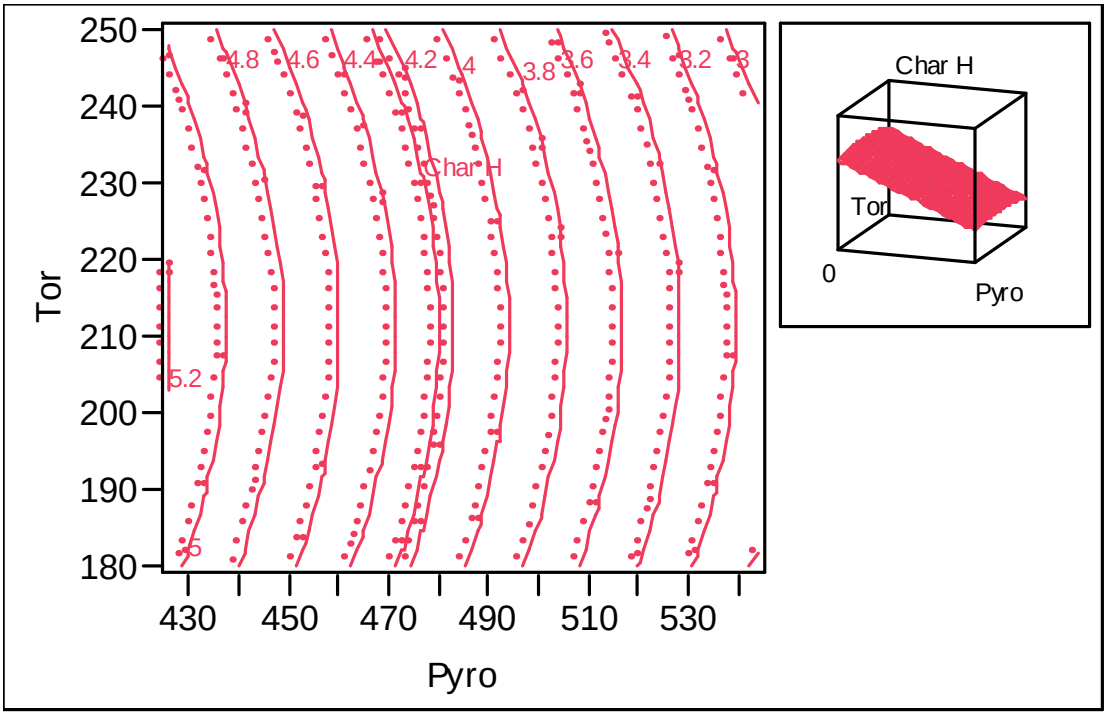
Tor
Pyro
Char H
5.2
5
4.8
4.6
4.4
4.2
4
3.8
3.6
3.4
3.2
3
250
240
230
220
210
200
190
180
430
450
470
490
510
530
Char H
Tor
0
Pyro

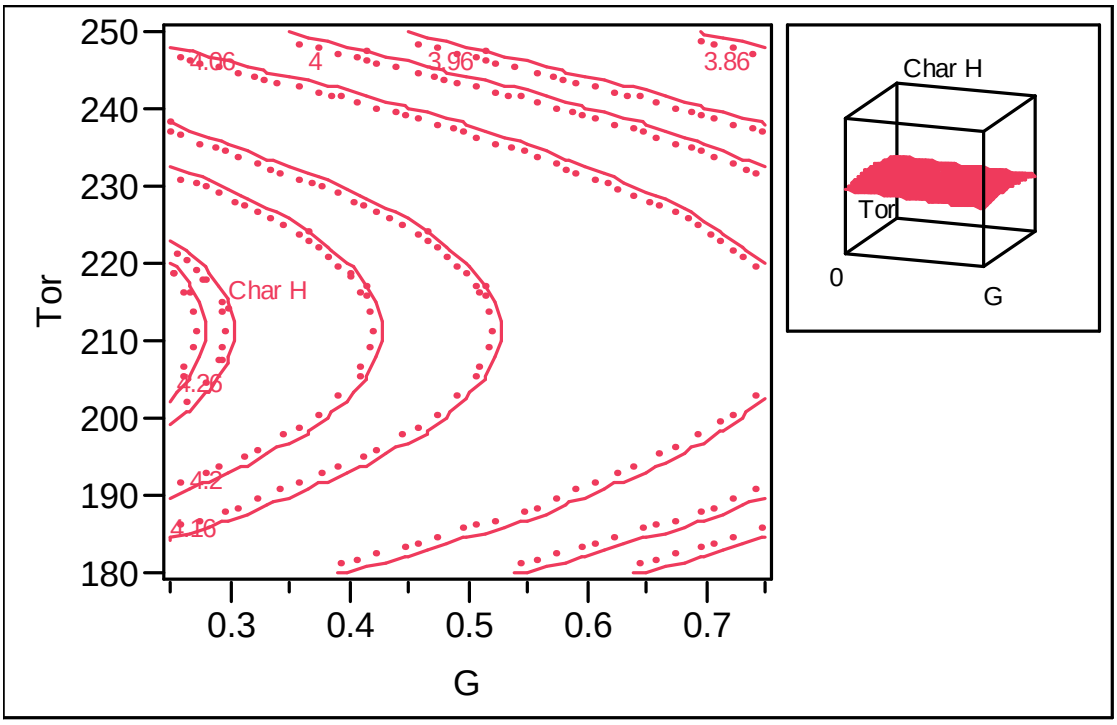
Tor
G
Char H
4.06
4
3.96
3.86
4.26
4.2
4.16
250
240
230
220
210
200
190
180
0.3
0.4
0.5
0.6
0.7
Char H
Tor
0
G

Response wt. % carbon in biochar for unwashed biomass

Key:
Pyro – Pyrolysis temperature
Char C – Carbon wt. % in biochar

Actual by Predicted Plot

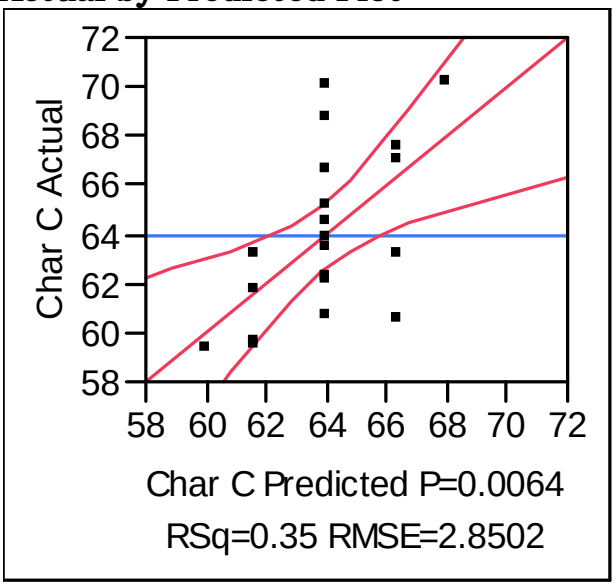

Summary of Fit

RSquare	0.345952
RSquare Adj	0.309616
Root Mean Square Error	2.850196
Mean of Response	63.9287
Observations (or Sum Wgts)	20

Parameter Estimates

Term	Estimate	Std Error	t Ratio	Prob>|t|
Intercept	30.98345	10.69611	2.90	0.0096
Pyro	0.0679283	0.022015	3.09	0.0064

Residual by Predicted Plot

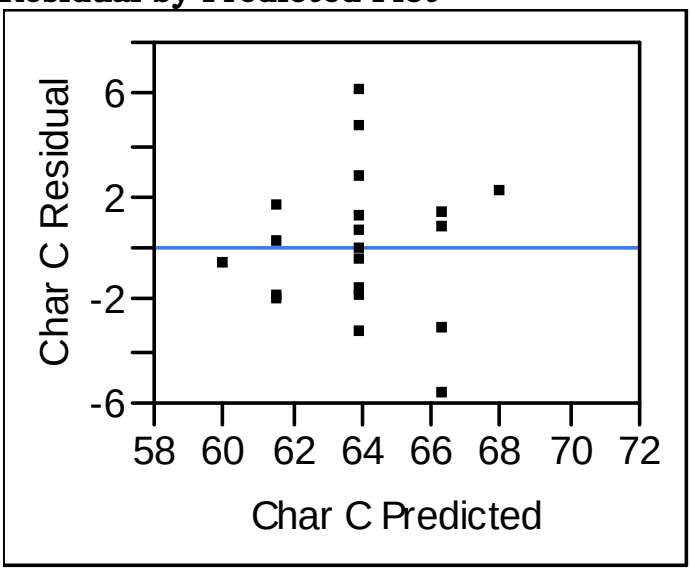

Prediction Profiler

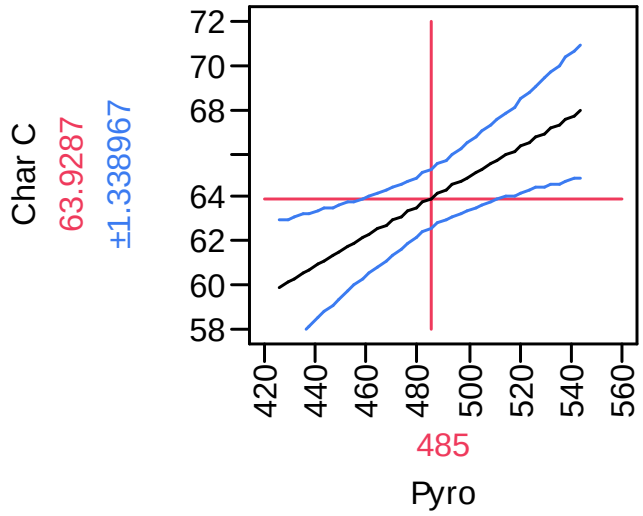

Response wt. % carbon in biochar for washed biomass

Key:
Pyro – Pyrolysis temperature
M – Moisture content
G – Grind size
Char C – Carbon wt. % in biochar

Actual by Predicted Plot

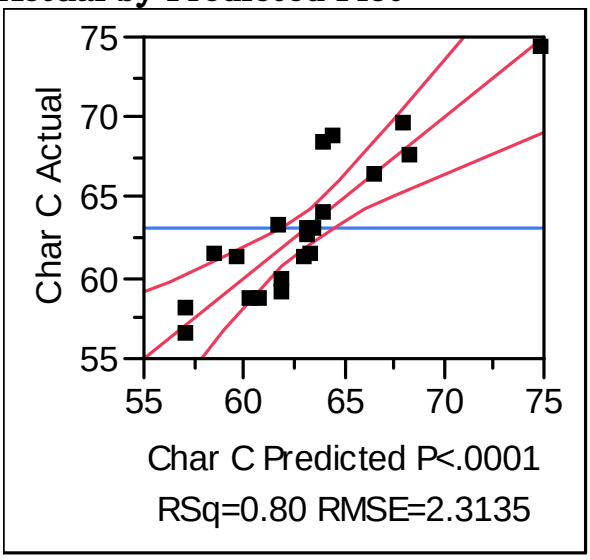

Summary of Fit

RSquare	0.80241
RSquare Adj	0.736547
Root Mean Square Error	2.313481
Mean of Response	63.08048
Observations (or Sum Wgts)	21

Parameter Estimates

Term	Estimate	Std Error	t Ratio	Prob>|t|
Intercept	16.6162	9.082596	1.83	0.0873
G	18.976474	3.021228	6.28	<.0001
Pyro	0.0782489	0.01833	4.27	0.0007
(G-0.5119)*(Pyro-483.333)	0.2749187	0.09151	3.00	0.0089
(Pyro-483.333)*(M-0.13444)	-0.704002	0.311724	-2.26	0.0392
(M-0.13444)*(M-0.13444)	-195.6274	188.3557	-1.04	0.3154

Residual by Predicted Plot

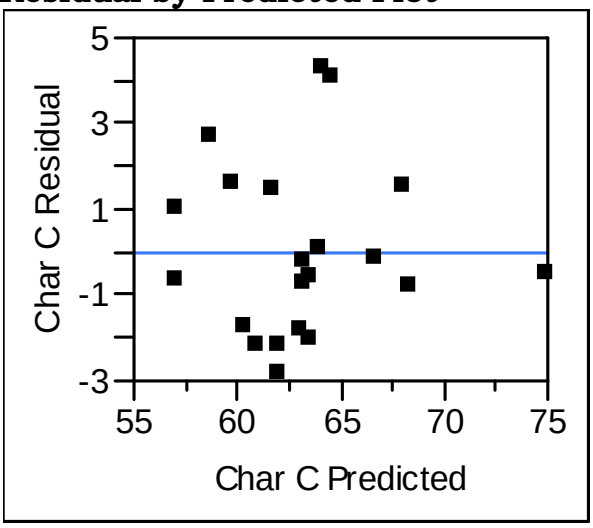

Contour Profiler

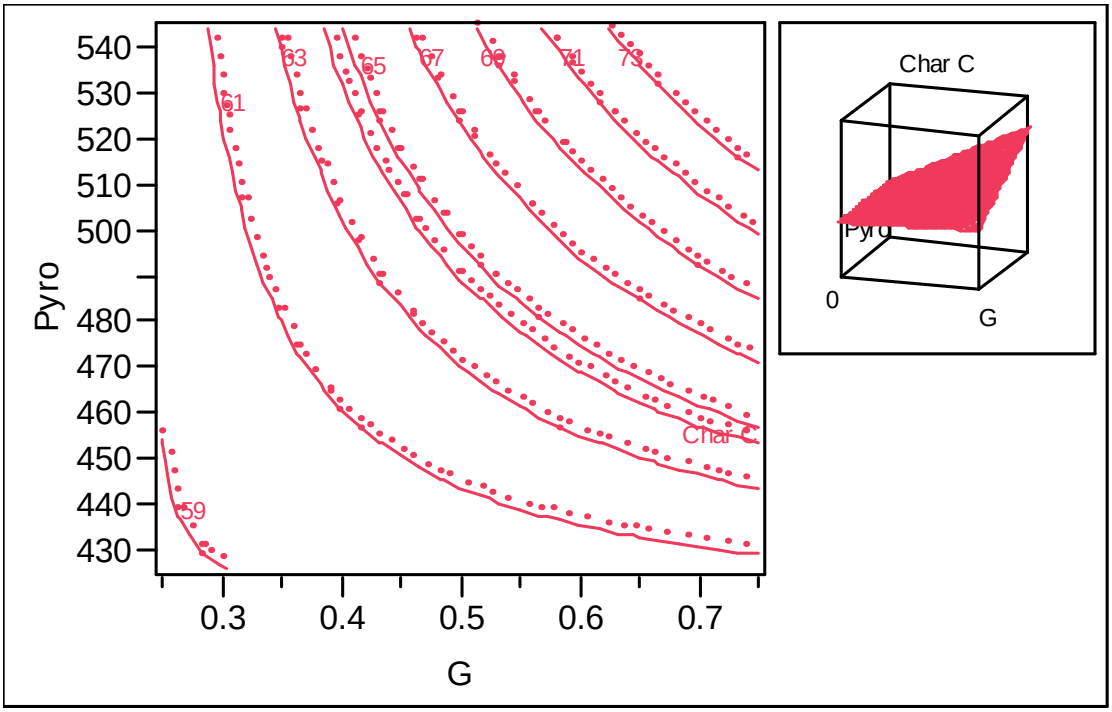

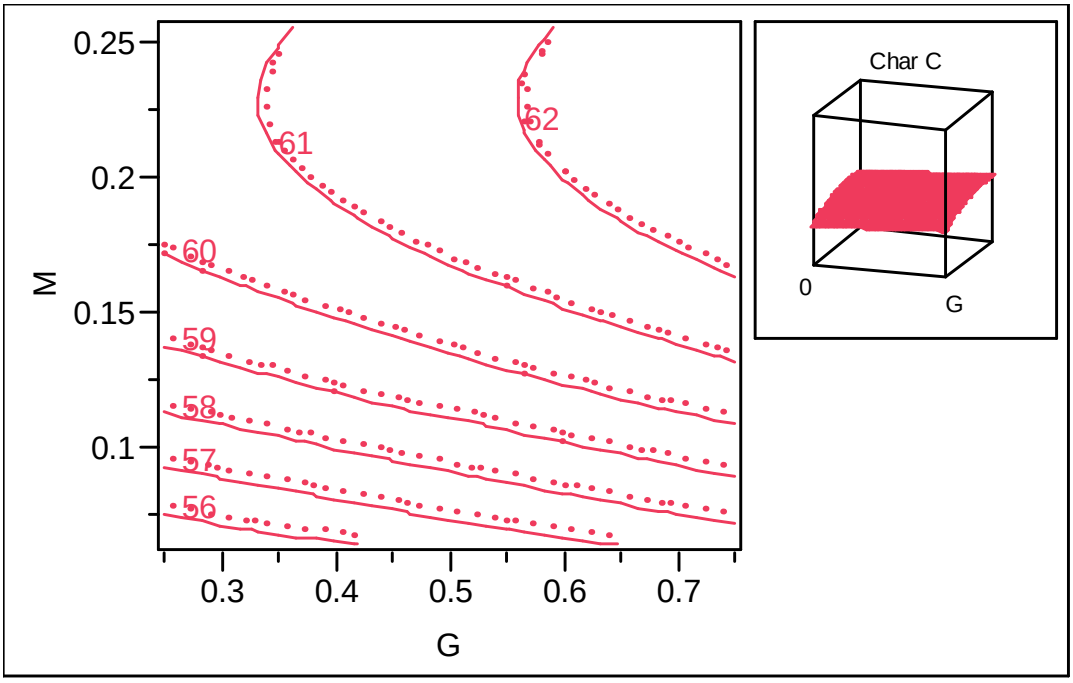
0.25
0.2
0.15
0.1
M
61
62
60
59
58
57
56
0.3
0.4
0.5
0.6
0.7
G
Char C
0
G

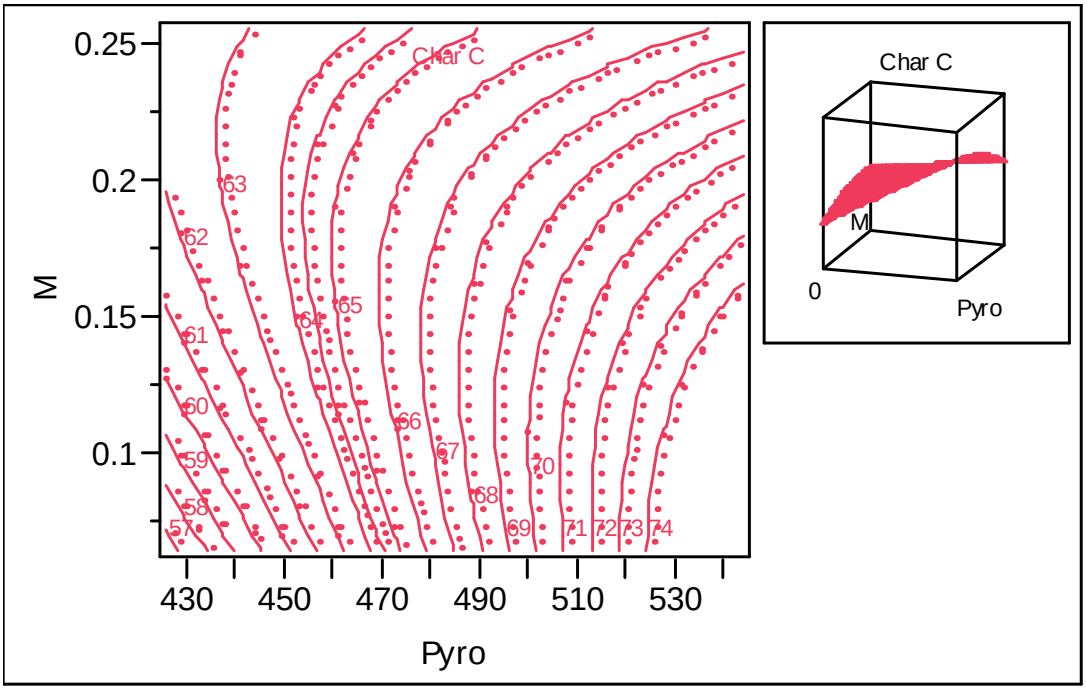
0.25
0.2
0.15
0.1
M
Char C
63
62
61
60
59
58
57
65
64
66
67
70
68
69
71
72
73
74
430
450
470
490
510
530
Pyro
Char C
M
0
Pyro

Response wt. % carbon in biochar for torrefied biomass

Key:
G – Grind size
Tor – Torrefaction temperature
Char C – Carbon wt. % in biochar

Actual by Predicted Plot

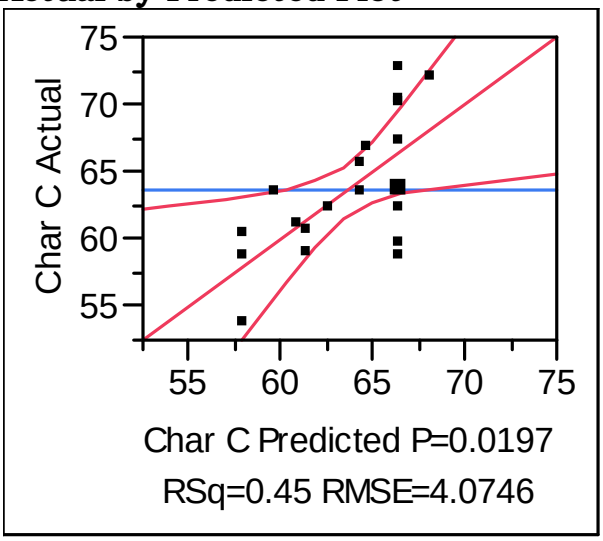

Summary of Fit

RSquare	0.450869
RSquare Adj	0.347907
Root Mean Square Error	4.074609
Mean of Response	63.5325
Observations (or Sum Wgts)	20

Parameter Estimates

Term	Estimate	Std Error	t Ratio	Prob>|t|
Intercept	46.97528	7.984869	5.88	<.0001
Tor	0.074124	0.038289	1.94	0.0708
G	6.9092174	5.264869	1.31	0.2079
(Tor-211.5)*(Tor-211.5)	-0.004289	0.001504	-2.85	0.0115

Residual by Predicted Plot

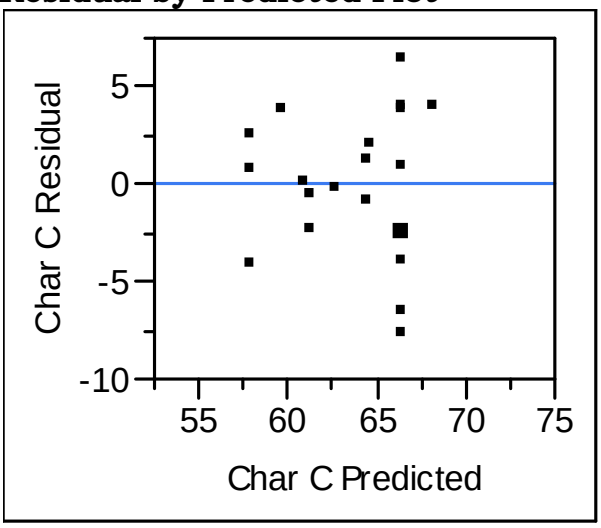

Contour Profiler

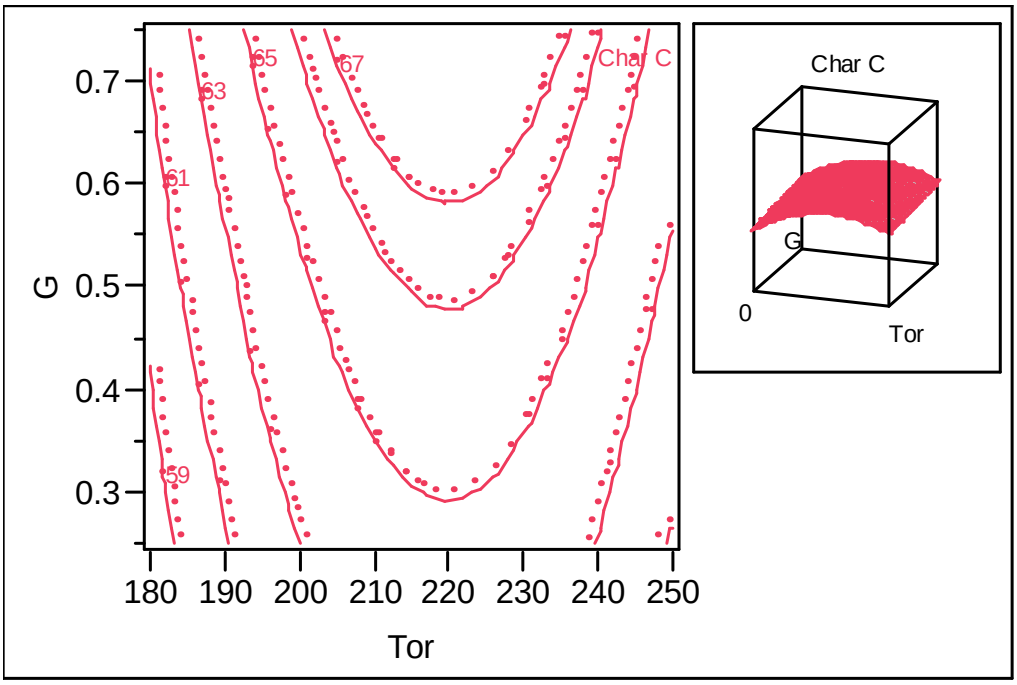

Response bio-oil fraction one wt. % yield for unwashed biomass

Key:
M – Moisture content
G – Grind size
SF1 % - Bio-oil fraction one wt. % yield

Actual by Predicted Plot

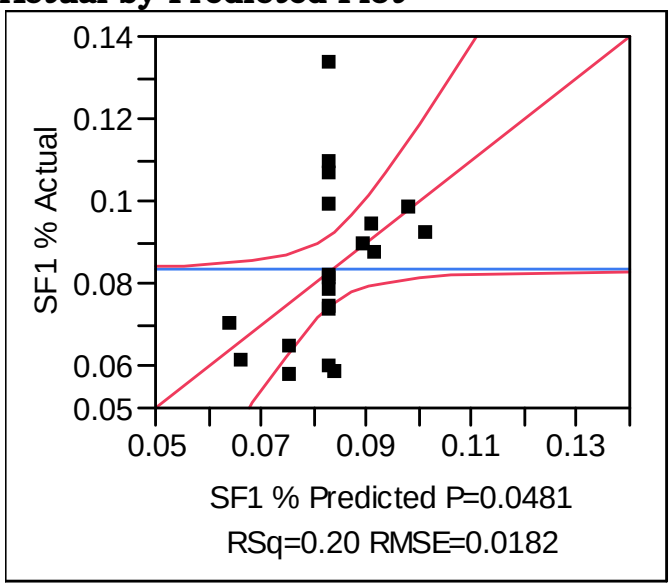

Summary of Fit

RSquare	0.199847
RSquare Adj	0.155395
Root Mean Square Error	0.01819
Mean of Response	0.08334
Observations (or Sum Wgts)	20

Parameter Estimates

Term	Estimate	Std Error	t Ratio	Prob>|t|
Intercept	0.0831247	0.004069	20.43	<.0001
(M-0.093)*(G-0.5)	3.4446965	1.62462	2.12	0.0481

Residual by Predicted Plot

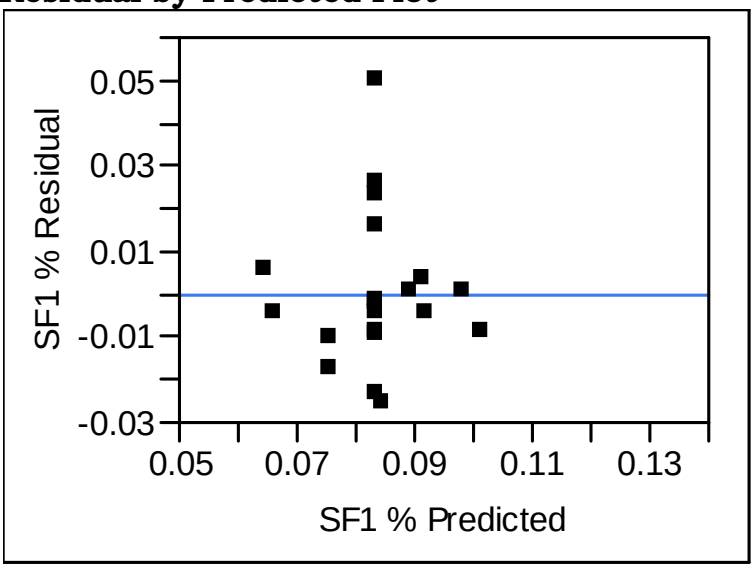

Contour Profiler

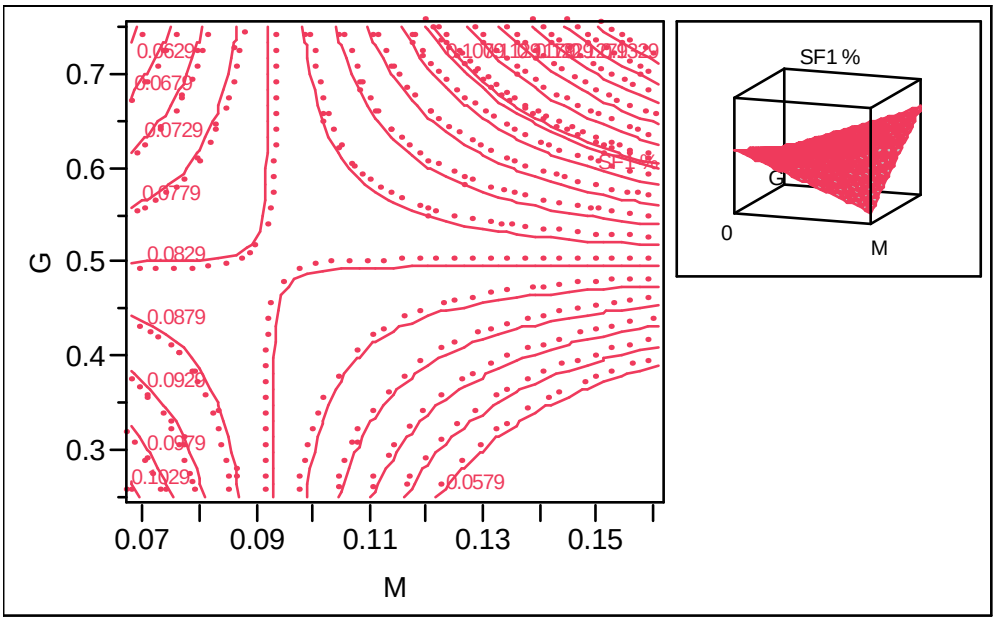

Response bio-oil fraction one wt. % yield for torrefied biomass

Key:
Pyro – Pyrolysis temperature
G – Grind size
Tor – Torrefaction temperature
SF1 % - Bio-oil fraction one wt. % yield

Actual by Predicted Plot

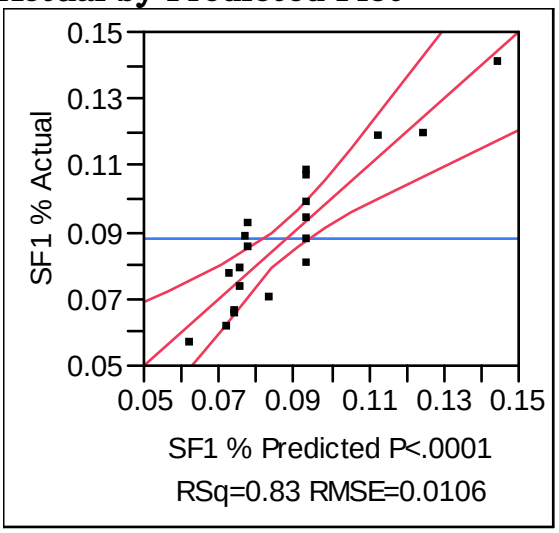

Summary of Fit

RSquare	0.826833
RSquare Adj	0.764987
Root Mean Square Error	0.010591
Mean of Response	0.088175
Observations (or Sum Wgts)	20

Parameter Estimates

Term	Estimate	Std Error	t Ratio	Prob>|t|
Intercept	-0.047456	0.042835	-1.11	0.2866
Pyro	0.0005341	8.562e-5	6.24	<.0001
Tor	-0.00055	0.000104	-5.31	0.0001
(Pyro-485)*(G-0.5)	-0.001777	0.000462	-3.85	0.0018
(Tor-211.5)*(G-0.5)	0.0018792	0.000483	3.89	0.0016
(G-0.5)*(G-0.5)	-0.276672	0.078219	-3.54	0.0033

Residual by Predicted Plot

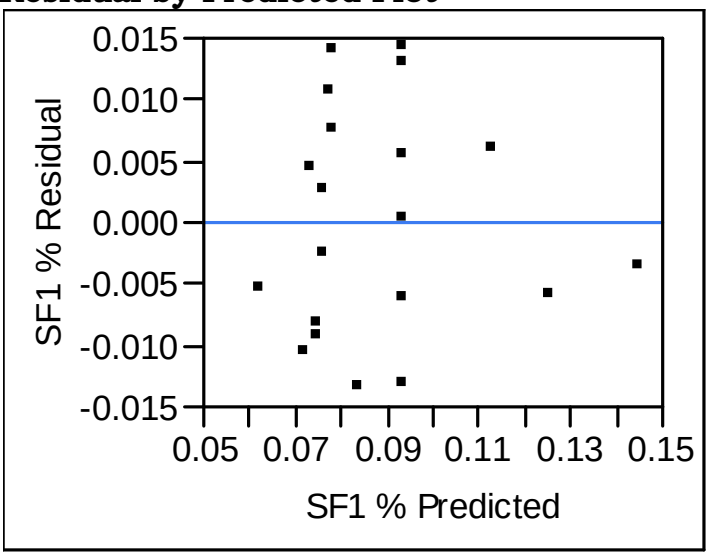

Contour Profiler

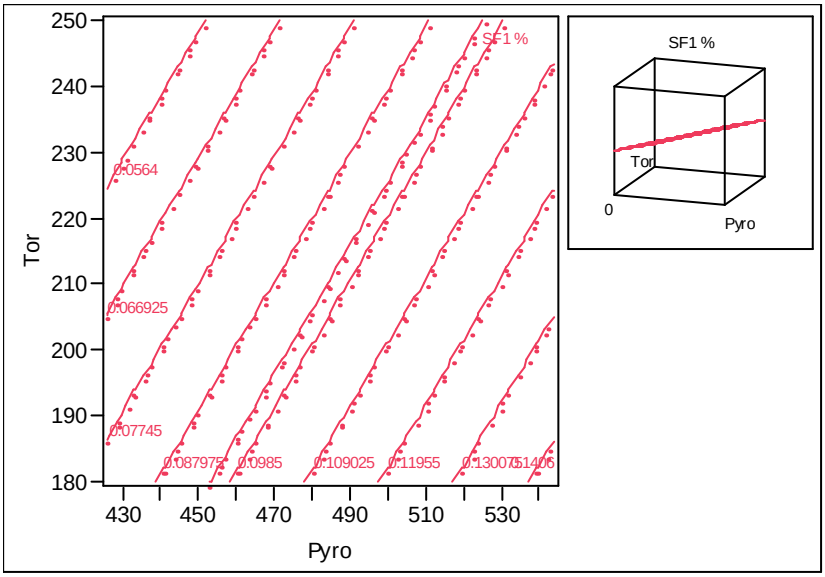

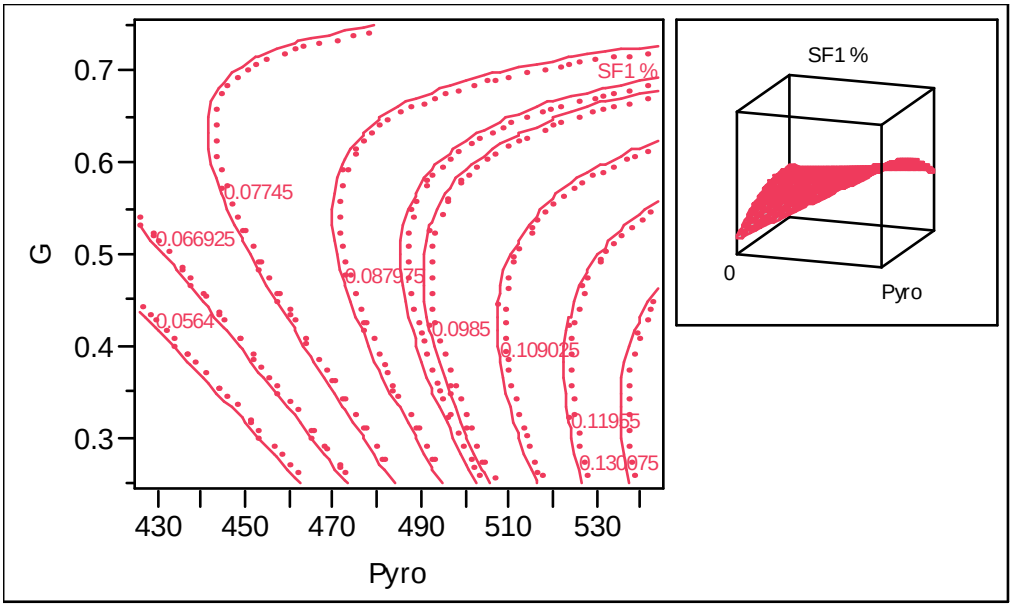
G
0.7
0.6
0.5
0.4
0.3
430
450
470
490
510
530
Pyro
SF1 %
0.07745
0.066925
0.087975
0.0564
0.0985
0.109025
0.11955
0.130075
SF1 %
0
Pyro

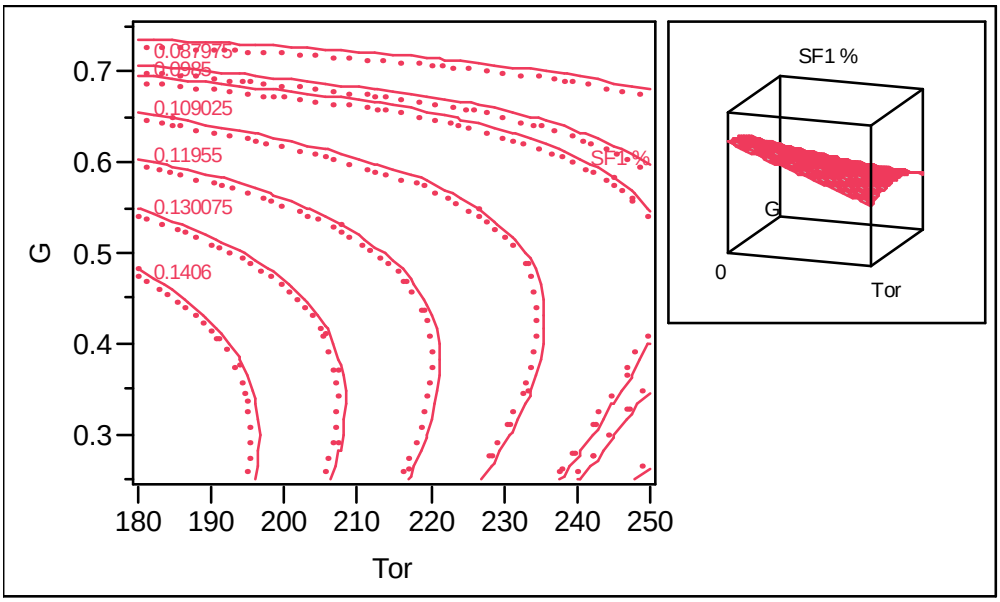
G
0.7
0.6
0.5
0.4
0.3
180
190
200
210
220
230
240
250
Tor
0.087975
0.0985
0.109025
0.11955
0.130075
0.1406
SF1 %
SF1 %
G
0
Tor

Response bio-oil fraction two wt. % yield for washed biomass

Key:

Pyro – Pyrolysis temperature
M – Moisture content
SF2 % - Bio-oil fraction two wt. % yield

Actual by Predicted Plot

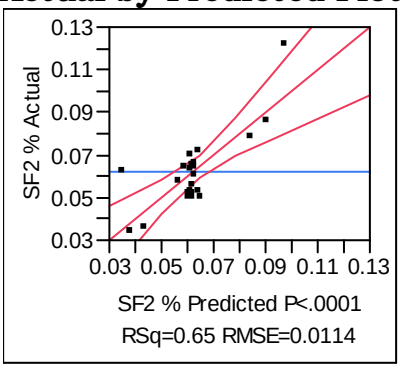

Summary of Fit

RSquare	0.645536
RSquare Adj	0.606151
Root Mean Square Error	0.011394
Mean of Response	0.06231
Observations (or Sum Wgts)	21

Parameter Estimates

Term	Estimate	Std Error	t Ratio	Prob>|t|
Intercept	-0.062228	0.042622	-1.46	0.1615
Pyro	0.0002554	8.818e-5	2.90	0.0096
(Pyro-483.333)*(M-0.13444)	0.0058303	0.001455	4.01	0.0008

Residual by Predicted Plot

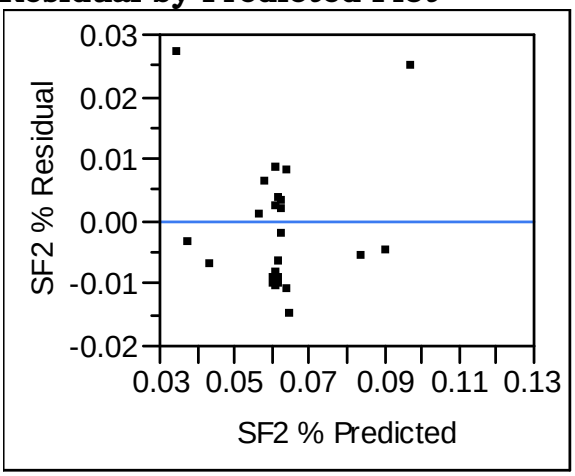

Contour Profiler

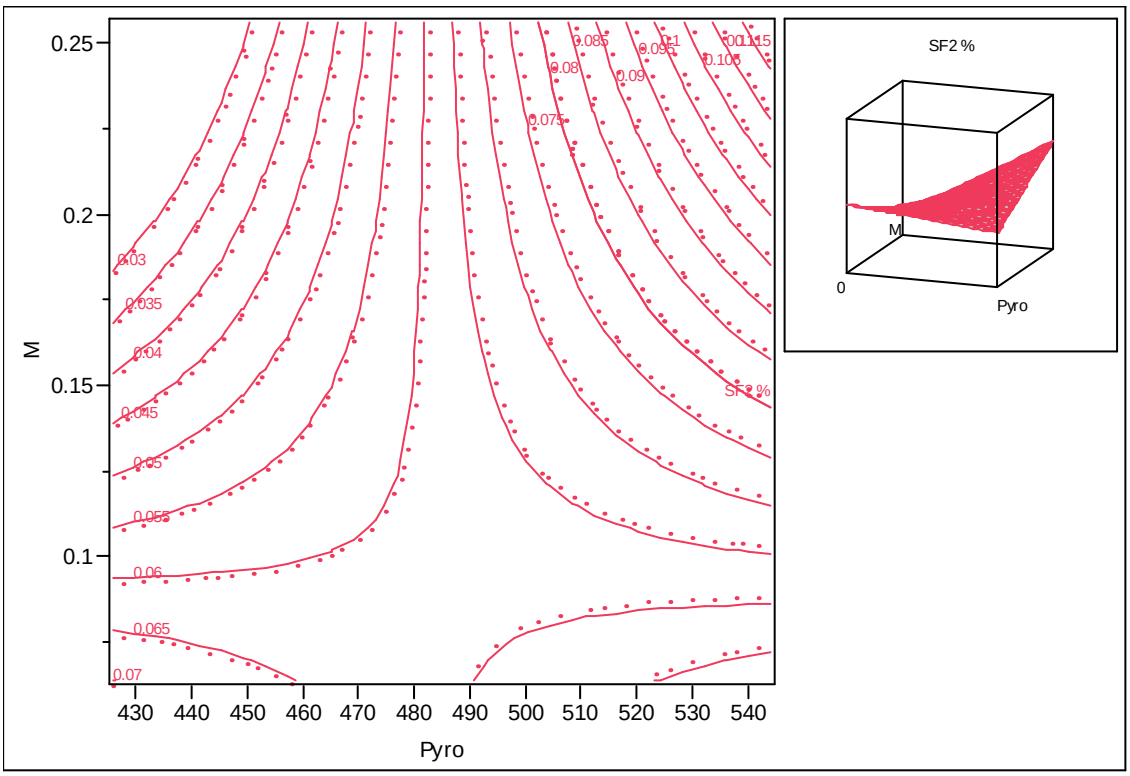

Response bio-oil fraction two wt. % yield for torrefied biomass

Key:
Pyro – Pyrolysis temperature
G – Grind size
SF2 % - Bio-oil fraction two wt. % yield

Actual by Predicted Plot

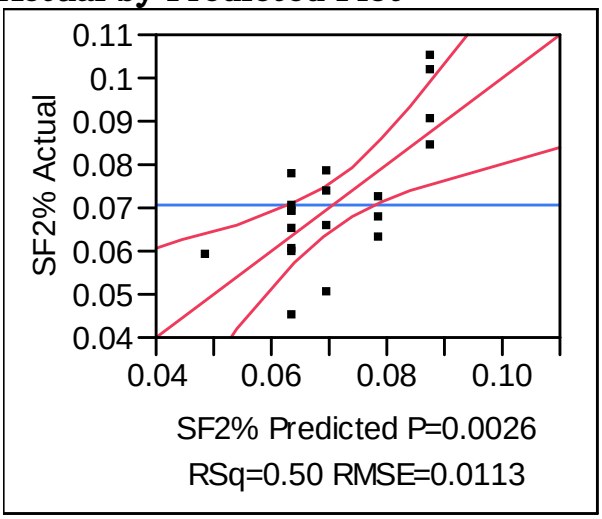

Summary of Fit

RSquare	0.503076
RSquare Adj	0.444614
Root Mean Square Error	0.011317
Mean of Response	0.070995
Observations (or Sum Wgts)	20

Parameter Estimates

Term	Estimate	Std Error	t Ratio	Prob>|t|
Intercept	0.185733	0.042544	4.37	0.0004
Pyro	-0.000252	8.741e-5	-2.88	0.0103
(G-0.5)*(G-0.5)	0.24144	0.080975	2.98	0.0084

Residual by Predicted Plot

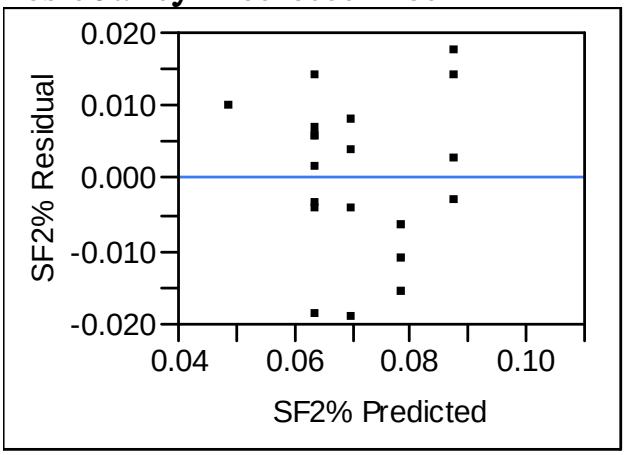

Contour Profiler

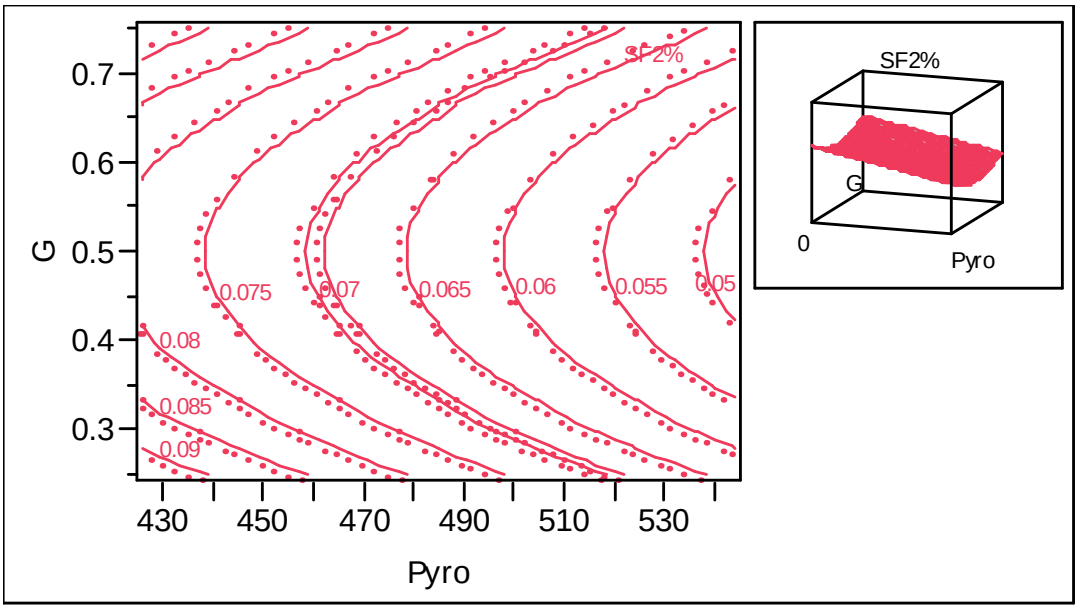

Response bio-oil fraction three wt. % yield for unwashed biomass

Key:
Pyro – Pyrolysis temperature
SF3 % - Bio-oil fraction three wt. % yield

Actual by Predicted Plot

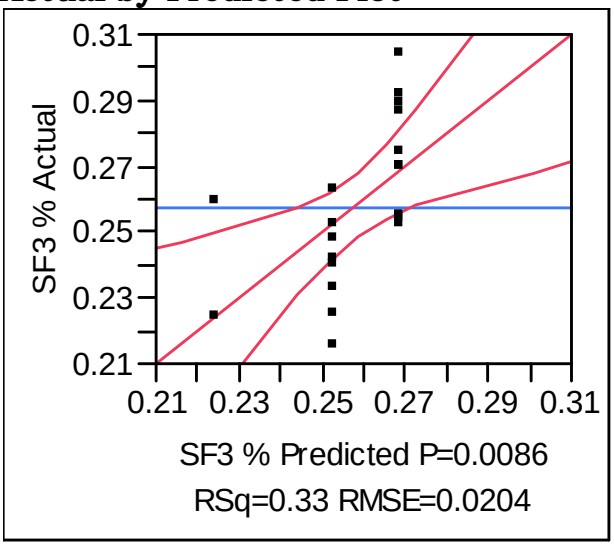

Summary of Fit

RSquare	0.325485
RSquare Adj	0.288012
Root Mean Square Error	0.020371
Mean of Response	0.25735
Observations (or Sum Wgts)	20

Parameter Estimates

Term	Estimate	Std Error	t Ratio	Prob>|t|
Intercept	0.2680315	0.005821	46.04	<.0001
(Pyro-485)*(Pyro-485)	-1.274e-5	4.324e-6	-2.95	0.0086

Residual by Predicted Plot

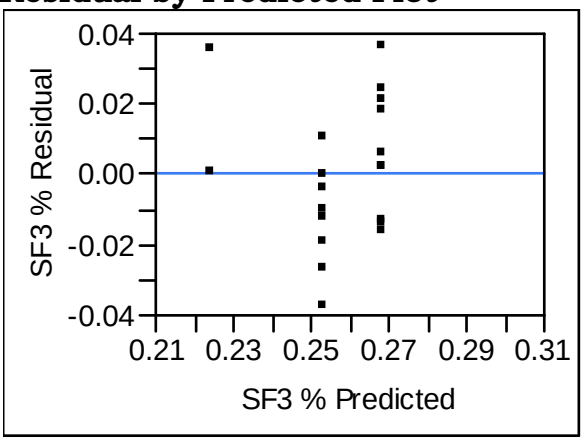

Prediction Profiler

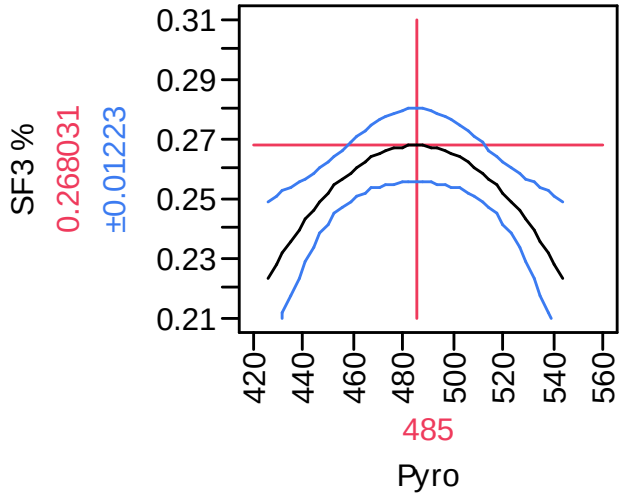

Response bio-oil fraction three wt. % yield for washed biomass

Key:
Pyro – Pyrolysis temperature
M – Moisture content
SF3 % - Bio-oil fraction three wt. % yield

Actual by Predicted Plot

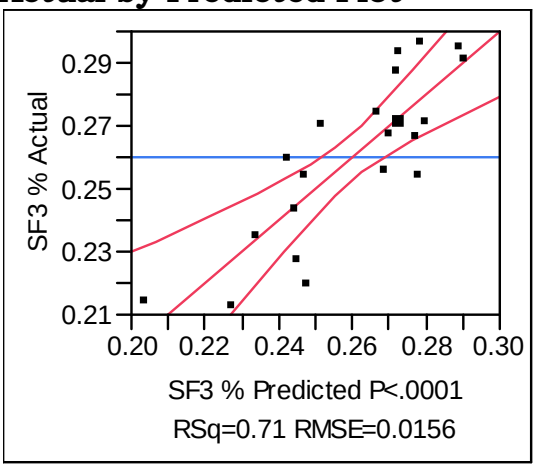

Summary of Fit

RSquare	0.706956
RSquare Adj	0.655243
Root Mean Square Error	0.015585
Mean of Response	0.259686
Observations (or Sum Wgts)	21

Parameter Estimates

Term	Estimate	Std Error	t Ratio	Prob>|t|
Intercept	0.0821296	0.056974	1.44	0.1676
Pyro	0.0004318	0.00012	3.60	0.0022
(Pyro-483.333)*(Pyro-483.333)	-1.763e-5	3.341e-6	-5.28	<.0001
(M-0.13444)*(M-0.13444)	-3.79123	1.118871	-3.39	0.0035

Residual by Predicted Plot

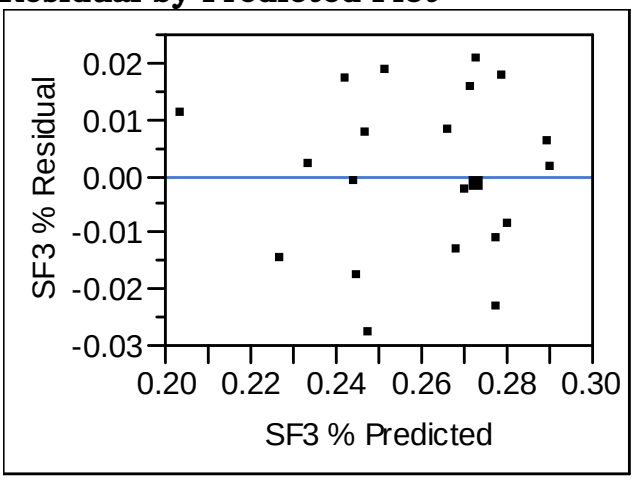

Contour Profiler

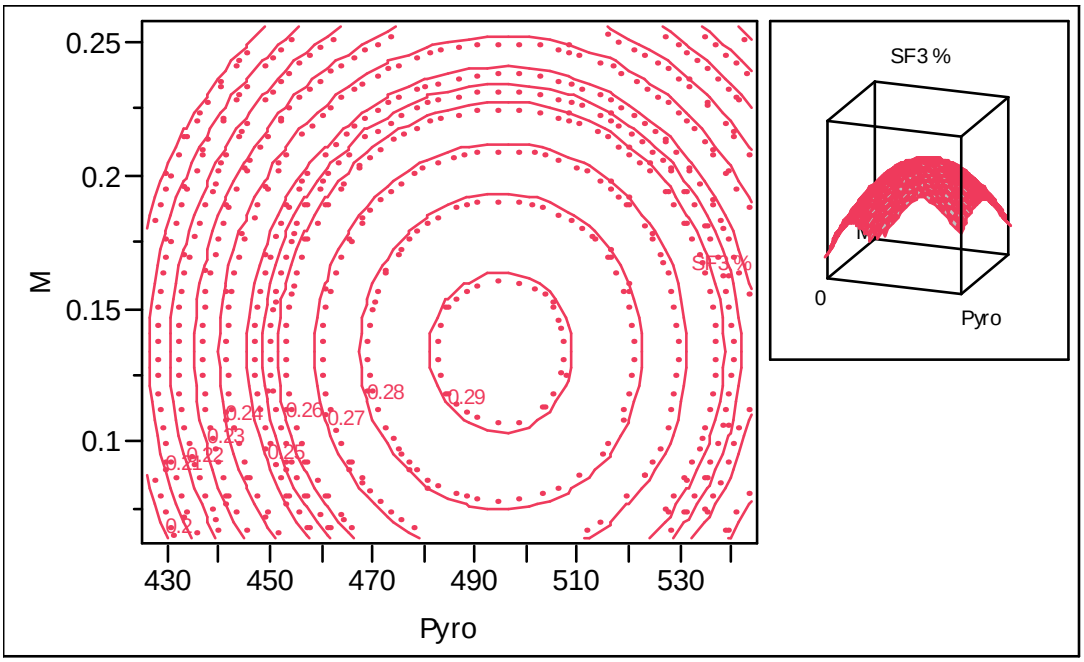

Response bio-oil fraction three wt. % yield for torrefied biomass

Key:
Pyro – Pyrolysis temperature
G – Grind size
SF3 % - Bio-oil fraction three wt. % yield

Actual by Predicted Plot

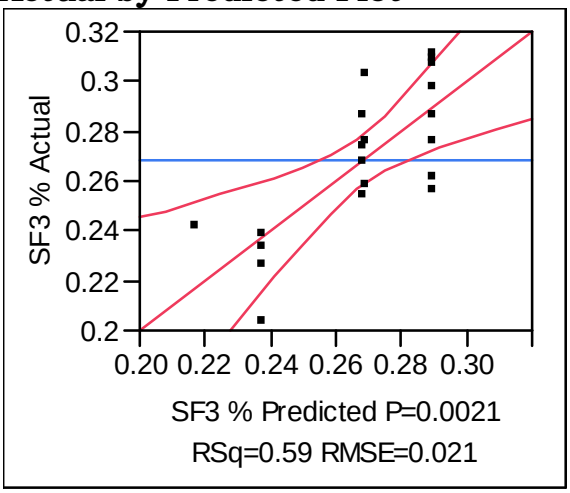

Summary of Fit

RSquare	0.590734
RSquare Adj	0.513996
Root Mean Square Error	0.020958
Mean of Response	0.26794
Observations (or Sum Wgts)	20

Parameter Estimates

Term	Estimate	Std Error	t Ratio	Prob>|t|
Intercept	0.0782639	0.078852	0.99	0.3357
Pyro	0.0004357	0.000162	2.69	0.0161
(Pyro-485)*(Pyro-485)	-1.349e-5	4.49e-6	-3.00	0.0084
(G-0.5)*(G-0.5)	-0.33042	0.151343	-2.18	0.0443

Residual by Predicted Plot

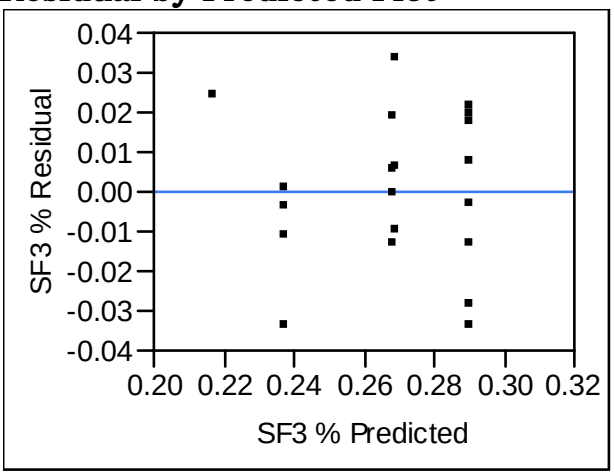

Contour Profiler

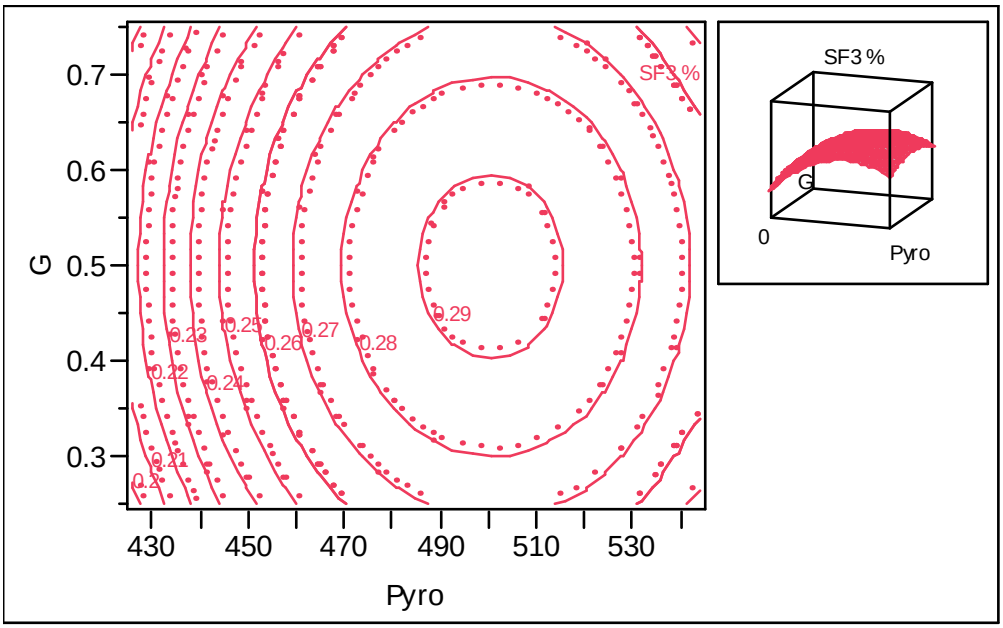

Response bio-oil fraction four wt. % yield for unwashed biomass

Key:
M – Moisture content
G – Grind size
SF4 % - Bio-oil fraction four wt. % yield

Actual by Predicted Plot

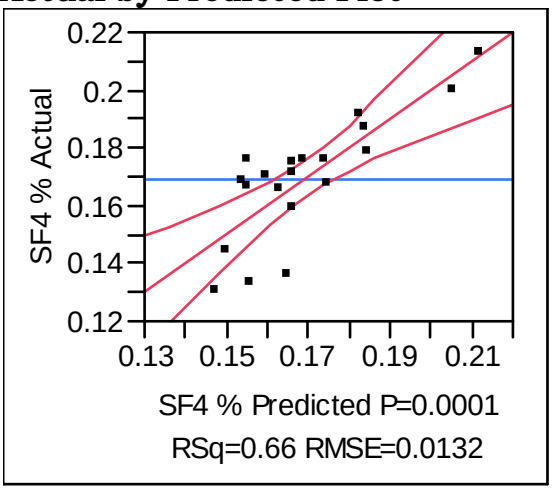

Summary of Fit

RSquare	0.657606
RSquare Adj	0.617325
Root Mean Square Error	0.013188
Mean of Response	0.16905
Observations (or Sum Wgts)	20

Parameter Estimates

Term	Estimate	Std Error	t Ratio	Prob>|t|
Intercept	0.0930685	0.014044	6.63	<.0001
M	0.623712	0.118556	5.26	<.0001
G	0.0359526	0.016683	2.16	0.0458

Residual by Predicted Plot

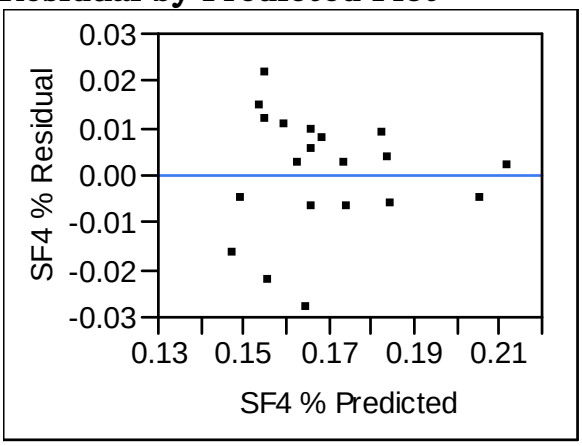

Contour Profiler

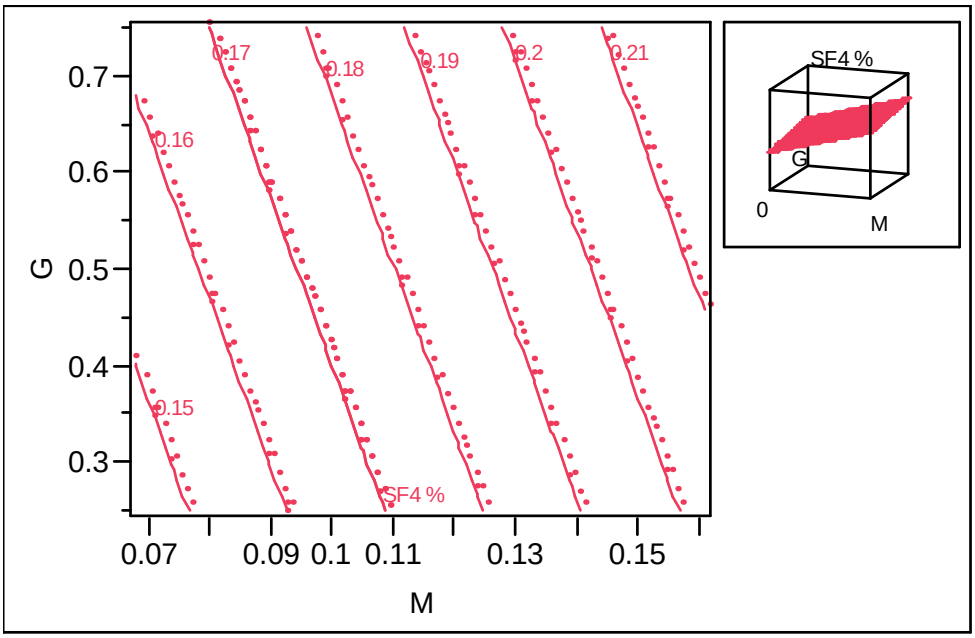

Response bio-oil fraction four wt. % yield for washed biomass

Key:
M – Moisture content
G – Grind size
SF4 % - Bio-oil fraction four wt. % yield

Actual by Predicted Plot

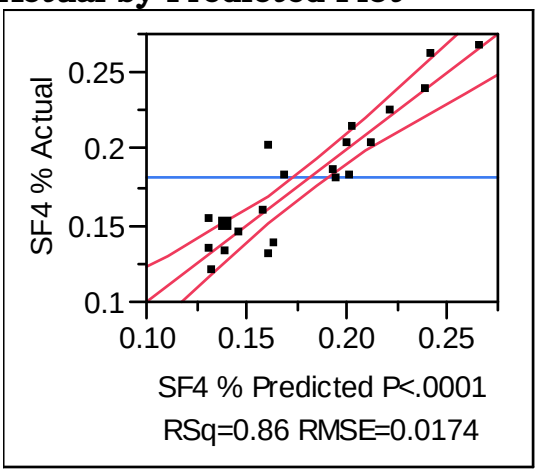

Summary of Fit

RSquare	0.855676
RSquare Adj	0.83964
Root Mean Square Error	0.017395
Mean of Response	0.180662
Observations (or Sum Wgts)	21

Parameter Estimates

Term	Estimate	Std Error	t Ratio	Prob>|t|
Intercept	0.071099	0.013761	5.17	<.0001
M	0.5736301	0.058308	9.84	<.0001
G	0.0633812	0.021027	3.01	0.0075

Residual by Predicted Plot

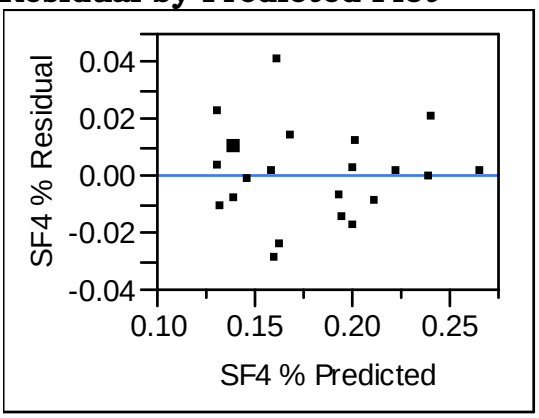

Contour Profiler

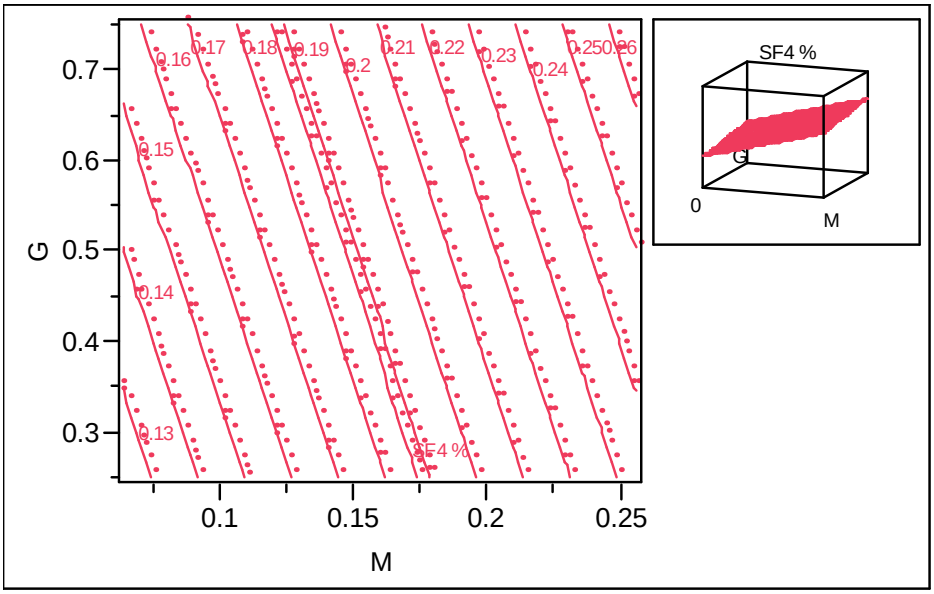

Response total bio-oil wt. % yield for unwashed biomass

Key:
M – Moisture content
G – Grind size
ST % - Total bio-oil wt. % yield

Actual by Predicted Plot

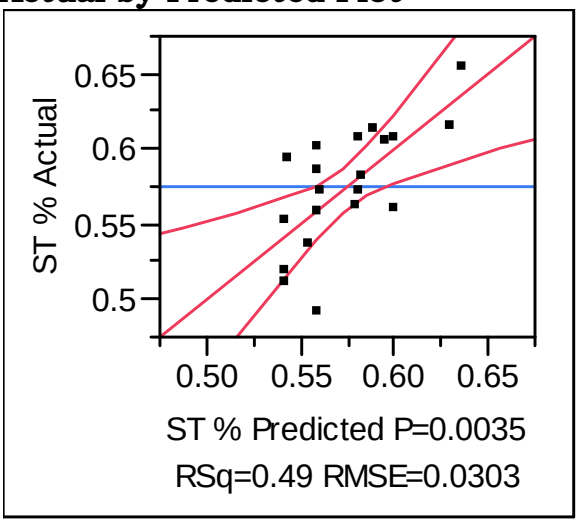

Summary of Fit

RSquare	0.486269
RSquare Adj	0.42583
Root Mean Square Error	0.030277
Mean of Response	0.57425
Observations (or Sum Wgts)	20

Parameter Estimates

Term	Estimate	Std Error	t Ratio	Prob>|t|
Intercept	0.5386989	0.028283	19.05	<.0001
M	0.6029069	0.275216	2.19	0.0427
(G-0.5)*(G-0.5)	-0.656616	0.219078	-3.00	0.0081

Residual by Predicted Plot

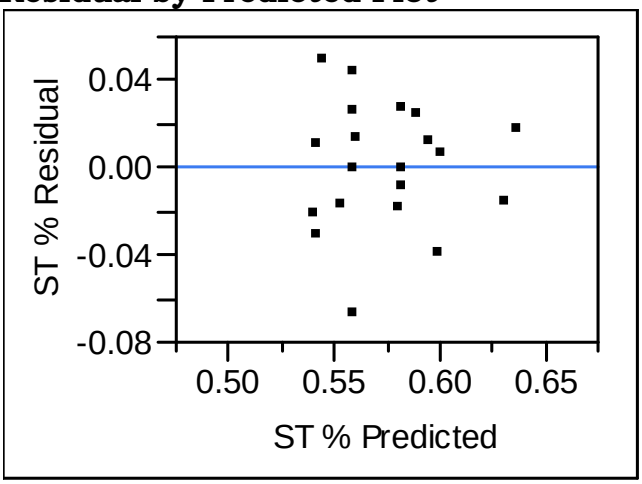

Contour Profiler

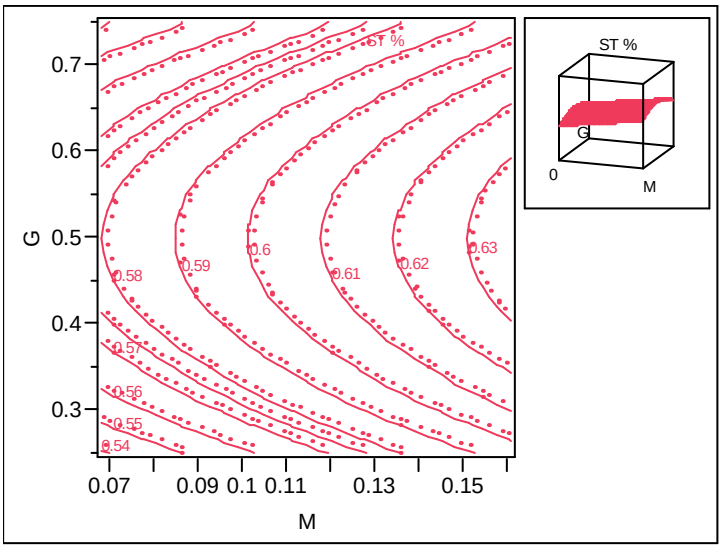

Response total bio-oil wt. % yield for washed biomass

Key:
Pyro – Pyrolysis temperature
M – Moisture content
G – Grind size
ST % - Total bio-oil wt. % yield

Actual by Predicted Plot

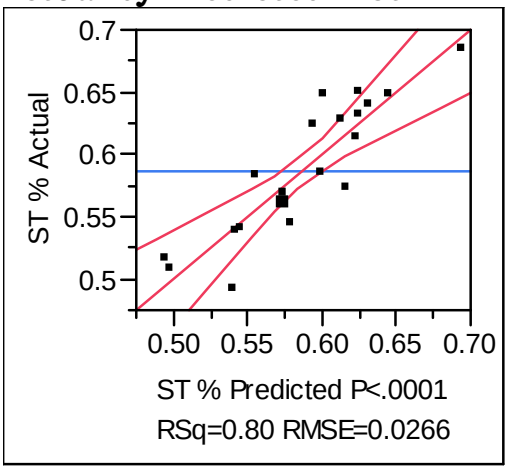

Summary of Fit

RSquare	0.804349
RSquare Adj	0.755436
Root Mean Square Error	0.026628
Mean of Response	0.586995
Observations (or Sum Wgts)	21

Parameter Estimates

Term	Estimate	Std Error	t Ratio	Prob>|t|
Intercept	-0.053674	0.09926	-0.54	0.5961
Pyro	0.0011424	0.000201	5.69	<.0001
M	0.4057305	0.091463	4.44	0.0004
G	0.0941871	0.032288	2.92	0.0101
(Pyro-483.333)*(Pyro-483.333)	-1.668e-5	5.748e-6	-2.90	0.0104

Residual by Predicted Plot

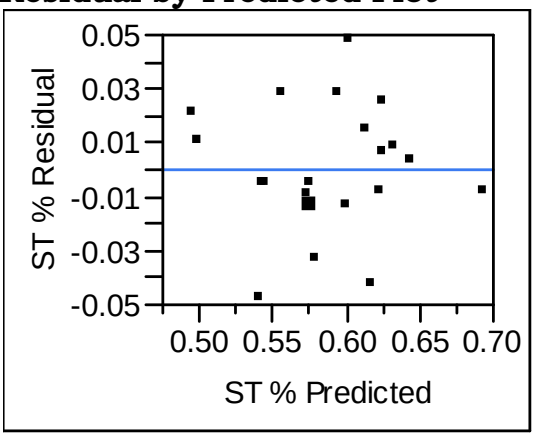

Contour Profiler

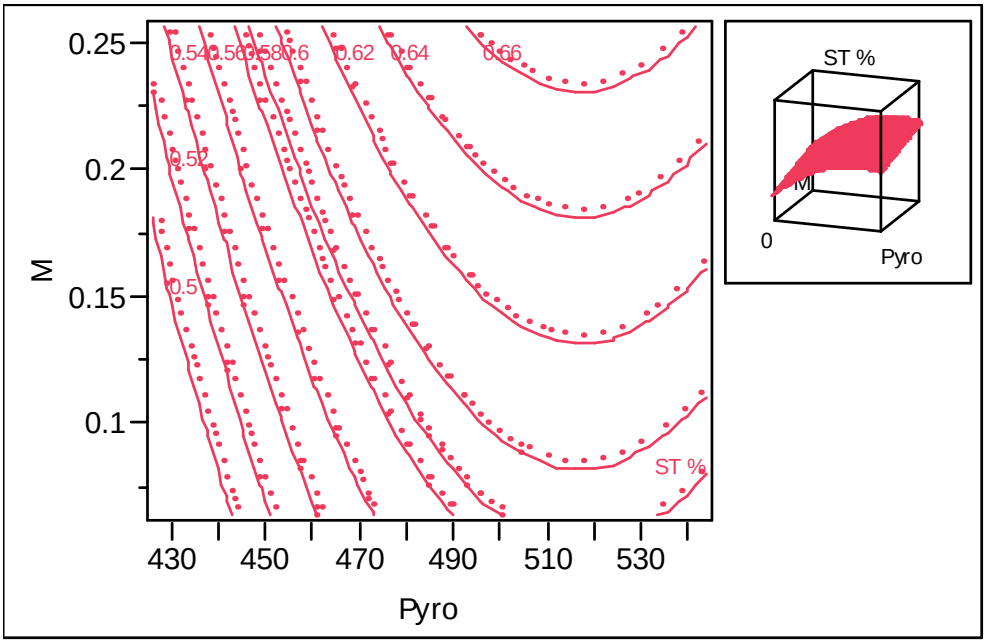

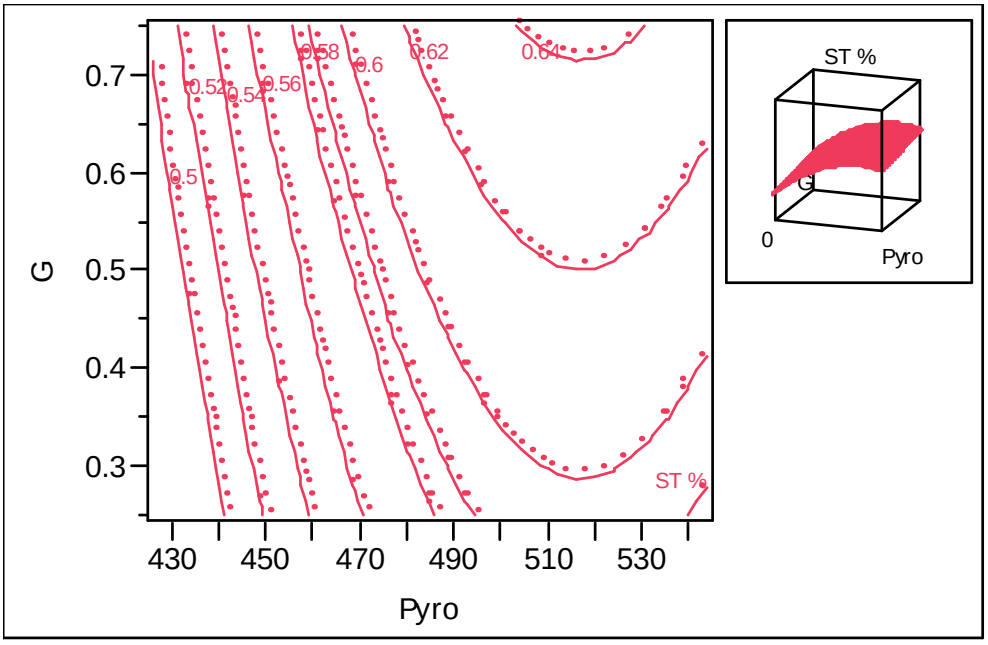
0.7
0.6
0.5
0.4
0.3
G
0.5
0.52
0.54
0.56
0.58
0.6
0.62
0.64
ST %
430
450
470
490
510
530
Pyro
ST %
G
0
Pyro

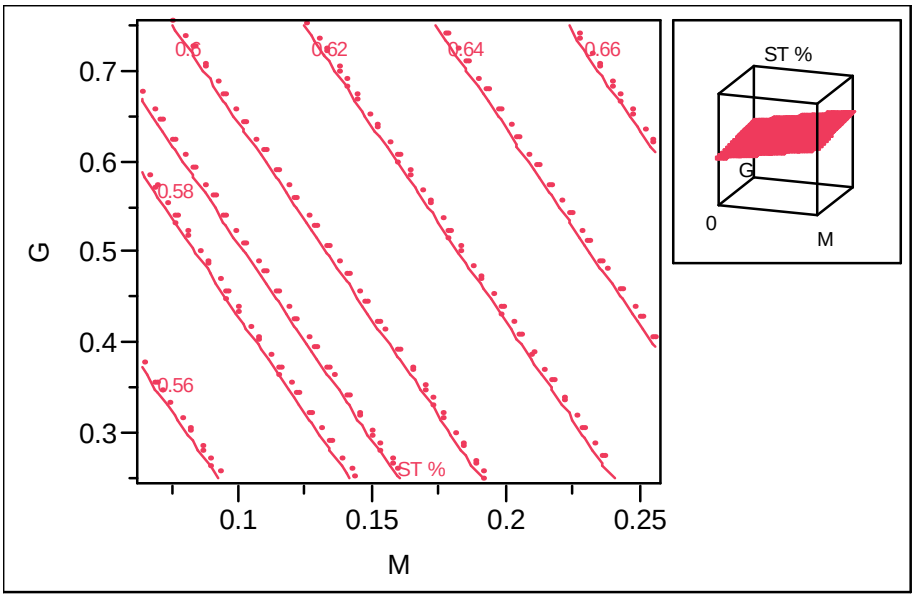
0.7
0.6
0.5
0.4
0.3
G
0.6
0.62
0.64
0.66
0.58
0.56
ST %
0.1
0.15
0.2
0.25
M
ST %
G
0
M

Response total bio-oil wt. % yield for torrefied biomass

Key:
Pyro – Pyrolysis temperature
Tor – Torrefaction temperature
ST % - Total bio-oil wt. % yield

Actual by Predicted Plot

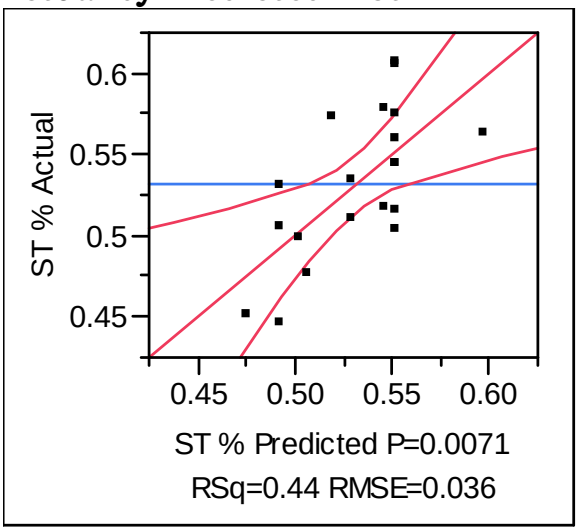

Summary of Fit

RSquare	0.441559
RSquare Adj	0.375861
Root Mean Square Error	0.035974
Mean of Response	0.5313
Observations (or Sum Wgts)	20

Parameter Estimates

Term	Estimate	Std Error	t Ratio	Prob>|t|
Intercept	0.1773079	0.13501	1.31	0.2065
Pyro	0.0007711	0.000278	2.77	0.0131
(Tor-211.5)*(Tor-211.5)	-3.331e-5	1.316e-5	-2.53	0.0215

Residual by Predicted Plot

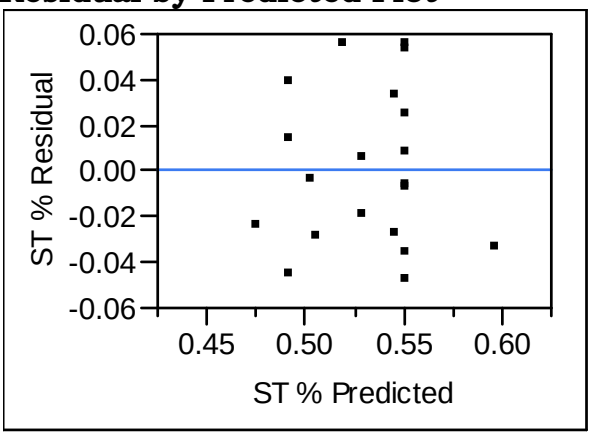

Contour Profiler

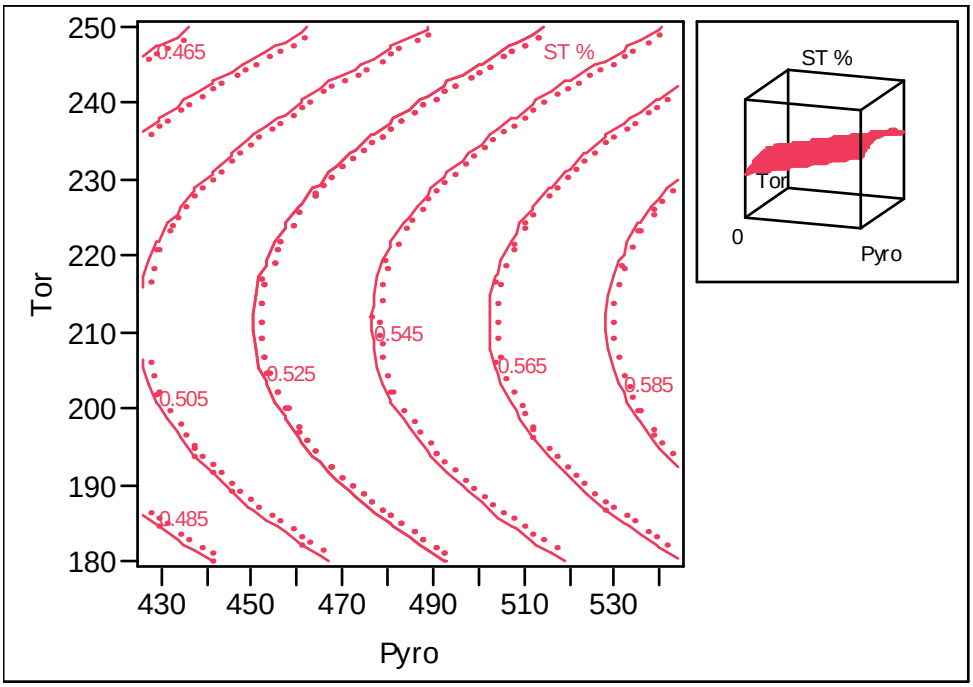

Response bio-oil fraction four moisture content (wt. %) for unwashed biomass

Key:
Pyro – Pyrolysis temperature
M – Moisture content
G – Grind size
SF4 moisture - Bio-oil fraction four moisture content

Actual by Predicted Plot

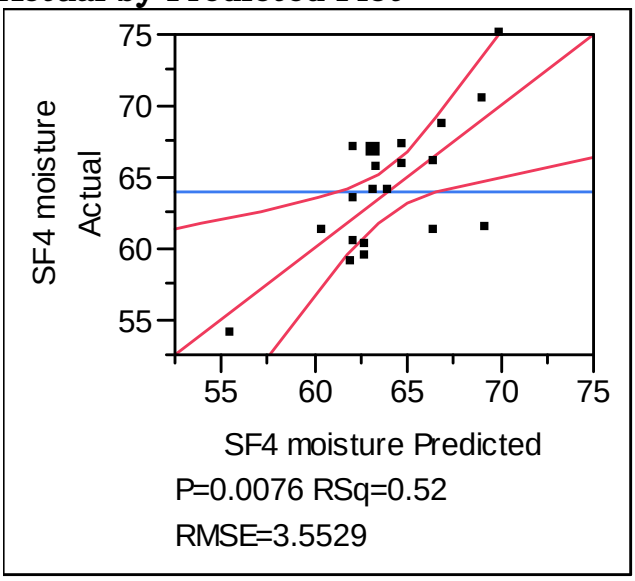

Summary of Fit

RSquare	0.515958
RSquare Adj	0.4252
Root Mean Square Error	3.552909
Mean of Response	63.984
Observations (or Sum Wgts)	20

Parameter Estimates

Term	Estimate	Std Error	t Ratio	Prob>|t|
Intercept	55.941773	3.077222	18.18	<.0001
M	86.941262	31.97565	2.72	0.0152
(M-0.093)*(G-0.5)	-692.9724	318.0093	-2.18	0.0446
(G-0.5)*(Pyro-485)	-0.35673	0.143753	-2.48	0.0246

Residual by Predicted Plot

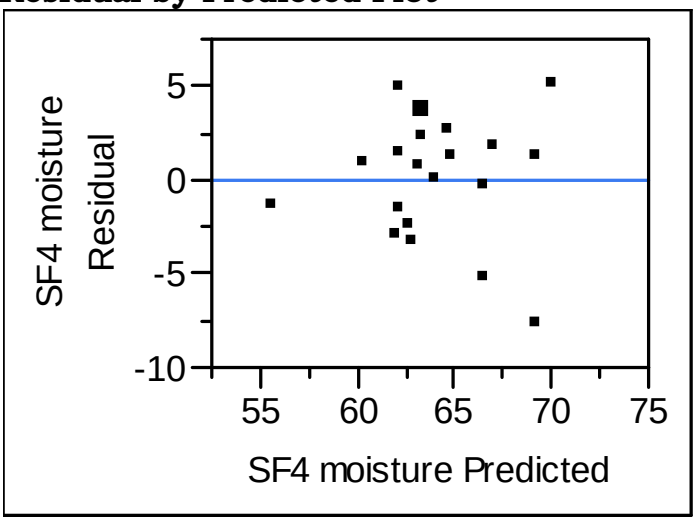

Contour Profiler

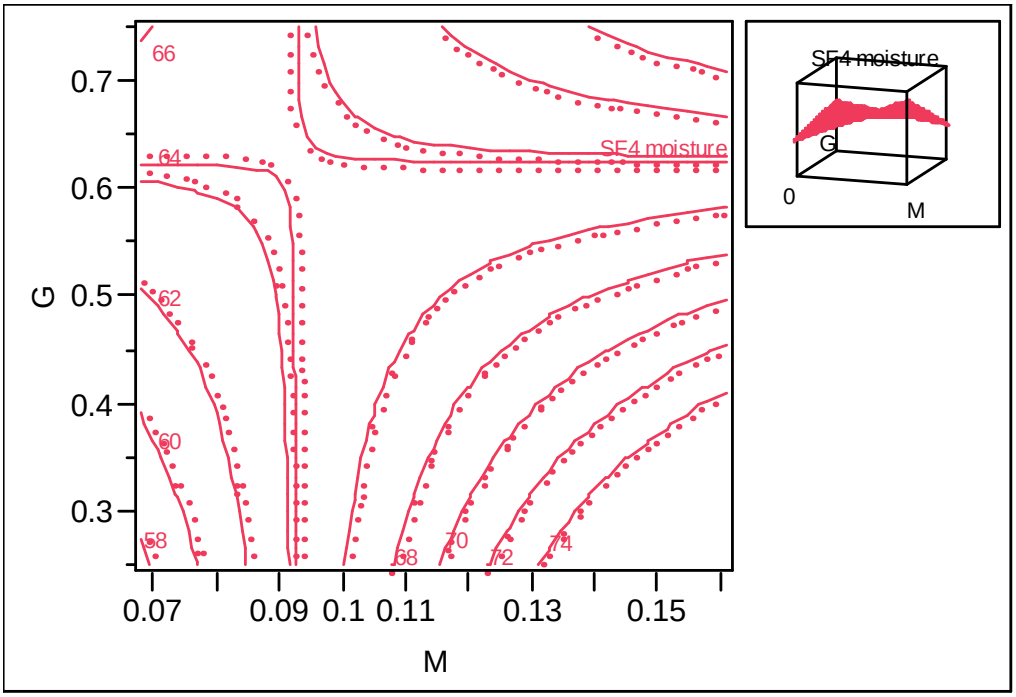

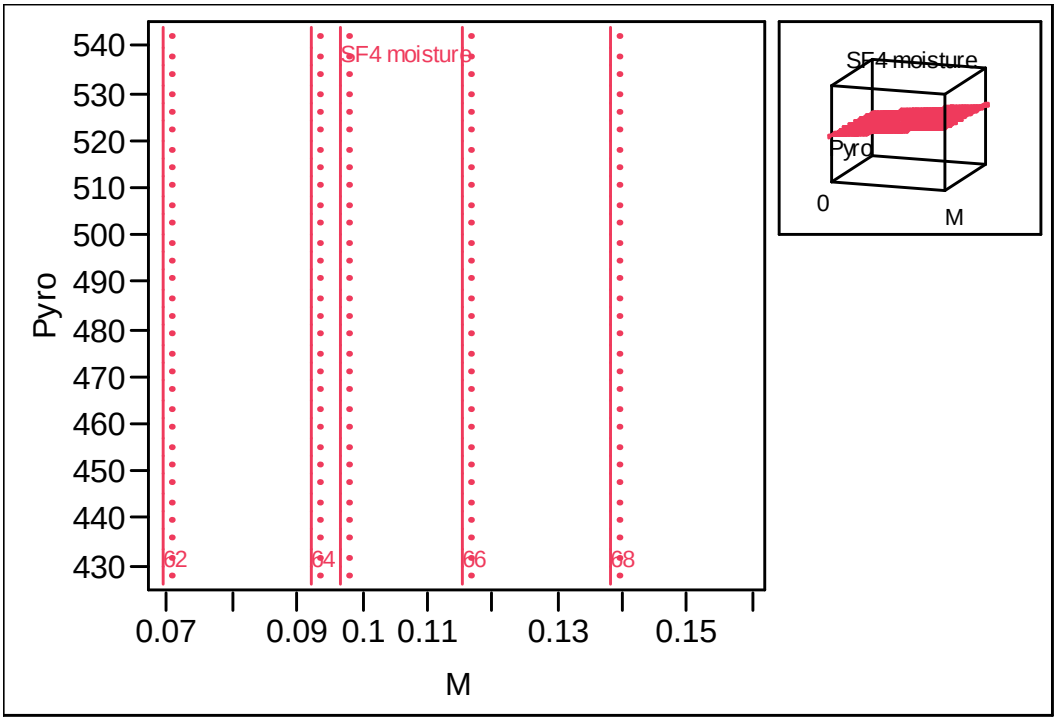
Pyro
540
530
520
510
500
490
480
470
460
450
440
430
SF4 moisture
62
64
66
68
0.07
0.09
0.1
0.11
0.13
0.15
M
SF4 moisture
Pyro
0
M

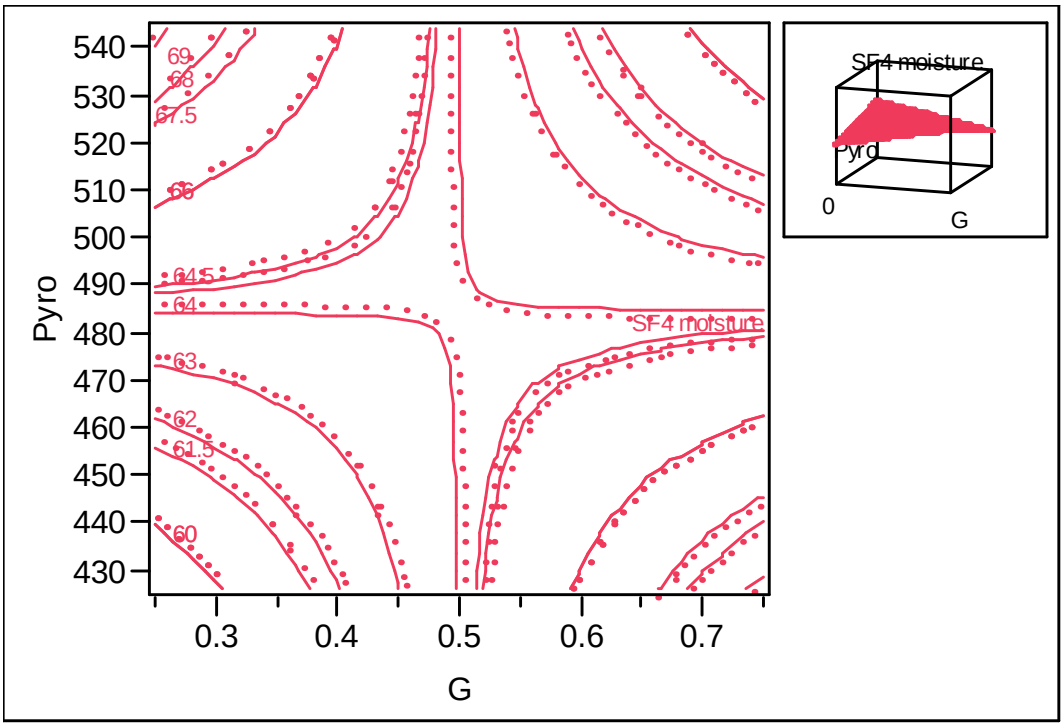
Pyro
540
530
520
510
500
490
480
470
460
450
440
430
69
68
67.5
66
64.5
64
63
62
61.5
60
SF4 moisture
0.3
0.4
0.5
0.6
0.7
G
SF4 moisture
Pyro
0
G

Response bio-oil fraction four moisture content (wt. %) for washed biomass

Key:
M – Moisture content
G – Grind size
SF4 moisture - Bio-oil fraction four moisture content

Actual by Predicted Plot

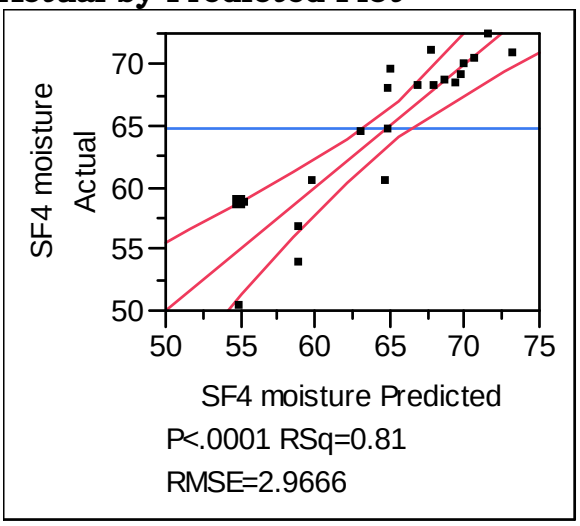

Summary of Fit

RSquare	0.811263
RSquare Adj	0.777956
Root Mean Square Error	2.966563
Mean of Response	64.80762
Observations (or Sum Wgts)	21

Parameter Estimates

Term	Estimate	Std Error	t Ratio	Prob>|t|
Intercept	50.452687	2.346986	21.50	<.0001
M	79.672156	10.23833	7.78	<.0001
G	7.1890222	3.629547	1.98	0.0640
(M-0.13444)*(G-0.5119)	-220.5669	54.67342	-4.03	0.0009

Residual by Predicted Plot

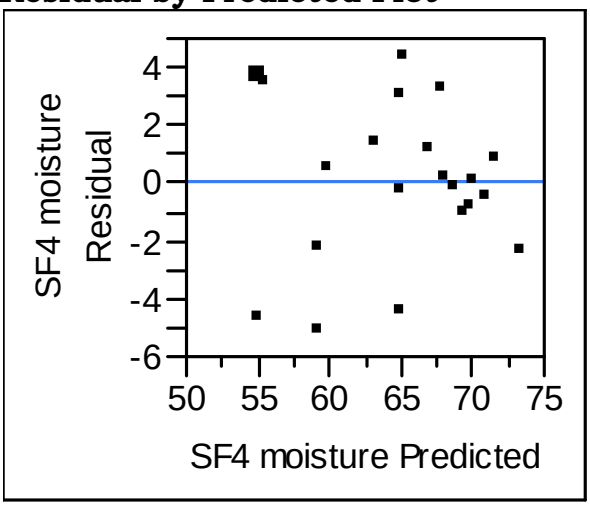

Contour Profiler

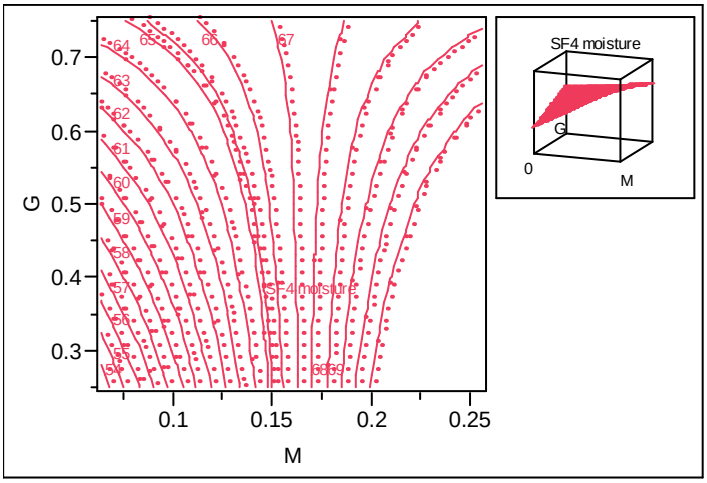

Response bio-oil fraction four moisture content (wt. %) for torrefied biomass

Key:
G – Grind size
Tor – Torrefaction temperature
SF4 moisture - Bio-oil fraction four moisture content

Actual by Predicted Plot

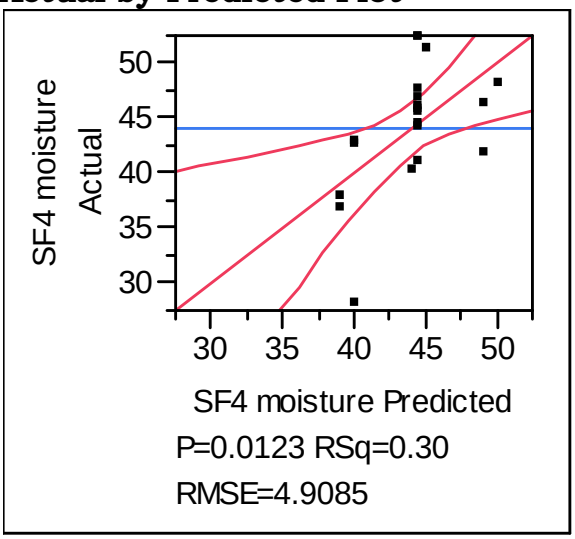

Summary of Fit

RSquare	0.300968
RSquare Adj	0.262133
Root Mean Square Error	4.908493
Mean of Response	44.0165
Observations (or Sum Wgts)	20

Parameter Estimates

Term	Estimate	Std Error	t Ratio	Prob>|t|
Intercept	44.51546	1.11211	40.03	<.0001
(Tor-211.5)*(G-0.5)	-0.57024	0.204838	-2.78	0.0123

Residual by Predicted Plot

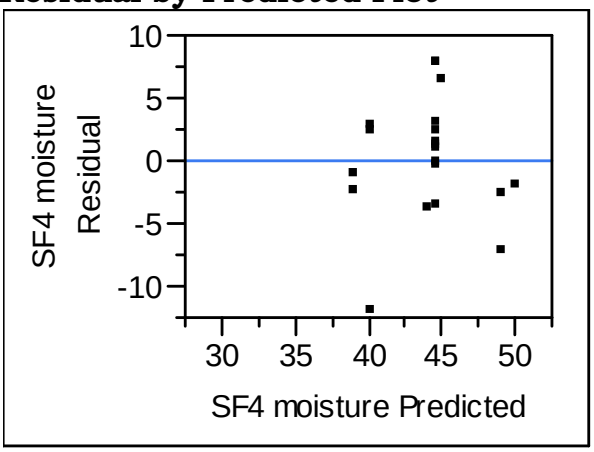

Contour Profiler

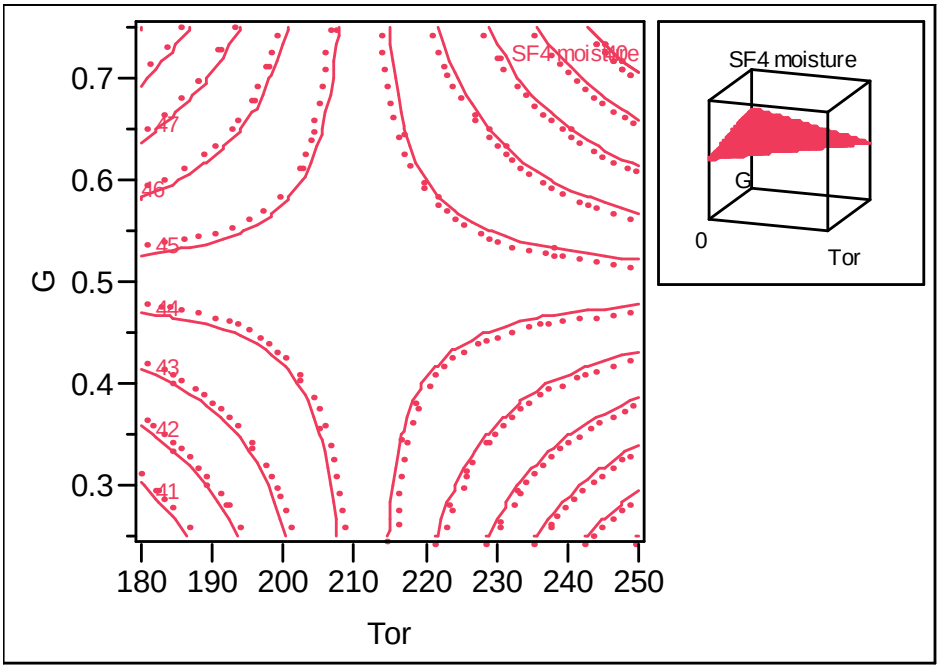

Response bio-oil fraction one water insoluble content (wt. %) for unwashed biomass

Key:
Pyro – Pyrolysis temperature
Ins 1 – Water insolubles content in bio-oil fraction one

Actual by Predicted Plot

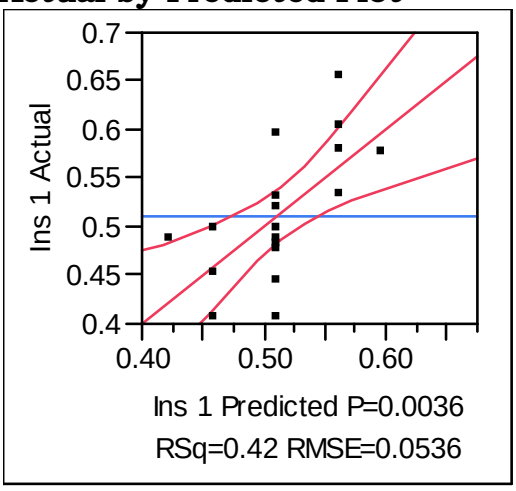

Summary of Fit

RSquare	0.421165
RSquare Adj	0.384988
Root Mean Square Error	0.053649
Mean of Response	0.511962
Observations (or Sum Wgts)	18

Parameter Estimates

Term	Estimate	Std Error	t Ratio	Prob>|t|
Intercept	-0.204712	0.210425	-0.97	0.3451
Pyro	0.0014718	0.000431	3.41	0.0036

Residual by Predicted Plot

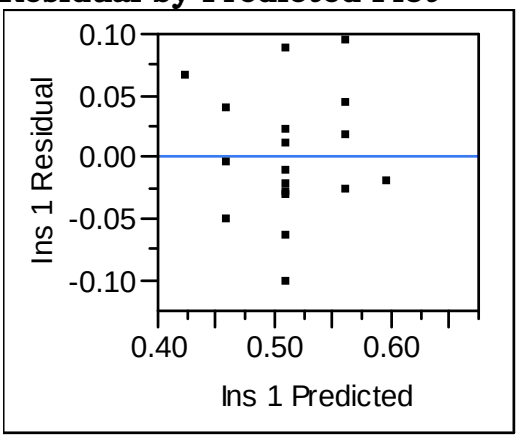

Prediction Profiler

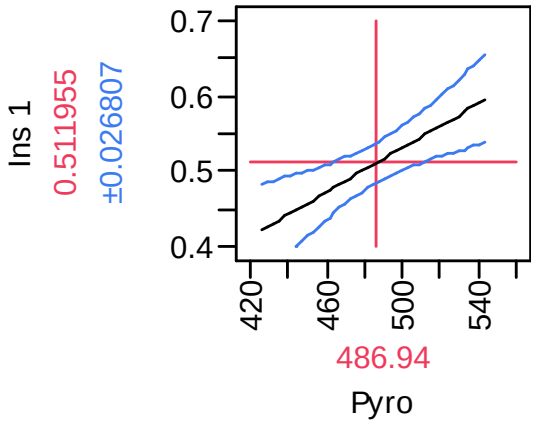

Response bio-oil fraction one water insoluble content (wt. %) for washed biomass

Key:
Pyro – Pyrolysis temperature
G – Grind size
Ins 1 – Water insolubles content in bio-oil fraction one

Actual by Predicted Plot

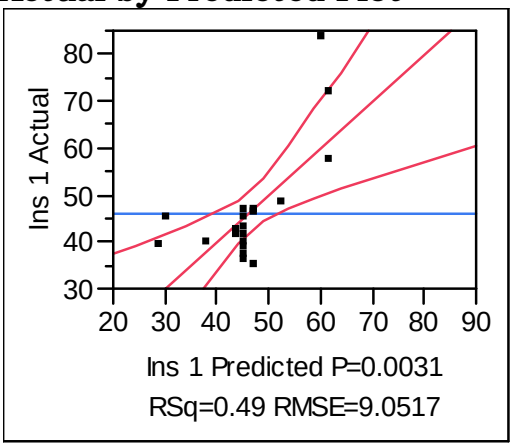

Summary of Fit

RSquare	0.493242
RSquare Adj	0.433623
Root Mean Square Error	9.051742
Mean of Response	46.035
Observations (or Sum Wgts)	20

Parameter Estimates

Term	Estimate	Std Error	t Ratio	Prob>|t|
Intercept	184.19517	35.94484	5.12	<.0001
Pyro	-0.256751	0.0715	-3.59	0.0023
G	-29.06903	11.62336	-2.50	0.0229

Residual by Predicted Plot

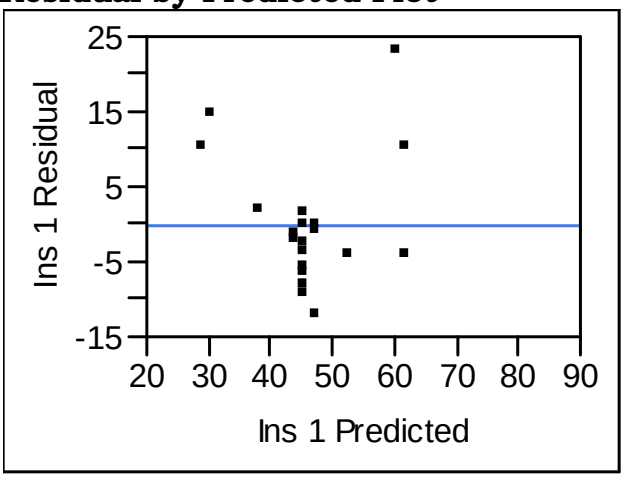

Contour Profiler

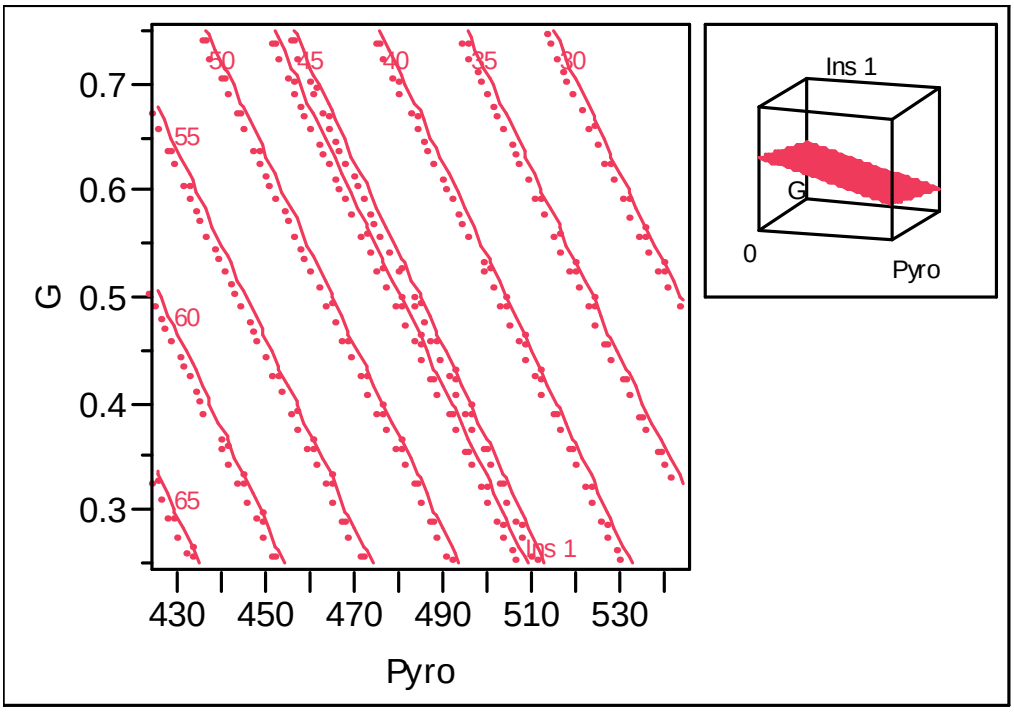

Response bio-oil fraction one water insoluble content (wt. %) for torrefied biomass

Key:
Pyro – Pyrolysis temperature
G – Grind size
Ins 1 – Water insolubles content in bio-oil fraction one

Actual by Predicted Plot

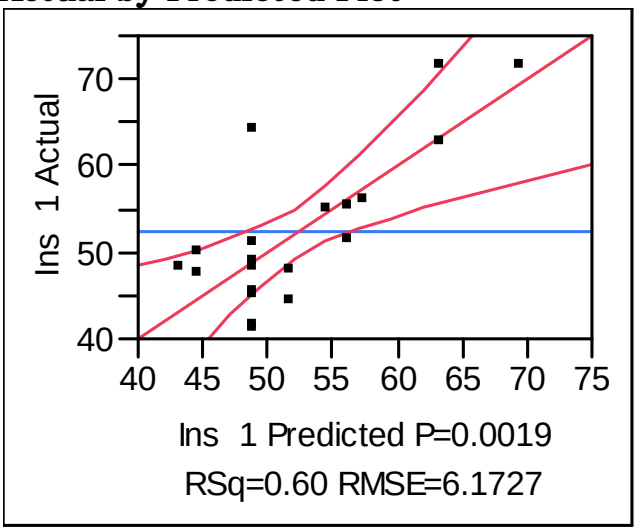

Summary of Fit

RSquare	0.595468
RSquare Adj	0.519618
Root Mean Square Error	6.172689
Mean of Response	52.255
Observations (or Sum Wgts)	20

Parameter Estimates

Term	Estimate	Std Error	t Ratio	Prob>|t|
Intercept	109.47429	23.51696	4.66	0.0003
G	-23.12	7.807903	-2.96	0.0092
Pyro	-0.101396	0.047677	-2.13	0.0494
(Pyro-485)*(Pyro-485)	0.0041973	0.00131	3.20	0.0055

Residual by Predicted Plot

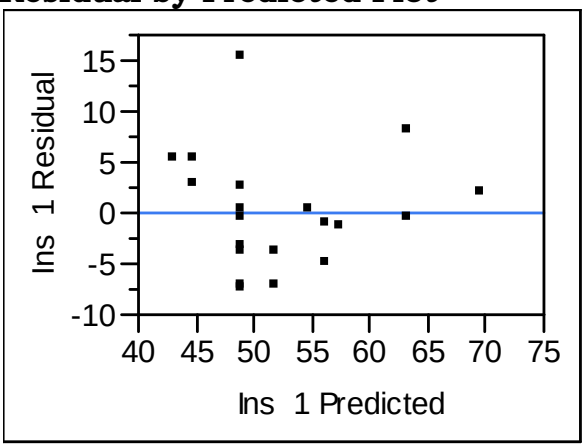

Contour Profiler

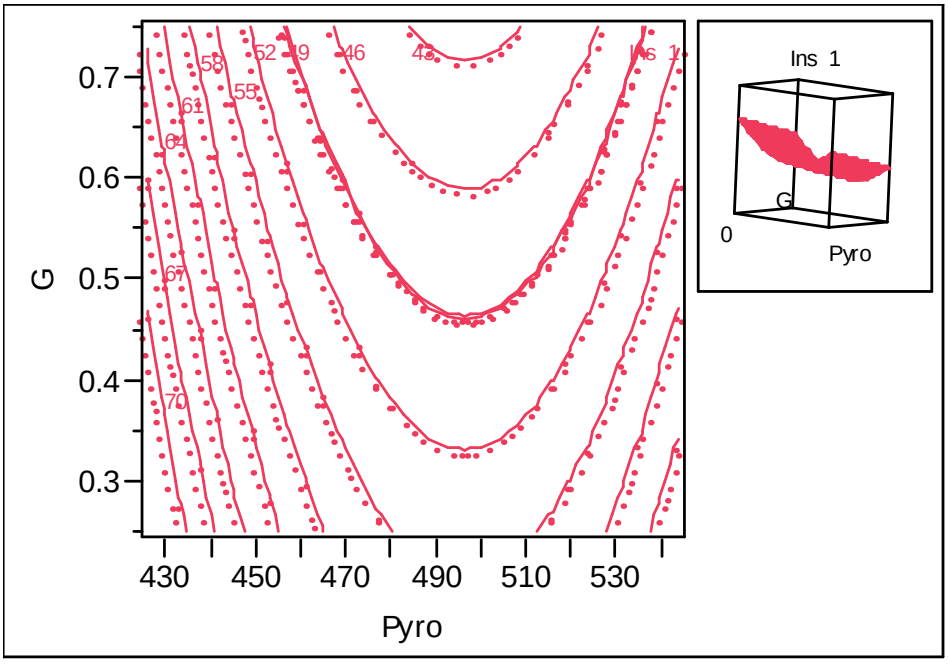

Response non-condensable gas wt. % yield for unwashed biomass

Key:
Pyro – Pyrolysis temperature
Gas % - Total non-condensable gas wt. % yield

Actual by Predicted Plot

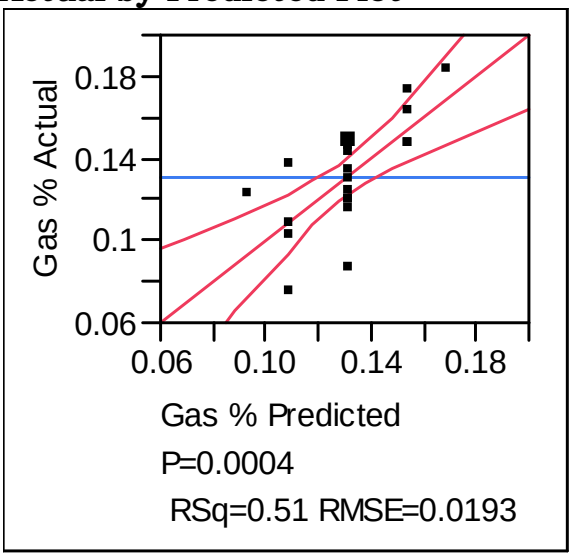

Summary of Fit

RSquare	0.509447
RSquare Adj	0.482194
Root Mean Square Error	0.01933
Mean of Response	0.13075
Observations (or Sum Wgts)	20

Parameter Estimates

Term	Estimate	Std Error	t Ratio	Prob>|t|
Intercept	-0.182321	0.072539	-2.51	0.0217
Pyro	0.0006455	0.000149	4.32	0.0004

Residual by Predicted Plot

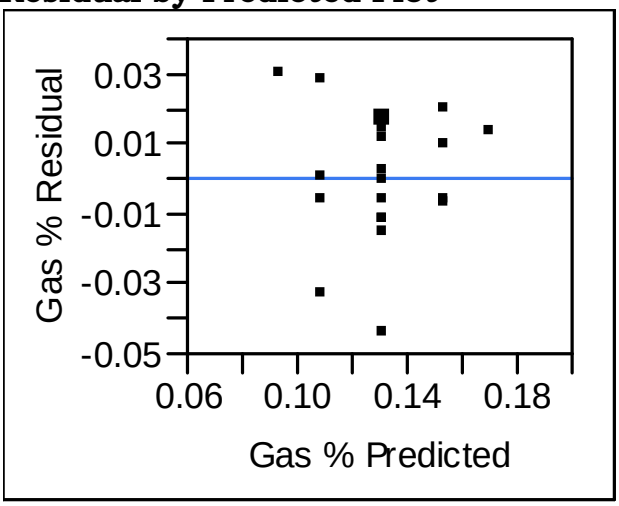

Prediction Profiler

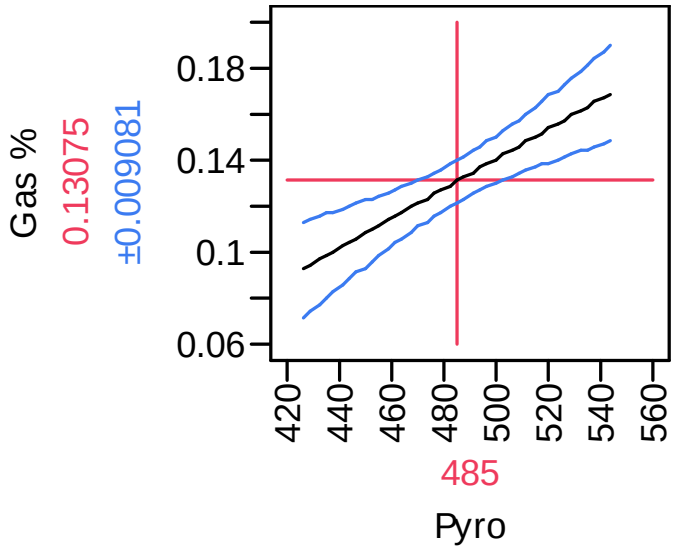

Response non-condensable gas wt. % yield for washed biomass

Key:
Pyro – Pyrolysis temperature
Gas % - Total non-condensable gas wt. % yield

Actual by Predicted Plot

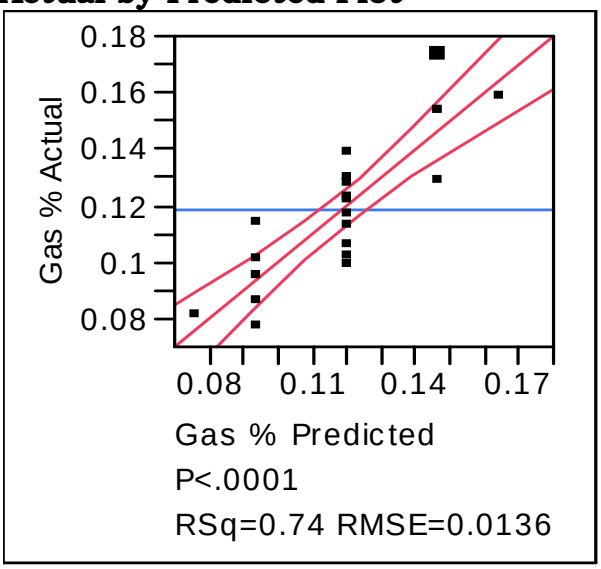

Summary of Fit

RSquare	0.740953
RSquare Adj	0.727318
Root Mean Square Error	0.013566
Mean of Response	0.11881
Observations (or Sum Wgts)	21

Parameter Estimates

Term	Estimate	Std Error	t Ratio	Prob>|t|
Intercept	-0.242203	0.049061	-4.94	<.0001
Pyro	0.0007469	0.000101	7.37	<.0001

Residual by Predicted Plot

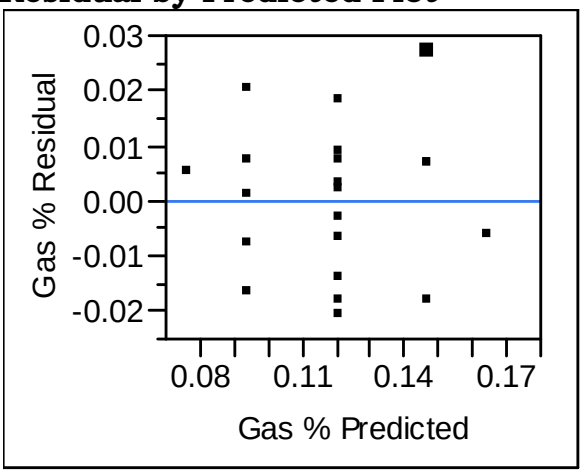

Prediction Profiler

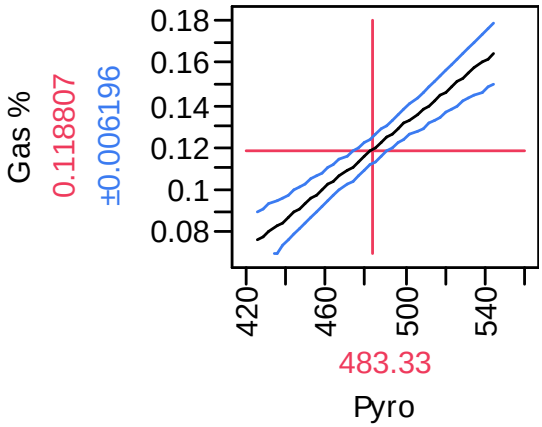

Response non-condensable gas wt. % yield for torrefied biomass

Key:
Pyro – Pyrolysis temperature
G – Grind size
Gas % - Total non-condensable gas wt. % yield

Actual by Predicted Plot

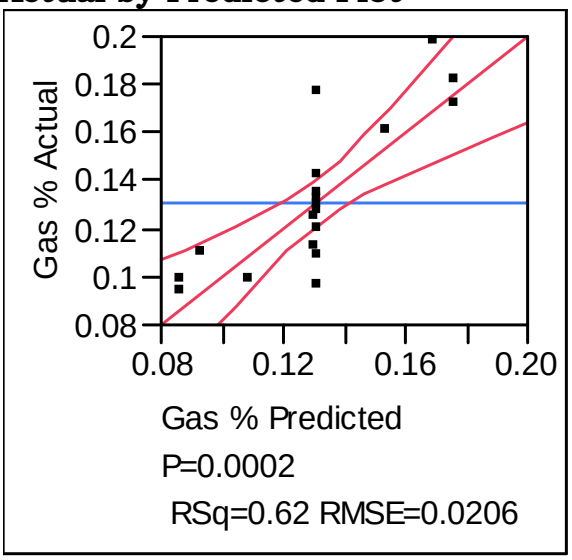

Summary of Fit

RSquare	0.624269
RSquare Adj	0.580065
Root Mean Square Error	0.020556
Mean of Response	0.13045
Observations (or Sum Wgts)	20

Parameter Estimates

Term	Estimate	Std Error	t Ratio	Prob>|t|
Intercept	-0.226729	0.078231	-2.90	0.0100
Pyro	0.0006445	0.000159	4.06	0.0008
G	0.0892	0.026002	3.43	0.0032

Residual by Predicted Plot

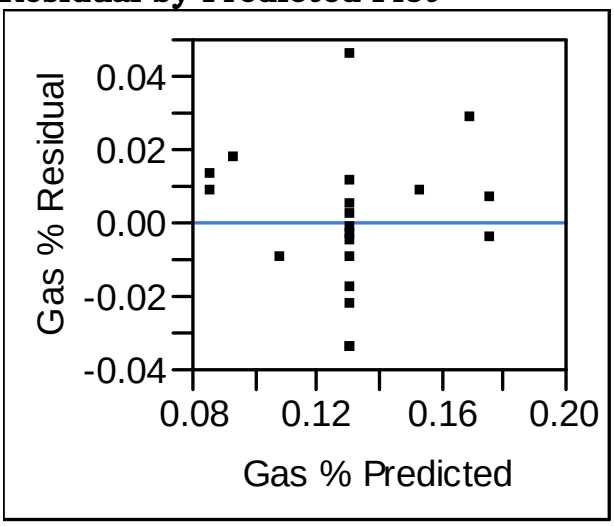

Contour Profiler

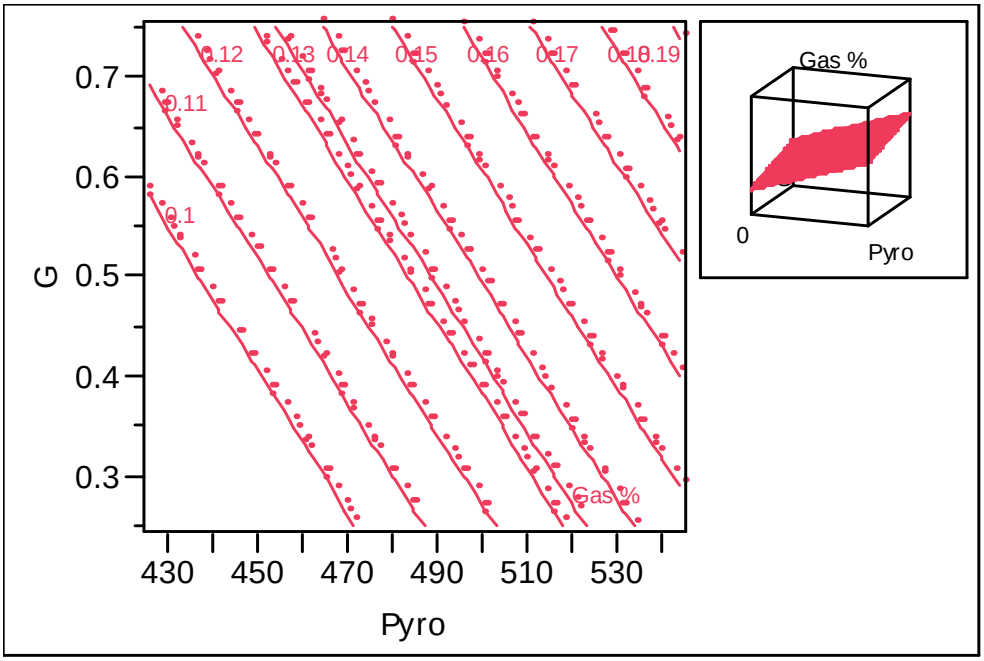

Response carbon monoxide concentration vol. % for unwashed biomass

Key:
Pyro – Pyrolysis temperature
M – Moisture content
CO - Total carbon monoxide vol. % yield in non-condensable gas, nitrogen free

Actual by Predicted Plot

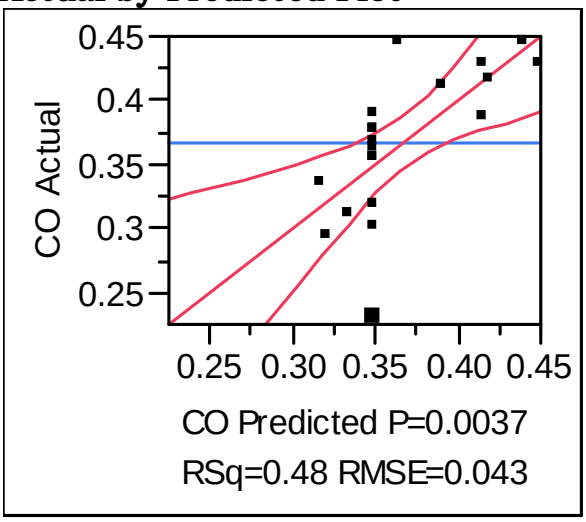

Summary of Fit

RSquare	0.48328
RSquare Adj	0.422489
Root Mean Square Error	0.042954
Mean of Response	0.366495
Observations (or Sum Wgts)	20

Parameter Estimates

Term	Estimate	Std Error	t Ratio	Prob>|t|
Intercept	0.3474672	0.012488	27.82	<.0001
(Pyro-485)*(Pyro-485)	3.1113e-5	1.04e-5	2.99	0.0082
(Pyro-485)*(M-0.093)	-0.090363	0.024106	-3.75	0.0016

Residual by Predicted Plot

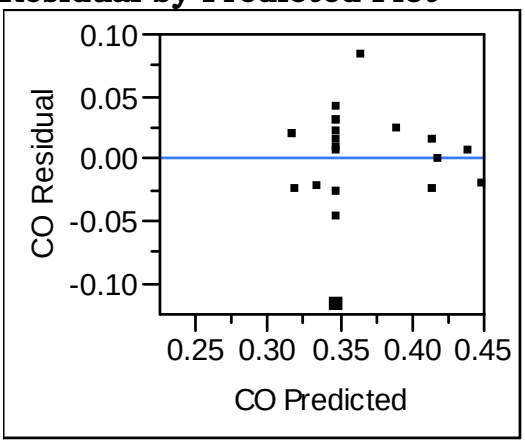

Contour Profiler

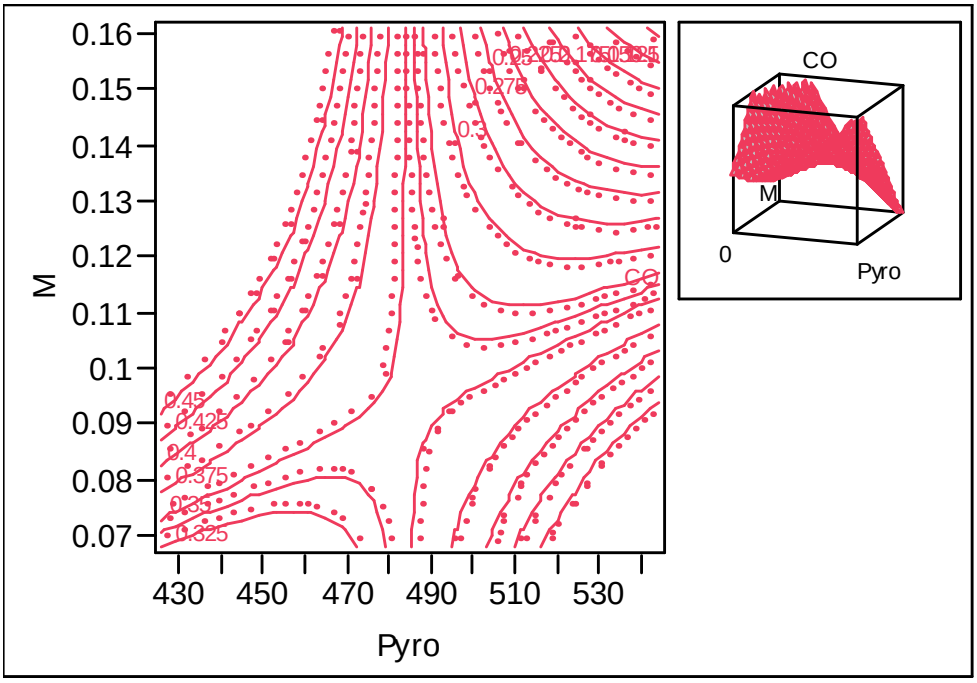

Response carbon monoxide concentration vol. % for washed biomass

Key:
Pyro – Pyrolysis temperature
M – Moisture content
G – Grind size
CO - Total carbon monoxide vol. % yield in non-condensable gas, nitrogen free

Actual by Predicted Plot

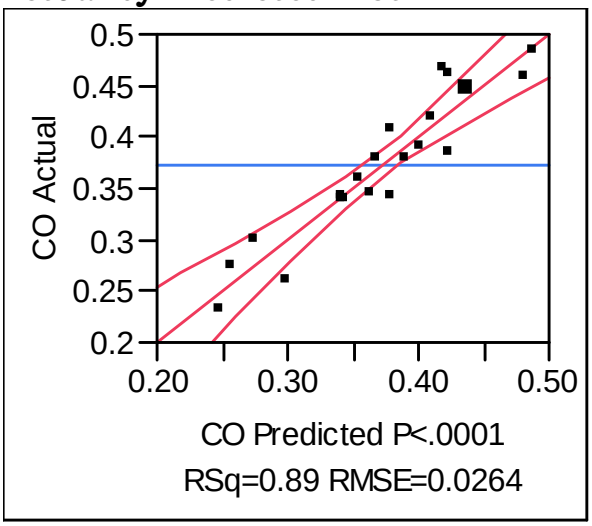

Summary of Fit

RSquare	0.885932
RSquare Adj	0.857415
Root Mean Square Error	0.026363
Mean of Response	0.371314
Observations (or Sum Wgts)	21

Parameter Estimates

Term	Estimate	Std Error	t Ratio	Prob>|t|
Intercept	-0.529672	0.099018	-5.35	<.0001
Pyro	0.0019557	0.000199	9.85	<.0001
M	-0.483279	0.089913	-5.37	<.0001
G	0.0704252	0.032054	2.20	0.0431
(G-0.5119)*(G-0.5119)	-0.471239	0.187196	-2.52	0.0229

Residual by Predicted Plot

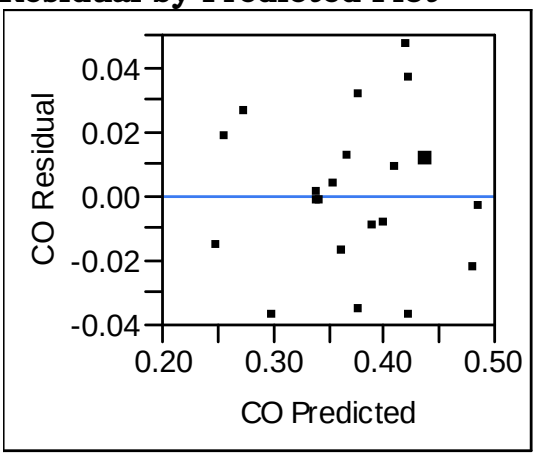

Contour Profiler

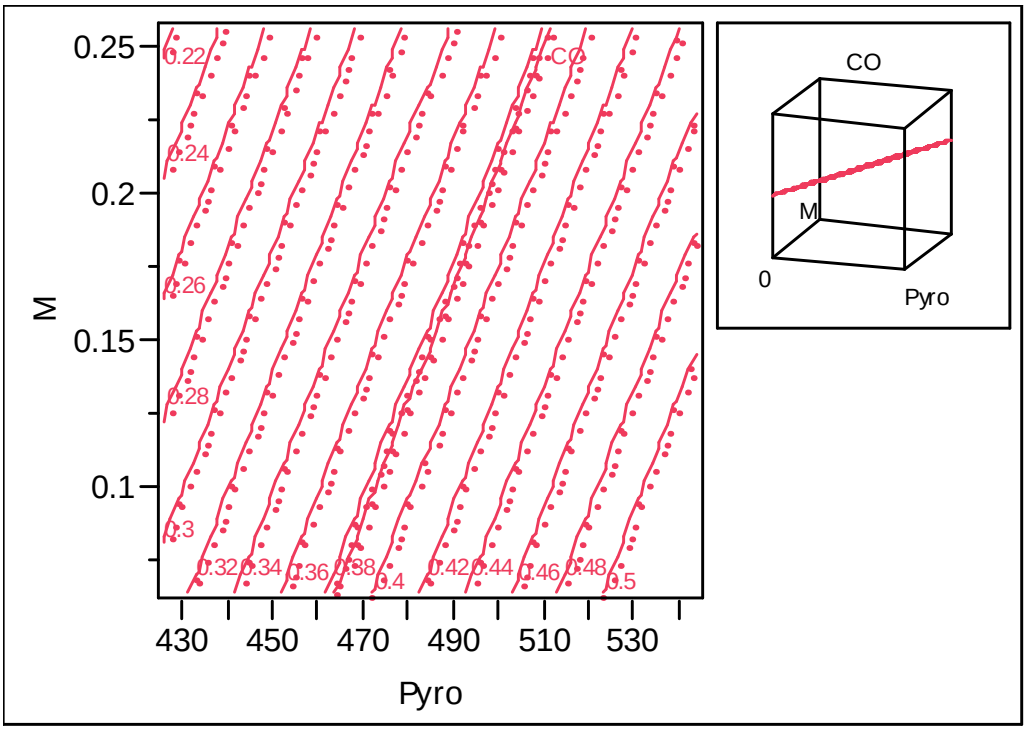

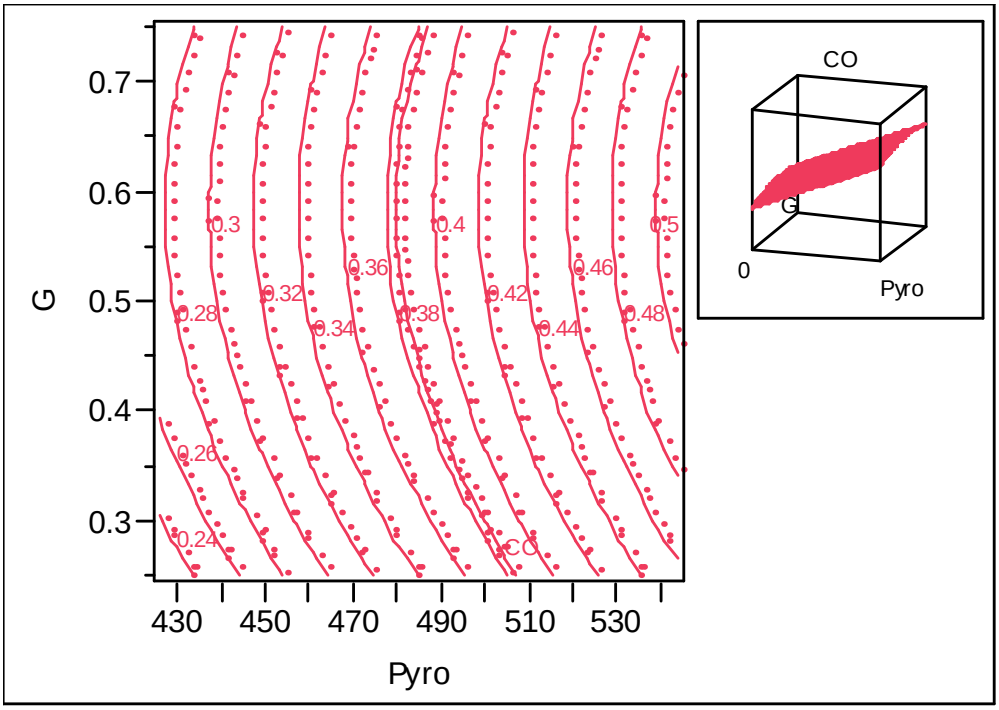
G
0.7
0.6
0.5
0.4
0.3
0.3
0.28
0.32
0.36
0.4
0.34
0.38
0.42
0.46
0.5
0.44
0.48
0.26
0.24
CO
430
450
470
490
510
530
Pyro
CO
G
0
Pyro

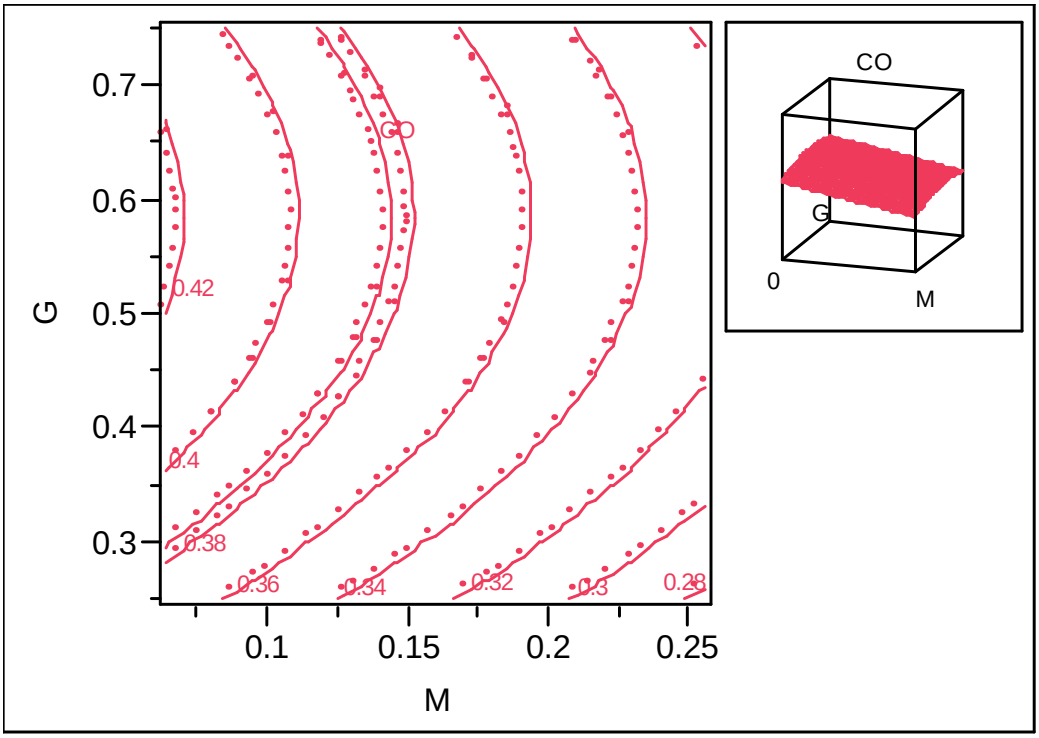
G
0.7
0.6
0.5
0.4
0.3
CO
0.42
0.4
0.38
0.36
0.34
0.32
0.3
0.28
0.1
0.15
0.2
0.25
M
CO
G
0
M

Response carbon monoxide concentration vol. % for torrefied biomass

Key:
Pyro – Pyrolysis temperature
G – Grind size
Tor – Torrefaction temperature
CO - Total carbon monoxide vol. % yield in non-condensable gas, nitrogen free

Actual by Predicted Plot

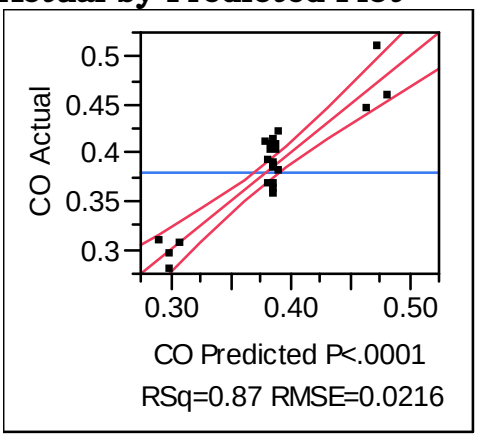

Summary of Fit

RSquare	0.869443
RSquare Adj	0.854083
Root Mean Square Error	0.021627
Mean of Response	0.38098
Observations (or Sum Wgts)	20

Parameter Estimates

Term	Estimate	Std Error	t Ratio	Prob>|t|
Intercept	-0.254676	0.082946	-3.07	0.0069
Pyro	0.00132	0.00017	7.75	<.0001
(G-0.5)*(Tor-211.5)	-0.005175	0.000921	-5.62	<.0001

Residual by Predicted Plot

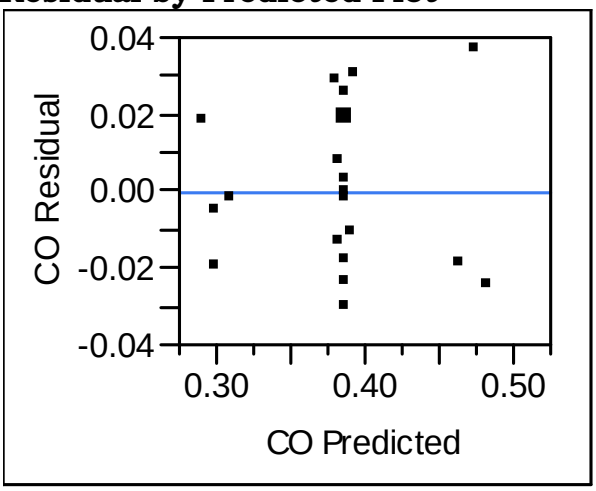

Contour Profiler

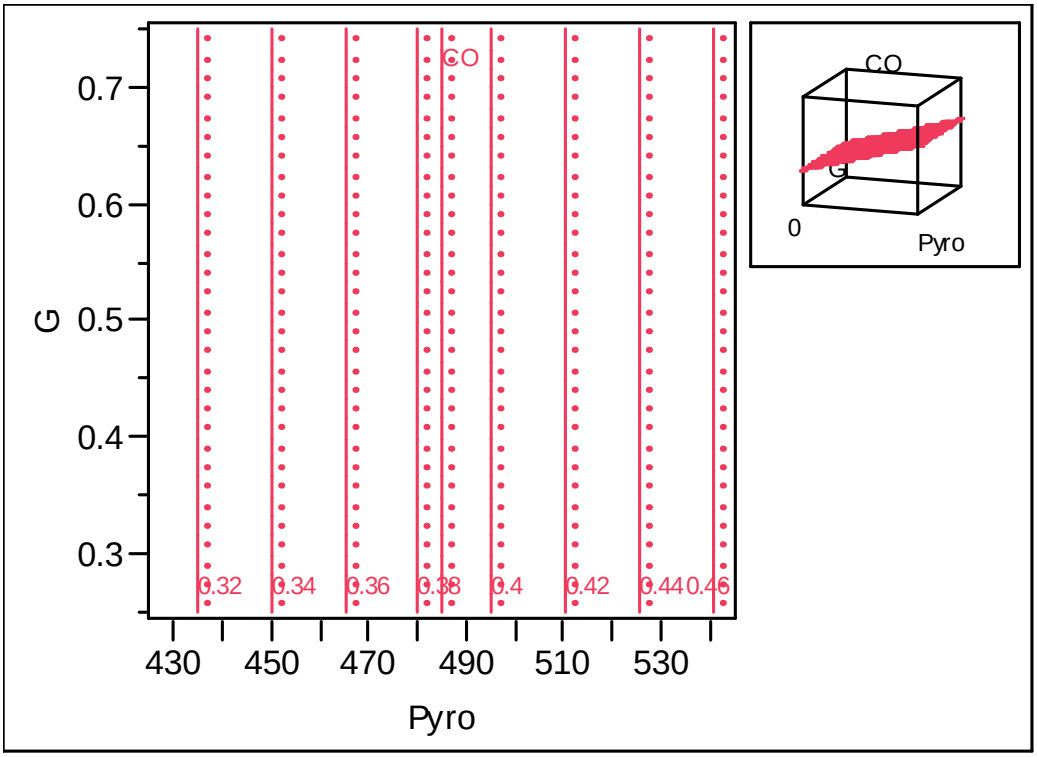

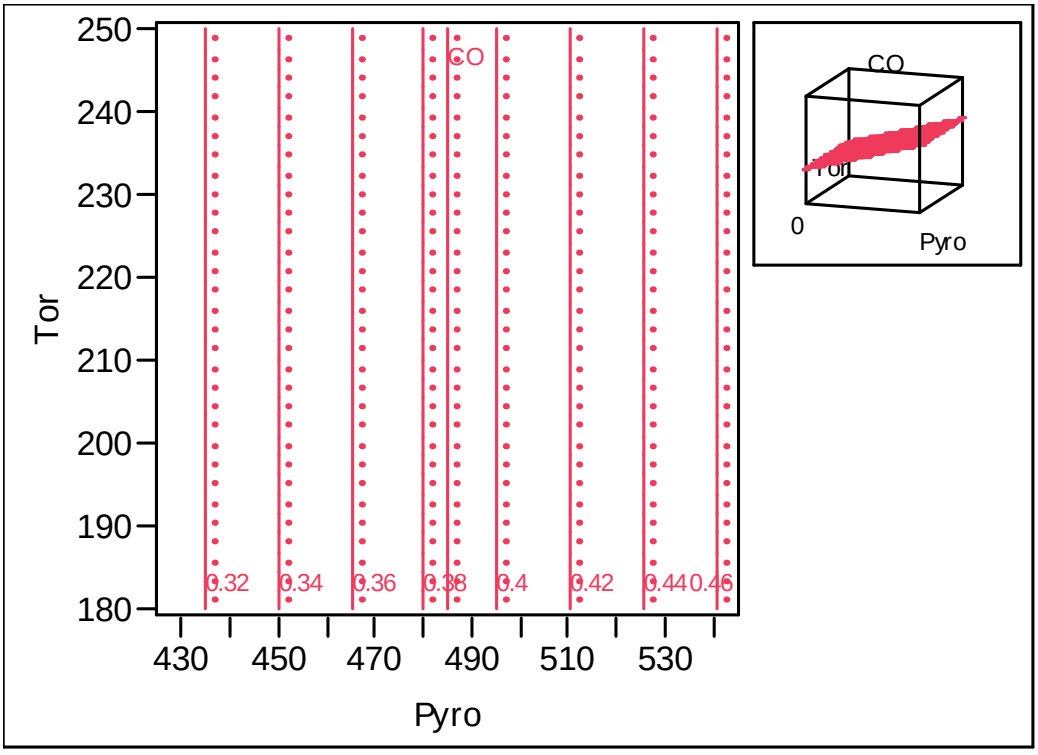
250
240
230
220
210
200
190
180
Tor
CO
0.32
0.34
0.36
0.38
0.4
0.42
0.44
0.46
430
450
470
490
510
530
Pyro
CO
Tor
0
Pyro

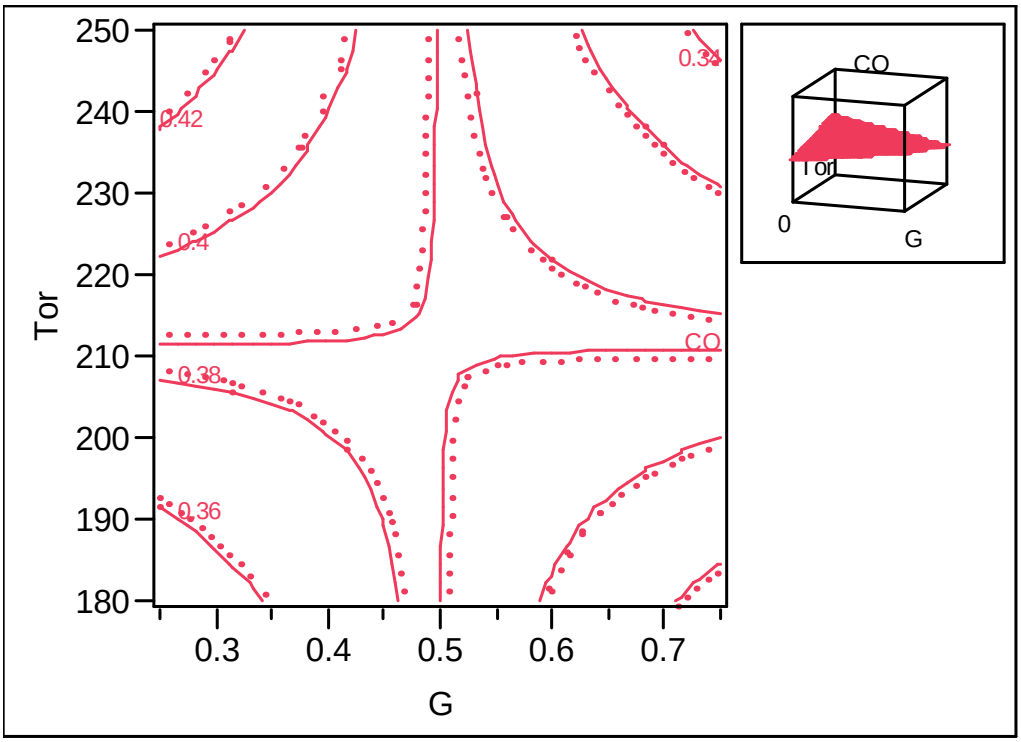
250
240
230
220
210
200
190
180
Tor
0.42
0.4
0.34
CO
0.38
0.36
0.3
0.4
0.5
0.6
0.7
G
CO
Tor
0
G

Response carbon dioxide concentration vol. % for unwashed biomass

Key:

Pyro – Pyrolysis temperature
CO2 - Total carbon dioxide vol. % yield in non-condensable gas, nitrogen free

Actual by Predicted Plot

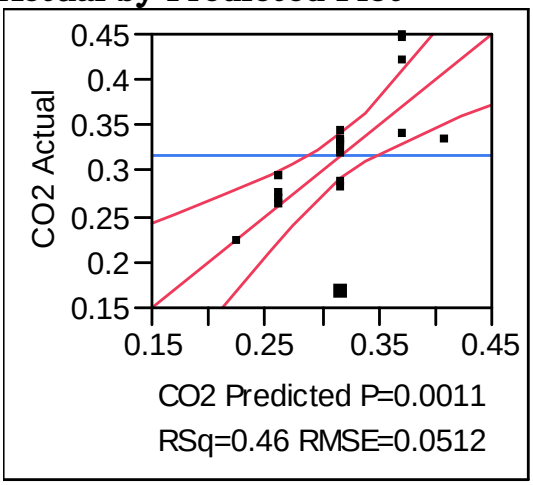

Summary of Fit

RSquare	0.457483
RSquare Adj	0.427344
Root Mean Square Error	0.051197
Mean of Response	0.316215
Observations (or Sum Wgts)	20

Parameter Estimates

Term	Estimate	Std Error	t Ratio	Prob>|t|
Intercept	1.0634194	0.19213	5.53	<.0001
Pyro	-0.001541	0.000395	-3.90	0.0011

Residual by Predicted Plot

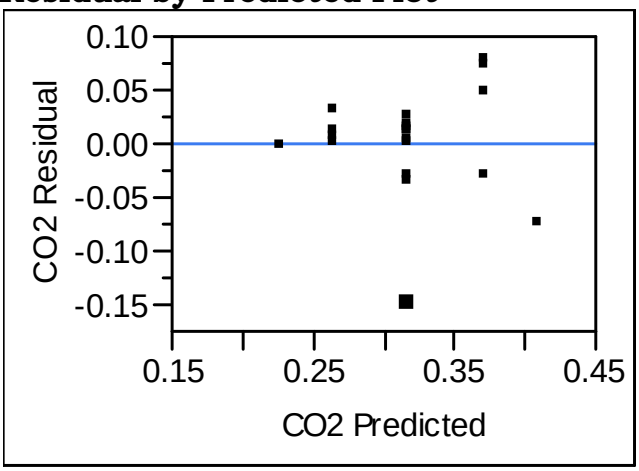

Prediction Profiler

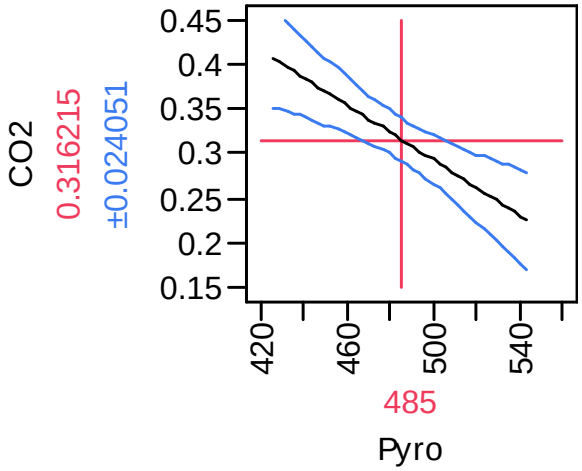

Response carbon dioxide concentration vol. % for washed biomass

Key:

Pyro – Pyrolysis temperature
M – Moisture content
G – Grind size
CO2 - Total carbon dioxide vol. % yield in non-condensable gas, nitrogen free

Actual by Predicted Plot

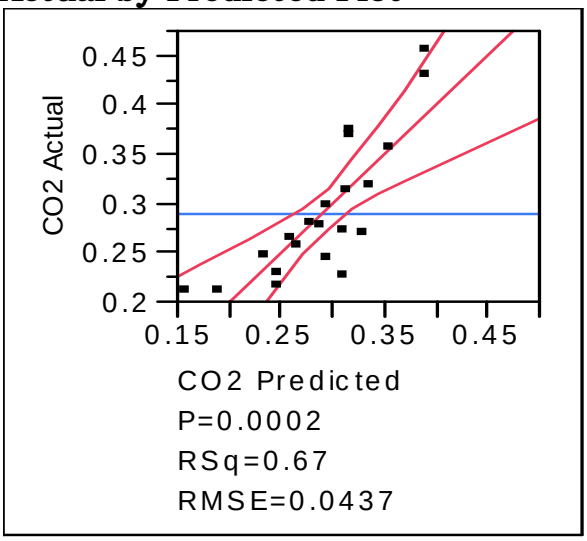

Summary of Fit

RSquare	0.670455
RSquare Adj	0.612301
Root Mean Square Error	0.04366
Mean of Response	0.290138
Observations (or Sum Wgts)	21

Parameter Estimates

Term	Estimate	Std Error	t Ratio	Prob>|t|
Intercept	1.0327794	0.157995	6.54	<.0001
Pyro	-0.00143	0.000328	-4.37	0.0004
M	-0.39174	0.147637	-2.65	0.0167
(Pyro-483.333)*(G-0.5119)	-0.003557	0.001686	-2.11	0.0500

Residual by Predicted Plot

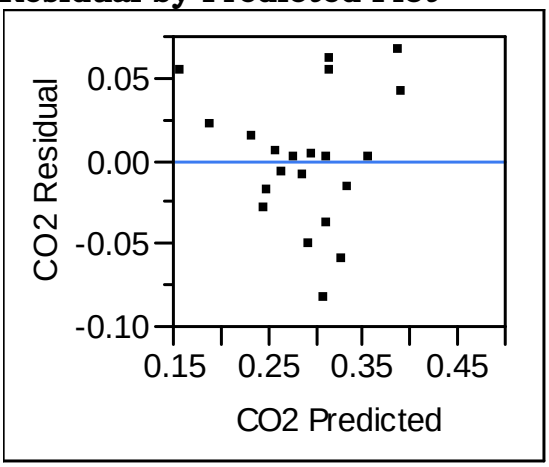

Contour Profiler

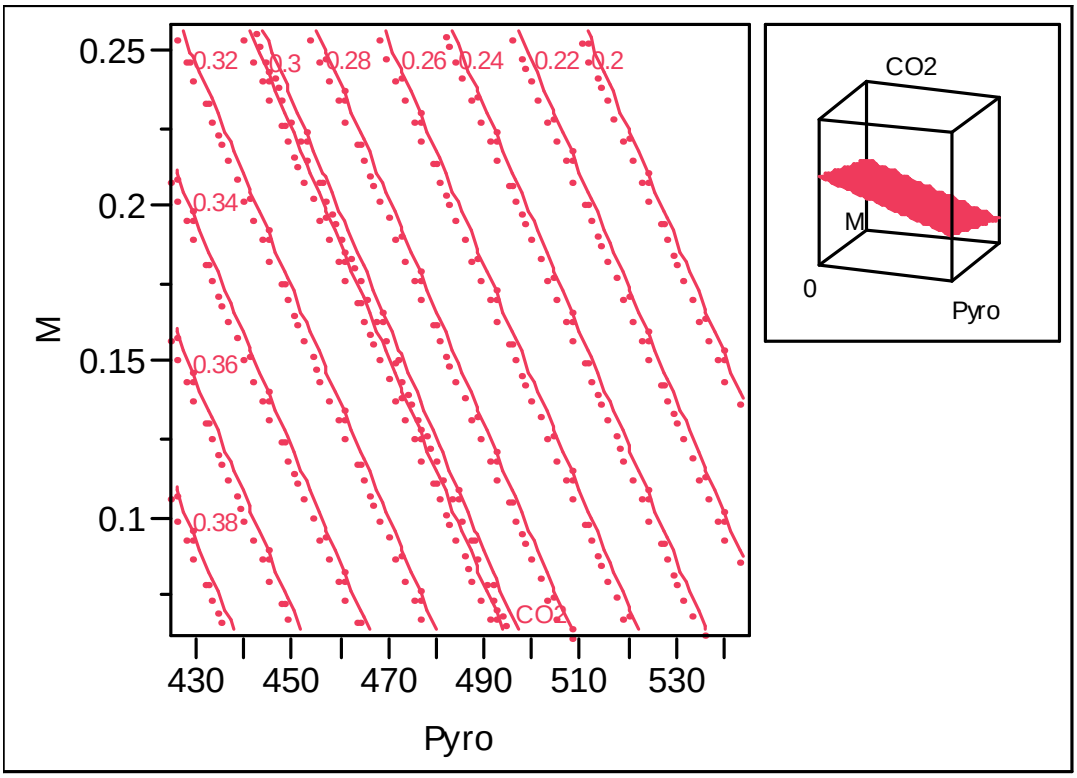

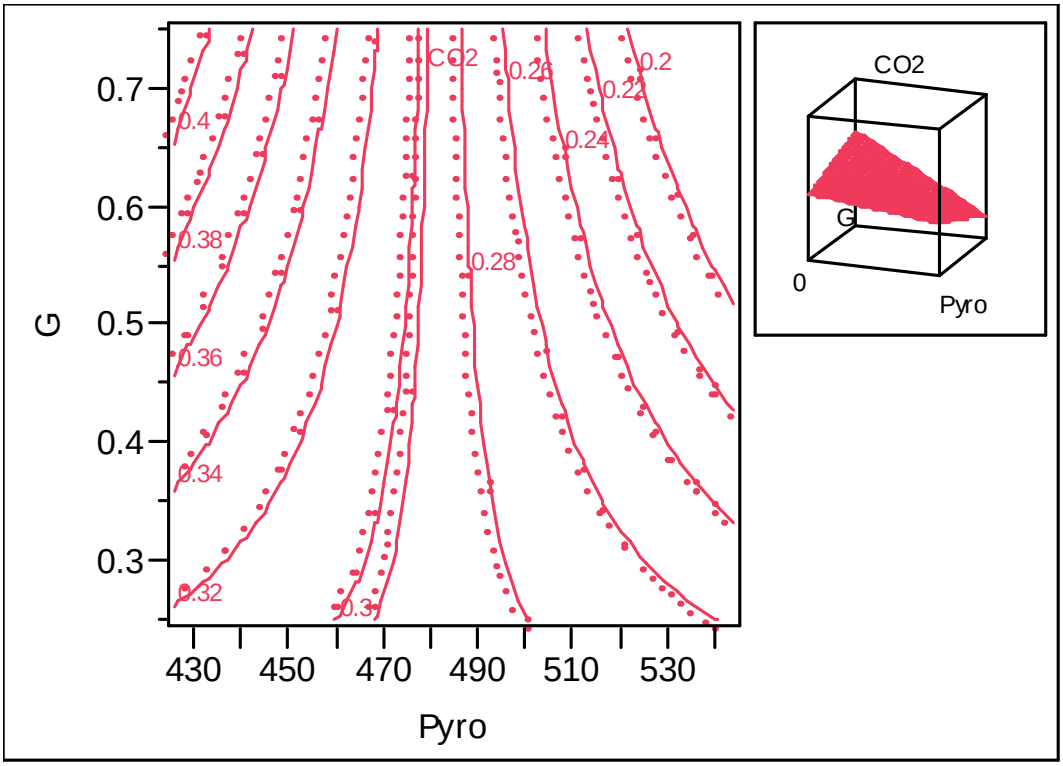
CO2
0.4
0.38
0.36
0.34
0.32
0.3
0.28
0.26
0.24
0.22
0.2
G
0.7
0.6
0.5
0.4
0.3
430
450
470
490
510
530
Pyro
CO2
G
0
Pyro

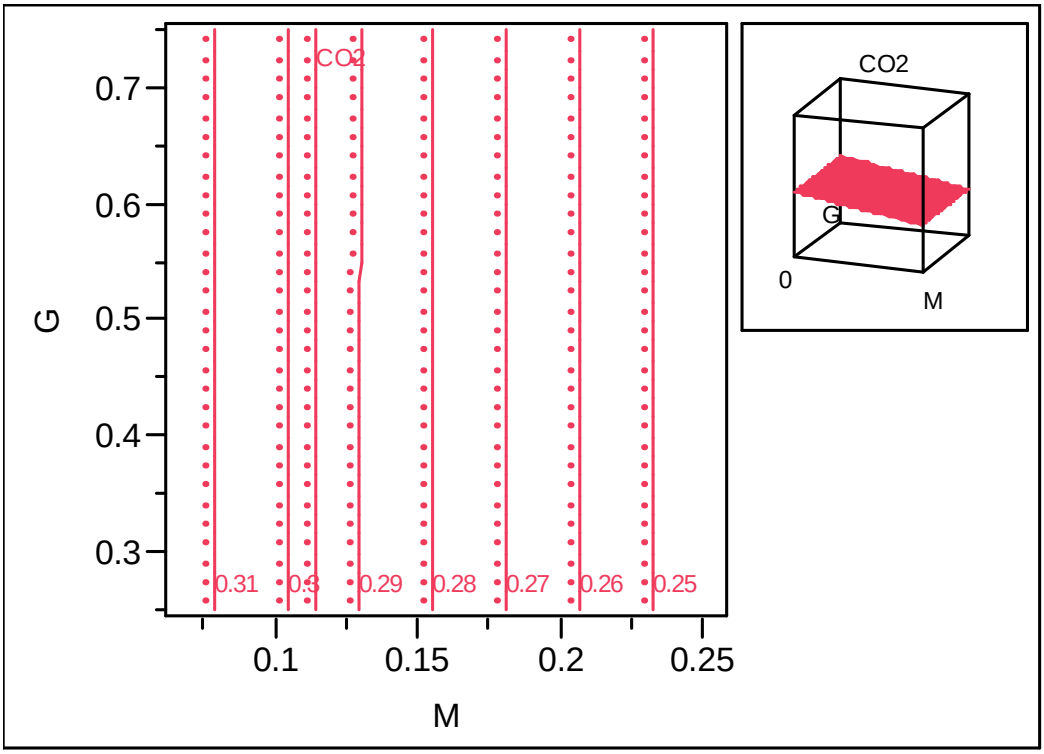
CO2
0.31
0.3
0.29
0.28
0.27
0.26
0.25
G
0.7
0.6
0.5
0.4
0.3
0.1
0.15
0.2
0.25
M
CO2
G
0
M

Response carbon dioxide concentration vol. % for torrefied biomass

Key:

Pyro – Pyrolysis temperature
G – Grind size
Tor – Torrefaction temperature
CO2 - Total carbon dioxide vol. % yield in non-condensable gas, nitrogen free

Actual by Predicted Plot

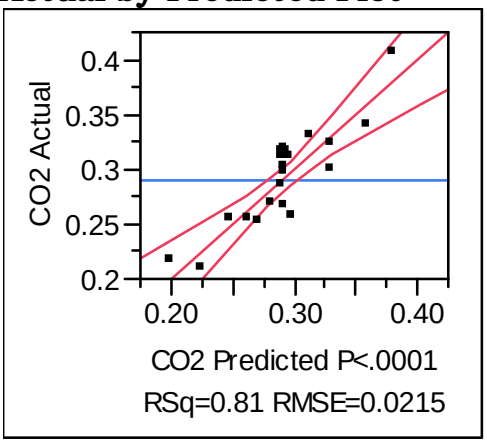

Summary of Fit

RSquare	0.811593
RSquare Adj	0.776266
Root Mean Square Error	0.021465
Mean of Response	0.290555
Observations (or Sum Wgts)	20

Parameter Estimates

Term	Estimate	Std Error	t Ratio	Prob>|t|
Intercept	0.9779957	0.08653	11.30	<.0001
Pyro	-0.001145	0.000172	-6.65	<.0001
Tor	-0.000611	0.0002	-3.06	0.0075
(Tor-211.5)*(G-0.5)	-0.003198	0.000917	-3.49	0.0030

Residual by Predicted Plot

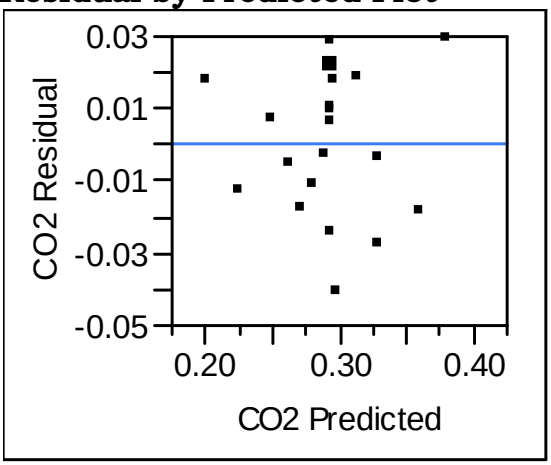

Contour Profiler

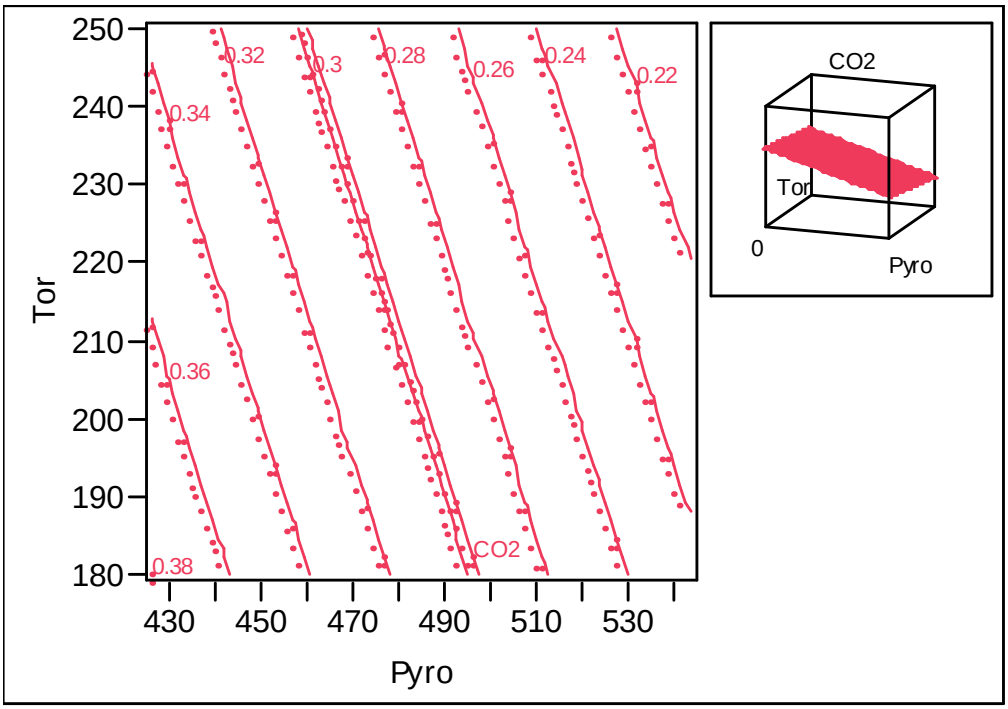

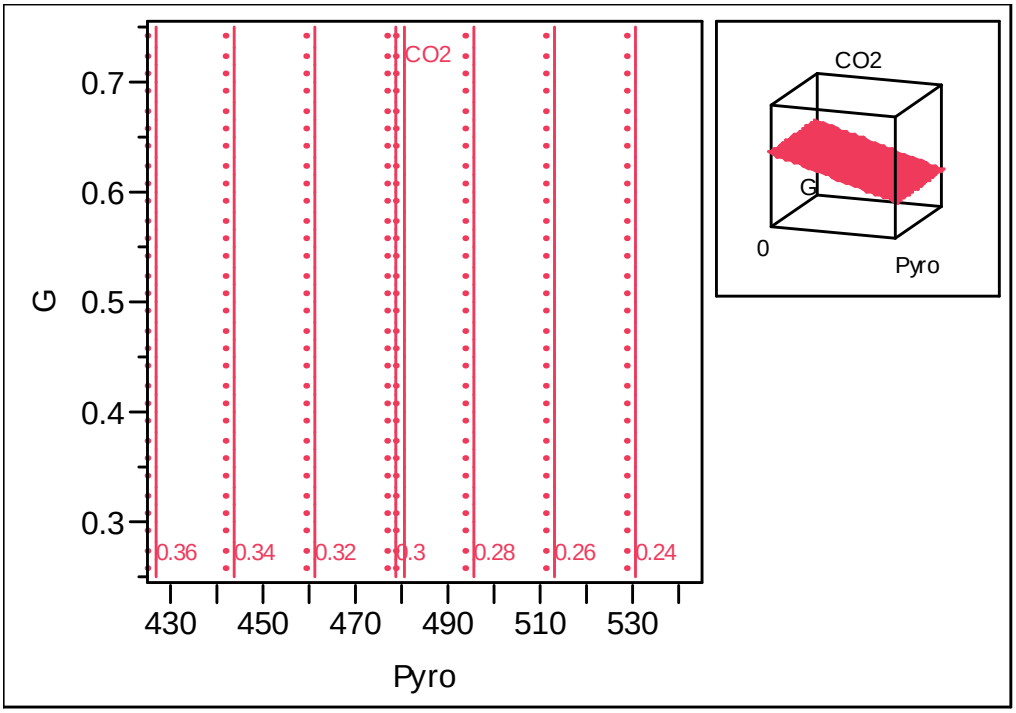
CO2
0.7
0.6
0.5
0.4
0.3
G
0.36
0.34
0.32
0.3
0.28
0.26
0.24
430
450
470
490
510
530
Pyro
CO2
G
0
Pyro

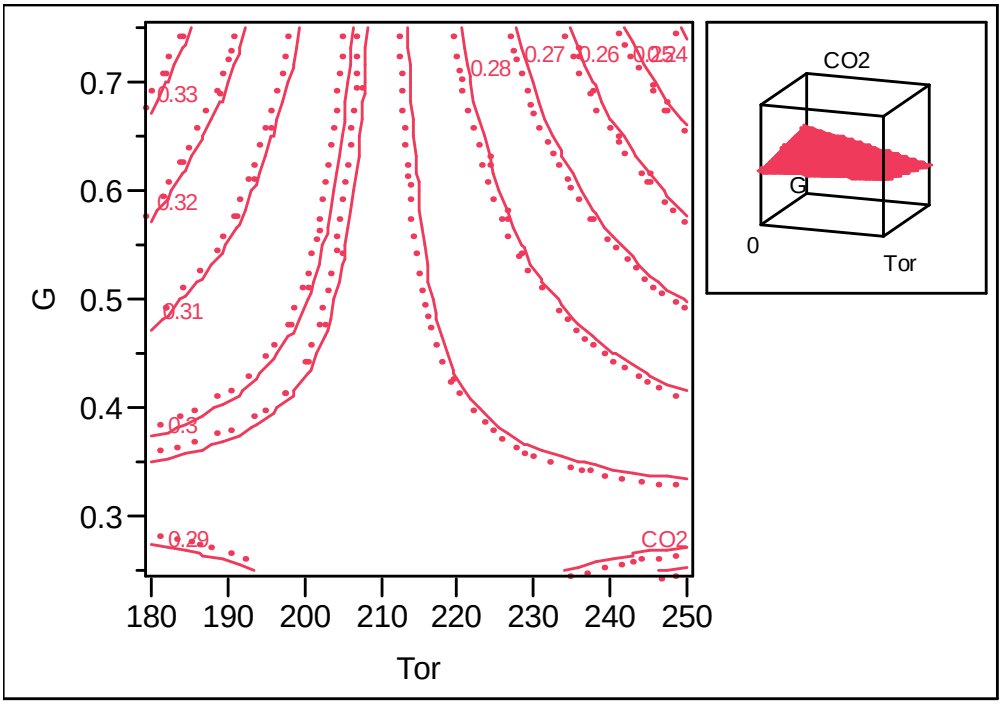
0.7
0.6
0.5
0.4
0.3
G
0.33
0.32
0.31
0.3
0.29
0.28
0.27
0.26
CO2
180
190
200
210
220
230
240
250
Tor
CO2
G
0
Tor

Response hydrogen gas concentration vol. % for washed biomass

Key:
Pyro – Pyrolysis temperature
G – Grind size
H2 - Total hydrogen vol. % yield in non-condensable gas, nitrogen free

Actual by Predicted Plot

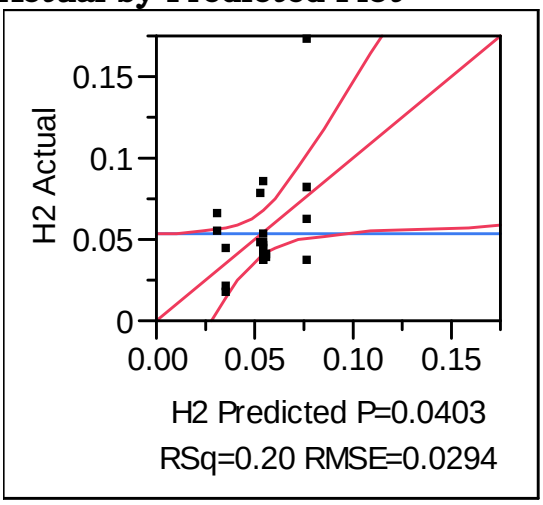

Summary of Fit

RSquare	0.203183
RSquare Adj	0.161245
Root Mean Square Error	0.029416
Mean of Response	0.053457
Observations (or Sum Wgts)	21

Parameter Estimates

Term	Estimate	Std Error	t Ratio	Prob>|t|
Intercept	0.0544451	0.006435	8.46	<.0001
(G-0.5119)*(Pyro-483.333)	0.0024897	0.001131	2.20	0.0403

Residual by Predicted Plot

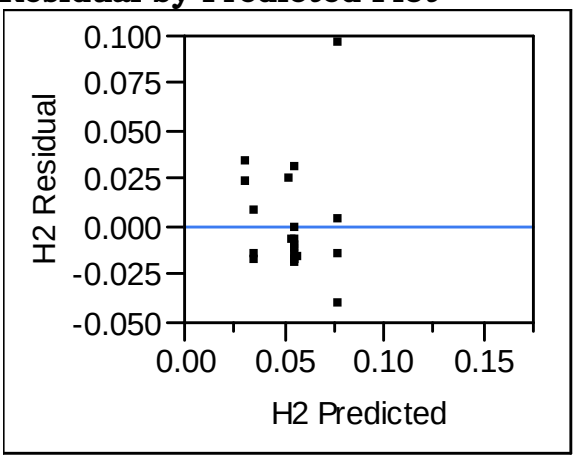

Contour Profiler

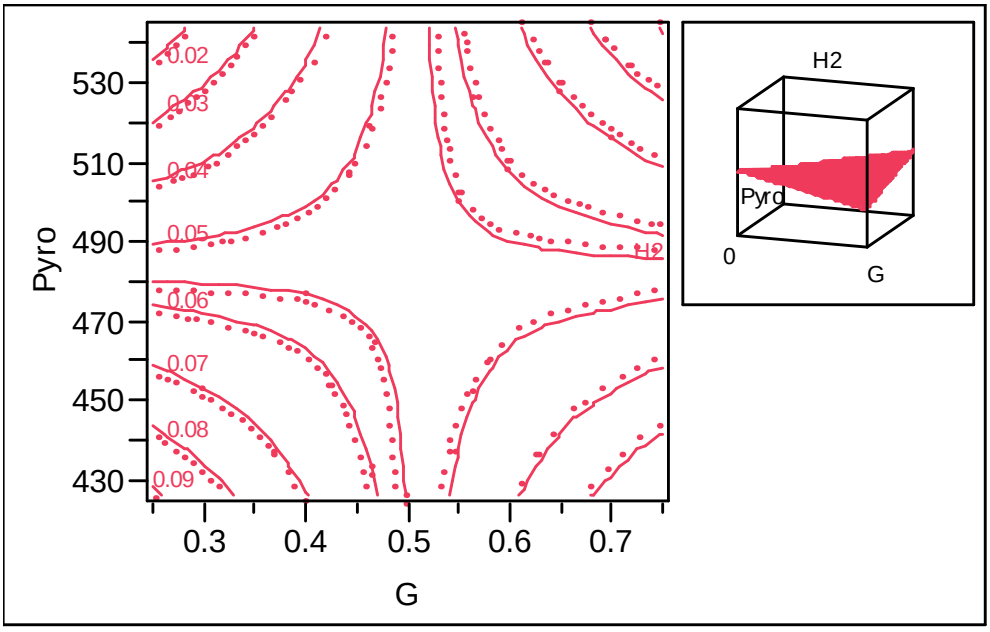

Response hydrogen gas concentration vol. % for torrefied biomass

Key:
Pyro – Pyrolysis temperature
H2 - Total hydrogen vol. % yield in non-condensable gas, nitrogen free

Actual by Predicted Plot

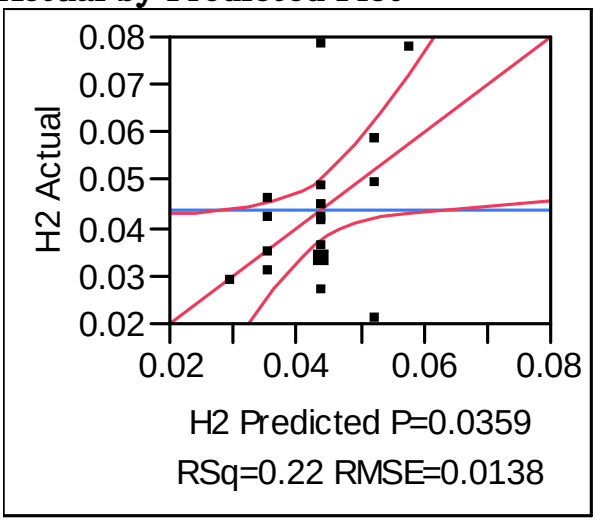

Summary of Fit

RSquare	0.222247
RSquare Adj	0.179038
Root Mean Square Error	0.013755
Mean of Response	0.043565
Observations (or Sum Wgts)	20

Parameter Estimates

Term	Estimate	Std Error	t Ratio	Prob>|t|
Intercept	-0.073296	0.051619	-1.42	0.1727
Pyro	0.0002409	0.000106	2.27	0.0359

Residual by Predicted Plot

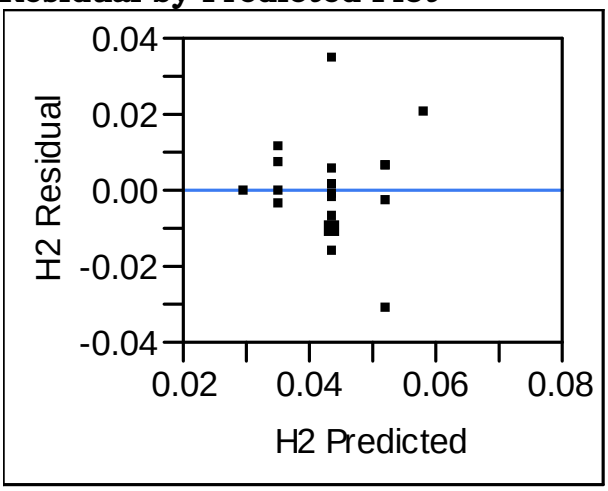

Prediction Profiler

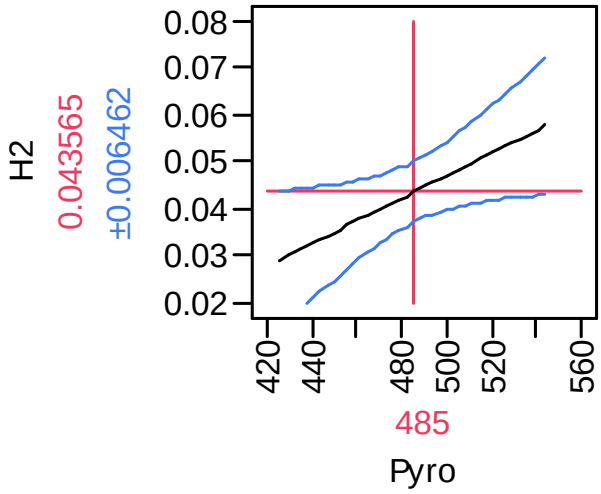

Response methane concentration vol. % for washed biomass

Key:
Pyro – Pyrolysis temperature
M – Moisture content
CH4 - Total methane vol. % yield in non-condensable gas, nitrogen free
Response CH4
Whole Model

Actual by Predicted Plot

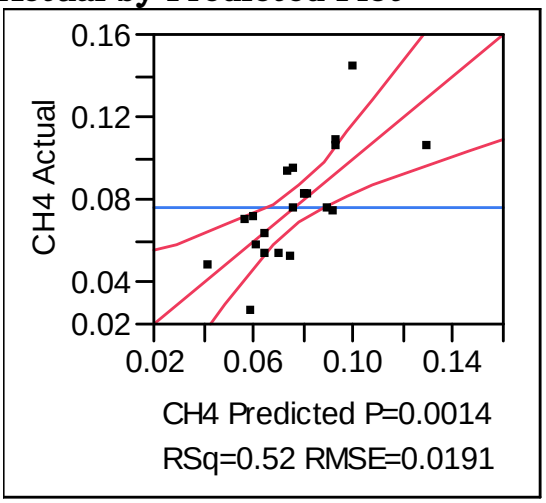

Summary of Fit

RSquare	0.518878
RSquare Adj	0.46542
Root Mean Square Error	0.019055
Mean of Response	0.076781
Observations (or Sum Wgts)	21

Parameter Estimates

Term	Estimate	Std Error	t Ratio	Prob>|t|
Intercept	-0.142973	0.069586	-2.05	0.0547
Pyro	0.0004239	0.000146	2.91	0.0094
(M-0.13444)*(M-0.13444)	3.5058943	1.350757	2.60	0.0183

Residual by Predicted Plot

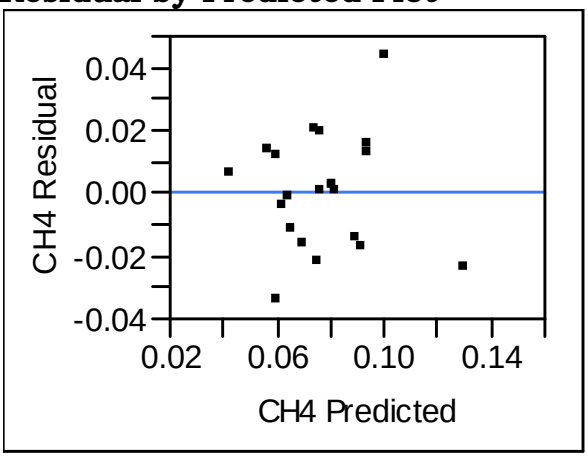

Contour Profiler

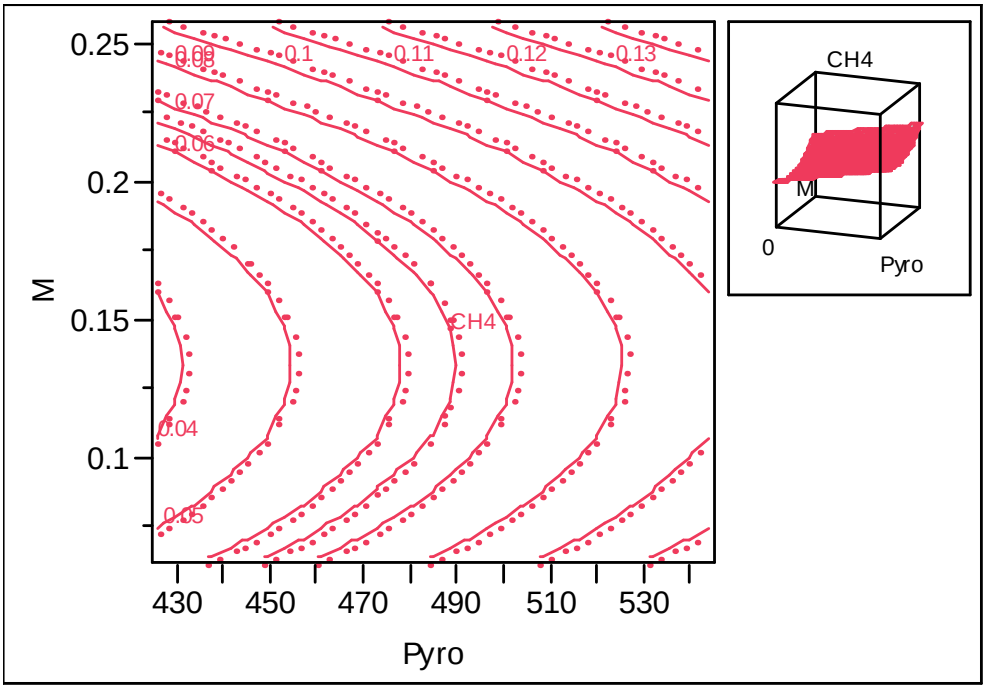

Response methane concentration vol. % for torrefied biomass

Key:

Pyro – Pyrolysis temperature
M – Moisture content
G – Grind size
T – Torrefaction temperature
CH4 - Total methane vol. % yield in non-condensable gas, nitrogen free
Response CH4

Actual by Predicted Plot

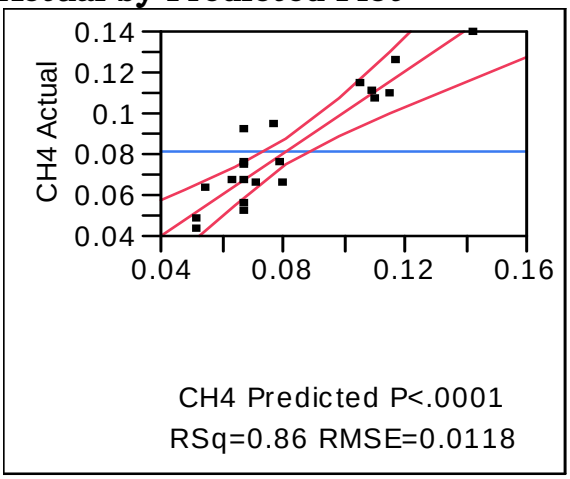

Summary of Fit

RSquare	0.863957
RSquare Adj	0.81537
Root Mean Square Error	0.011843
Mean of Response	0.081665
Observations (or Sum Wgts)	20

Parameter Estimates

Term	Estimate	Std Error	t Ratio	Prob>|t|
Intercept	-0.239642	0.047388	-5.06	0.0002
Tor	0.0004027	0.000113	3.56	0.0032
Pyro	0.0004003	0.000093	4.31	0.0007
G	0.0522439	0.015313	3.41	0.0042
(Tor-211.5)*(Tor-211.5)	1.8574e-5	4.408e-6	4.21	0.0009
(Pyro-485)*(Pyro-485)	5.6585e-6	2.539e-6	2.23	0.0427

Residual by Predicted Plot

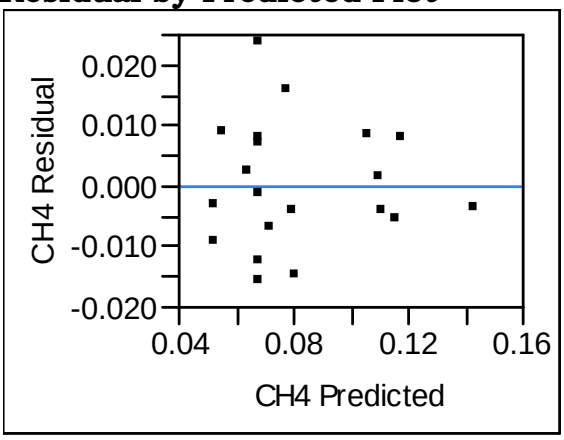

Contour Profiler

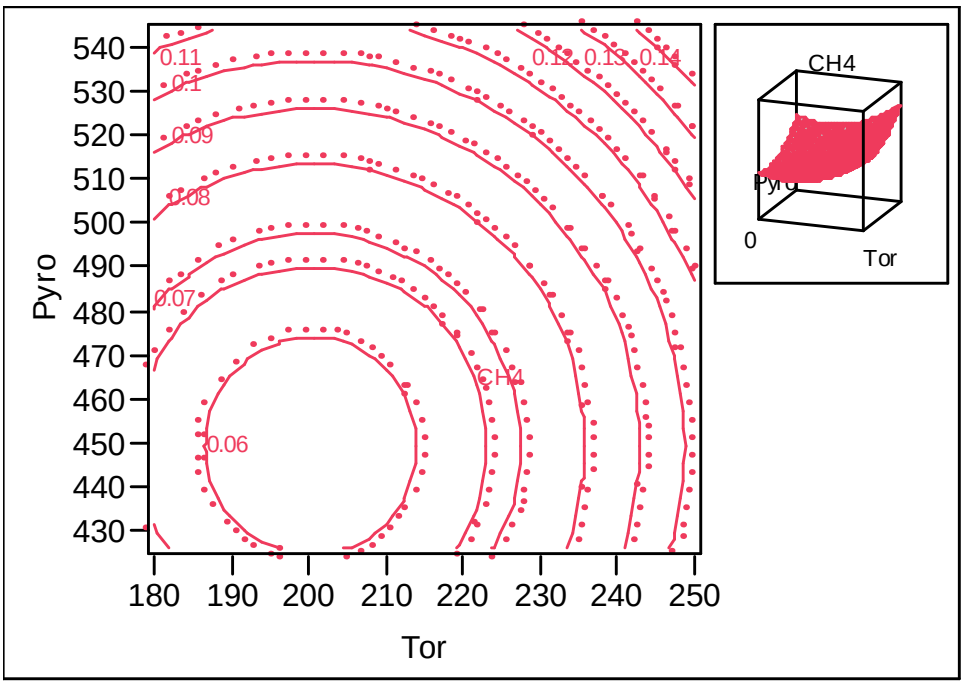

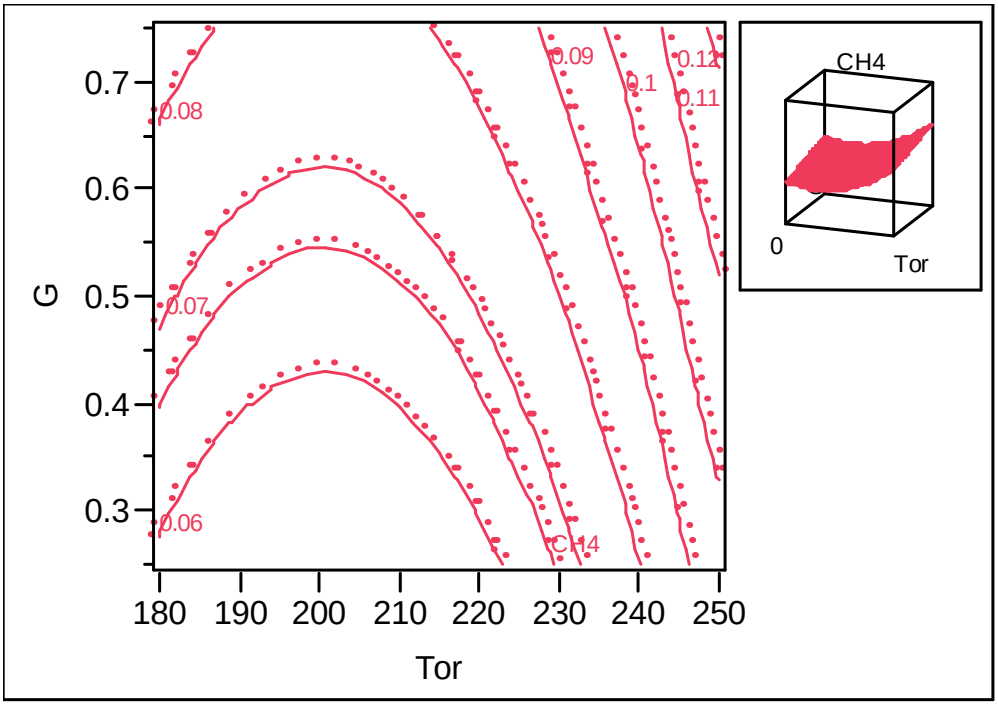
G
0.7
0.6
0.5
0.4
0.3
0.08
0.07
0.06
0.09
0.1
0.11
0.12
CH4
180
190
200
210
220
230
240
250
Tor
CH4
0
Tor

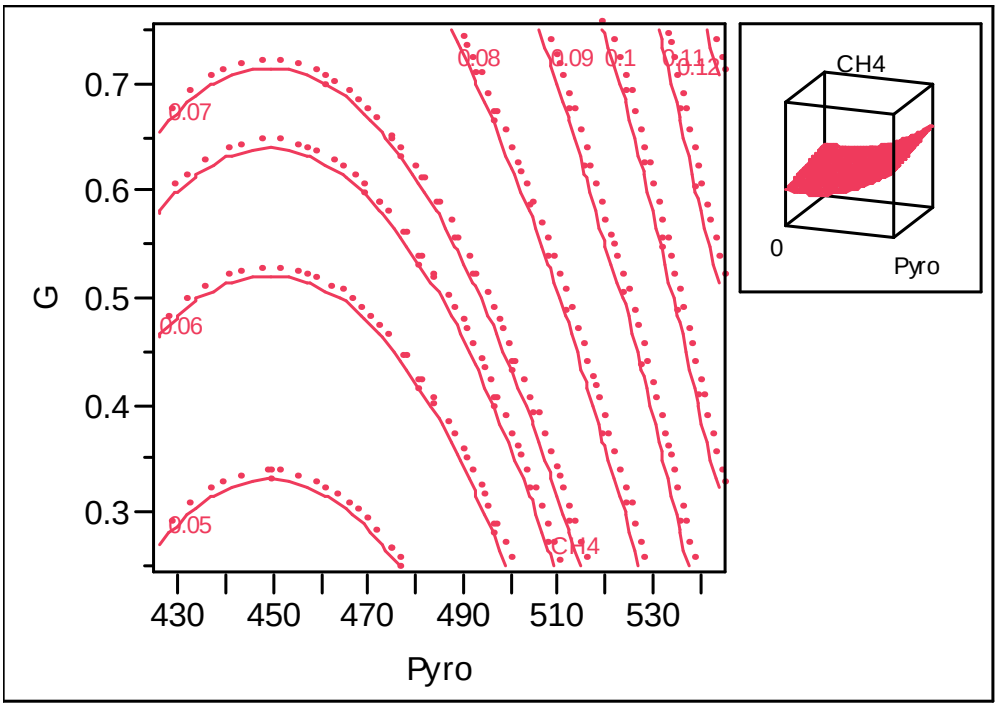
G
0.7
0.6
0.5
0.4
0.3
0.08
0.09
0.1
0.11
0.12
0.07
0.06
0.05
CH4
430
450
470
490
510
530
Pyro
CH4
0
Pyro

ACKNOWLEGEMENTS

I would like to take this opportunity to express my thanks to those who helped me with various aspects of conducting research and the writing of this thesis. First and foremost, Dr. Robert C. Brown for his guidance, patience and support throughout this research and the writing of this thesis, also my graduate committee members for their efforts and contributions to this work: Dr. Raj Raman and Dr. James Bernard. I would also like to thank Dr. Justinus Satrio for starting me into this research field and assisting me in the early stages of my research, Dr. Samuel Jones for his patience through the development, experimentation, and reporting stages of my research, Dr. Daren Daugaard for his assistance and guidance, as well as the ConocoPhillips Company for providing the funding and guidance for this research project, and lastly, my wife, Jill, for her eternal patience, support, and editing assistance to prepare and present this document.

Special thanks to:

Fellow graduate students in CSET for insight, assistance, and critiquing, CSET lab technicians for putting up with the long hours and frustrating days in the lab to complete the analysis critical to this study, and all other CSET staff members for their priceless assistance through my graduate assistantship.